

**Assessing the response of T cells to *Mycobacterium tuberculosis*
lipids**

Inauguraldissertation

zur

Erlangung der Würde eines Doktors der Philosophie
vorgelegt der
Philosophisch-Naturwissenschaftlichen Fakultät
der Universität Basel

von

Anthony COLLMANN

Aus Porcelette, France

Basel, 2008

Genehmigt von der Philosophisch-Naturwissenschaftlichen Fakultät

Auf Antrag von

Prof. Jean Pieters (Fakultätsverantwortlicher)

Prof. Gennaro De Libero (Dissertationleiter)

Prof. Regine Landmann-Suter (Korreferent)

Basel, den 11.11.2008

Prof. Dr. Eberhard Parlow, Dekan

Acknowledgments

“To be successful in Science...and in whatever you do, you must learn to think with two years in advance...”

These are the first words I heard when I arrived in the Lab of Experimental Immunology, at the beginning of my Ph.D. training, here in Basel. They were from my chief and mentor, and will sound in my head forever. For the wise advices, for scientific rigor, and unconditional support, I would like to express my gratitude and deepest respect to you, Gennaro. Be sure what you taught me will have major impact on my future career, and be convinced after these years spent under your guidance I consider you now as a friend.

I would also like to thank all the past (Sabrina, Samantha, David, Hans-Jürgen, Jens, Maria, Karimi, Vera, Manu...) and present (Lucia, Nino, Lena, Marco & Marco, Federica, Paula, Michael...) members of the Lab, with whom I shared so many nice and tough times (but that's what life is made of...). I hope you enjoyed all these moments as I did. I know I'm probably not the easiest guy to cope with, but be proud...you managed! I'm sure we'll meet again...

Sorry for those I forgot...you know who you are!

Thanks to all my collaborators as well! You are too numerous to mention, and I invite to refer to all the papers we wrote together. Also in your case, I might have been tough sometimes, but be sure I'm proud of what we achieved.

Thanks to the members of my Thesis Committee: Prof. Jean Pieters, Prof. Regine Landmann, and Prof. Ed Palmer.

To you who made me the man I am: my brother Nicolas, my grandmother Yvonne, my lovely parents and parents in law, and all close friends and family members.

We still have a long road to travel together...

And last, to my wonderful wife, Emilie. What I feel for you cannot be described by words...you are the flame...

I dedicate this work to all of you...

TABLE OF CONTENTS

ABBREVIATIONS.....	9
ABSTRACT	13
INTRODUCTION	15
Genetic history of CD1 and MHC molecules	15
Structure of CD1 proteins.....	18
CD1a.....	19
CD1b.....	20
CD1c.....	21
CD1d.....	21
CD1e.....	22
Structures of ternary CD1-lipid-TCR complexes	22
CD1 expression patterns	25
CD1 assembly	28
CD1 trafficking.....	30
Structure, biology and functions of Lipid Antigens	32
Self Lipid Antigens.....	32
Microbial Lipid Antigens	37
Lipid Antigen Presentation.....	42
Lipid uptake by APCs and intracellular trafficking	42
Antigen processing and loading onto CD1.....	45
Persistence of CD1-lipid antigen complexes	46
Lipid-reactive TCRs and selection of CD1-restricted T cells	46
CD1-restricted T cells implication in disease	49
Therapeutic applications of Lipid Antigens	52

CHAPTER 1.....	55
Mycolic acids constitute a scaffold for mycobacterial lipidic antigens stimulating CD1b-restricted T cells.....	55
Systematic approach.....	57
Results	57
Characterization of the Z5B71 T cell clone.....	57
Chemical characterization of the lipid antigen.....	61
Stimulation of T cells by hemi-synthetic GroMM (sGroMM)	65
Structural requirements of GroMM for immunogenicity.....	69
Presentation of GroMM is CD1b-restricted and CD1e-independent	72
<i>M. tuberculosis</i> -infected DCs stimulate Z5B71 T cells.....	74
GroMM-reactive T cells are not detected in patients with active tuberculosis.....	75
Discussion.....	79
 CHAPTER 2.....	 83
Fatty acyl structures of <i>Mycobacterium tuberculosis</i> sulfoglycolipid govern T cell immunogenicity	83
Results	86
Synthesis of diacylated SGLs with linear fatty acids.....	86
Palmitoyl-sulfoglycolipids with an additional linear fatty acyl-chain bind to soluble human CD1b.....	87
SGL analogs with linear fatty acyl chains are not stimulatory	89
Hemisynthetic SGLs containing <i>M. tuberculosis</i> mycolipenic and mycosanoic acids are immunogenic	90
The number of C-methyl branched groups controls the antigenicity of the SGL analogs.....	92

The length of the conventional acyl chain located at the position 2 of the trehalose core modulates SGL antigenicity	93
The absolute configuration of the C-methyl branched chiral carbons is sensed by the TCR	95
Stimulation of Ac ₂ SGL-specific T cells by plate-bound shCD1b:SGL complexes	96
Discussion	99
CHAPTER 3.....	102
Design of lipid-based subunit vaccines	102
Results	106
GroMM immunogenicity is increased by lipidic adjuvants and structural modifications of its hydrophobic tail	106
PIMs and GroMM do not increase Ac ₂ SGL immunogenicity.....	110
Lipid binding proteins can be used to increase Ac ₂ SGL immunogenicity	112
DCs from CD1b-transgenic mice present SGLs to Ac ₂ SGL-specific T cells in a CD1b-restricted manner	114
Generation of shCD1b:SGL12 dimers to stain CD1b-restricted Ac ₂ SGL-specific T cells	116
Immunization of CD1b-transgenic mice with synthetic SGLs leads to priming and expansion of SGL-specific T cells	117
Discussion	118
CONCLUSIONS	121
MATERIALS AND METHODS	123
Reagents.....	123

Bacterial Strain and Culture Conditions.....	123
Cell Culture	123
T Cell Activation Assays	124
Analysis of CD1 Restriction	124
Pulsing and infection of DCs with <i>M. tuberculosis</i>	125
Lipidic Fractions Used for Generation of T Cell Clone.....	125
Lipidic fractions from several actinomycetes.....	125
Purification of the GroMM from <i>M. bovis</i> BCG	125
GroMM Acetylation	126
GroMM Saponification	126
GroMM Synthesis	126
MALDI-<i>Tof</i>-MS.....	127
NMR Analysis.....	128
Recognition of GroMM by Lymphocytes from Tuberculosis	
Patients and Healthy Donors	128
Molecular Modeling	129
Synthesis of sulfoglycolipids.....	129
Preparation of <i>M. tuberculosis</i> multimethyl fatty acids for hemisynthesis.....	130
Synthesis of multimethylated fatty acids	131
Analysis of shCD1b protein:SGL complexes by IEF	131
Generation of shCD1b and <i>in vitro</i> SGL binding assays.....	131
Capillary isoelectrofocusing (cIEF)	132
Cloning, expression and purification of SCP-2 and hTAP	132
Generation of shCD1b:SGL12 dimers.....	133
Flow Cytometry	133
APPENDIX	134
Work discussed in the present thesis	134
 Mycolic acids constitute a scaffold for mycobacterial lipidic antigens stimulating CD1b-restricted T cells.....	134

Fatty acyl structures of <i>Mycobacterium tuberculosis</i> sulfoglycolipid govern T cell immunogenicity	134
Other participations.....	135
Synthesis of Diacylated Trehalose Sulfates: Candidates for a Tuberculosis Vaccine.....	136
A Naturally Occurring Mutation in CD1e Impairs Lipid Antigen Presentation	141
Differential alteration of lipid antigen presentation to NKT cells due to imbalances in lipid metabolism	146
 CURRICULUM VITAE	157
 REFERENCES	161

ABBREVIATIONS

α GalCer	alpha-galactosylceramide
Ac ₂ SGLs	diacylated sulfoglycolipids
AHR	airway hyperreactivity
AP-2	adaptor protein complex-2
AP-3	adaptor protein complex-3
APC	antigen-presenting cell
ApoE	apolipoprotein E
β_2 m	beta 2-microglobulin
BCG	bacillus Calmette-Guérin
BSA	bovine serum albumin
CDR	complementarity-determining region
cIEF	capillary isoelectric focusing
CNS	central nervous system
COSY	correlation spectroscopy
DAT	di-acylated trehalose
DC	dendritic cell
DDMs	didehydroxymycobactins
DMSO	dimethylsulfoxide
<i>e.g.</i>	<i>exempli gratia</i>
EAE	experimental autoimmune encephalomyelitis
ELISA	enzyme linked immunosorbent assay
ER	endoplasmic reticulum
FACS	fluorescence activated cell sorting
FATP	fatty acid transport protein
FCS	fetal calf serum
Flt-3L	FMS-like tyrosine kinase 3 ligand
GC	gas chromatography
G-CSF	granulocyte-colony stimulating factor
GlcMM	glucose monomycolate
GM2A	GM2-activator protein

GM-CSF	granulocyte-monocyte colony stimulating factor
GPI	glycosylphosphatidyl inositol
GroMM	glycerol monomycolate
GSL-1	α -glucuronosyl-ceramide
GSL-1'	α -galacturonosyl-ceramide
GVHD	Graft-versus-host disease
hr	hour(s)
hCD1d	human CD1d
HDL	high-density lipoprotein
HLA	human leukocyte antigen
HOHAHA	homonuclear Hartmann-Hahn
HPLC	high performance liquid chromatography
HRP	horse radish peroxidase
HS	human serum
hTAP	human tocopherol associated protein
<i>i.e.</i>	id est
IEF	isoelectric focusing
IFN γ	interferon gamma
Ig	immunoglobulin
iGb3	isoglobotrihexosylceramide
Ii	invariant chain
IL-4	interleukin-4
IL-12	interleukin-12
IL-18	interleukin-18
iNKT	invariant natural killer T
kDa	kilo Dalton
LAM	lipoarabinomannan
LBP	Lipid binding protein
LC	Langerhans cell
LDL	low-density lipoprotein
LM	lipomannan
LRP	LDL-R-like protein

LTP	lipid transfer protein
mAb	monoclonal antibody
MAIT	mucosal invariant T cells
MALDI- <i>Tof</i> -MS	matrix-assisted laser desorption/ionization- <i>time-of-flight</i> -mass spectrometry
MAPK	mitogen-associated protein kinase
mCD1d	mouse CD1d
MDR-TB	multidrug-resistant tuberculosis
MHC	major histocompatibility complex
MPDs	mannosyl phosphodolichols
MPIs	mannosyl phosphoisoprenoids
MPMs	mannosyl β -1-phosphomycoketides
MS	multiple sclerosis
MTP	microsomal triglyceride transfer protein
MVB	multivesicular bodies
MyD88	myeloid differentiation factor 88
NK	natural killer
NMR	nuclear magnetic resonance
PAT	penta-acylated trehalose
PBMC	peripheral blood mononuclear cells
PBS	phosphate buffered saline solution
PC	phosphatidylcholine
PE	phosphatidylethanolamine
PI	phosphatidylinositol
PI3P	phosphatidylinositol 3-phosphate
PPD	purified protein derivative
ppm	parts per million
PRR	pattern recognition receptor
PS	phosphatidylserine
PIMs	phosphatidylinositol mannosides
SAP	saposin
SCP-2	Sterol carrier protein-2

SGLs	sulfolglycolipids
shCD1b	soluble human CD1b
TAP	transporter associated with antigen processing
TAT	tri-acylated trehalose
TB	tuberculosis
TCR	T cell receptor
TDM	trehalose-dimycolate
TGF	tumor growth factor
Th	T helper
TLR	toll-like receptor
TMM	trehalose-monomycolate
TNF	tumor necrosis factor
VLDL	very-low-density lipoprotein
vs.	versus
WT	wild-type
XDR-TB	extensively resistant tuberculosis

ABSTRACT

Most vaccines used nowadays are created using inactivated or attenuated compounds from micro-organisms. Advances in basic immunology and molecular biology opened the gate for consequent improvement of vaccination strategies. The vast majority of successful vaccines developed so far functions through production of specific antibodies, thus allowing rapid eradication of the disease's causative agent. However, intracellular bacterial pathogens like *Mycobacterium tuberculosis* hide from immune attack by antibodies within cells, and their virulence is related to their capacity to survive for prolonged times within macrophage phagosomes by blocking lysosomal delivery and subsequent degradation. Therefore, design of more effective vaccination strategies is needed to ensure efficient killing of this type of pathogens. The discovery of CD1 molecules, that present lipidic antigens from the bacterial cell wall to T cells, might be an additional step in this direction. In this dissertation, we used chemical and biochemical approaches to identify and synthesize lipid antigens, as well as T cell activation assays, molecular biology tools, and transgenic mice to evaluate the potential of lipid antigens to be included in subunit vaccines.

In a first series of studies, we identified glycerol monomycolate (GroMM) as a mycobacterial lipid antigen that activates CD1b-restricted T cells, and confirmed its immunogenicity during the course of infection by *M. tuberculosis*. GroMM efficiently stimulates T cells from PPD-positive healthy donors, but not from non-infected donors nor patients with active tuberculosis. These data suggest that GroMM-reactive T cells are primed during infection and may contribute to protection against pathogenic mycobacteria, rendering GroMM an interesting candidate for further evaluation to be used in vaccination strategies.

A second series of studies dealt with a lipid antigen from *M. tuberculosis* previously identified in our laboratory, *i.e.* diacylated sulfoglycolipids (Ac₂SGL). Sulfoglycolipid (SGL) analogs were synthesized in order to study the structural constraints governing binding to CD1b and generation of immunogenic CD1b-SGL complexes. Comparison of these analogs sharing the same trehalose-sulfate polar head but differing in the structure of their acyl tails showed that the number of C-methyl substituents, the configuration of the chiral centers, and the respective localization of the two different acyl chains on the polar head are important

structural elements that must be considered for the design of sulfoglycolipid analogs with potential use as vaccine subunits.

In a third series of experiments, we began pre-clinical *in vivo* studies in CD1b-transgenic mice that we have generated, using the most immunogenic synthetic SGL analog. CD1b:SGL dimers allowed us to follow successful priming and expansion of CD1b-restricted SGL-reactive T cells after immunization. Finally, we have investigated different ways to increase immunogenicity by facilitating lipid solubilisation and transport into antigen presenting cells (APCs).

Altogether, the data obtained and discussed in the present dissertation go through the first stages of a vaccine's development, from identification of candidate antigens to pre-clinical *in vivo* studies in mice. Confirmation of the protective effect of the lipid antigens described herein will determine whether they can be considered as candidate compounds of a subunit vaccine.

INTRODUCTION

Genetic history of CD1 and MHC molecules

The MHC locus is present in the genomes of all mammals and is spanning over 3,600 kb of chromosome 6 in humans with 128 functional genes and 96 pseudogenes [1, 2]. Many of these genes are directly involved in various aspects of the adaptive immune system, but there are others involved in innate immunity and some that have functions completely unrelated to the immune system [3]. The MHC locus is itself part of linear array genes on chromosome 6 in humans that is at least partially duplicated on three other chromosomes in most jawed vertebrates [3-5]. These four paralogous regions located on chromosomes 1, 6, 9, and 19 in humans are collectively referred to as the MHC paralogy group.

To fully appreciate the evolutionary history of the MHC, we must return to the sea. The sea lancelet, or amphioxus, is a cephalochordate that is thought to represent a critical transitional form that eventually led to the emergence of true vertebrates [6]. Amphioxus possess a locus of genes referred to as the proto-MHC. These proto-MHC genes are quadruplicated on four different chromosomes in jawed vertebrates, thus forming the core gene set of the MHC paralogy group. The homologs of the proto-MHC genes are found within the present-day mammalian MHC locus, and it is this cluster of genes that is thought to be the primordial genomic scaffold on which MHC I, MHC II, and other members of the MHC-based adaptive immune system later evolved. It is estimated that a duplication of the proto-MHC occurred approximately 600 million years ago in an early jawless vertebrate ancestor after splitting of from the cephalochordate lineage [4, 7, 8]. A second duplication is thought to have occurred in an early jawed vertebrate ancestor after splitting off from the jawless vertebrate lineage [9, 10]. This ancestral species subsequently gave rise to all jawed vertebrates, carrying with it the four paralogous copies of the proto-MHC found today, one of which forms the core of the actual MHC locus. Whether two rounds of genome duplication took place, or a single round plus extensive localized segmental duplications, is still a matter of debate.

However, the precise genetic progenitor of MHC I and MHC II antigen presentation molecules remains a mystery. Several theories have been proposed to explain how these genes may have initially evolved [11].

The CD1 human locus was discovered in 1979 [12], whereas the antigen-presenting function of CD1 molecules has been highlighted in the early 90's [13]. The hypothesis that CD1 and MHC I antigen presentation molecules share a common ancestry is strongly supported by sequence alignments and structural data. But the precise age of CD1 relative to MHC I has remained unresolved. Bearing in mind that the collection of genomic sequence data from lower vertebrates is still ongoing, the data examined so far suggests that CD1 may be more recent than MHC I. Evidence of CD1 homologs in both birds and mammals implies that a primordial CD1 gene was present in the common ancestor of both groups. The separation of birds and mammals from a common reptilian ancestor into two distinct lineages is one of the major milestones in vertebrate evolution: the Synapsid-Diapsid (S-D) split. Mammals emerged from the Synapsid lineage while birds derive from the Diapsid [14]. Fossil evidence led to the conclusion that the divergence between Synapsid and Diapsid lineages occurred approximately 310 million years ago [14, 15]. Thus, the age of CD1 gene family can be pushed back to before the existence of true mammals. Molecular clock analysis calculations evaluated the separation of MHC I and CD1 at approximately 384 million years ago [16]. This timing corresponds closely with the appearance of the first tetrapods in the Devonian fossil record roughly 365-385 million years ago [17]. These data suggest that the emergence of CD1 in the vertebrate genome occurred in the reptiliform lineage after the amphibian-reptile split, close to the water-to-land transition.

The clear homology between MHC I and CD1 using both the amino acid sequence alignment and crystal structure data suggests that CD1 arose by gene duplication of a primordial MHC I. The human CD1 locus is located on chromosome 1 and is therefore unlinked to the MHC locus on chromosome 6 [18]. The CD1 gene(s) likely translocated from a primordial MHC locus in an early mammalian ancestor after the bird-mammal split 310 million years ago. Selective pressure has been proposed as an explanation [19].

The human CD1 gene family is composed of five nonpolymorphic genes (CD1A, -B, -C, -D, and -E). It seems that the CD1 family of genes arose in an early mammalian ancestor, prior to the initial diversification of mammals around 125 million years ago in the Cretaceous period [20-22].

The MHC I requires a complex network of accessory molecules for effective presentation of peptides [23]. It seems that at least a subset of CD1 lipid antigens do not require internalization or processing to bind CD1 for subsequent recognition by T cells. These short-

chain lipid and glycolipid antigens can be loaded directly onto fixed APC for recognition by T cells [24-28]. Therefore, an early CD1 isoform would not necessarily require specialized molecules for antigen acquisition, internalization, processing, loading, or even the need for deep intracellular trafficking [25]. The initial evolutionary divergence of CD1 would therefore not be constrained by the need for specialized accessory proteins. However, lipid binding proteins and transport molecules, like saposins and ApoE [29, 30], that are not strictly CD1-specific but also have alternative physiological roles, may, to a certain extent, be considered as accessory molecules. Thus, it is also possible that the existence of any or all CD1 accessory molecules preceded the emergence of CD1. The transition from a single CD1 gene to an extended gene family probably occurred by duplication and neofunctionalization in a manner similar to other multigene families, including MHC I itself. Each of the CD1 isoforms has evolved a slightly different intracellular pattern of traffic and it has been postulated that this allows the CD1 proteins to broadly survey the intracellular environment of an APC for potential lipid antigens [26, 31, 32].

Structure of CD1 proteins

Although CD1 molecules are found in all mammalian species studied to date, the following data will focus only on human and mouse CD1 for which crystal structures are publicly available. The human CD1 antigen-presenting molecules were originally classified in group 1 (CD1a, CD1b, and CD1c) or group 2 (CD1d), while only CD1d is expressed in mice [20]. CD1e does not present lipids to T cells because it is not detectable on the cell surface, but it participates in intracellular lipid processing and subsequent loading onto other CD1 family members within endosomes. This is why CD1e is considered as a third group of CD1 molecules [33, 34]. CD1 are expressed as glycosylated proteins and are structurally similar to their peptide-presenting, MHC class I analogs. CD1 molecules form a stable, noncovalently associated heterodimer with beta 2-microglobulin (β_2m) of approximately 49 kDa, including N-linked carbohydrates. Like MHC class I, the ectodomain, or CD1 heavy chain, is organized into three domains, α_1 , α_2 and α_3 , and is anchored in the cell membrane by a transmembrane domain. The α_1 and α_2 domains combine to form the central binding groove of each CD1 isotype and differ from one another in primary amino acid sequence and three-dimensional structure, whereas the α_3 -domain is highly conserved among all isotypes and associates with β_2m . A tyrosine-based sorting motif, composed of tyrosine, two spacer amino acids, plus a hydrophobic amino acid (YXXZ), is encoded on the short cytoplasmic tail of CD1b, CD1c and CD1d to which adaptor proteins bind, but is absent in human CD1a [35]. This motif is directly responsible for the difference of sorting between the CD1 isoforms, CD1b-d recycling into late endosomal compartments [26, 27, 35, 36], whereas CD1a recycles into early endosomes [37].

The CD1 binding grooves are composed of two main pockets, named A' and F', and are found in CD1a, CD1b and CD1d [38]. CD1b has an additional C' pocket and T' tunnel [39]. The central binding groove is formed by two anti-parallel α -helices (α_1 and α_2), which sit on top of a six-stranded β -sheet platform. The groove is deeper and narrower than the cleft observed for binding peptides in classical MHC class I or II [40]. The overall three-dimensional structures of individual members of the CD1 family are similar to one another, but amino acid substitutions in the α_1 - α_2 superdomain are responsible for shaping the individual grooves and for the formation of isotype-specific pockets. The pockets and tunnels

are hydrophobic and accommodate the lipid backbone of all CD1 antigens. The carbohydrate or peptide headgroups are exposed at the cell surface and serve as the major T cell epitopes.

CD1a

CD1a has the smallest of the binding groove with a volume of $\sim 1,350 \text{ \AA}^3$, which allows about 36 carbon atoms to fit into [41]. CD1a has an unusual A' and F' pocket structure compared to the other isoforms (**Figure 1**). The A' pocket is not directly connected to the CD1 surface and is only accessible through the more exposed F' pocket. The CD1a groove can be described as a long tube that terminates at the end of the A' pocket and has its only entrance through the F' pocket. This means that the length of any alkyl chain that can be inserted into the A' pocket is restricted by this unique, blunt-ended pocket and is predicted to correspond to approximately C_{16} .

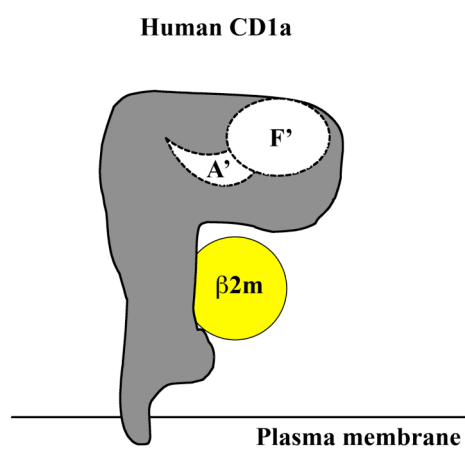


Figure 1: Two-dimensional schematic rendering of CD1a groove and its constituent A' and F' pockets, drawn based on the silhouette of the crystal structure of human CD1a. Interdomain contacts between the α_1 -helix and α_2 -helix close the top of the A' pocket, so that ligands enter the groove through the F' portal. In yellow is the $\beta 2m$.

CD1b

Human CD1b has the largest binding groove ($\sim 2,200 \text{ \AA}^3$) among the CD1 proteins described to date. Thus, CD1b can bind the largest of the CD1 antigens, including long chain fatty acids up to approximately C_{80} . The binding groove is composed of four interconnected pockets (A', C', F', and T') [39] (**Figure 2**). CD1b has a C' pocket that originates near the junction of the A' and F' pockets, descends into the groove and connects directly to the outer surface of CD1b via a structure known as the C' portal, which is located distal to the TCR interaction surface. This second connection between the interior of the groove and the outer surface of CD1 might allow egress of alkyl chains that exceed the capacity of the C' pocket, which corresponds approximately to C_{16} .

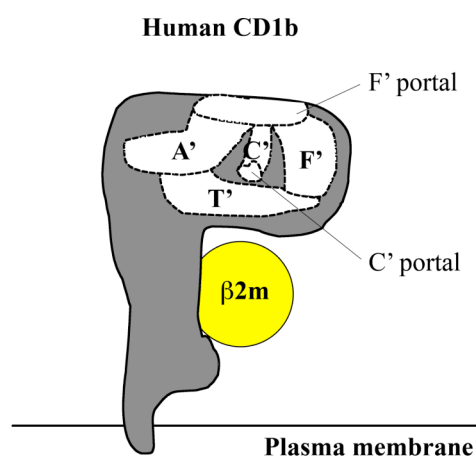


Figure 2: Two-dimensional schematic rendering of CD1b groove and its constituent A', C', F' and T' pockets, drawn based on the silhouette of the crystal structure of human CD1b. Interdomain contacts between the α_1 -helix and α_2 -helix close the top of the A' pocket, so that ligands enter the groove through the F' portal. Human CD1b has a second entrance and/or exit at the bottom of the C' pocket, known as the C' portal. In yellow is the $\beta 2m$.

CD1c

No crystal structure of CD1c is available yet. Information about its structure is inferred from amino acid sequence similarities with other CD1 proteins and the chemical structures of the antigens it presents. It seems that the individual pockets of the CD1c binding groove are unlikely to be as narrow as the A' pocket of CD1a, but instead will have a slightly greater diameter or multiple side pockets to accommodate the methyl groups from the antigens alkyl chains [40]. Sequence alignments with other CD1 isotypes suggest that CD1c is likely to have an open-ended A' pocket, like CD1b. The presence of an alternate exit portal, like the C' portal of CD1b, is also a possibility. However, no T' tunnel is predicted for CD1c, and it may also lack a C' pocket.

CD1d

The first crystal structure of mouse CD1d was obtained in 1997 and described only the two A' and F' pockets [38] (**Figure 3**). The binding groove of mouse CD1d has an approximate volume of $\sim 1,650 \text{ \AA}^3$ [40]. Empty binding grooves have not been observed for mouse CD1d that comes from natively folded protein, so it seems plausible that a pocket-stabilizing factor is bound until it is replaced with another antigen during its trafficking through various intracellular compartments. More recent structures of human and mouse CD1d revealed a complex hydrogen-bonding network responsible for the orientation and the high affinity binding of lipid antigens inside the groove [42-47].

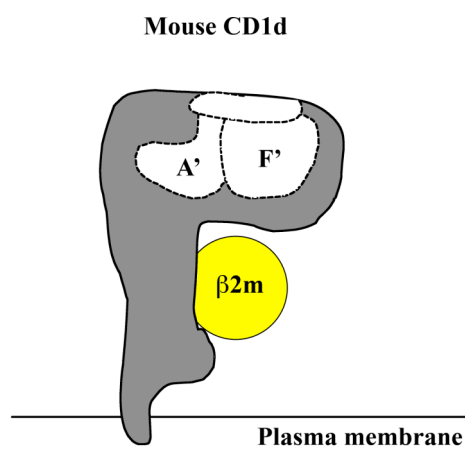


Figure 3: Two-dimensional schematic rendering of mCD1d groove and its constituent A' and F' pockets, drawn based on the silhouette of the crystal structure of mouse CD1d. Interdomain contacts between the α_1 -helix and α_2 -helix close the top of the A' pocket, so that ligands enter the groove through the F' portal. In yellow is the $\beta 2m$.

CD1e

No crystal structure of CD1e is available yet. Like other CD1 molecules, CD1e is noncovalently associated with $\beta 2m$. However, its α -chain is cleaved between the α_3 and the transmembrane domain in late endosomal compartments, generating by this way soluble CD1e, which represents the CD1e active form [33, 34]. A recent model suggests that CD1e binds glycolipids in a central cavity, similar to the binding of other CD1 members [34].

Structures of ternary CD1-lipid-TCR complexes

The CD1-lipid complexes interact with TCR $\alpha\beta$, but crystal structures of ternary CD1-lipid-TCR complexes are not available yet for group 1 CD1 molecules. Models of CD1a-lipopeptide-TCR and CD1b-mycolic acid-TCR exist, and suggest that the TCR adopts a diagonal positioning similar to MHC-TCR complexes [48, 49]. The crystal structure of the ternary complex hCD1d- α GalCer-TCR (V α 24-J α 18, V β 11) has recently been solved and determined to 3.2 Å resolution (**Figure 4**) [50]. The iNKT TCR bound approximately parallel to the long axis of the CD1d-antigen-binding cleft, which is distinct from the broad range of

“diagonal” footprints observed for MHC class I-restricted TCRs. The total buried surface area of binding between the iNKT TCR and CD1d is approximately 910 Å², below the range observed at the TCR-peptide-MHC interface [51]. The α -chain contributes more per cent of the buried surface area than the β -chain (65.5% versus 34.5%, respectively). The iNKT TCR α -chain interactions are mediated only by the complementarity-determining region (CDR3) α and CDR1 α loops. The CDR1 α loop interacts solely with the α GalCer, whereas the CDR3 α loop straddles the antigen-binding cleft, interacting with the α 1-helix, the α 2-helix and α GalCer. α GalCer protrudes minimally from the CD1d cleft with only the glycosyl head exposed for recognition by the iNKT TCR, interacting solely with the CDR1 α and CDR3 α loops. The plasticity of the iNKT TCR regarding other ligands is attributed to the CDR3 β loop, that contributes only 6% of the buried surface area. The CDR2 β loop contributes 27.5% of the buried surface area, contacts CD1d, and seems to have an important role, although yet undefined, in enabling a CD1d-restricted response.

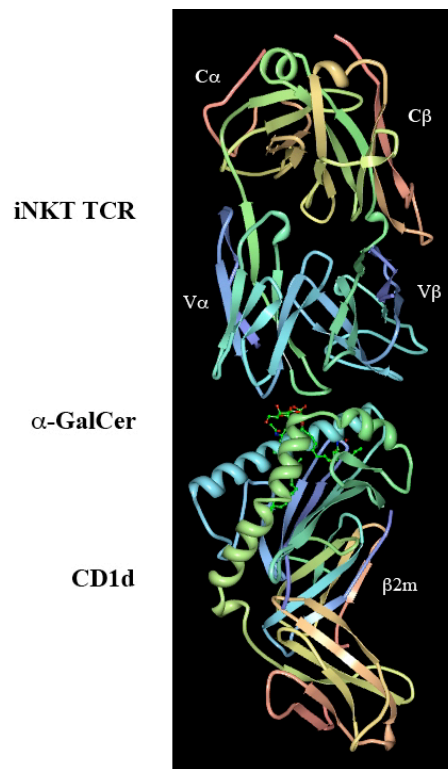


Figure 4: Overview of the human CD1d- α GalCer-iNKT TCR ternary complex. hCD1d heterodimer is on the bottom; α GalCer is in the middle; iNKT TCR α -chain and β -chain are on the top. The $\beta 2m$ is behind the CD1d molecule.

CD1 expression patterns

Group 1 CD1 molecules are almost exclusively found on professional antigen presenting cells (APCs) and thymocytes. They are expressed on double positive (CD4⁺CD8⁺) cortical thymocytes and with less intensity on CD4⁺ and CD8⁺ single positive thymocytes [52].

CD1a is expressed on Langerhans cells (LCs) [53]; on peripheral dendritic cells (DCs) [54]; on DCs differentiated from CD14⁺ monocytes with interleukin-4 (IL-4) and granulocyte-monocyte colony stimulating factor (GM-CSF) when cultured with fetal calf serum (FCS) [13, 55-58]; on DCs differentiated from CD34⁺ hematopoietic progenitor cells by culture with GM-CSF and tumor necrosis factor (TNF) [59-61]; and on mature DCs [62, 63]. Recent data indicate that CD1a surface expression is stabilized by serum lipids [24].

CD1b is expressed on the very same types of DCs than CD1a (see references above), except Langerhans cells. In addition, CD1b is expressed also on dermal and lymph node interdigitating DCs [64]. CD1b expression has also been found on perivascular inflammatory cells and hypertrophic astrocytes of chronic-active MS lesions, whereas its expression in chronic-silent multiple sclerosis (MS) lesions is limited to a few perivascular astrocytic foot processes and occasional macrophages [65]. These data suggest a specific role for CD1b in the active disease.

CD1c is also expressed on the same types of DCs than CD1a (see references above) and on Langerhans cells [53]; but also on dermal and lymph node interdigitating DCs [64]; on a subpopulation of circulating peripheral B cells [54, 66]; in lymph node mantle zones and germinal centers [64, 67, 68]; and on marginal zone B cells in the spleen [67]. CD1c can be induced by B cell activation, and has been proposed as a marker for distinguishing B cell populations, in particular mantle zone B cells [69].

CD1b and CD1c expression on the surface of DCs do not change during maturation, but CD1a expression decreases slightly [62, 63]. It should also be pointed out that infection with *M. tuberculosis* upregulates CD1a, CD1b and CD1c expression in CD1⁻ myeloid precursors [70]. CD1a, CD1b and CD1c expression is also induced on dermal granulomas DCs of patients with tuberculoid form of leprosy, being associated with active cellular immunity, but not with the lepromatous form, suggesting that downregulation of CD1 molecules might constitute an immune evasion strategy [71]. CD1a and CD1c have also been reported on DCs

in the inflamed synovium of rheumatoid arthritis [72]. In human breast cancer, tumor-infiltrating CD1-positive DCs have been reported, and their presence correlated with prognosis [73, 74]. In a cutaneous T cell lymphoma named mycosis fungoides, CD1b and CD1c expression is increased [75], whereas CD1c is downregulated in B chronic lymphocytic leukemia [76]. Recently, the beta herpes virus human cytomegalovirus has been shown to inhibit transcription and to block cell surface localization of group 1 CD1 molecules [77].

Here must be pointed out that group 1 CD1 molecules are not expressed on the surface of macrophages, rendering cross-priming and subsequent presentation by DCs essential in the case of infection by intracellular pathogens like *M. tuberculosis*.

In peripheral blood, human (h) CD1d is expressed on B cells, monocytes and activated T cells [78]. Cortical thymocytes also express hCD1d, but its expression is downregulated in medullary thymocytes and absent on naïve peripheral T cells. However hCD1d is re-expressed upon activation of peripheral T cells [79, 80]. It is also present on monocyte-derived macrophages and DCs, and dermal DCs [81, 82]. In the lymph node, hCD1d is expressed on DCs in the paracortical T cell zones and on mantle zone B cells, but not on any cells of the germinal center [78, 83]. It has also been detected in epithelial cells of the small bowel and colon [84], as well as on hepatocytes, bile duct epithelium, pancreas, kidney, endometrium, testis, epididymis, conjunctiva, breast, skin, tonsils, and vascular smooth muscle cells [85]. In the skin, hCD1d is found on keratinocytes, endothelium, eccrine ducts, acrosyringium, and the piloosebaceous unit except for dermal papillae and hair matrix cells [86]. hCD1d is also expressed in anagen phase growing hair [87]; in spindle-shaped cells found under the oral epithelium in noninflamed sections of periodontal biopsies [88]; and on trophoblast cells [89].

Several isoforms of hCD1d have been described [78, 89-93], with a certain degree of tissue-specificity and differences in glycosylation. Also, regulation of hCD1d is dependent on cell type-specific factors [94]. It should also be noticed that hCD1d is more abundantly expressed on the colonic epithelium of patients with inflammatory bowel disease [85], as well as in the affected tissues of patients suffering of Crohn's disease and ulcerative colitis [95]. Several liver diseases involve alterations in hCD1d expression as well [85, 96, 97]. hCD1d is also expressed in epithelioid granuloma cells in both primary biliary cirrhosis and sarcoidosis. Primary biliary cirrhosis patients express hCD1d on epithelial cells of the small bile duct

[98], and upregulation is important on hepatocytes infected with hepatitis C virus [99]. Other diseases influenced by hCD1d upregulation include psoriasis [85, 86] and experimental autoimmune encephalomyelitis [100]. Many tumors express hCD1d, including acute myeloid leukemias, juvenile myelomonocytic leukemias, acute lymphoblastic leukemias, B cell chronic lymphocytic leukemias, gliomas and brain tumor vasculature, and cutaneous T cell lymphomas [101-105].

Mouse (m) CD1d is expressed in thymus, lymph node, liver, stomach epithelium, small intestine and colon [96]. mCD1d is present in all fetal organs but only in thymus, spleen, liver and lung of adult mice [106]. It is also expressed on T cells, B cells, macrophages and hepatocytes [107]; on bone marrow cells, DCs, and intraepithelial lymphocytes [108]. Further analysis of the mouse hematopoietic compartment identified mCD1d expression in multiple lineages, including B cells, T cells, macrophages, CD11c⁺ DCs, thymocytes, thymic stromal cells, and thymic DCs [109, 110]. High mCD1d expression is also detected on splenic marginal zone B cells [109, 111, 112]. It is also present on endometrial endothelial cells of the cervix and fallopian tubes [113]; and on collecting ducts and blood vessels of the pancreas [114].

The mouse genome contains two CD1 genes, CD1d1.1 and CD1d1.2, which are 95% identical. They are equally expressed in the thymus, but CD1d1.1 is the predominant transcript in other tissues [115]. It seems that mouse CD1 mRNA levels correlate with surface protein expression, indicating that transcriptional regulation might modulate surface concentrations of mCD1d [116]. These two mCD1d isoforms may have close functions, but CD1d1.2 seems to play little role *in vivo* [117]. Variants with different glycosylation also exist for mCD1d [106].

In contrast to the regulation of group 1 CD1 proteins, surface levels of human and mouse CD1d remain quite constant over a wide range of experimental conditions [78, 108], even if they have a tendency to be upregulated upon infection with *Leishmania infantum* and mycobacteria [118, 119]. However, CD1d surface level has been shown to be downregulated by certain viruses, primarily through increased internalization [120, 121], probably reflecting immunoevasion strategies. As for CD1b and CD1c molecules, T cell recognition can also be altered via impairment of CD1d lysosomal trafficking, preventing binding of its dedicated lipid antigens [122].

Rat CD1d has similar tissue distribution to that seen in mouse, plus expression in heart, kidney and lung [123]; and on intestinal villi of enterocytes [124].

Thus, the wide tissue distribution of CD1d and its location on many parenchymal and endothelial cells differs markedly from the group 1 CD1 proteins. Expression of group 1 and group 2 CD1 molecules has also been demonstrated in CD68⁺ lipid-laden foam cells in atherosclerotic lesions, but not in normal arterial specimens [125]. In autoimmune thyroiditis, CD1 bearing DCs and CD1c-positive B cells were detected in inflamed thyroid tissues [68].

CD1e localizes to the Golgi of immature DCs, then in the lysosomes upon maturation, where it is cleaved into a soluble form [126]. Its strict intracellular localization excludes any direct interaction with T cells, but CD1e is required for lysosomal degradation of phosphatidylinositol mannoside (PIM)₆ and subsequent activation of CD1b-restricted T cells [34]. Here must be pointed out that a naturally occurring mutation in CD1e has recently been shown to prevent its correct assembly and transport to late endosomal compartments, thus being directly responsible for an altered immune response to complex glycolipid antigens [127]. Splicing variants have also been described for CD1a, CD1c, and CD1e molecules [33, 128], but their precise characterization is still unclear.

CD1 assembly

CD1 assembly and N-glycosylation takes place in the endoplasmic reticulum (ER) (**Figure 5**). CD1 molecules utilize some of the same chaperones as do MHC class I molecules, but CD1 folding and assembly reveal subtle differences. Calnexin and calreticulin are ER chaperones that bind β 2m-free CD1d heavy chains, but not β 2m-bound (on the contrary to MHC class I molecules), and disulfide bond formation is mediated by the associated ERp57 [129]. The fully oxidized CD1d heavy chains dissociate from these chaperones, and the majority of CD1d heavy chains then bind β 2m before exiting the ER. A small fraction of CD1d heavy chains is also able to exit the ER without association with β 2m and reach the plasma membrane [91, 130].

The exit of MHC class I molecules from the ER requires occupation of their peptide-binding groove with proteasome-derived peptides that are translocated into the ER by the transporter associated with antigen processing (TAP) [131, 132]. Similarly, the peptide-binding groove of MHC class II molecules is occupied through its association with invariant chain, which

also serves to target the multimeric complex to the endocytic system [131]. In the case of CD1 molecules, they acquire self lipid ligands in the ER, which influences their surface expression and antigen presentation function. Nascent CD1d associates with phosphatidylcholine (PC) [45], maybe also with spacer molecules [43], as do CD1b [133]. Phosphatidylinositol-containing compounds including glycosylphosphatidyl inositol (GPI) were eluted from CD1d molecules expressed in TAP-deficient cells [134], and PI was detected in association with a soluble form of CD1d containing the KDEL ER retention signal [135]. GPI and PI abundant expression in the ER suggest that assembly of CD1d with cellular phospholipids occurs in this compartment [136]. Microsomal triglyceride transfer protein (MTP) is an ER-resident lipid transfer protein (LTP) that has been proposed to be critical for proper assembly and antigen presentation function of CD1d, probably via transfer of lipids onto CD1d [137-139]. Recently, MTP has also been shown to be involved in the functioning of group 1 CD1 molecules, by regulating both endogenous and endosomally-loaded exogenous lipid antigen presentation [140].

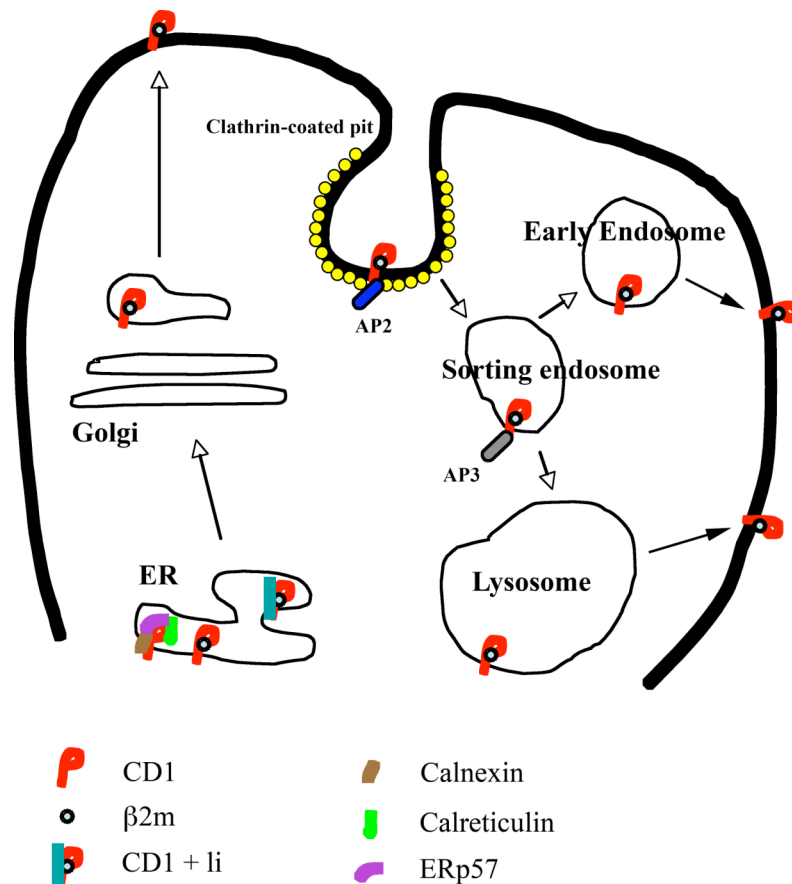


Figure 5: Assembly and intracellular trafficking of CD1 molecules. Assembly of CD1 molecules takes place in the ER with the help of chaperones named calnexin, calreticulin, and ERp57. CD1 associate noncovalently with β 2m, then traffic to the Golgi and the plasma membrane. A fraction of CD1 molecules associates with the invariant chain (Ii) which promotes trafficking to late endosomal compartments. Surfaces CD1b-d molecules are internalized in clathrin-coated pits, associate with AP-2, and move to sorting endosomes. There, they move to late endosomes/lysosomes upon AP-3 binding. CD1a recycles only in early endosomes.

CD1 trafficking

After assembly in the ER, the majority of CD1 molecules follow a secretory route via the Golgi where N-glycosylation is achieved and traffic directly to the plasma membrane [141]. Once on the plasma membrane, the CD1 molecules can be internalized and enter the endocytic pathway (**Figure 5**). It seems that the cytoplasmic tails of CD1 play a primary role in their trafficking to intracellular compartments [36, 141-143]. The cytoplasmic tails of

CD1b, CD1c, hCD1d and mCD1d contain a tyrosine-based sorting motif that bind the adaptor protein complex-2 (AP-2) at the plasma membrane, which allows sorting of CD1 and other transmembrane cargo proteins into clathrin-coated pits [142, 144]. CD1b internalization is also mediated by dynamin [141], which is thought to be involved in membrane fission. CD1a does not contain any apparent sorting motifs in its cytoplasmic tail, but was found in clathrin-coated pits and clathrin-coated vesicles in *in vitro*-derived DCs and freshly isolated LCs, a type of DCs resident in the epidermis [27, 37]. CD1a can also be internalized in a clathrin- and dynamin-independent manner, and it follows a Rab22a- and ARF6-dependent recycling pathway in HeLa cells, similarly to other cargo internalized independently of clathrin [145]. Ii has recently been found in association with CD1a at the cell surface of immature DCs and proposed to be a key regulator of its surface expression, as Ii silencing induces CD1a accumulation at the cell surface [146].

After internalization, both CD1a and CD1c molecules have been shown to traffic to early recycling endosomes and co-localize with early recycling compartment markers [27, 37, 144], where CD1b is almost absent [27].

CD1b and mCD1d molecules recycle in late endosomal/lysosomal compartments. In the case of CD1b, a role for the adaptor protein complex-3 (AP-3) in its recycling has been proposed [147]. CD1c is also present in the lysosomes [63], but does not bind to AP-3 [147], suggesting that an AP-3 independent pathway for CD1 trafficking to lysosomal compartments also exists [144]. mCD1d trafficking to lysosomes has been proposed to be mediated by AP-3 [143, 148, 149], but also by association with the MHC class II-Ii complex [129].

CD1e trafficking is different from other CD1 molecules, as it is not present on the plasma membrane, and maturation of DCs modify its localization [126]. In immature DCs, membrane-bound CD1e stays in the Golgi, and traffics to late endosomal compartments upon maturation where it is cleaved and becomes soluble [33, 34]. The cytoplasmic domain of CD1e consists of 53 to 61 amino acids, and does not contain any specific targeting motif, but is essential to intracellular retention and Golgi accumulation of CD1e [150]. Its traffic to LE/lysosomes seems to be facilitated by ubiquitination of the cytoplasmic domain, a phenomenon increased upon DCs maturation [150].

Structure, biology and functions of Lipid Antigens

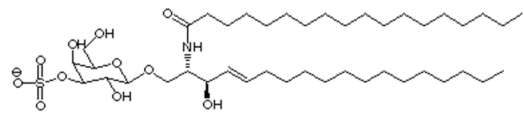
To discuss lipid antigens, a first distinction between T cells has to be made. Indeed, antigens presented by CD1d molecules are recognized by T cells that express a semi-invariant TCR ($V\alpha 24$ - $J\alpha 18$ and variable $V\beta 11$ chains in humans, $V\alpha 14$ - $J\alpha 18$ and $V\beta 8.2$, $V\beta 7$ or $V\beta 2$ chains in mice). This type of T cells also expresses markers characteristic of natural killer cells, and is therefore named invariant (i) NKT cells. Antigens presented by group 1 CD1 molecules (and in some cases also CD1d) are recognized by T cells expressing a variety of TCR heterodimers, apparently without bias for unique V or J genes. Human CD1-restricted T cells may express CD4, CD8, or are CD4 and CD8 double-negative. Initial studies have shown that lipid-specific T cells can easily be detected in the circulating blood [151, 152], even at frequencies close to classical MHC-restricted and peptide-specific T cells [153].

Self Lipid Antigens

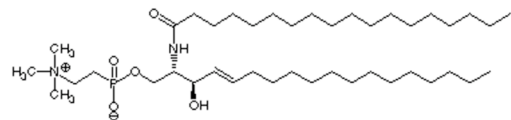
Self lipids that stimulate T cells can be subdivided into three prominent groups, *i.e.* sphingolipids, gangliosides and phospholipids (**Figure 6**).

SPHINGOLIPIDS

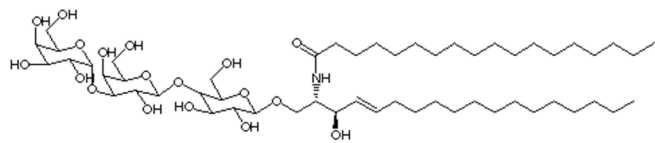
sulfatide



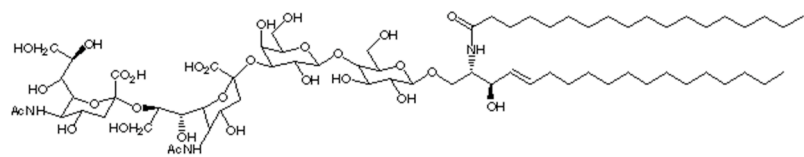
sphingomyelin



iGb3

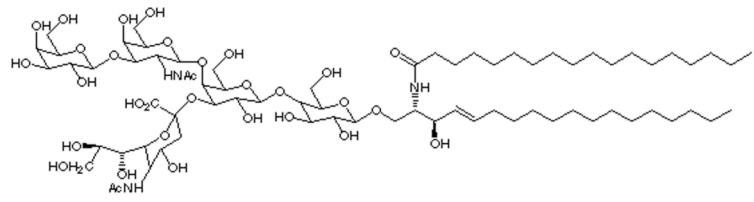


GD3

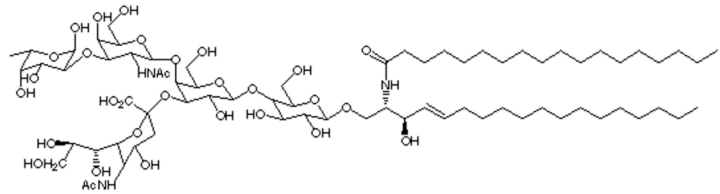


GANGLIOSIDES

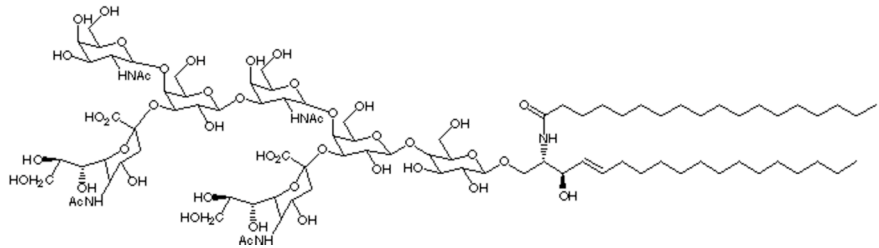
GM1



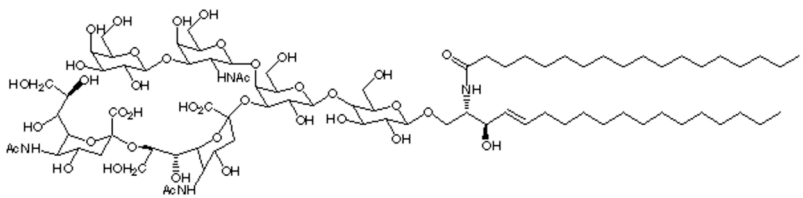
Fucosyl-GM1



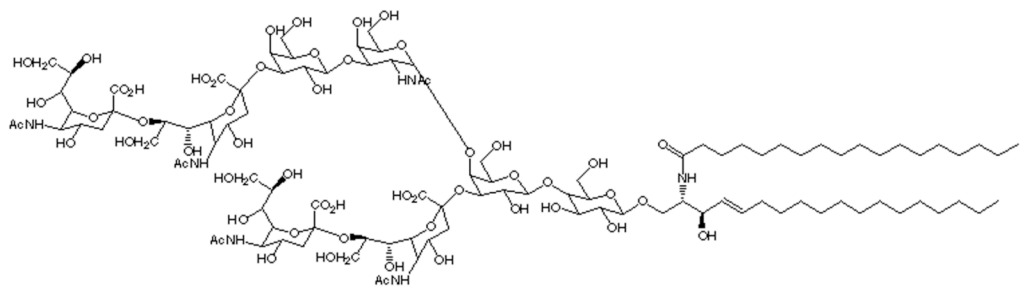
GalNac GD1a



GD1b



GQ1b



PHOSPHOLIPIDS

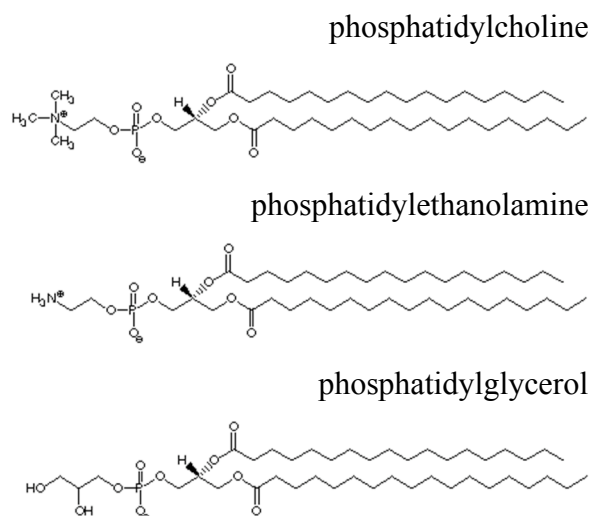


Figure 6: Structures of immunogenic self lipids presented by CD1 molecules.

The backbone of the sphingolipids is made of the basic alcohol sphingosine, or a related long-chain base usually between 14 and 24 carbon atoms long. Sphingomyelin is found in all cell membranes, and is composed of a ceramide (sphingosine plus an amide linkage with a fatty acid) with additional phosphate and choline. Addition of glucose or galactose to a ceramide leads to glycosylceramides. The hydrophobic lipid moiety of glycosphingolipids is of primary importance in terms of immunogenicity [28], as the lipid tail is involved in binding onto CD1. The length of the acyl chains, as well as their degree of saturation and rigidity, also seem to play a role [28, 154-157]. The positioning of the polar part of lipid antigens is influenced by the lipid moiety. The polar head makes direct interactions with the α -helices of the CD1 molecule, thus contributing to the formation of stable CD1-lipid complexes. It also interacts directly with the TCR. At this stage, it must be pointed out that, despite the fine antigen specificity of the TCR, lipid-specific T cells also show a certain degree of cross-reactivity between different lipid antigens.

Immunogenic lipids are synthesized by enzymes at different places in the cell. For example, the enzymes responsible for ceramide synthesis are on the cytosolic membrane leaflet of the ER [158]. LTPs are implicated in the transfer of lipids between intracellular compartments. In the case of ceramide, CERT allows its transport to the trans-Golgi cisternae [159]. But ceramide can also be translocated inside the luminal membrane of the ER where it is used to

generate galactosylceramide [160]. Ceramide is the common precursor of sphingomyelin and glycosphingolipids. Sphingomyelin is mainly synthesized in the luminal part of Golgi apparatus vesicles [161], then traffics to the plasma membrane following the secretory pathway. Glycosphingolipids synthesis also occurs in the Golgi. Glucosylceramide is synthesized on the cytosolic leaflet of the Golgi apparatus [162]. Glucosylceramide is then either transported to the plasma membrane by a non-Golgi pathway and degraded [163], or translocated in the luminal leaflet of Golgi vesicles for further addition of sugars. Addition of a galactose to a glucosylceramide gives a lactosylceramide, that is the common precursor of other glycosphingolipids. GM3 and GD3 are synthesized in early Golgi compartments, whereas complex gangliosides are predominantly synthesized in the *trans* Golgi [164, 165]. Glycosphingolipids and sphingomyelin reach then the noncytosolic leaflet of membranes following the secretory pathway. Phospholipids, at last, are synthesized on the cytosolic leaflet of the ER, then move to the luminal one, where they can assemble with nascent CD1d [43, 45] and CD1b [133] molecules.

Regulation of antigenic self lipid synthesis is influenced by intrinsic properties of glycosyltransferases, such as enzymatic kinetics and localization, but also by the relative abundance and activity of such enzymes [166, 167]. On the other side, physicochemical characteristics, trafficking capacity and availability of the sugar substrates are also factors of primary importance for further synthesis. Accumulation of glycosphingolipids also might influence the regulation of glycosyltransferases at the gene level.

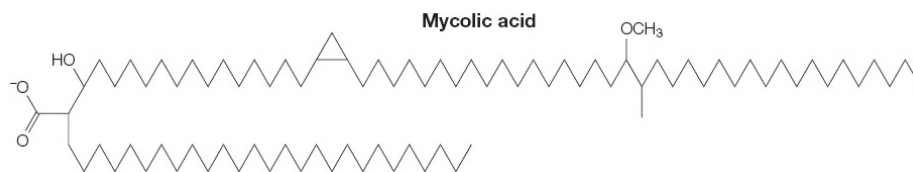
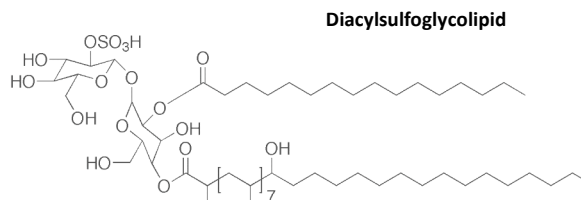
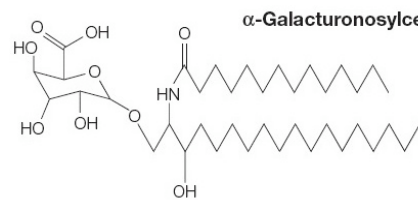
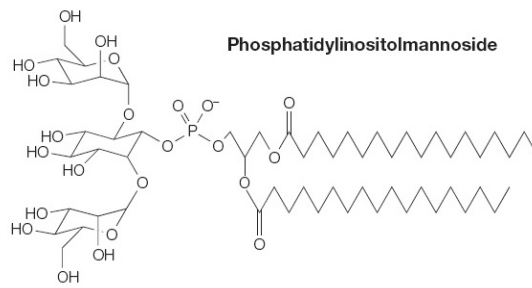
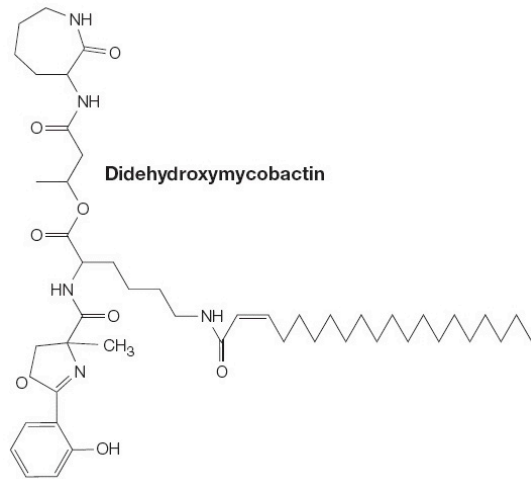
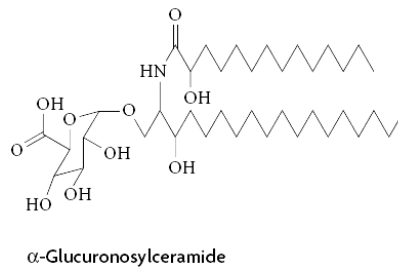
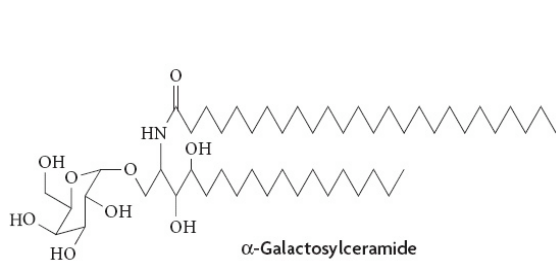
As described above, immunogenic self lipids are synthesized in the ER and Golgi. The lipids synthesized in the ER are transferred to other organelles by LTPs [168], that bind and transport lipids across aqueous phases. Specific transfer between donor and acceptor membranes is due to the presence of unique LTP protein domains. Again, biophysical characteristics inherent to each lipid can lead to preferential pathways when they are part of a vesicle. It may be the case for glycolipids with similar structures but differing in the length of their lipid tail, the ones with shorter tails recycling preferentially to early endosomes while the ones with long chains recycle to late endosomes [25]. The late endosomal compartment allows an additional sorting step into multivesicular bodies (MVB), that might help lipid loading onto CD1 molecules, as might do the presence of LTPs such as saposins (SAPs) and GM2-activator protein (GM2A) [30].

During assembly in the ER, nascent CD1d associates with PC [45], maybe also with spacer molecules [43], as do CD1b [133]. These spacers stabilize CD1d and CD1b during their traffic to the cell membrane. Recycling in low-pH endosomal compartments facilitate loading of other lipid antigens. Indeed, changes in the proton concentration influence the charged state of residues in flexible areas in the superior and lateral walls of the A' pocket of CD1b, thus regulating the conformation of the CD1 groove and controlling the size and rate of antigens captured [169]. A subpopulation of CD1d also forms complexes with the invariant chain (Ii) and class II molecules [129, 170]. CD1a, that lacks tyrosine containing cytoplasmic tail motifs, only recycles in early endosomes. Phospholipids recycling in early endosomes are then efficiently presented by CD1a [155]. On the contrary, complex glycolipids traffic to late endosomes where they are loaded onto resident CD1 molecules, namely CD1b, CD1c, and CD1d. Sulphatide, a major component of myelin, can be presented by CD1a, CD1b and CD1c molecules [171].

High numbers of T cells recognizing self lipid antigens are present in the blood of patients suffering from MS [153]. Myelin lipids seems to be highly immunogenic [172-174], and it is likely that the specific T and B cell responses are correlated with the progression of MS. It should also be noticed that bacterial infection promotes *de novo* synthesis and recognition of self lipid antigens [175].

Microbial Lipid Antigens

The first microbial lipid antigen described was mycolic acid [176]. Many others have now been identified, presented by CD1a [177], CD1b [178-180], CD1c [181], and CD1d [182-187] (**Figure 7**).



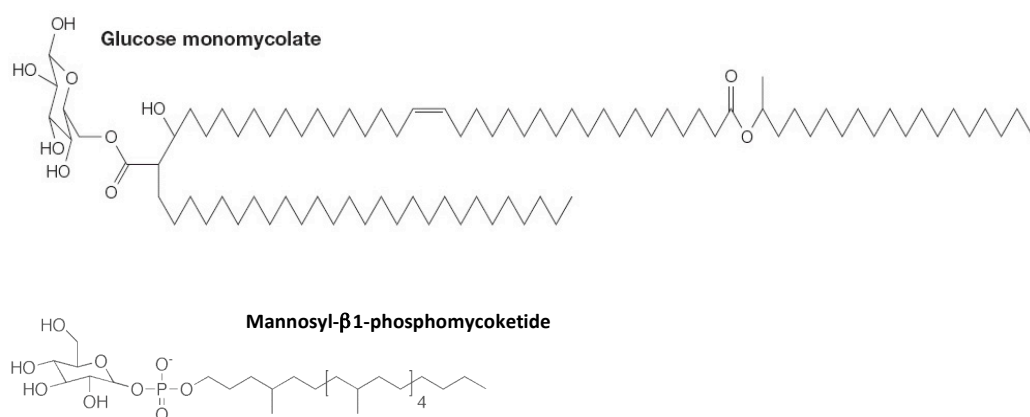


Figure 7: Non exhaustive structures of immunogenic microbial lipids presented by CD1 molecules.

Didehydroxymycobactins (DDMs) are lipopeptides composed of a complex peptidic headgroup linked to a single alkyl chain of approximately 20 carbons. They may be direct metabolic precursors of mycobactins, that are mycobacterial lipopeptides with iron-scavenging properties [177]. These siderophores, presented by CD1a molecules, are of primary interest as they might be important for mycobacterial growth and virulence according to the complex enzymatic machinery devoted to their synthesis. Thus, DDMs may represent an early warning system highlighting intracellular pathogen infection. Again, length and saturation of the alkyl chain, as well as the headgroup, play critical roles in recognition by T cells [48, 177].

CD1b-restricted foreign lipid antigens all derive from the mycobacterial cell envelope and have no close structural homologues in mammalian cells. They include lipoarabinomannan (LAM), lipomannan (LM), phosphatidylinositol mannosides (PIMs) [34, 180, 188], glucose monomycolate (GlcMM) [179], and sulfoglycolipids (SGLs) [178].

Mycolic acids are a family of characteristic α -branched, β -hydroxy fatty acids produced by *M. tuberculosis* and other species of actinomyces. They constitute about 40% of the cell wall skeleton of mycobacteria, corynebacteria and *Nocardia* [189]. Mycolic acids present in the mycobacterial cell wall can be separated into three classes (α , methoxy, keto) and are between 70 and 90 carbons large, up to 26 carbons long, with meromycolate chains about 60 carbons plus additional functional groups (methyl branches, cyclopropane rings, or double bonds). They might increase rigidity and lower permeability of the cell wall. Compounds that

inhibit their synthesis, such as isoniazid and ethionamide, are used as antituberculosis drugs, confirming their importance for *M. tuberculosis* survival [189]. It seems that naturally occurring variations in the lipid tail structure are not critical for recognition of GlcMM by LND5, a CD1b-restricted $\alpha\beta$ T cell clone [179]. Whether this can be considered a general rule is still an open question, especially because DN1, another CD1b-restricted $\alpha\beta$ T cell clone, is sensitive to structural differences in the meromycolate chain [49]. However, in both cases, the glucose headgroup seemed of primary importance for GlcMM recognition [49, 179]. It should also be noticed that mycobacteria are unable to synthesize GlcMM *de novo*, and need to acquire exogenous glucose from host's infected tissues, indicating that GlcMM generation may be restricted to pathogenic mycobacteria capable of infection [190].

Mycobacterial glycosylphosphatidylinositols are CD1b-restricted lipid antigens with a phosphatidyl inositol core [180]. One subset, named PIMs, contain varying numbers of mannose residues, are restricted to actinomycetes [189] and are major components of the outer leaflet of the mycobacterial plasma membrane. LM and LAM are multiglycosylated extensions of the PIMs. LAM is heterogenous in structure, with variations between different mycobacterial species in terms of whether and how distal arabinose moieties possess a terminal mannose unit. LAM exerts a wide range of biological activities, including diverse effects on phagocyte chemotaxis and function, DC function and T cell migration and activation [191]. LAM and PIMs also induce group 1 CD1 proteins expression in human myeloid cells via toll-like receptor (TLR)2 [70]. TLRs are instructive pattern recognition receptors (PRRs) providing APCs with signals that regulate their capacity to elicit T cell responses [192]. Both hydrophilic and carbohydrate structures are important for recognition of LM, LAM and PIMs [180].

SGLs have recently been identified as CD1b-restricted antigens recognized by *M. tuberculosis*-specific T cells [178]. They are mycobacterial cell envelope molecules that possess a trehalose 2' sulfate core acylated by two to four fatty acids. These fatty acids can be palmitic (C₁₆), stearic (C₁₈), hydroxyphthioceranoic (C₃₂), or phthioceranoic (C₃₂). They also seem to exert many biological activities, including anti-tumor activity [193]. The extent of their expression in *M. tuberculosis* correlates with strain virulence in guinea pigs models [194]. The active antigenic species have been shown to be diacylated sulfoglycolipids (Ac₂SGLs) containing hydroxyphthioceranoic and either palmitic or stearic acid chains.

Presentation of Ac₂SGLs is efficient during infection, and induces production of IFN γ by specific human T cells and subsequent killing of intracellular bacteria *in vitro* [178].

The first CD1c-restricted antigens to be defined structurally were isolated from lipids in the cell wall of both *M. avium* and *M. tuberculosis* [181], and shown to be closely related to mannosyl β -1-phosphomycoketides (MPMs). They are also referred to as mannosyl phosphoisoprenoids (MPIs), because of their structure containing a single fully saturated alkyl chain similar to isoprenoid lipids, with methyl branches at every four carbons. Their structure is close to mammalian mannosyl phosphodolichols (MPDs), with an identical mannosyl β -1 headgroup, but with lipid tails that are saturated and much shorter in the case of mycobacterial MPMs. The stimulatory MPM antigens are only present in cell wall extracts from mycobacteria and are restricted to species that can infect human cells [195]. Also in the case of MPMs, both headgroup and alkyl chain are of primary importance for recognition by T cells [181, 195, 196]. All CD1a-, b- and c restricted foreign antigens defined to date derive from mycobacteria, suggesting a role for group 1 CD1-restricted responses in immunity to these pathogens. These CD1 molecules are expressed at the site of mycobacterial infection, and their expression correlates with effective host immune response in leprosy patients [71, 197, 198]. It seems that group 1 CD1-restricted T cells preferentially secrete Th1 cytokines [199, 200], thus contributing to protective immunity to mycobacteria and rendering antigens presented by these molecules good candidates for vaccine formulations.

It should be noticed that CD1d binds α -galactosylceramide (α -GalCer), a foreign glycosphingolipid from marine sponges resembling mammalian ceramides [201]. α -GalCer is composed of a sphingosine base, an amide-like acyl chain, and an O-linked galactose sugar with an α -linkage, whereas mammalian ceramides possess a β -linkage. It is still unclear whether α -GalCer has to be considered as an antigen or an agonist, since it has not been found elsewhere than in sponges. However, mice treated with α -GalCer have increased resistance to infection by viruses, mycobacteria and trypanosomes. GPI structures linked to proteins derived from protozoan pathogens were the first lipids proposed to function as exogenous antigens for iNKT cells [202]. PIM₄ [183], as well as other phosphatidylinositol (PI)-related lipids derived from protozoan parasites [182], have also been proposed as foreign antigens restricted by CD1d. These three types of putative antigens are still a matter of debate. Recent data show that bacterial glycosphingolipids with α -anomeric linkages, such as

α -glucuronosyl-ceramide (GSL-1) and α -galacturonosyl-ceramide (GSL-1'), as well as sulfatide variants, are presented by CD1d and are capable to activate iNKT cells [184-187]. Recently, threitolceramide has also been shown to behave as an agonist, but it is unclear whether such nonglycosidic compounds are naturally synthesized [203]. Group 2 CD1-restricted T cells have been implicated in broad antimicrobial responses to bacterial, parasite, viral and fungal infections [204]. They are currently considered as linking innate and adaptive immunity.

Lipid Antigen Presentation

Lipid uptake by APCs and intracellular trafficking

Phase fluid antigens are extensively taken up by APCs via macropinocytosis. In the case of exogenous lipids, many other mechanisms might play a significant role (**Figure 8**).

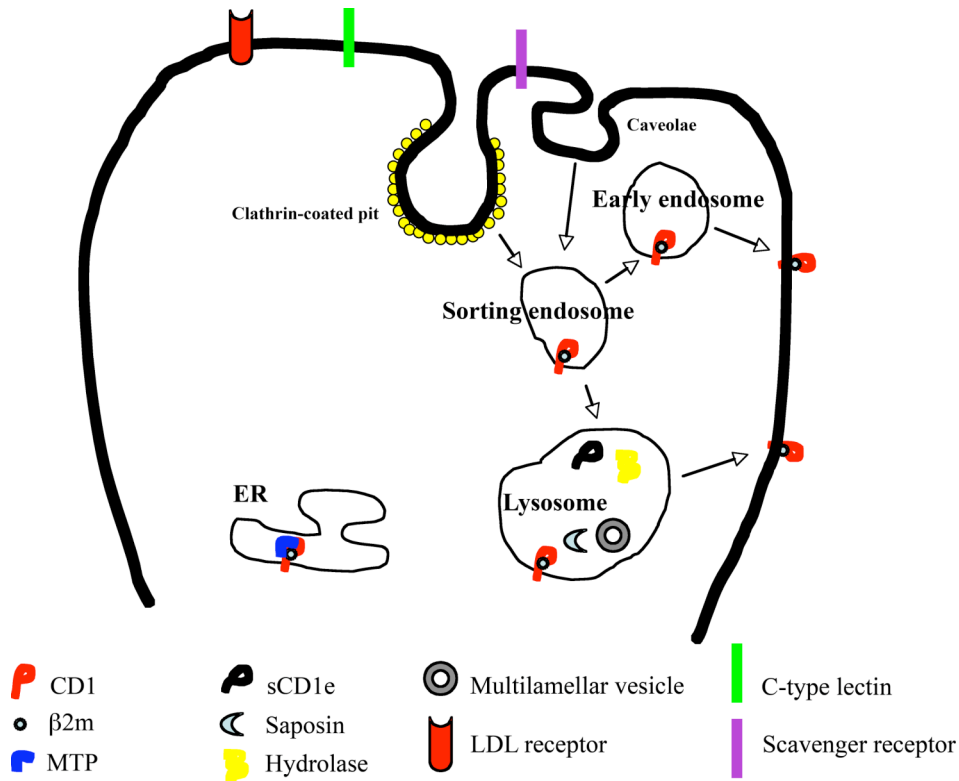


Figure 8: Internalisation and loading of lipid antigens onto CD1 molecules. In the ER, nascent CD1 are stabilized by resident lipids, and MTP is thought to facilitate this process. Exogenous lipid antigens enter the cell by phagocytosis or interaction with LDL receptors, C-type lectins, or scavenger receptors. Then, exogenous lipids traffic to late endosomal/lysosomal compartments through clathrin-coated pit vesicles. Plasma membrane-resident lipids are internalized through clathrin-coated vesicles as well, but also through caveolae, and their distribution to sorting endosomes is probably controlled by their intrinsic physico-chemical properties. In the lysosomes, complex glycolipids are processed by enzymes, with the participation of LTPs and CD1e.

The majority of circulating lipids are transported as soluble complexes bound to lipoproteins [205]. These lipoproteins organize lipids into particles of variable density called very-low-density lipoprotein (VLDL), low-density lipoprotein (LDL) and high-density lipoprotein (HDL). The core of these particles is largely composed of triglycerides and cholesteryl esters, sphingolipids, and fat-soluble vitamins. Apolipoprotein E (ApoE) has recently been proposed as a carrier, present in the serum, that binds exogenous lipid antigens and increases their uptake by DCs via lipoprotein receptors, as well as their subsequent presentation by CD1 molecules [29]. Scavenger receptors, like CD36 and SR-B1, as well as LDL-R-like protein

(LRP), may also participate in lipid uptake through binding of ApoE or lipidic ligands [206-208]. Even if LRP and scavenger receptors have not yet been implicated in CD1-based antigen uptake, they look like attractive candidates. Thus, lipoprotein receptors and scavenger receptors are cell surface receptors that have the capacity to bind lipid particles.

Other cell-surface receptors bind glycans instead of particles. It is the case of C-type lectins, like the macrophage mannose receptor (MMR) or langerin, that allow distribution of lipids into the endocytic compartments, hence participating in CD1 antigen presentation [27, 209, 210].

The uptake of lipids into the endocytic system may also occur based on their incorporation into the plasma membrane that is then taken up as part of general endocytic processes [211], thus being receptor-independent. Phagocytosis, macropinocytosis, micropinocytosis that is clathrin-mediated or -independent, all result in the uptake of the plasma membrane that may have incorporated lipid antigens. The so-called rafts (cholesterol- and sphingolipid-rich plasma membrane microdomains) may differentially incorporate lipid antigens based on their resident lipid composition [212]. Both rafts and caveolae (caveolin-containing subdomains of glycolipid rafts) are internalized [213], and might deliver lipid antigens to CD1-loading endosomal compartments. CD1a is enriched in detergent-resistant membrane microdomains that are essential for efficient CD1a-mediated antigen presentation [145]. Disruption of these lipid rafts inhibits CD1a-restricted presentation [146]. ABC transporters are pumps also involved in lipid trafficking across the bilayer [214], and fatty acid transport proteins (FATPs) have been found to mediate uptake of long chain fatty acids as well [215, 216].

Finally, uptake of apoptotic bodies from cells infected with microbes by APCs may also lead to lipid antigen presentation via the CD1 molecules of the APCs [217].

Cellular membranes show regulated changes in their density within a single membrane, and individual organelles differ in their membrane lipid composition. Because lipids do not display recognized targeting motifs, it is thought that their distribution is controlled by their chemical and physical properties [218, 219]. Glycerophospholipids and sphingolipids are major constituents of cellular membranes, and many of the CD1 ligands fall into one of these two lipid groups, raising the possibility that membrane microdomains may potentially contribute to sorting lipid antigens [213]. It has also been shown that lipid analogs that differ only in the length and saturation of their tails are sorted distinctly [220]. Similarly, it seems that GlcMM with long alkyl chains is preferentially sorted to late endosomal compartments,

whereas it is not the case for GlcMM with shorter ones [25]. Early recycling compartments are rich in cholesterol and sphingolipids, whereas late endosomal/lysosomal ones are enriched in neutral lipids such as triglycerides and cholesterol esters [218]. It seems that the differential trafficking of both lipids and CD1 molecules enables a broad intracellular survey of the cell. In the context of mycobacterial infection, antigen delivery in the right compartment is a critical point, as prevention of lysosomal delivery is a strategy developed by pathogens to escape innate immunity [221, 222]. For information, a leukocyte-specific protein named coronin 1 has recently been shown to act as a primary player in phagosomal-lysosomal fusion blockade, ensuring survival of mycobacteria inside macrophages [223].

Antigen processing and loading onto CD1

Lipid loading onto CD1 molecules can take place in both extra- and intracellular compartments, from the cell surface to the lysosomes, including the ER and early recycling compartments (**Figure 8**). Loading of α GalCer onto CD1d happens either on the plasma membrane or in lysosomes [224]. Late endosomes/lysosomes provide an ideal environment for antigen processing and loading, *i.e.* processing enzymes and acidic conditions. For example, mycobacterial PIM₆ is processed to PIM₂ by lysosomal α -mannosidase with the help of CD1e [34]. LTPs have recently been proposed for lipid extraction from membrane bilayers and transfer onto CD1 molecules. It is the case for SAPs and GM2A [30, 225, 226]. SAPs A, B, C and D are enzymatically inactive glycoproteins generated by endosomal proteolytic cleavage of the precursor prosaposin, while GM2A is encoded on a separate gene. SAPs localize to late endosomes/lysosomes and assist glycosphingolipid degradation [227]. The SAPs share lipid-binding and membrane-perturbing properties, but differ in their binding specificity and mode of action. SAP C interacts directly with, and activates, the enzyme glucosylceramide- β -glucosidase for glucosylceramide degradation [228-230]. SAP B interacts with a variety of sphingolipids and facilitates their digestion by specific lysosomal enzymes [231-236]. All the four saposins are capable of transferring phosphatidylserine (PS); and SAP A, B and C transfer sulfatide to CD1d [30]. In addition, SAP-dependent antigen processing and loading pathways have also been noted for human CD1b-presented glycolipid antigens of microbial origin [226]. GM2A associates with β -hexosaminidase A and assists GM2 degradation. GM2A can bind GM2, but also GT1b bound to CD1d and remove it from

the CD1d antigen-binding groove [30]. However, it has recently been shown that lysosomal accumulation of lipids impairs lipid antigen presentation, and therefore should be considered in the interpretation of immunological deficiencies observed in the presence of lipid metabolic disorders [237].

Persistence of CD1-lipid antigen complexes

Prolonged exposition of CD1-lipid antigen complexes on the surface of APCs facilitates interaction with specific T cells, thus affecting their immunogenicity. CD1b and CD1c molecules form immunogenic complexes with half-life shorter than 24 h, whereas CD1a persists at least three days, as measured on living DCs [171]. CD1d complexes with different glycosphingolipids have a half-life longer than 24 h [43, 238, 239]. This difference might be ascribed to the intracellular compartment wherein CD1 molecules traffic, with a faster degradation of the immunogenic complexes in LE/lysosomes.

Lipid-reactive TCRs and selection of CD1-restricted T cells

Lipids are recognized by T lymphocytes that express $\alpha\beta$ TCRs and are called “unconventional” T cells because they might have different properties than “conventional” T cells that recognize peptides presented by MHC class I and class II proteins. The group of unconventional T cells also includes MHC class I-reactive T cells that co-express NK cell receptors such as NK1.1, and T cells reactive with nonclassical class I or class Ib molecules. T cells reactive with CD1d can express a semi-invariant TCR ($V\alpha 24$ - $J\alpha 18$ and variable $V\beta 11$ chains in humans, $V\alpha 14$ - $J\alpha 18$ and $V\beta 8.2$, $V\beta 7$ or $V\beta 2$ chains in mice) [240-243], or not [244, 245]. The T cells reactive with human CD1a, CD1b, and CD1c molecules have diverse TCRs [204, 246]. In general, T cells reactive to a particular CD1 molecule can express either CD4, CD8, or are double negative [247]. The large percentage of double negative CD1 reactive T cells suggests that the TCRs of glycolipid reactive T cells may be co-receptor independent. This would be of primary importance as the co-receptors enhance both TCR avidity [248] and transduction of the signal [249].

iNKT cells, that are CD1d-restricted, are naturally occurring memory-like populations with the capacity to produce both pro- and anti-inflammatory cytokines rapidly after TCR

engagement. iNKT cells have the capacity to alter the initiation of an adaptive immune response by augmenting or dampening the early immune response, or by diverting it in either a T helper type 1 or T helper type 2 direction. In the thymus, T cell precursors recombine genes of their TCR β and α loci and test the paired chains against the pool of self-MHC-antigen complexes expressed predominantly by epithelial cells for positive selection and dendritic cells, among others, for negative selection. T cell precursors with intermediate-affinity $\alpha\beta$ TCRs mature, while those with high- and low-affinity are deleted. After random TCR rearrangements, iNKT cells are positively selected by other double positive cortical thymocytes that probably express CD1d in association with endogenous glycolipids [250, 251], and the positive selection signal is thought to be agonistic [252]. How or whether negative selection occurs remains controversial. Then, iNKT cells undergo differentiation and maturation [253-256]. Even if the thymic development of iNKT cells shares features with the development of conventional CD4⁺ and CD8⁺ T cells, iNKT cells differentiation requires genes involved in the presentation or recognition of the selecting antigen such as *CD1d*, *TCR J α 18*, *prosaposin*, *hexosaminidase B*, *ap3*, and *cathepsin L* [257, 258]. Some signaling molecules and transcription factors are required as well for iNKT cells differentiation. They include fyn, SLAM-associated-protein, DOCK2, T-bet, IL-15 and members of the ets and NF- κ B families [149, 257-260]. iNKT cells are usually identified by staining using tetramers composed of CD1d and α GalCer or α GalCer analogs. Interestingly, and contrary to peptide-MHC complexes [261], iNKT TCR binding to α GalCer-CD1d complexes was not found to be temperature-dependent [238, 262], suggesting low versatility in CD1d-lipid-TCR binding. It also seems that the avidity interactions between CD1d-lipid complexes and the TCR of iNKT cells are stronger than the ones observed for peptide reactive T cells [44, 239, 248, 262-264]. Affinities and half-life of CD1d-lipid complexes with iNKT TCR vary according to the structure of the lipidic compound [238, 262, 263], but CD1d complexes with different glycosphingolipids have a relatively long half-life, *i.e.* more than 24 h [43, 238, 239]. Crystal structures of several human TCRs that bind α GalCer have been solved [265, 266], and recently also the mouse TCR that recognizes the complex mCD1d-iGb3 [47]. Each TCR has an architecture similar to conventional TCRs, with two immunoglobulin (Ig)-like V domain (V α and V β) and two constant (C α and C β) domains. The glycolipid-CD1d-specific binding surface of the TCR contains a pocket formed by complementarity-determining regions

CDR1 α , CDR3 α , CDR1 β and CDR3 β , and seems to be flexible due to conformational changes of the CDR3 loops [47, 266]. It should be noticed that, even if nearly all iNKT cells are α GalCer-reactive [241], some heterogeneity in lipid-reactivity exists, probably reflecting the diversity of the β chain. Thus, some iNKT cells react to GD3 [267] and phospholipids such as PI and phosphatidylethanolamine (PE) [154, 268, 269].

CD1d-dependent NKT cells that do not express the invariant V α 14-J α 18 rearrangement also exist [244, 245, 270, 271], and they are called type II NKT cells [272]. Type II NKT cells are not dependent on the ability of CD1d to traffic to endosomes for their autoreactivity [273], contrary to iNKT cells for which CD1d trafficking to endosomes is required for selection [143] and autoreactivity [273]. iNKT and type II NKT cells seem to be functionally distinct [274, 275], and iNKT are less abundant than type II in human bone marrow [276]. Type II NKT cells are likely to recognize diverse antigens [244], including sulfatide [175] and nonlipidic sulfonate-containing small molecules [277].

Mucosal invariant T cells (MAIT) are a second population of invariant NKT cells found in mice and humans. They express an invariant V α 19-J α 33 TCR in mice and V α 7.2-J α 33 rearrangement in humans. They are reactive to MR1, a non-polymorphic MHC class I-like antigen-presenting molecule. CD1d and MR1 are encoded in the same region of chromosome 1 in a locus paralogous to the MHC [278]. The majority of mouse V α 19i MAIT cells are NK1.1⁺ and double negative, they express a restricted set of V β regions, are selected by hematopoietic cells in the thymus, and rapidly produce effector cytokines such as IL-4 after TCR activation [279, 280]. However, V α 19i MAIT cells are functionally different from iNKT cells, as V α 19i MAIT cells are uniquely dependent upon B lymphocytes and the gut flora for their normal accumulation in the periphery, and are enriched in the intestinal lamina propria [279, 280]. It has also been suggested that V α 19i MAIT cells are reactive to mannose-containing glycolipids presented by MR1 [281, 282].

The T cells reactive with group 1 CD1 molecules recognize a variety of antigens including mycolic acids, phospholipids, glycosphingolipids, polyisoprenols glycolipids, diacylated sulfoglycolipids, and lipopeptides [204]. Group 1 CD1-reactive T cells are a diverse set of lymphocytes that can express either CD4, CD8, or are double negative. They can react to self, foreign, or both type of antigens [283]. $\alpha\beta$ T cells restricted to CD1a, CD1b, or CD1c are highly diverse, with junctional diversity in both the α and β chains and N nucleotide

additions [246, 283]. The $\alpha\beta$ TCR is the most frequently expressed, but also $\gamma\delta$ T cells expressing V δ 1 are reactive to CD1a [155] and CD1c [284].

CD1-restricted T cells implication in disease

CD1 molecules have the potential to function as key components of a microbial recognition system that alerts the immune system to the presence of pathogens harboring relevant lipid targets as part of their essential structure. However, the importance of this system in adaptive and innate immune responses is not completely evaluated yet. The function of the group 1 CD1 isoforms seems closely linked to adaptive immunity, while group 2 CD1 molecules have been predominantly associated with innate immunity.

One major limitation to the study *in vivo* of CD1-restricted T cell responses is the absence of group 1 CD1 molecules and CD1e in mice. Nevertheless, they express CD1d, making them valuable models for the study of group 2 CD1-restricted T cells.

The effect of infection on group 1 CD1 proteins expression is unclear. Positive or negative modulation depends on several factors including the pathogen involved, the differentiation state of the APC at the time of infection, or even the local microenvironment [70, 71, 285-291]. Group 1 CD1-restricted T cells specific for *M. tuberculosis* are generally detectable only in humans with positive tuberculin skin tests, which are indicative of previous infection with *M. tuberculosis* [152, 178, 181], corresponding to sustained memory responses characteristic of adaptive immunity. Animal models expressing group 1 CD1 molecules, including guinea pigs, rabbits, cows, and nonhuman primates, may be useful for further studies. Infection and vaccination studies in guinea pigs have already provided significant results, including protection against virulent *M. tuberculosis* organisms [292, 293], highlighting the fact that group 1 CD1-restricted T cell responses can be potentially exploited for development of novel vaccination strategies against *M. tuberculosis* and possibly other organisms that contain relevant lipid antigens.

Group 2 CD1-restricted T cells are also thought to contribute to immunity against infection. Indeed, α GalCer treatment has been shown to improve the outcome of infection, indicating that iNKT cells have the potential to enhance immunity against microbial pathogens [294-296]. Several microbial lipids that bind CD1d have been identified, but it is still uncertain whether CD1d-restricted T cells that recognize these antigens are elicited during infection

[154, 182-185, 297, 298]. During infection, cytokines and TLR signals increase CD1d levels on APCs, which promote NKT cell activation [119, 121, 299]. TLR ligands expressed by microbial pathogens can also induce cells such as macrophages or DCs to produce soluble mediators that co-stimulate NKT cell activation [185, 300], thus validating a model in which pathogen-induced TLR-dependent IL-12 production co-stimulates a weak TCR signal generated by the recognition of self antigens presented by CD1d and leads to NKT cell activation during infection. CD1d-restricted T cells can act as direct effector cells via cytotoxicity or granzyme [301], and their IFN γ production can activate macrophages to become more microbicidal. In addition, iNKT cells can rapidly generate large amounts of IL-4 and IFN γ , that can modulate the function of other cells, by activating NK cells [302, 303], inducing MHC on macrophages and DCs, and modulating the T helper (Th)1/Th2 balance of CD4⁺ T cell responses [156, 157, 239, 304-307]. In the case of *Streptococcus pneumoniae* or *Pseudomonas aeruginosa* infections, the number of iNKT cells in the lung increase, and they produce cytokines such as tumor necrosis factor (TNF) and macrophage inflammatory protein-2, which lead to the accumulation of neutrophils in the lung and subsequent phagocytosis of the pathogens [308, 309]. CD1d-restricted NKT cells are also thought to have an early impact on immunity to *Borrelia burgdorferi*, the causative agent of Lyme disease, by regulating inflammatory reactions [310]. They are also implicated in regulation of inflammation subsequent to infection with parasites [311-317]. Viral infection can modulate CD1d expression [318] or trafficking [122]. For example, HIV-1 downregulates CD1d expression by increasing its internalization from the cell surface [120], whereas hepatitis C virus increases CD1d levels on hepatocytes and infiltrating mononuclear cells of patients with the chronic form of the disease [99, 319]. Studies on mouse models of autoimmune diseases, including Experimental Autoimmune Encephalomyelitis, Diabetes, Arthritis, and Lupus, clearly pointed out a critical role for iNKT cells in regulation of autoimmunity. Even if results are still controversial regarding the mode of action, it seems that protection is rather mediated by Th2 cytokines produced by iNKT cells than Th1 ones [156, 157, 320-335]. Also for dextran sodium sulfate-induced colitis, an experimental model of Crohn's disease, activation of iNKT cells seems to have a protective effect [336]. In humans, the number of iNKT cells in the peripheral blood of patients is reduced in systemic sclerosis [337], multiple sclerosis [338-340], and other autoimmune diseases [341-343]. Their putative role in type 1 diabetes is still a matter of debate [344-347]. iNKT cells also appear to play a critical role in

allergic inflammatory responses, particularly in the development and pathogenesis of asthma and airway hyperreactivity (AHR) [348-351]. The fact that iNKT cells are relatively resistant to corticosteroid treatment renders them a target of choice for the establishment of new medications [352-355]. Subsets of iNKT cells with restricted cytokine profiles have already been described: human CD4⁺ iNKT cells produce both Th1 and Th2 cytokines, whereas CD4⁻ CD8⁻ or CD8⁺ produce only Th1 cytokines and exhibit greater cytotoxic activity [356, 357]. CD4⁺ iNKT cells with a Th2-restricted profile also exist [348]. iNKT cells are also involved in allergic diseases other than Asthma, including Contact Sensitivity, a skin reaction mediated by conventional CD4⁺ T cells, dependent upon the presence of IL-4⁺ iNKT cells [358] and CD1d glycolipid presentation [359]. Some studies also indicate an imbalance in CD4⁺ iNKT cells in atopic dermatitis, but little is known about their precise involvement [360-362].

To date, only CD1d-restricted T cells have been implicated in tumor immunity, maybe reflecting the fact their study is more easily addressed experimentally as CD1d is the only member of the CD1 family present in the mouse genome. Mice lacking iNKT cells are more susceptible to tumor growth, with both an earlier onset of tumor development and higher tumor incidence [363], suggesting that iNKT cells play a role in mediating anti-tumor immunity. Antigenic lipids may either come directly from the tumor, and/or could also correspond to altered endogenous ones. For example, the ganglioside GD3 is a tumor-released glycolipid antigen that is cross-presented to iNKT cells by APCs rather than directly by the tumor cells themselves [267]. α GalCer was isolated during a screen for anti-cancer agents [364, 365], possess a potent anti-tumor activity [366-369], and iNKT cells are required for its effectiveness [368, 370]. Patients with malignant melanoma or prostate cancer have decreased numbers of circulating iNKT cells [371, 372]. iNKT cells functions in leukemia have also been studied, and they are able to efficiently kill the tumor cells [101, 102, 104]. In patients with progressive multiple myeloma, iNKT cells have an impaired ability to secrete IFN γ [373]. Intra-tumor iNKT cell frequency has recently been identified as a prognostic factor in primary colorectal carcinomas, the prognosis being improved for patients exhibiting high iNKT cell infiltration [374]. In another study, it has also been shown that the number of iNKT cells is diminished in the liver of colon cancer patients with hepatic metastasis [375]. It seems that also noninvariant CD1d-restricted NKT cells are able to regulate tumor immunity [376-379] and autoimmunity [380], thus broadening even more the impact of CD1-related

immune responses. In humans, noninvariant CD1d-restricted NKT cells have been identified in the bone marrow [276], and among the intrahepatic lymphocytes of patients with hepatitis C [381].

Therapeutic applications of Lipid Antigens

Current vaccination strategies using recombinant viruses are facing limitations due to high responses against the viral proteins, which out-number responses specific for recombinant protein antigens [382, 383]. Advances in molecular technology have permitted the design of synthetic protein vaccines, providing immunotherapy with a degree of specificity that has not been possible using traditional vaccines based on live attenuated pathogens or whole inactivated organisms. Such specificity is providing a platform for the design of T cell therapies for infectious diseases and cancer. Optimisation of such vaccination strategies requires a deeper understanding of the signals that the immune system coordinates to respond to pathogenic infections. Compounds that mimic these signals, such as those capable of activating CD1-restricted T cells, should therefore be exploited in current vaccination protocols. That is the reason why microbial lipids, which are the products of multistep enzymatic synthesis and are often significantly different from mammalian lipids, appear to be perfect targets for vaccine development. Furthermore, the minimal polymorphisms present in the CD1 genes suggest that vaccination with microbial lipids has the potential to stimulate protective immunity in ethnically diverse populations.

As described above, CD1d-restricted NKT cells rapidly release large amounts of both Th1 and Th2 cytokines, and are able of both enhancing and suppressing immune responses [304]. The existence of functionally distinct subsets of CD1d-restricted T cells [357, 384, 385] may explain the different outcomes following their activation. Fine-tuning their activation *in vivo* might be of primary importance for therapeutic purposes.

α GalCer has been tested in phase I clinical trials involving patients with solid tumors, metastatic malignancies and non-small cell lung carcinoma [386-389]. These tests demonstrate that α GalCer can be safely used to activate iNKT cells in human cancer patients, although they displayed various efficacy. Other strategies involve modification of α GalCer itself to bias the iNKT cell-mediated response towards secretion of Th1 or Th2 cytokine profiles [156, 306], polarization of iNKT cells *in vitro* before transfer into patients [390], or

addition of cytokines during therapy to enhance efficacy of α GalCer [391, 392]. Addition of α GalCer to tumor vaccination schedules has also proven to be an effective way of boosting antigen-specific CD4⁺ and CD8⁺ T cell responses in mice [393-395], a phenomenon mainly dependent on the ability of iNKT cells to stimulate DC maturation and cross-presentation. In this case, both glycolipid and peptide antigen must be presented by the same APCs for effective enhancement of T cell responses [395]. Injections of α GalCer or OCH, a sphingosine-truncated analog of α GalCer, confer protection against type I diabetes and experimental autoimmune encephalomyelitis (EAE) via Th2 responses [156, 396, 397]. However, treatment with soluble α GalCer can also induce long-term anergy in the iNKT cell subset [398-400].

It has been shown that cytokines have the ability to induce iNKT cell tumor immunity. Administration of IL-12 at low doses prevents the growth of tumors in an iNKT and NK cell-dependent fashion [401-406]. IL-18 combination with IL-12 induce iNKT cell-dependent tumor rejection and enhances NK cell function [407]. In addition, GM-CSF-secreting irradiated whole cell tumor vaccines have shown good efficacy in mouse models [408]. They seem to require the presence of iNKT cells [409], and have some potential in clinical settings [410]. Recently, therapy with a pegylated form of granulocyte-colony stimulating factor (G-CSF) was shown to mediate potent anti-leukemia responses in an iNKT cell-dependent manner [411]. Another example is treatment with progenipoiectin-1, a chimeric cytokine of G-CSF and FMS-like tyrosine kinase 3 ligand (Flt-3L). Progenipoiectin-1-mediated expansion of donor CD1d-restricted NKT cells has been proved important to reduce Graft-versus-host disease (GVHD) in a model of allogeneic stem cell transplantation [411].

Apparently, effective activation of CD1d-restricted T cells *in vivo* is dependent on the route of administration of the activating ligand. Intravenous and intraperitoneal injection of DCs loaded with α GalCer leads to CD1d-restricted T cell activation and subsequent cytokine production [395, 400], whereas subcutaneous administration seems less effective [394], possibly due to the low frequency of CD1d-restricted T cells in the region of injection [398]. The adjuvant effect of CD1d-dependent NKT cell stimulation was also observed after nasal [412] or oral administration of protein vaccine and α GalCer [413, 414].

It also seems that iNKT cell-mediated anti-tumor responses can be augmented by chemokines [415], as chemokines enhances the migration and subsequent activation of effector cells.

Overall, the results of initial clinical trials are encouraging. Future trials should be based on the use of stimulatory CD1-restricted T cell agonists which would ensure optimal DC maturation without over-stimulating T cells. Identification of compounds with the ability to modulate the lymphokine profile appears of primary importance. Design of agonists with variable TCR binding affinity and variable CD1 binding stability might allow such tuning of the immune response.

CHAPTER 1

Mycolic acids constitute a scaffold for mycobacterial lipidic antigens stimulating CD1b-restricted T cells

(These results have been accepted for publication in Chemistry & Biology)

Mycobacterium tuberculosis, the causative agent of tuberculosis, is a microbial pathogen that stimulates both conventional and unconventional T cells upon infection. As described before, conventional T cells utilize a TCR $\alpha\beta$ to recognize peptide antigens presented by MHC class I or MHC class II molecules on the surface of APCs. Unconventional T cells comprise TCR $\gamma\delta$ cells specific for mycobacterial phosphorylated ligands, and TCR $\alpha\beta$ cells that recognize lipid antigens presented by CD1 molecules [40, 416, 417]. CD1 are MHC class I-like molecules and comprise five members (CD1a, b, c, d and e). CD1a-d directly interact with the TCR, whereas CD1e is involved in processing of mycobacterial PIM₆ and therefore plays a role in CD1b-restricted immune response [34]. CD1-restricted T cells are activated during the course of *M. tuberculosis* infection [152, 178, 181], and might contribute to protection during infection since they exhibit effector functions, including cytotoxicity and secretion of pro-inflammatory cytokines, which in turn promote macrophage bactericidal activity. Some lipids from the mycobacterial envelope have been shown to be immunogenic (**Figure 9**), and are considered as promising candidates to enhance the protective effects of subunit vaccine formulations [418, 419]. Indeed, lipid antigens present interesting features: first, selection-induced structural variation is unlikely as they are products of multi-step biosynthesis; and second, stimulatory lipids might be immunogenic in the entire population due to limited CD1 polymorphism.

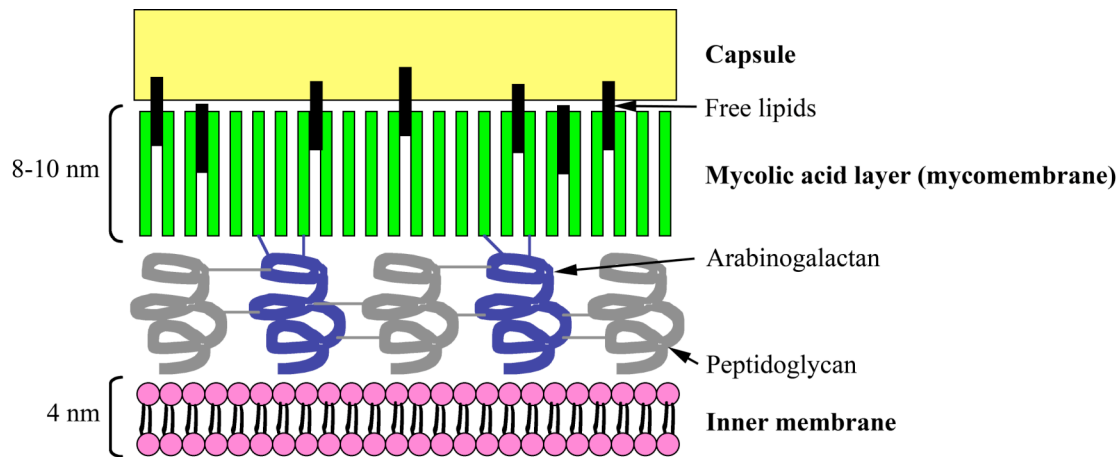


Figure 9: Schematic representation of the cell envelope of *M. tuberculosis*. The cell wall is mainly composed of peptidoglycan (grey), arabinogalactan (blue), and mycolic acids (green), all three structures being covalently linked. The mycomembrane has low fluidity, and its outer part contains various free lipids, including phenolic glycolipids, SGLs and PIMs, that are intercalated with the mycolic acids. Most of these free lipids are specific for mycobacteria. The outer layer (capsule) mainly contains polysaccharides (glucan and arabinomannan).

Vaccination of guinea pigs with *M. tuberculosis* lipids has already been shown to improve the course of the pulmonary pathology [292, 293]. Here, we tried to further characterize the repertoire of mycobacterial lipidic antigens in search for new candidates to be included in subunit vaccines.

Systematic approach

In order to identify new antigenic lipids from mycobacteria, we developed a systematic approach consisting of extraction of lipids from mycobacteria, fractionation of these extracts according to polarity and charge, and generation of T cell clones with the fractionated material [178]. T cell activation assays allow to define the antigenic lipid species after additional fractionation steps. The stimulatory species is then identified using chemical and biochemical techniques, and the responding T cell clone is further characterized. The antigen-specific T cell response is then assessed *in vitro* using cells and samples from patients.

Results

Characterization of the Z5B71 T cell clone

T cell clones were generated using three types of crude mycobacterial lipidic fractions differing in their polarity and charge [178]. One of these clones, named Z5B71, was isolated after stimulation with a lipid fraction isolated from *M. bovis* bacillus Calmette-Guérin (BCG) and enriched in PIM₂. Z5B71 T cells use a TCR $\alpha\beta$ and are CD4⁺. They were reactive to lipidic extracts from all mycobacterial species tested, *i.e.* *M. bovis* BCG, *M. smegmatis*, *M. gastri*, *M. marinum*, *M. fortuitum*, *M. xenopi*, *M. kansasii*, *M. tuberculosis* H37Ra and H37Rv, and also to lipids isolated from *Corynebacterium glutamicum* and *Nocardia asteroides* (**Figure 10A** and **10B**). This means that the immunogenic lipid is probably ubiquitous in bacteria belonging to the Corynebacteria-Mycobacteria-Nocardia group.

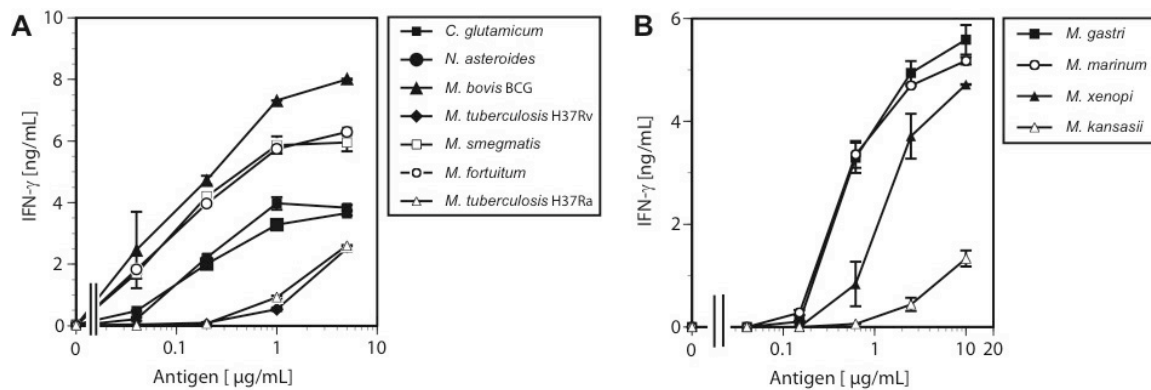


Figure 10: Immunogenicity of lipidic fractions from various bacterial species of the Corynebacteria-Mycobacteria-Nocardia group (A and B). IFN γ release was used to quantify T cell activation and is expressed as the mean ng/mL (\pm SD; n=3). The data are representative of three independent experiments.

In all tests, the *M. bovis* BCG extract always appeared the most stimulatory, suggesting that the antigen is more abundant in this species. As *M. bovis* BCG glycolipid diversity is lower compared to that of *M. tuberculosis*, we decided to use *M. bovis* BCG lipid extracts to isolate and identify the stimulatory antigen. The lipid extract was first partitioned by acetone precipitation (Figure 11A), and the acetone insoluble fraction showed the strongest activity (Figure 11B). A further methanol precipitation allowed us to determine that the methanol-insoluble fraction was the most stimulatory (Figure 11C). This latter fraction was then fractionated on a silica gel column and eluted with chloroform containing increasing amounts of methanol (Figure 11A).

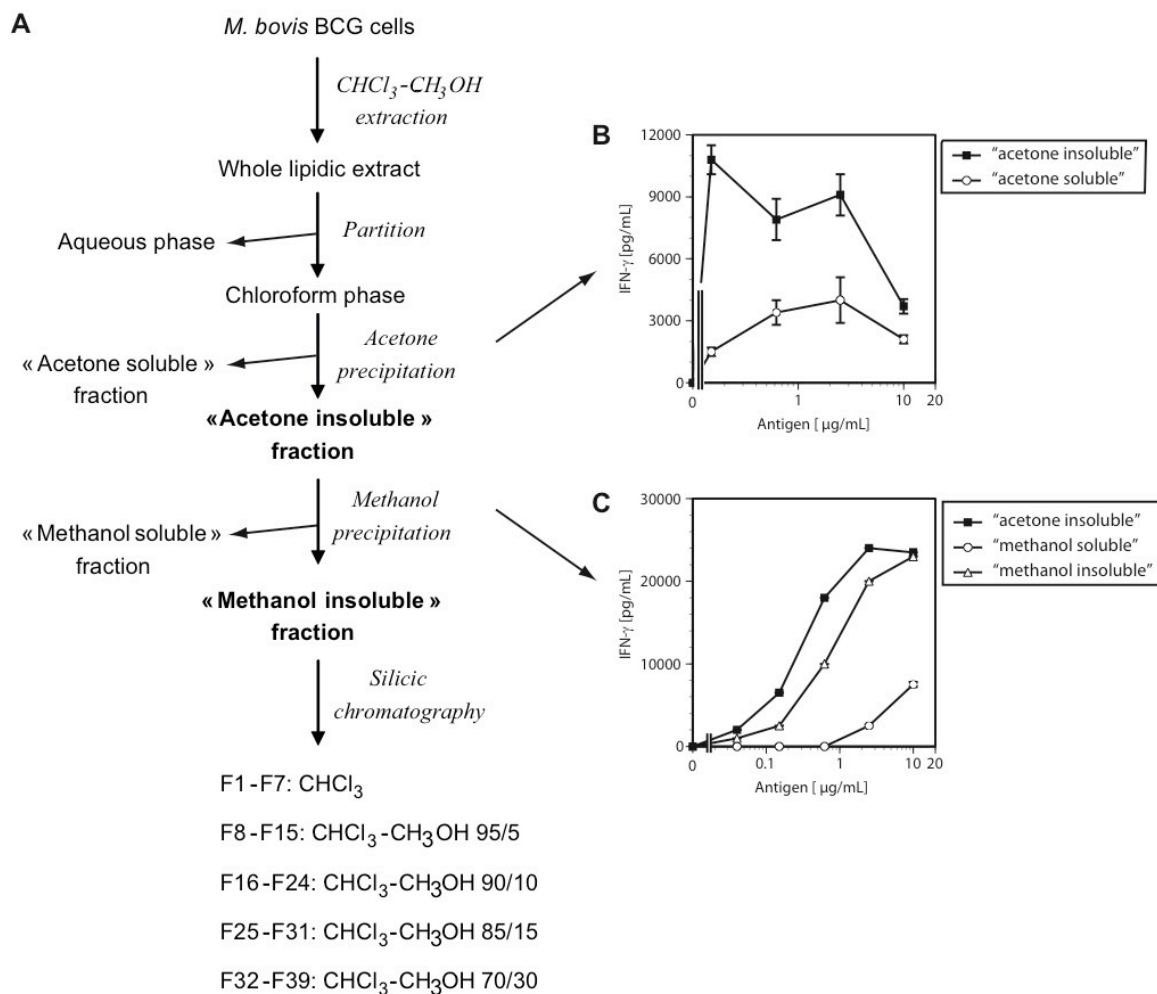


Figure 11: (A) Purification scheme of GroMM from *M. bovis* BCG. (B and C) The purification was followed by assessing immunogenicity of the lipidic fractions. IFN γ release was used to quantify activation of the T cell clone Z5B71 and is expressed as the mean pg/mL (\pm SD; n=3). The data are representative of three independent experiments. Purification was done by collaborators.

Fractions 5 to 9, eluted with chloroform or chloroform/methanol 95/5 (v/v), were able to stimulate Z5B71 T cells (**Figure 12**).

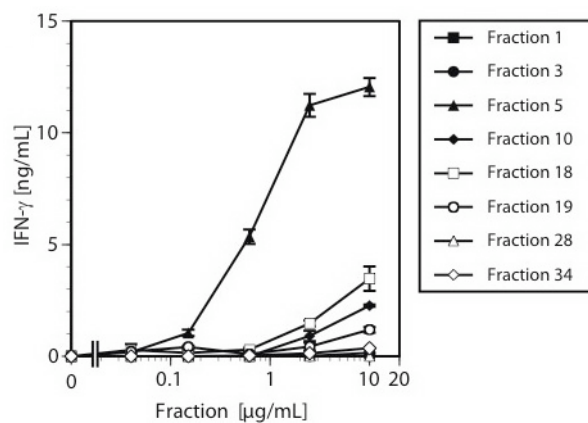


Figure 12: Immunogenicity of acetone insoluble/methanol insoluble lipidic fractions. IFN γ release was used to quantify T cell activation and is expressed as the mean ng/mL (\pm SD; n=3). The data are representative of three independent experiments.

The homogeneity of the product contained in these fractions was confirmed by thin layer chromatography (**Figure 13**).

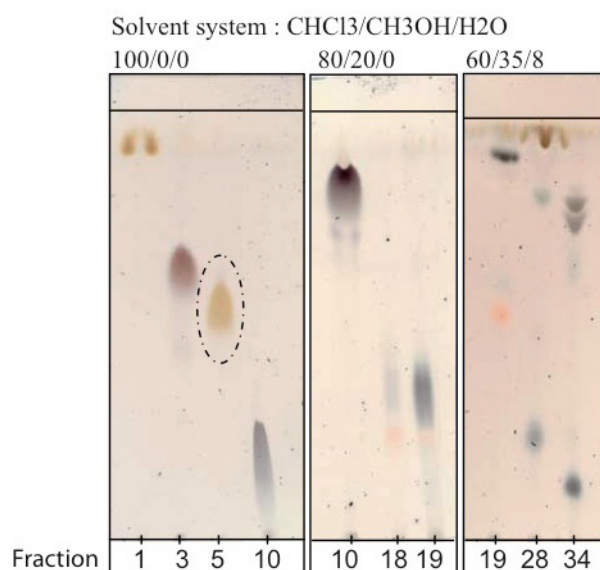


Figure 13: TLC analysis of eight representative fractions (fractions 1, 3, 5, 10, 18, 19, 28 and 34) obtained after purification of acetone insoluble/methanol insoluble lipids by silica chromatography. The encircled spot corresponds to the active compound. TLC was done by collaborators.

Chemical characterization of the lipid antigen

Fractions 5 to 9 were pooled, and the product was analysed by matrix-assisted laser desorption/ionization-*time-of-flight*-mass spectrometry (MALDI-*ToF*-MS) and nuclear magnetic resonance (NMR). The positive mode MALDI mass spectrum showed a complex pattern of peaks assigned to cationized sodiated molecular ions $[M+Na]^+$ (**Figure 14A**). The main peaks were characterized by 28 mass units difference, suggesting differences of two methylenic units between each molecular species, possibly reflecting heterogeneity in fatty acid length.

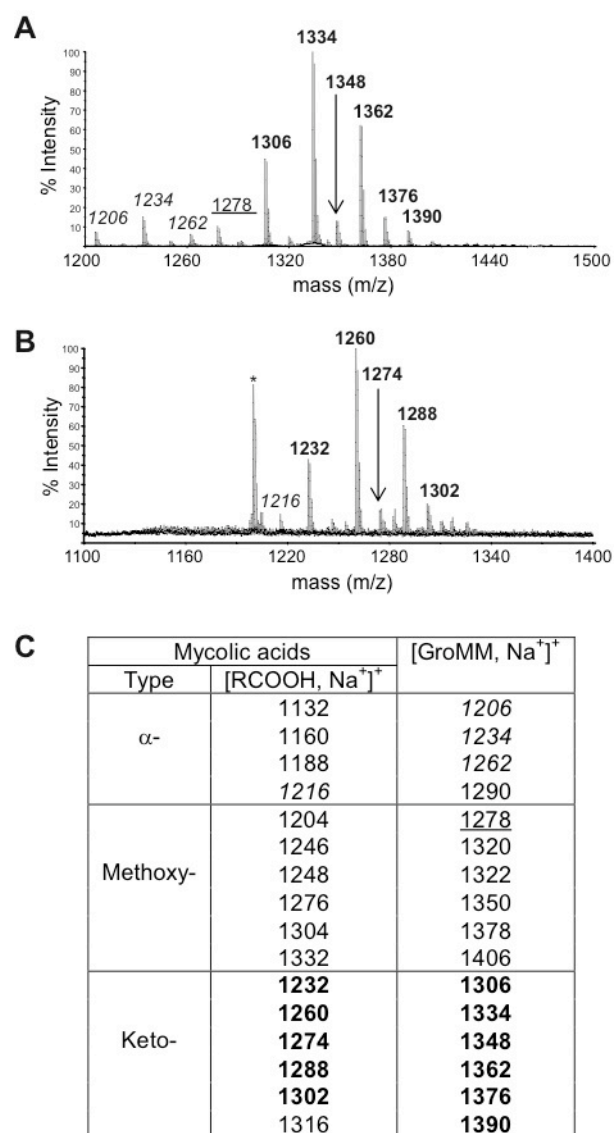


Figure 14: (A) MALDI-*Tof*-MS analysis in positive mode of *M. bovis* BCG GroMM. (B) Mycolic acids obtained after alkaline hydrolysis of *M. bovis* BCG GroMM. The asterisk corresponds to a contaminant. (C) Estimated masses of sodium adducts corresponding to expected mycolic acids and subsequent GroMM. MALDI-*Tof*-MS analysis was done by collaborators.

To confirm this assumption, the product was hydrolyzed under alkaline conditions and the fatty acids were analysed by gas chromatography (GC) (not shown) and MALDI-*Tof*-MS (Figure 14B). The positive mode MALDI mass spectrum revealed a series of peaks typical of mycolic acids [420]. Mycolates are classified into α-mycolates, methoxymycolates, and

ketomycolates, according to the presence of various chemical functions on the meromycolic chain [421]. *M. tuberculosis* contains a ratio α -mycolates/oxygenated mycolates (*i.e.* methoxymycolates and ketomycolates) of 1/1, while *M. bovis* BCG contains predominantly ketomycolates [422]. In agreement with these data, peaks at m/z 1232, 1260, 1274, 1288 and 1302 (**Figure 14B**) were assigned to $[M+Na]^+$ forms of ketomycolates (**Figure 14C**). The 74 atomic mass units difference with the native product suggested that the latter consisted of one mycolic acid esterifying a glycerol residue. In line with this, MALDI-MS analysis of the peracetylated molecule (not shown) showed a displacement of 126 mass units, indicating the presence of three alcohol functions. Identification of glycerol monomycolate (GroMM) as a novel antigen was supported by 1D 1H NMR analysis (**Figure 15E** and **15D**).

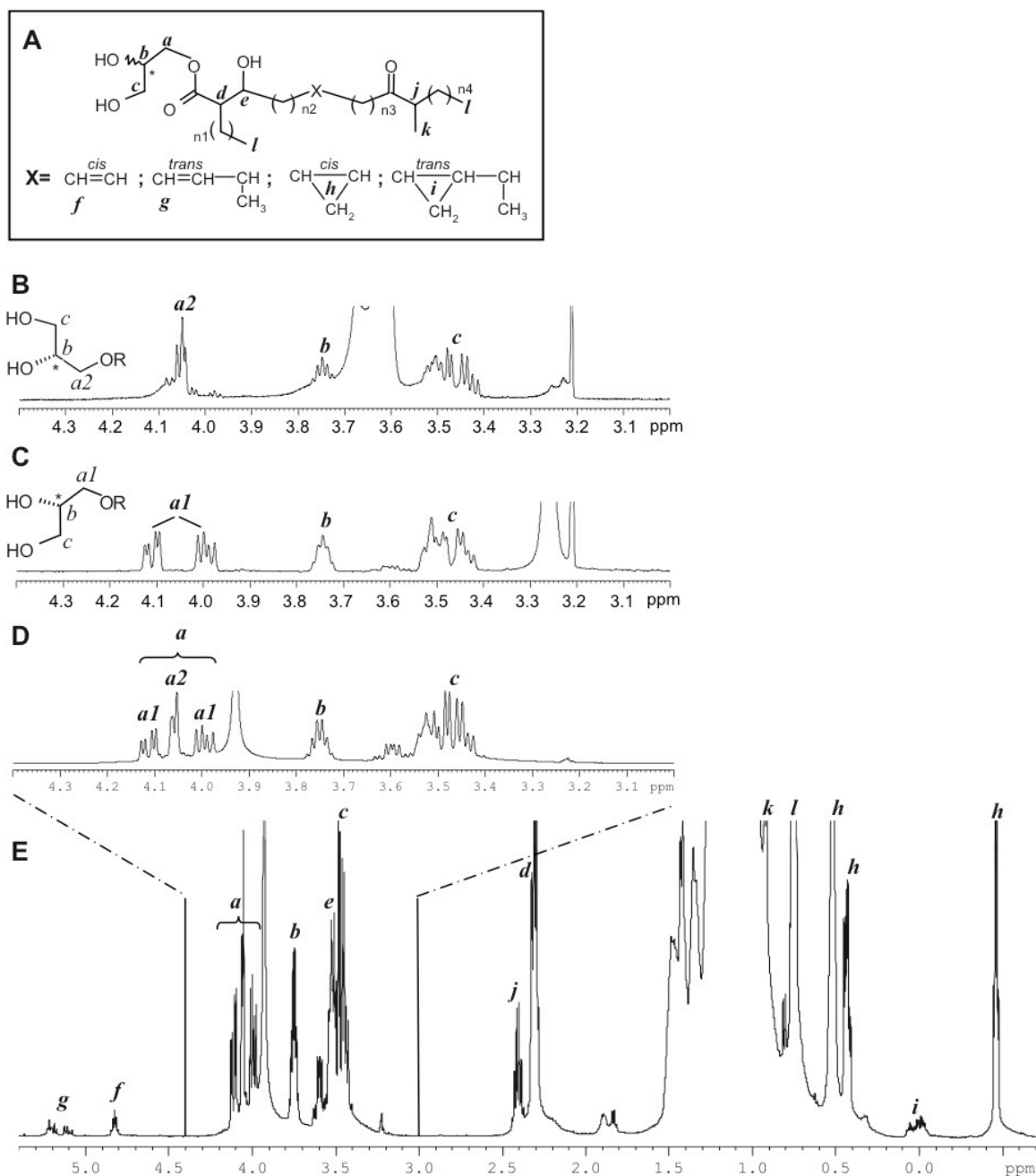


Figure 15: Structure determination of natural *M. bovis* BCG GroMM (**D** and **E**), synthetic (S)-1-O-mycoloyl-glycerol (**C**), and (R)-1-O-mycoloyl-glycerol (**B**) by ¹H NMR analysis. Specific GroMM protons signals are annotated a to k and are assigned on the structure of the major forms of *M. bovis* BCG GroMM, i.e. esterified by ketomycolic acids, presented in (**A**). n1=19, 21 or 23; n2 and n4= 15, 17 or 19; n3=12 to 17; glycerol protons signals are annotated a to c. In (**B**) and (**C**), R corresponds to mycolic acid. NMR analysis was done by collaborators.

The resonances typical of mycolic acids were assigned according to published studies [422-424]. Protons *d* (δ 2.31) and *e* (δ 3.53, multiplet), which correlate together on the 2D ^1H - ^1H correlation spectroscopy (COSY) spectrum (not shown), were assigned to the protons of the carbons carrying the α -chain and the β -hydroxyl group, respectively (**Figure 15A**). The protons *j* (δ 2.41, multiplet) and *k* (δ 0.92, doublet), which also correlate together on the COSY spectrum, were assigned to the $-\text{CHCH}_3-$ group in the distal portion of the meromycolic chain. The signal *l* (δ 0.75, triplet) was assigned to the protons of the terminal methyl groups of the α - and meromycolic chain. The multiplets at δ -0.46, δ 0.44 and δ 0.52 (labeled *h*), that correlate together on the COSY spectrum, are the characteristic signals of the cyclopropanic function protons. Signals around 5 parts per million (ppm) (*g* at δ 5.16 and *f* at δ 4.83) correspond to olefinic protons, indicating that a small proportion of the mycoloyl chains contain ethylenic groups. Protons *a* (δ 4.11, 4.06 and 3.99), *b* (δ 3.75) and *c* (δ 3.47) (**Figure 15D**), which correlate together on the 2D ^1H - ^1H homonuclear Hartmann-Hahn (HOHAHA) spectrum (not shown), were assigned to glycerol protons (**Figure 15A**). However, protons *a* were divided into two independent spin systems, *a1* (δ 4.11 and 3.99) and *a2* (δ 4.06) (**Figure 15D**), whose definitive assignment was made by NMR analysis of synthetic GroMM analogs.

Stimulation of T cells by hemi-synthetic GroMM (sGroMM)

To confirm GroMM antigenicity, analogs were chemically synthesized (**Figure 16**) using mycolates isolated from *M. tuberculosis* H37Rv (**figure 17B**).

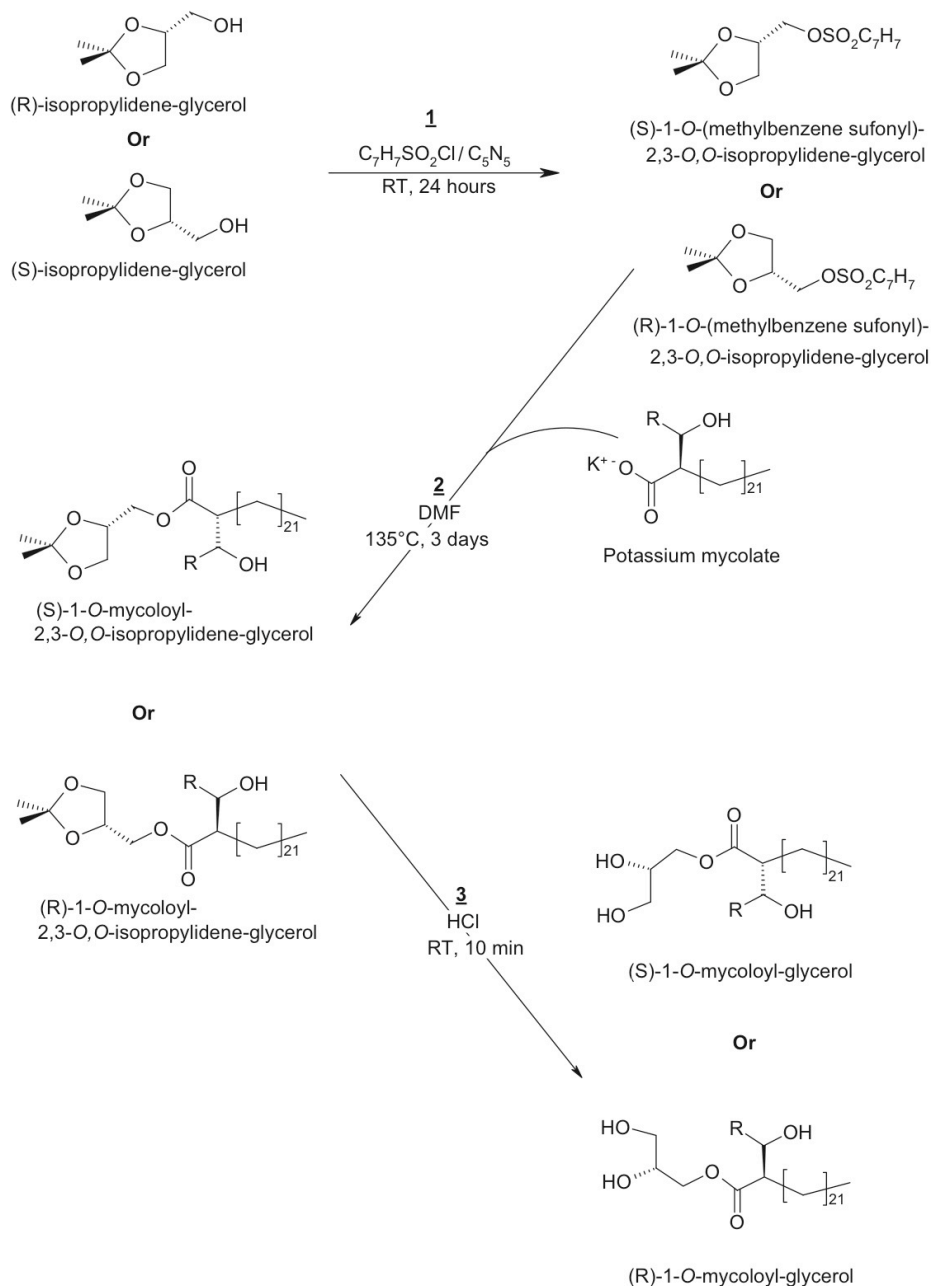


Figure 16: Synthesis scheme of (S)-1-O-mycoloyl-glycerol and (R)-1-O-mycoloyl-glycerol. Synthesis was done by collaborators.

The chemical synthesis was started using (R)- and (S)-isopropylidene-glycerol, activated by p-toluene-sulfonyl [425] (**Figure 16**). The esterification of glycerol by mycolic acids was realized by heating (R) or (S)-isopropylidene-glycerol in the presence of potassium mycolates [426]. Both isopropylidene-mycoloyl-glycerol isomers were then deprotected under acidic

conditions giving synthetic (R)- or (S)-GroMM (s(R)-GroMM and s(S)-GroMM, respectively). The MALDI mass spectra of both sGroMM (**Figure 17A**) were in agreement with the expected mass distribution of GroMM bearing *M. tuberculosis* H37Rv mycolic acids (**Figure 17B**).

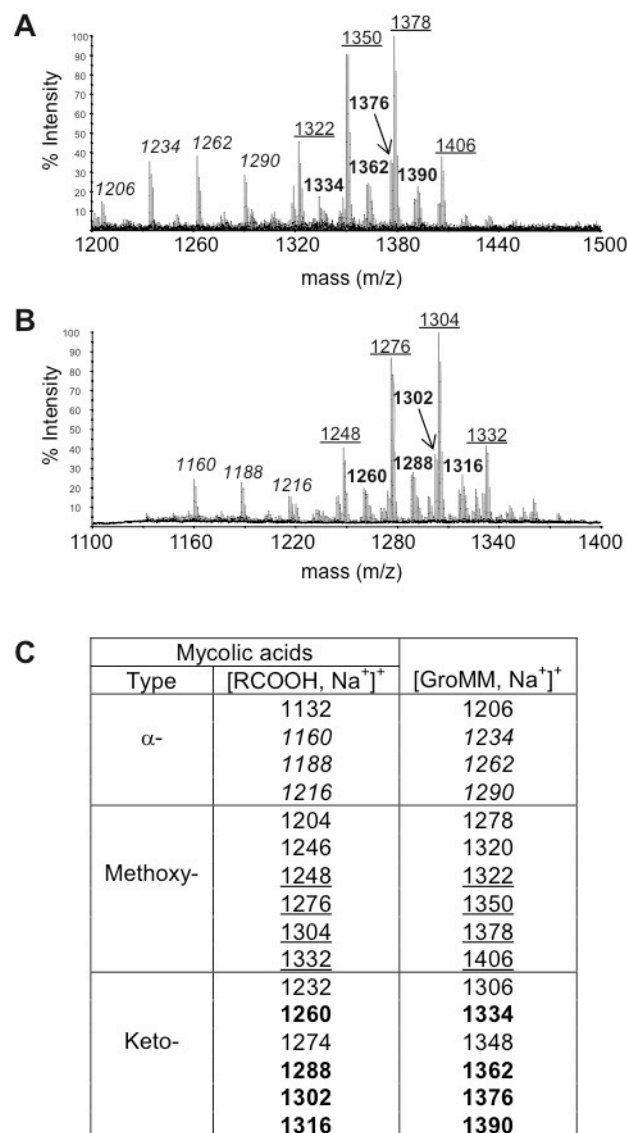


Figure 17: (A) MALDI-*Tof*-MS analysis in positive mode of synthetic GroMM. (B) MALDI-*Tof*-MS analysis in positive mode of the *M. tuberculosis* H37Rv mycolic acids used for synthesis. (C) Estimated masses of sodium adducts corresponding to expected mycolic acids and subsequent GroMM. MALDI-*Tof*-MS analysis was done by collaborators.

Both sGroMM were then analysed by 1D ¹H NMR (Figure 15B and 15C). The analysis of the (S)-1-O-mycoloyl-glycerol (s(S)-GroMM) showed *a* protons (designated *a*1) with chemical shifts at 4.00 and 4.12 ppm (Figure 15C), while the analysis of the (R)-1-O-mycoloyl-glycerol (s(R)-GroMM) showed *a* protons (designated *a*2) resonating at 4.05 ppm (Figure 15B). These data allowed us to conclude that natural GroMM, which shows *a*1 and

a2 resonances of similar intensity (**Figure 15D**), is composed of both stereoisomers in equal proportions. When these analogs were used to stimulate Z5B71 T cells, s(R)-GroMM was more active than s(S)-GroMM, and the natural compound had an intermediate activity (**Figure 18**).

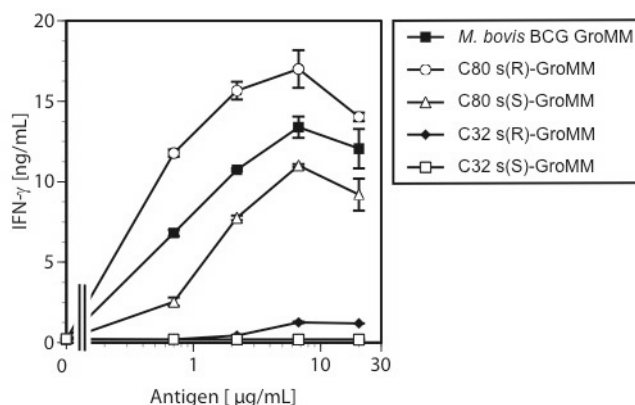


Figure 18: Immunogenicity of hemi-synthetic GroMM. In C32 or C80 s(S)- or s(R)-GroMM, C32 corresponds to corynomycolic acids and C80 to mycolic acids, (S) corresponds to (S)-1-O-mycoloyl-glycerol and (R) to (R)-1-O-mycoloyl-glycerol. IFN γ release was used to quantify T cell activation and is expressed as the mean ng/mL (\pm SD; n=3). The data are representative of three independent experiments.

These data confirmed both nature and structure of the natural antigen, and show that one diastereoisomer is preferentially recognized by the TCR of Z5B71 T cells.

Structural requirements of GroMM for immunogenicity

Free mycolates may form stimulatory complexes with CD1b [176, 179]. However, mycolates and corynomycolates tested in our assay did not activate Z5B71 T cells (not shown), highlighting the crucial role of the glycerol moiety for TCR recognition. Acetylation of the hydroxyl groups of glycerol was then carried out to evaluate the importance of the alcohol functions. The presence of an acetyl substituent on the position *c* of glycerol (**Figure 15A**) did not abolish T cell reactivity, but the presence of two acetyl substituents (on both positions *b* and *c*) did (**Figure 19A**). These data suggest that the hydroxyl group in position *b* is implicated in recognition by T cells. GroMM was also submitted to periodic acid cleavage and reduction, in order to generate glycol-monomycolate, and this compound showed a

drastically reduced ability to stimulate T cells (**Figure 19A**), demonstrating the importance of the position *c*. We next investigated whether other natural mycolate derivatives were able to stimulate Z5B71 T cells. Interestingly, GlcMM, another lipid antigen presented by CD1b [179], was able to activate this T cell clone (**Figure 19B**).

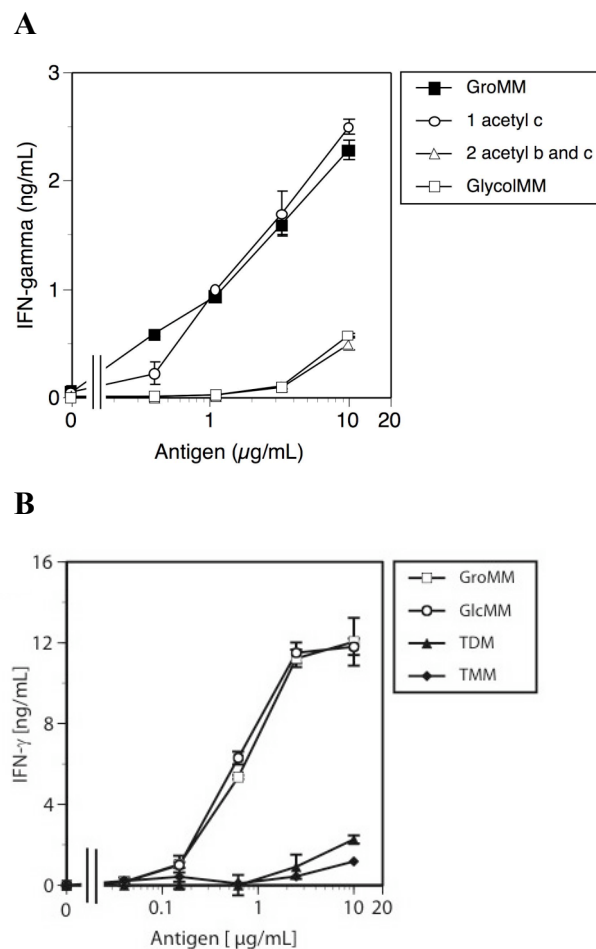


Figure 19: (A) Importance of the alcohol functions of the glycerol head on T cell stimulation. Position *c* was acetylated alone, or both *b* and *c* were acetylated. (B) Immunogenicity of *M. bovis* BCG mycolate derivatives. IFN γ release was used to quantify T cell activation and is expressed as the mean ng/mL (\pm SD; n=3). The data are representative of three independent experiments.

However, neither trehalose-monomycolate (TMM) nor trehalose-dimycolate (TDM) were stimulatory (**Figure 19B**). The importance of the number and the structure, in particular the length, of the acyl chain(s) on the glycerol unit was investigated by testing the immunogenicity of different commercial glycerides. Mono-, di- and triglycerides bearing

conventional palmitic acids did not stimulate Z5B71 T cells (not shown). Hemi-synthetic GroMMs were prepared using corynomycolates (*i.e.* C₃₂ mycolic acid) isolated from *C. glutamicum*. Even at high doses, T cell stimulation with both R and S isomers was very inefficient (**Figure 18**). However, GlcMM isolated from *C. glutamicum* (*i.e.* with corynomycolates) showed about the same activity as *M. phlei* GlcMM (*i.e.* with C₈₀ mycolic acid) (**Figure 20**).

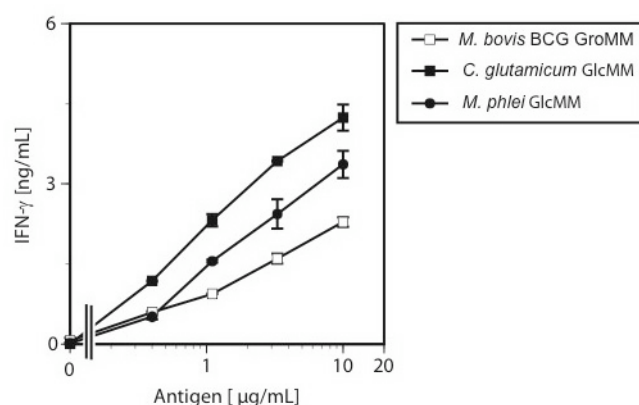


Figure 20: Immunogenicity of GlcMM from *C. glutamicum* and *M. phlei*. IFN γ release was used to quantify T cell activation and is expressed as the mean ng/mL (\pm SD; n=3). The data are representative of three independent experiments.

Collectively, these results show that both fatty acid and hydrophilic head influence stimulation of Z5B71 T cells.

Presentation of GroMM is CD1b-restricted and CD1e-independent

To determine GroMM restriction, we used CD1-transfected APCs. Only APCs expressing CD1b were stimulatory (**Figure 21**).

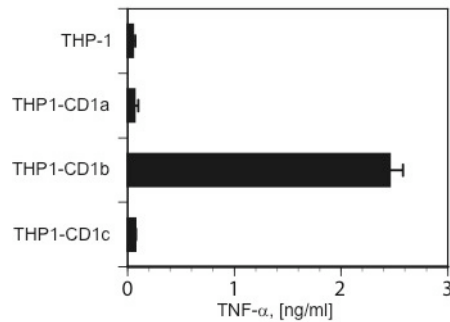


Figure 21: Presentation of GroMM to Z5B71 T cells by CD1-transfected THP-1 cells. TNF α release was used to quantify T cell activation and is expressed as the mean ng/mL (\pm SD; n=3). The data are representative of three independent experiments.

In addition, the stimulation was inhibited by anti-CD1b blocking monoclonal antibodies (mAbs), but not by other anti-CD1 mAbs (**Figure 22**).

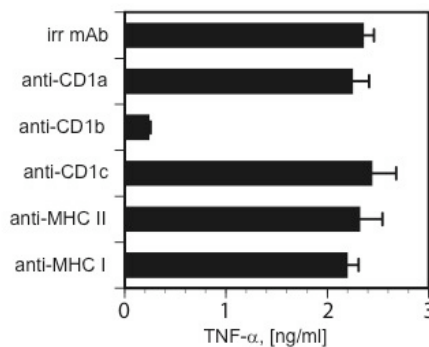


Figure 22: mAbs-mediated inhibition of T cell activation. TNF α release was used to quantify T cell activation and is expressed as the mean ng/mL (\pm SD; n=3). The data are representative of three independent experiments.

Since CD1e may facilitate presentation of complex mycobacterial lipids [34], we investigated whether GroMM antigenicity is influenced by CD1e. Similar T cell responses were observed

using APCs expressing only CD1b or both CD1b and CD1e (**Figure 23**), thus demonstrating that CD1e is not required for presentation of GroMM to T cells.

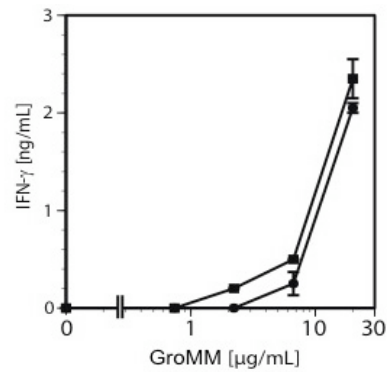


Figure 23: Presentation of GroMM to Z5B71 T cells is CD1e-independent. THP-1-CD1b (■) and THP-1-CD1b-CD1e (●) cells were used as APCs. IFN γ release was used to quantify T cell activation and is expressed as the mean ng/mL (\pm SD; n=3). The data are representative of three independent experiments.

***M. tuberculosis*-infected DCs stimulate Z5B71 T cells**

To determine whether mycobacterial lipids stimulating Z5B71 T cells are antigenic during the course of the infection, we pulsed human DCs with heat-killed *M. tuberculosis* and found strong activation (**Figure 24**).

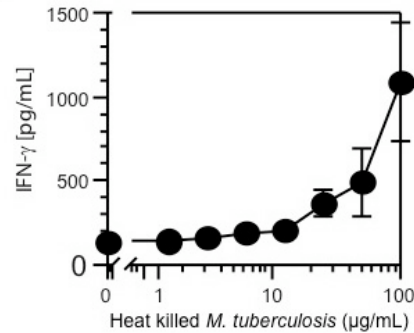


Figure 24: Activation of Z5B71 T cells by human DCs pulsed with heat-killed *M. tuberculosis*. IFN γ release was used to quantify T cell activation and is expressed as the mean pg/mL (\pm SD; n=3). The data are representative of three independent experiments.

As Z5B71 T cells were reactive, we then infected human DCs with *M. tuberculosis* (**Figure 25**).

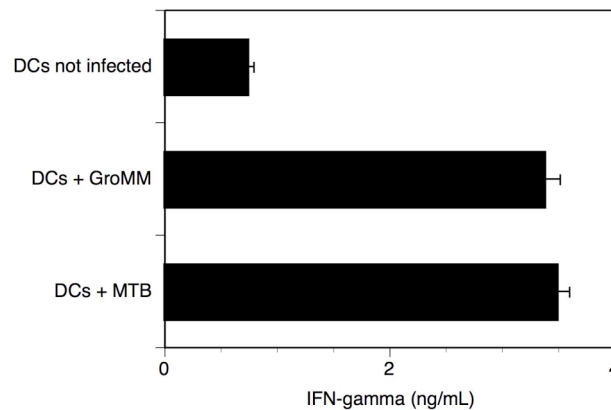


Figure 25: Activation of Z5B71 T cells by human DCs infected with living *M. tuberculosis*. IFN γ release was used to quantify T cell activation and is expressed as the mean ng/mL (\pm SD; n=3). The data are representative of three independent experiments.

Infected APCs were also able to stimulate GroMM-specific T cells, confirming the immunogenicity of these antigens during infection. These data also confirm that GroMM forms immunogenic complexes with CD1b upon phagosomal internalization of bacteria.

**GroMM-reactive T cells are not detected in patients
with active tuberculosis**

The next step was to determine whether T cells in the peripheral blood of human donors recognize GroMM. We collected blood samples from patients classified as naïve (or purified protein derivative (PPD)-negative) (n=10), with latent *M. tuberculosis* infection (n=19), BCG-immunized (n=22), and with active *M. tuberculosis* infection (n=11). Then, we measured IFN γ release after stimulation with GroMM. Significant responses were observed with the blood from BCG-immunized donors and donors with latent infection (**Figure 26**). However, no responses were observed with the blood from naïve donors and donors with active tuberculosis (**Figure 26**), although the ones with active tuberculosis vigorously responded to PPD (not shown).

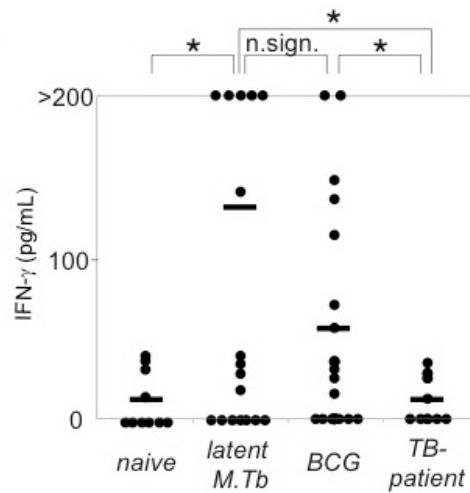


Figure 26: GroMM reactivity of naïve donors (n=10), donors with latent *M. tuberculosis* infection (n=19), BCG-immunized donors (n=22), and donors with active *M. tuberculosis* infection (n=11). Black circles show individual donors, horizontal bars represent the average for each group. One asterisk indicates a confidence interval greater than 95%. A confidence interval below 95% was considered insignificant. IFN γ release was used to quantify T cell activation and is expressed as the mean pg/mL. GroMM reactivity of donors was assessed by collaborators.

We also verified the CD1-restriction of the reactive T cells, and a cocktail of blocking antibodies directed against group 1 CD1 molecules inhibits GroMM-induced IFN γ secretion (**Figure 27**). In contrast, anti-MHC class I antibodies were not inhibitory (not shown).

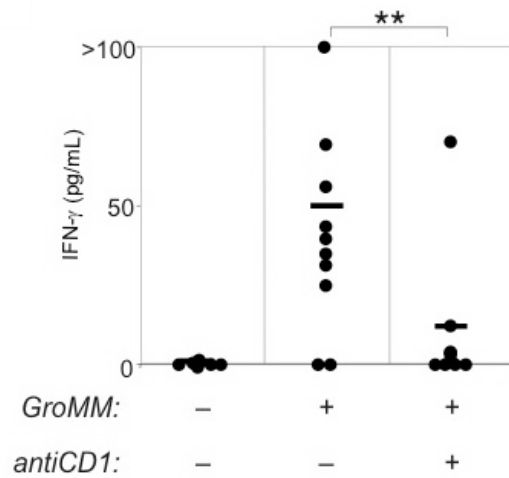


Figure 27: Inhibition of T cell activation by anti-CD1 mAbs for ten PPD-positive healthy donors. Black circles show individual donors, horizontal bars represent the average for each group. Two asterisks indicate a confidence interval greater than 99%. A confidence interval below 95% was considered insignificant. IFN γ release was used to quantify T cell activation and is expressed as the mean pg/mL. Inhibition of T cell activation using blood from donors was assessed by collaborators.

The specificity of the *ex vivo* lipid reactivity was addressed testing the reactivity of five PPD-reactive donors to three unrelated mycobacterial lipids: GroMM, PIM₂ and DAT (**Figure 28**). One donor responded only to DAT, two responded only to GroMM, one only to PIM₂, and one to both GroMM and DAT. This indicates that the *ex vivo* T cell responses are specific for individual lipids and not due to cross-reactivity.

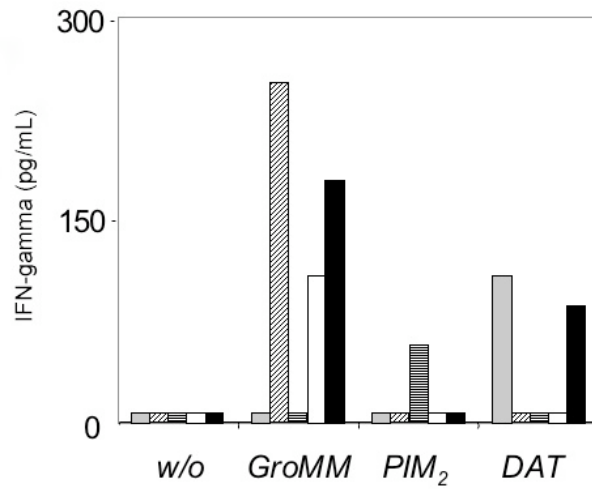


Figure 28: *Ex vivo* T cell responses are specific for individual lipid antigens. Each donor is represented by a bar, and reactivity to three unrelated mycobacterial lipids (GroMM, PIM₂ and DAT) was assessed. IFN γ release was used to quantify T cell activation and is expressed as the mean pg/mL. Lipid reactivity of donors was performed by collaborators.

Altogether, these data show that GroMM-specific T cells are expanded after mycobacterial infection and are no longer detectable during active disease.

Discussion

The mycobacterial envelope contains a large number of diverse lipid molecules. Among them, CD1-restricted antigens have been identified, which are represented by: i) mycoloyl-based molecules, such as free mycolic acids [176] and GlcMM [179]; ii) mannosyl-phosphatidylinositol-based glycolipids represented by LAMs [180], LMs [180], and PIMs [34, 188]; iii) sulfoglycolipids [178]; iv) lipopeptides [177]; and v) polyketides [181].

Here, we identified GroMM as a mycoloyl-based lipid antigen presented by CD1b. GroMM is thought to be inserted in the outer part of the mycomembrane and is present in many mycobacterial species, including *M. bovis* BCG [427], *M. tuberculosis* [428-430], but also *Nocardia*, *Corynebacteria*, and *Gordona* bacterial cells [431].

Hemi-synthesis of GroMM analogs, (R)-1-O-mycoloyl-glycerol (s(R)-GroMM) and (S)-1-O-mycoloyl-glycerol (s(S)-GroMM), allowed us to assess structural contributions to immunogenicity. Both diastereoisomers stimulated Z5B71 T cells, s(R)-GroMM being more active than s(S)-GroMM. Shortening the mycolic acid chain almost abrogated immunogenicity of the GroMM analogs, in line with previous studies showing that GlcMM with long alkyl chains (C₈₀) requires internalization and trafficking through late endosomal compartments for efficient presentation whereas GlcMM with short alkyl chains (C₃₂) can be loaded onto CD1b on the cell surface [25]. The fact that Z5B71 T cells react to both GlcMM and GroMM argue for the presence of a common epitope. By chemical degradation, we found that GroMM corresponds to the minimal structure required for recognition by Z5B71 T cells, raising the question of how cross-reactivity between these two lipids may occur. The crystal structure of GlcMM bound to CD1b [432] shows that the arginine in position 79 of the α 1 helix (R79) of CD1b makes a hydrogen bond with the oxygen of the alcohol function on the C4 of glucose (**Figure 29A**), possibly stabilizing a specific orientation of the sugar.

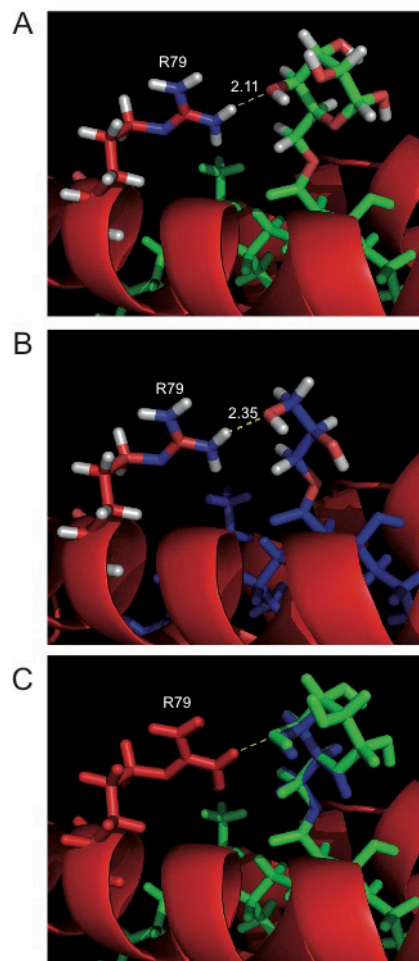


Figure 29: Models resulting from molecular modeling calculations for CD1b-GlcMM (A) and CD1b-GroMM (B) complexes. The resulting structures were superimposable (C), with glycerol well superposed on a part of the glucosidic ring. Both glucose and glycerol are found in close contact with R79. Molecular modeling was done by collaborators.

Superimposition of GroMM and GlcMM structures shows that the hydroxyl in position *c* of GroMM might correspond to OH-4 of the glucosyl unit of GlcMM, whereas the hydroxyl in position *b*, corresponding to the oxygen atom of the sugar ring, might be available for a cognate interaction with the TCR (**Figure 29B** and **29C**). This model might explain the recognition of both GlcMM and GroMM structures by the Z5B71 T cell clone. Using these T cells, we also found that the mycolic acid length is important for stimulation by GroMM, but less for stimulation by GlcMM. The current paradigm is that fatty acyl chain length affects positioning of the polar head and its subsequent interaction with the TCR [25, 190, 307, 432]. This parameter might be more critical for GroMM because the number of possible

interactions with the TCR is more limited with glycerol than with glucose. Taken together, these data suggest that mycolic acids may constitute a scaffold for lipidic antigens, which supports binding to CD1b and facilitates interaction of different polar heads with the TCR. This resembles the scaffold nature of ceramide and diacylglycerol moieties found with other lipid antigens [433, 434], and thus reveals a more general rule in which scaffold molecules which are well suited for CD1 binding confer immunogenicity to a large number of lipid molecules.

The observation that GroMM, GlcMM and free mycolic acid are all presented by CD1b molecules is probably caused by the unique presence of intricate and connected hydrophobic pockets in CD1b. Crystallographic data have revealed how the meromycolate chain of GlcMM completely occupies the A' T' and F' channels of CD1b and protrudes out of the F' channel, possibly interacting with the TCR, whereas the α -chain occupies the C' channel [432]. In addition, CD1b traffics through the phagosome [435] and might facilitate formation of immunogenic complexes with mycobacterial lipid antigens released in the phagosomes. CD1b binds and present C₈₀ lipidic antigens using a pH-dependent mechanism [169] and does not require cellular enzymes or lipid cleavage [436]. In the latter study, it has been proposed that lipids with long acyl chains are loaded in an intact form, and protrude through a portal near the bottom of the CD1b groove. Although we cannot formally exclude that the meromycolate chain of GroMM is partially degraded before forming antigenic complexes with CD1b, it is more likely that it is stimulatory in its native form. This is supported by the fact that GroMM analogs with short fatty acids are poorly immunogenic. In addition, GroMM from *M. bovis* BCG is still immunogenic when presented by APCs lacking CD1e, a CD1 family member involved in processing of complex glycolipid antigens [34].

GroMM stimulates T cells in the peripheral blood of human donors that were BCG-immunized or with latent *M. tuberculosis* infection. However, no stimulation is observed in the case of patients with active *M. tuberculosis* infection. This contrasts with the response to Ac₂SGL, which is detectable in donors with both latent and active *M. tuberculosis* infection [178]. Several hypothesis might explain why patients with active *M. tuberculosis* infection failed to respond to GroMM. One could be that in investigated patients a general and non-specific tumor growth factor (TGF)- β -mediated immune suppression prevents *in vitro* response, as described for the initial phase of the acute disease [437]. However, this is unlikely as T cell responses to mycobacterial protein antigens were readily detectable in the

peripheral blood of the same donors. It is also possible that GroMM-specific T cells are sequestered in inflamed tissues, as suggested for Ag85-specific CD8⁺ T cells [438]. A third possibility is that GroMM-specific T cells participate in protection and limit growth of the bacilli. The absence of these T cells might then directly contribute to appearance of clinically active disease. The fact that GroMM-specific T cells recognize mycobacteria-infected cells and release pro-inflammatory cytokines are in accordance with this hypothesis. Evaluation of the protective value of GroMM will shed light on its putative use in subunit vaccine formulations against tuberculosis.

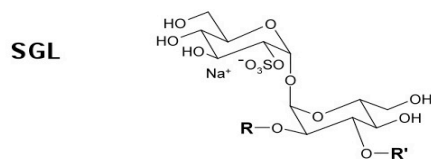
CHAPTER 2

Fatty acyl structures of *Mycobacterium tuberculosis* sulfoglycolipid govern T cell immunogenicity

(These results have been submitted to the Journal of Immunology)

According to crystal structures of CD1:mycobacterial lipid complexes, it is thought that acyl appendages are used to anchor lipids to the CD1 proteins, thus providing a correct conformation and facilitating contact between the hydrophilic part of the lipids and the TCR [439]. As described before (see **Figures 1, 2, and 3**), the human CD1a antigen-binding groove is composed of two pockets, A' and F' [41]; whereas the human CD1b groove is compartmentalized in three pockets, A', C' and F', directly accessible from the surface, plus the T' tunnel that interconnects the A' and F' pockets, leading to a 70 Å-long superchannel [39]. This T' tunnel, unique to CD1b, arises from substitution at positions 98 and 116 of bulky residues by glycine residues, compared to other CD1 isoforms. The C' pocket is, seemingly, also unique to CD1b. This large antigen-binding cavity may allow optimal accommodation of antigens with an overall lipid length of C₆₂-C₆₅ onto CD1b [40]. The two acyl chains of Ac₂SGL antigens, *i.e.* a palmitoyl (or stearyl) and a C₂₆-C₄₀ hydroxyphthioceranoic acid (a dextrogyre multimethyl-branched fatty acid [178]) (**Table I**), fit within the CD1b groove and seem to accommodate in the C' pocket and the A'-T'-F' channel, respectively. Indeed, it was suggested from the crystal structure of the CD1b:GlcMM complex that the C₄₉ meromycolic chain fully occupied the A'-F'-T' superchannel, whereas the C₈ α-chain only partially filled the C' channel [432]. Mapping of the CD1b:GlcMM molecular determinants responsible for recognition by T cells supported a critical role for the hydrophilic cap, whereas the length and structure of the acyl chains seemed of lesser importance [179, 190]. However, microbial and host glycolipids do share identical polar moieties, still suggesting that acyl appendages may allow some kind of discrimination.

As Ac₂SGLs may represent ideal candidates for novel subunit lipid vaccines, we performed a detailed investigation of the acyl chains structural requirements contributing to Ac₂SGL immunogenicity by using synthetic SGL analogs (**Table I**).



	R	R'
Ac₂SGL	Palmitoyl / Stearoyl	(32)
SGL1	Palmitoyl	(16) Palmitoyl
SGL2	Palmitoyl	(16)
SGL3	Palmitoyl	(30) Triacontanoyl
SGL4	Palmitoyl	(22) (24)
SGL5	Palmitoyl	(18)
SGL6	Palmitoyl	(22)
SGL7	Palmitoyl	(24)
SGL8	Palmitoyl	(24)
SGL9	Palmitoyl	(20)
SGL10	Palmitoyl	(22)
SGL11	Palmitoyl	(24)
SGL12	Palmitoyl	(24)
SGL13	Palmitoyl	(26)
SGL14	(8) Octanoyl	(24)
SGL15	(24) Tetracosanoyl	(24)
SGL16	(22)	Palmitoyl
SGL17	Palmitoyl	(22)

Table I: Structure of the *M. tuberculosis* sulfoglycolipid (Ac₂SGL) and the synthetic SGL analogs. R and R' numbers under brackets correspond to the number of methylene units of the aliphatic linear chain. For Ac₂SGL, R' corresponds to the most abundant homologue. Mono-, di- and trimethyl-branched fatty acids are pure stereoisomers, while unsaturated tetra and penta are 88% and saturated tetra is 83%. R and S correspond to the configuration of the respective chiral center.

Results

Synthesis of diacylated SGLs with linear fatty acids

Ac₂SGLs are glycolipid antigens synthesized by virulent *M. tuberculosis* strains and stimulate CD1b-restricted $\alpha\beta$ T cells [178]. The hydrophilic part is composed by a 2'-O-sulfate- α,α -D-trehalose acylated on position 2 with a palmitic or stearic acid, and on position 3 with a hydroxyphthioceranoic acid (**Table I**). The most abundant hydroxyphthioceranoic homologue is a dextrogyre 32 carbon atoms long chain with 8 C-methyl branched groups; all C-methyl bearing stereocenters belonging to the *L* series [440]. To determine whether this unique hydroxyphthioceranoil residue is important for stimulation of specific T cells, a chemical approach was developed (**Figure 30**) in order to synthesize a series of SGLs in which the hydroxyphthioceranoic acid had been replaced by linear fatty acids such as palmitic (C₁₆) (SGL1), 16-hydroxypalmitic (SGL2) and melissic acid (C₃₀) (SGL3) (**Table I**).

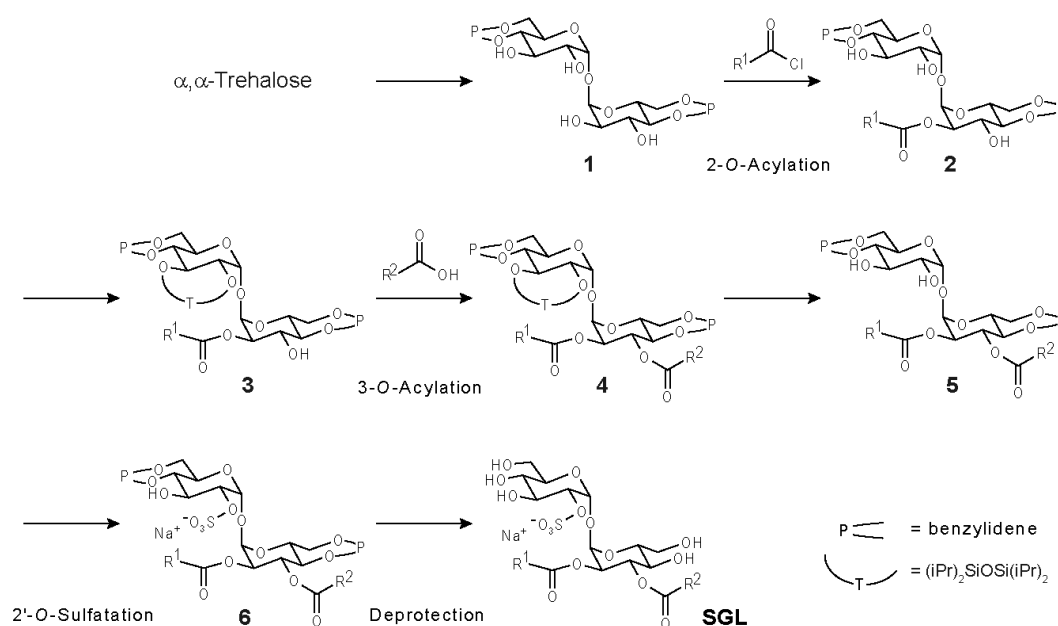


Figure 30: General route for synthesis of SGLs. The synthesis is based on a 7-step reaction sequence (**1** to **SGL**) with an overall product yield of about 5%. Synthesis was done by collaborators and is described in Materials and Methods.

Palmitoyl-sulfoglycolipids with an additional linear fatty acyl-chain bind to soluble human CD1b

To investigate the immunogenicity of synthetic SGLs, we first monitored their binding *in vitro* to soluble human CD1b (shCD1b) expressed in mouse cells. The shCD1b showed one major band in gel IEF electrophoresis (**Figure 31A**), and one peak in the capillary IEF (cIEF) electrophoregram (**Figure 31B**). These forms were assigned to shCD1b loaded with endogenous chaperon lipids including PC and a C₄₁₋₄₄ spacer lipid [133].

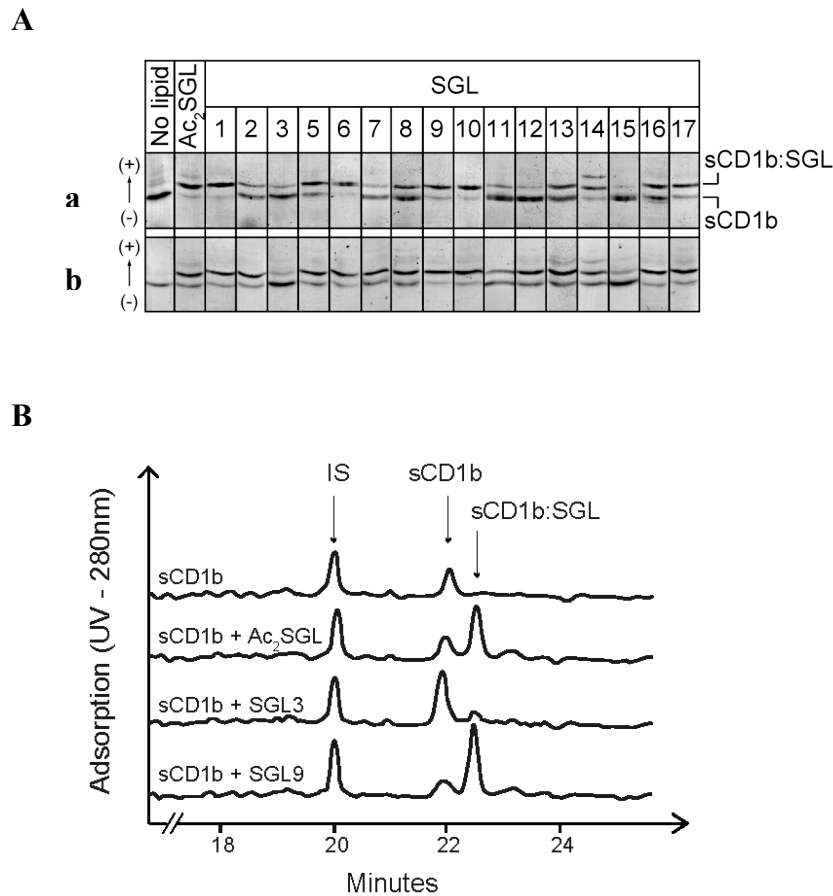


Figure 31: (A) IEF gel analysis of SGL binding onto shCD1b. Incubation of shCD1b and SGL was done in the absence (a) or presence (b) of taurocholate. Proteins were revealed by Coomassie R350 staining. (B) Illustrative electrophoregrams (UV 280 nm) corresponding to shCD1b incubated in the absence or presence of Ac₂SGL, SGL3 or SGL9; in the presence of taurocholate. IS, internal standard; the second peak corresponds to shCD1b without SGL, the third peak corresponds to shCD1b loaded with negatively-charged SGL. IEF and cIEF were done by collaborators.

Incubation of shCD1b with Ac₂SGL resulted in the appearance of a second band in IEF tentatively assigned to the shCD1b:Ac₂SGL complexes. cIEF electrophoregram analysis of shCD1b incubated with Ac₂SGL in presence of detergent showed an additional peak at higher migration time, thus supporting the formation of shCD1b:Ac₂SGL complexes as well. The difference in electrophoretic behavior compared with native shCD1b arises from the modification of the isoelectric point caused by displacement of the neutral endogenous ligand PC by negatively charged Ac₂SGL. Integration of the electrophoregram peak revealed that 70% of shCD1b was complexed with Ac₂SGL (Figure 32).

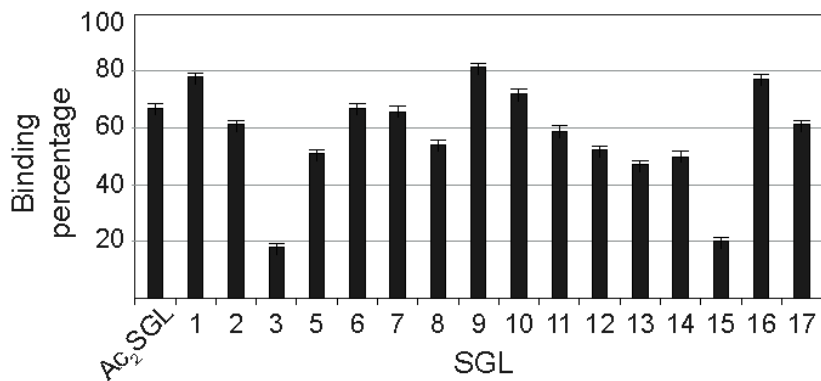


Figure 32: SGL binding onto shCD1b. shCD1b was incubated with the SGLs in presence of taurocholate, followed by cIEF analysis. The peaks assigned to shCD1b and shCD1b:SGL complexes were integrated and used to determine the percentage of shCD1b loaded with SGLs.

Similarly, IEF methods were used to determine the percentage of shCD1b molecules loaded with other SGLs. SGL1 and SGL2, with short linear acyl chains consisting of palmitic and 16-hydroxypalmitic acids at position 3 (**Table I**), formed similar amounts of shCD1b:SGL complexes (60-80%), resembling the natural Ac₂SGL (**Figures 31A** and **32**). In contrast, very inefficient binding of C₃₀-acylated SGL3 was observed (~20%), irrespective of the presence or absence of detergent during loading (**Figures 31A** and **32**).

SGL analogs with linear fatty acyl chains are not stimulatory

The stimulatory activity of the synthetic SGLs was evaluated in a classical T cell stimulation assay using human DCs as APCs. Ac₂SGL-specific T cells were reactive to Ac₂SGL, but not to SGL1, SGL2, or SGL3 (**Figure 33A**).

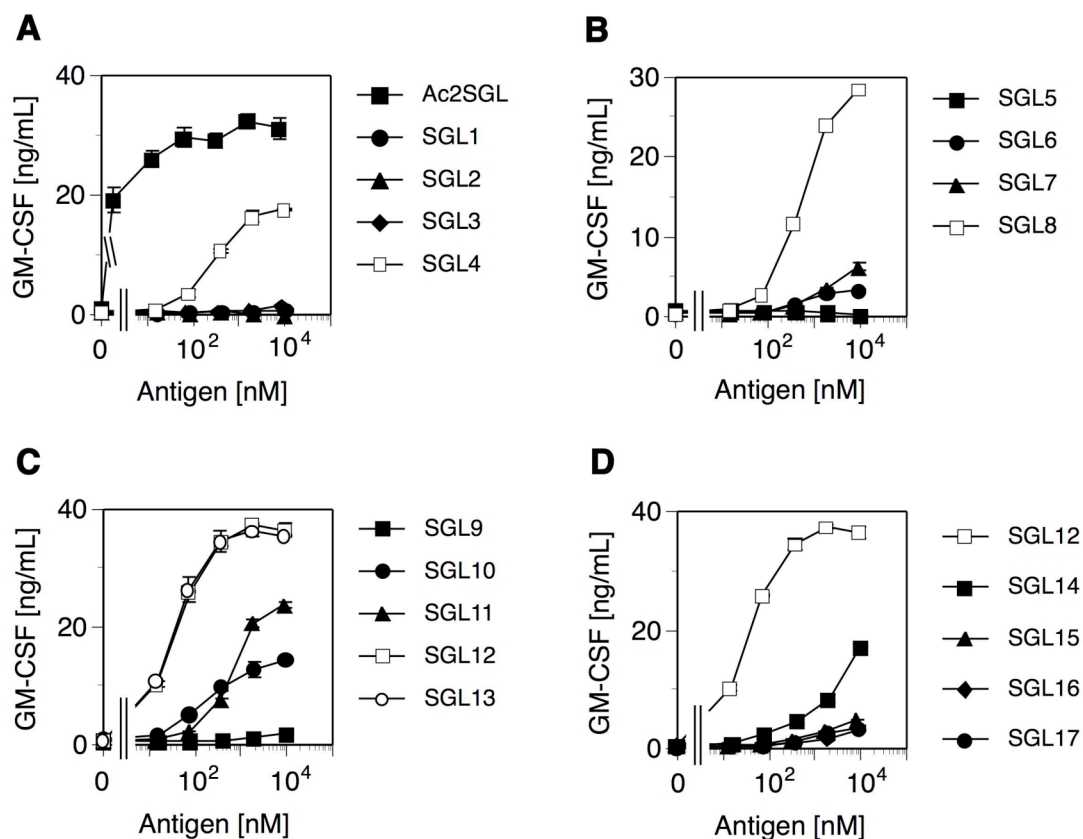


Figure 33: Immunogenicity of SGLs. Human DCs were pre-incubated with different concentrations of natural Ac₂SGL or synthetic SGLs before addition of T cells. GM-CSF release was used to quantify T cell activation and is expressed as the mean ng/mL (\pm SD; n=3). Each panel shows the T cell response to different SGL analogs. The data are representative of three independent experiments.

Since SGL1 and SGL2 efficiently bind to shCD1b, their lack of immunogenicity might be due to the absence of branched C-methyl groups on the aliphatic chain.

Hemisynthetic SGLs containing *M. tuberculosis* mycolipenic and mycosanoic acids are immunogenic

To assess the role of C-methyl groups substituting the fatty acyl chain, hemisynthetic SGLs containing *M. tuberculosis* mycolipenic and mycosanoic acyl chains were prepared. Dextrogyre di- and tri-methyl branched fatty acids, such as mycosanoic and the α,β -unsaturated mycolipenic acids are present in the envelope of *M. tuberculosis* as acyl substituents of di-, tri-, and penta-acylated trehalose (DAT, TAT, and PAT, respectively)

[441]. A mixture of these fatty acids, containing also conventional fatty acids, was obtained by alkaline hydrolysis of *M. tuberculosis* DAT and TAT, and introduced in position 3 of 2-O-palmitoyl- α,α -D-trehalose derivative **3** following the general strategy depicted in (**Figure 30**). The structure of the resulting hemisynthetic SGL4 was supported by ^1H NMR (not shown) and MALDI-*Tof*-MS (**Figure 34**) and appeared as a mixture of C_{22} mycosanoic and C_{24} mycolipenic acid-substituted sulfoglycolipids (m/z 1009.5, m/z 1049.6).

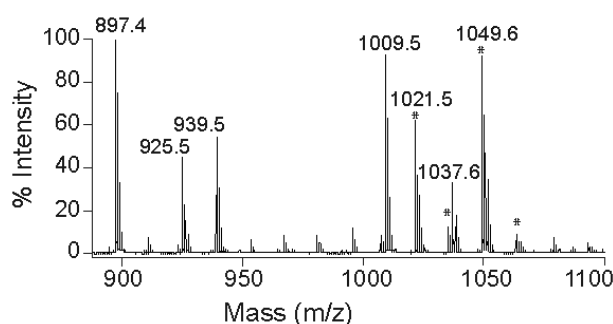


Figure 34: MALDI-*Tof*-MS analysis in positive mode of the semi-synthetic sulfoglycolipid analog SGL4. Peaks with * correspond to SGL4 with unsaturated mycolipenic acids (**Table D**); m/z 1009.5 typifies SGL4 with C_{22} mycosanoic acid; m/z = 897.4, 925.5 and 939.5 correspond to SGL4 with two palmitic acids, one palmitic and one stearic, one palmitic and one tuberculostearic, respectively. MALDI-*Tof*-MS analysis was done by collaborators.

SGL4 mass spectrum also showed the presence of SGLs acylated by conventional $\text{C}_{16}/\text{C}_{16}$ (m/z 897.4), $\text{C}_{16}/\text{C}_{18}$ (m/z 925.5) and $\text{C}_{16}/\text{C}_{19}$ (m/z 939.5) fatty acids. SGL4 was immunogenic, although less than natural Ac_2SGL (**Figure 33A**). The lower activity of SGL4 might be attributed to the presence of non-antigenic forms containing conventional fatty acids. These data are in line with our hypothesis, strongly suggesting that branched methyl groups are required to confer immunogenicity to SGLs.

The number of C-methyl branched groups controls the antigenicity of the SGL analogs

To test whether the number of methyl-branched acyl appendages influence immunogenicity, dextrogyre multimethyl-branched saturated and α,β -monounsaturated fatty acids were synthesized and coupled to 2-O-palmitoyl- α,α -D-trehalose derivative **3** (**Figure 30**), leading to the corresponding SGLs (**Table I**). Binding of each SGL analog onto shCD1b was investigated by IEF (**Figure 31A** and **31B**) and compared to that of Ac₂SGL. SGL5, SGL6, SGL7, and SGL8, containing respectively saturated fatty acids with one, two, three, and four C-methyl branched groups, showed efficient binding onto shCD1b, from 54% to 64% (**Figure 32**). In contrast, SGL9 to SGL13 analogs, that are characterized by the presence of α,β -unsaturated fatty acids, formed less complexes with shCD1b as the number of branched methyl groups increased. cIEF analysis confirmed a drop from 80% to 50% when the number of C-methyl groups increased from 1 to 5 (**Figure 32**). The SGL analogs esterified with saturated fatty acids were immunogenic when the number of C-methyl groups was equal to two (SGL6), and immunogenicity drastically increased with four methyl groups (SGL8) (**Figure 33B**). Also in the case of unsaturated SGLs, immunogenicity was observed with two methyl groups (SGL10), and increased progressively with three and four methyl groups (SGL11 and SGL12, respectively) (**Figure 33C**). Therefore, a direct correlation was observed between the immunogenicity of the SGL analogs and the number of C-methyl groups that substitute the aliphatic tail at the position 3 of the trehalose core. SGL13, which contains 5 branched methyl groups, showed exactly the same stimulatory capacity as SGL12 (**Figure 33C**), suggesting that the presence of additional branched methyl groups attached at carbons after C-8 does not improve antigenicity. SGL12, which is characterized by the (4S,6S,8S)-2,4,6,8-tetramethyltetracos-2-enoyl appendage, and SGL13, by the (4S,6S,8S,10S)-2,4,6,8,10-pentamethylhexacos-2-enoyl appendage, were the most immunogenic synthetic SGLs. It should also be noticed that the SGL analogs with α,β -unsaturated fatty acids were more immunogenic than the corresponding ones with saturated fatty acids, despite the fact that the hydroxyphthioceranoic acid of the natural Ac₂SGL is a saturated one (**Figure 33B** and **33C**). SGL12 and SGL13 showed similar efficacy, if not better, to that of Ac₂SGL since all three lipids induced release of similar high amounts of GM-CSF by T cells (**Figure 35A**). However, both SGL12 and SGL13 were less potent than

Ac₂SGL since higher doses were necessary to induce half maximal cytokine release. These effects are clearly depicted by the Lineweaver-Burk plot of the same data (**Figure 35B**), where all three lipids cross the efficacy axis (y axis) at close intercepts, whereas they are separated on the potency axis (x axis).

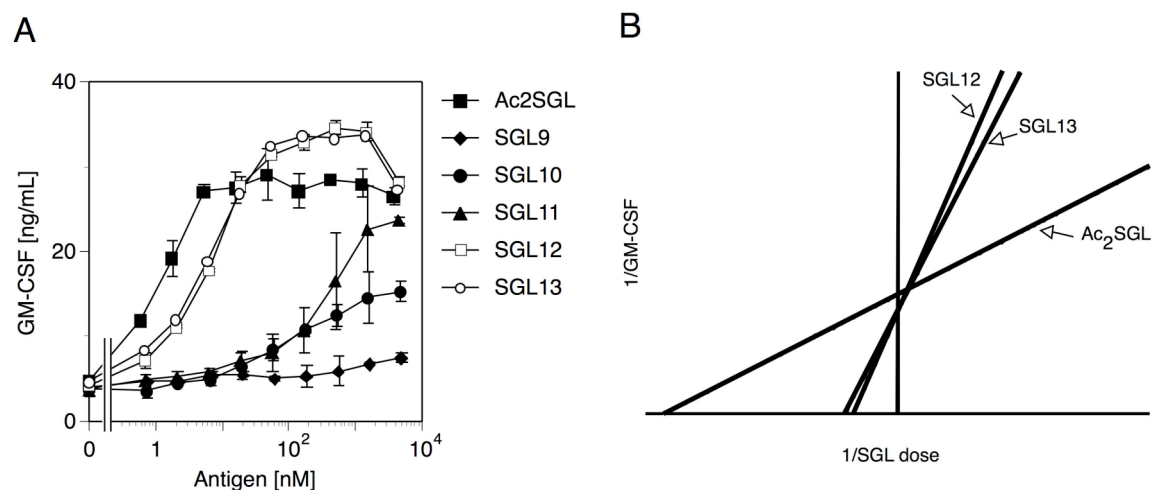


Figure 35: Immunogenicity of synthetic SGLs containing an α,β -unsaturated multimethyl aliphatic chain in position 3 of the trehalose core. **(A)** Human DCs were pre-incubated with different concentrations of natural Ac₂SGL or synthetic SGLs before addition of T cells. GM-CSF release was used to quantify T cell activation and is expressed as the mean ng/mL (\pm SD; n=3). The data are representative of three independent experiments. **(B)** Lineweaver-Burk plot comparing efficacy (y axis intercept) and potency (x axis intercept) of Ac₂SGL, SGL12, and SGL13.

These findings indicate that the branched methyl decorations of the acyl chain located at the position 3 of the SGL's trehalose core govern T cell stimulation.

The length of the conventional acyl chain located at the position 2 of the trehalose core modulates SGL antigenicity

To get further insights into the role of the acyl appendages for TCR recognition, we studied whether the length of the acyl chain located at position 2 of the trehalose unit would affect the binding onto shCD1b and/or T cell recognition. Two other SGL analogs with C₈ (SGL14) and C₂₄ (SGL15) linear acyl chains on position 2 were synthesized. These SGLs share the same (4S,6S,8S)-2,4,6,8-tetramethyltetracos-2-enoyl appendage at position 3

(Table I). Substitution of C₁₆ by C₂₄ acyl chain led to a drastic reduction in binding onto shCD1b, with only 20% of shCD1b:SGL15 complexes formed **(Figure 32)**. On the contrary, substitution by C₈ acyl chain resulted in 50% of shCD1b:SGL14 complexes formed. In addition, possibly as a consequence, stimulation of Ac₂SGL-specific T cells with SGL15 was very weak, whereas SGL14 was active, albeit less than SGL12 **(Figure 33D)**. The unexpected low binding of SGL15 onto shCD1b probably reflects the difficulty to accommodate one of the two C₂₄ aliphatic chains attached either at position 2 or 3 of the trehalose head inside the C' channel of CD1b. A C₂₄ long acyl chain might prevent insertion inside the C' pocket of CD1b. To test this hypothesis, we synthesized another SGL analog (SGL16) with a C₂₂ acyl chain at position 2 (dimethyldocos-2-enoyl acyl) and a C₁₆ (palmitoyl acyl) at position 3 **(Table I)**. SGL16 was then compared to SGL10, acylated by the same fatty acids but at the conventional position **(Table I)**. Up to 80% of shCD1b formed complexes with SGL16 **(Figure 32)**, showing that swapping the short with the long acyl appendages in position 2 and 3 did not alter binding to CD1b. However, SGL16 was not immunogenic **(Figure 33D)**. These findings can be explained by the capacity of the C₂₂ long chain at position 2 to accommodate inside the A'-T'-F' superchannel and the C₁₆ at position 3 to insert into the C' channel. As a consequence, the SGL16 trehalose-sulfate epitope probably rotates by 180° compared to its position in complexes involving Ac₂SGL, and is not capable of engaging the specific TCR anymore **(Figure 36)**.

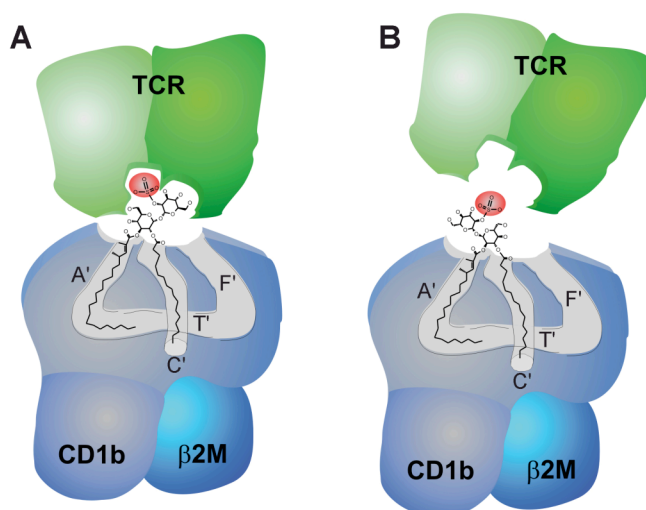


Figure 36: Schematic drawings of CD1b:SGL complexes interacting with the specific TCR. **(A)** CD1b:SGL10 complex forming stimulatory interactions with the TCR. **(B)** CD1b:SGL16 complex unable to form stimulatory interactions. SGL10 and SGL16 have the same acyl chains, but in permuted positions. The drawing shows insertion in the C' pocket of the C₁₆ acyl chain attached to either C2 (in SGL10) or to C3 (in SGL16). This allows both SGLs to bind shCD1b. However, only SGL10 forms the stimulatory complex interacting with the TCR.

Taken together, these data demonstrate that SGL analogs are immunogenic when they carry an aliphatic chain equal to, or shorter than C₁₈ (stearoyl acyl) at position 2 of the trehalose core, and when they carry a long multimethyl-saturated chain, or α,β -unsaturated fatty acyl appendage, at position 3. In addition, the length of fatty acid chains at positions 2 and 3 of the trehalose core might select the CD1b channel (A'-T'-F' vs. C') to fill, thus controlling the orientation of the polar head.

The absolute configuration of the C-methyl branched chiral carbons is sensed by the TCR

Hydroxyptioceranoic acids are dextrogyre multimethyl-branched saturated fatty acids [441, 442]. To better define the contribution of the chiral carbon stereochemistry to T cell recognition, we synthesized the analog SGL17 (**Table I**) by coupling the levogyre (R)-2,4-dimethyldocos-2-enoic acid at position 3 of 2-O-palmitoyl- α,α -D-trehalose derivative **3**

(Figure 30). The only structural difference between SGL17 and SGL10 is the absolute configuration of the chiral carbon of the acyl chains at position 3 of the trehalose core. Binding onto shCD1b was similar for both SGL analogs **(Figure 32)**, but only SGL10 was stimulatory **(Figure 33D)**. These data demonstrate that the configuration of the aliphatic chiral carbons affects TCR recognition.

Stimulation of Ac₂SGL-specific T cells by plate-bound shCD1b:SGL complexes

Differences in antigen trafficking to late endosomes [179] or in loading onto CD1b molecules *in vivo* may affect immunogenicity. The reduced potency of the most active synthetic analogs, compared to natural Ac₂SGL, as well as lack of activity of analogs that proved capable of binding to shCD1b *in vitro*, might then be ascribed to events occurring in living APCs. To exclude such possibilities, we investigated the stimulatory capacity of plate-bound shCD1b:SGL complexes. Plate-bound shCD1b complexed with Ac₂SGL induced strong T cell activation **(Figure 37)**, whereas control groups stimulated with unloaded shCD1b or without shCD1b were not activated, thus confirming the antigen-specificity of the T cell response.

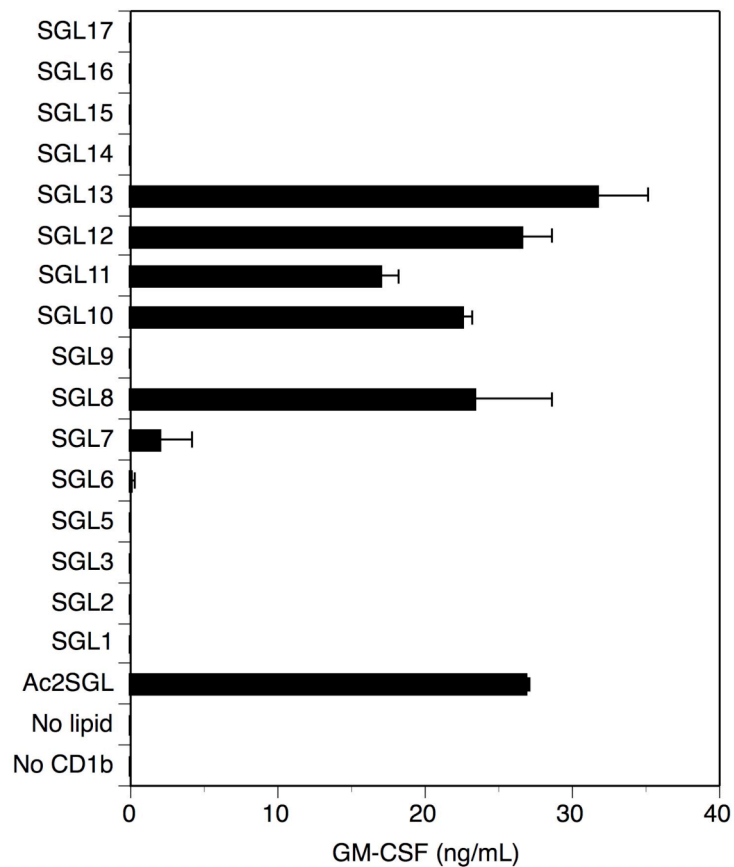


Figure 37: Stimulatory capacity of shCD1b:SGL complexes. Complexes were coated on 96 well plates before addition of T cells. GM-CSF release was used to quantify T cell activation and is expressed as the mean ng/mL (\pm SD; n=3). The data are representative of three independent experiments.

The shCD1b complexes formed with SGL8, SGL10, SGL12 and SGL13 were as active as Ac₂SGL, whereas SGL7 and SGL11 were less active than the natural compound (**Figure 37**). When the plate-bound assay results were compared to those obtained with living DCs, the shCD1b complexes formed with SGL7, SGL8, SGL11, SGL12 and SGL13 stimulated T cells like SGL-pulsed living DCs. SGL10 was more stimulatory in the plate-bound assay than with living DCs. Whether this difference is ascribed to more efficient formation of ternary complexes *in vitro* will be subject of future studies. The data obtained with the plate-bound assay confirmed: i) lack of immunogenicity of SGL analogs with linear acyl chains; ii) the decisive role of the chirality of the fatty acid attached at the position 3 of the trehalose (SGL17 vs. SGL10); iii) the TCR sensitivity to length changes on acyl chain at the position 2

of the trehalose (SGL14 *vs.* SGL12); and iv) the dramatic effect of aliphatic tail permutation at the position 2 and 3 (SGL16 *vs.* SGL10).

Discussion

The diacylated sulfoglycolipid antigen (Ac₂SGL) is produced by virulent Mycobacteria and stimulates CD1b-restricted T cells [178] with bactericidal activity. Ac₂SGL is characterized by the presence of dextrogyre multimethyl-branched fatty acids assigned, for the most abundant homolog, to C₃₂-hydroxyphthioceranoic acids at the position 3 of a 2'-O-sulfate- α,α -D-trehalose, the position 2 being acylated by a palmitic or stearic acid [178]. We systematically changed the type of aliphatic chains and tested each SGL analog using three different assays: i) Loading of SGLs to soluble human CD1b; ii) T cell activation with living DCs; and iii) T cell activation with plate-bound recombinant shCD1b. The combined evaluation of these tests allowed us to identify three experimentally supported rules governing Ac₂SGL immunogenicity.

The first rule is that the type of aliphatic chain is sensed by the TCR. Replacement of the hydroxyphthioceranyl appendage by conventional fatty acids, *i.e.* palmitic (SGL1) or hydroxypalmitic (SGL2), abrogates T cell stimulation, but not binding to CD1b. Replacement of the hydroxyphthioceranyl tail by a linear C₃₀ aliphatic appendage (SGL3) abrogates both binding to shCD1b and T cell activation. Thus, irrespective of the chain length (C₁₆ or C₃₀) these SGL variants are not immunogenic when presented by professional antigen-presenting cells such as DCs. Since SGL1 and SGL2 bind to shCD1b and are not stimulatory, they probably do not engage the TCR because the complexes formed with CD1b do not correctly expose the trehalose-sulfate epitope that activates T cells. Previous studies provided initial evidences that acyl appendages affect T cell stimulation [28, 154, 196] although it was not investigated whether binding to CD1 or interaction with the TCR were affected. Other studies reported that α GalCer analogs with short chains behave as weak agonists [156] and generate complexes with CD1d which interact with low affinity with the TCR [307].

The second rule is that the T cell stimulatory activity of Ac₂SGL depends on the presence of branched-methyl groups on the aliphatic tail at position 3 of the trehalose-sulfate. Indeed, at least two C-methyl branches in the fatty acids of SGL analogs are required for immunogenicity. A possible explanation is that insertion of ramified chains inside the CD1b pocket induces discrete conformational changes of CD1b amino-acid residues directly contacting the TCR. The terminal aliphatic C-methyl groups are close to the Ac₂SGL hydrophilic cap, and presumably contact residues of or beneath the CD1b α 1- α 2 helices. This

assumption is supported by lack of immunogenicity of SGL17 analog, which binds efficiently to CD1b and differs from the active SGL10 only in the absolute configuration of the C-methyl chiral carbon atoms. A previous study investigating T cell response to GlcMM reported that presentation of GlcMM to CD1b-restricted T cells is not affected by substantial variations in its lipid tail [179]. In the case of GlcMM, the proximal decoration is separated from the hydrophilic cap by at least 17 methylene units, and it was proposed that it lays deep inside the CD1b hydrophobic pocket [432]. This localization may explain why decorations are of lesser importance in the GlcMM-specific T cell responses, whereas they are essential in the case of Ac₂SGL in which the methyl groups are proximal to the ester bond linking the fatty acid to trehalose. This hypothesis is in agreement with the finding that addition of further methyl groups beyond 4 to SGL analogs does not enhance T cell response. Indeed, SGL13 that contains a fifth branched-methyl group on C-10 is as active as SGL12 that contains only four branched-methyl groups.

The third rule is that the length of the two aliphatic tails dictates in which CD1b pocket they will become inserted. The crystal structure of CD1b:SGL suggests that A' and C' are filled by the SGL acyl appendages (Garcia-Alles et al. manuscript in preparation). The C' pocket appears to behave as a molecular ruler, accommodating aliphatic chains with maximum lengths of 16-18 carbons. Thus, SGL10, SGL12 and SGL13, presenting a C₁₆ acyl chain at position 2 and C₂₂/C₂₄ at position 3, bind to CD1b and stimulate T cells. On the contrary, introduction of a short fatty acid at position 2 of the trehalose (C₈, SGL14) preserves binding to shCD1b, but dramatically decreases antigenicity. In addition, the presence of two C₂₄-long fatty acids at the positions 2 and 3 (SGL15) abolishes both binding to CD1b and T cell recognition. This finding confirms that the presence of C₁₆/C₁₈ aliphatic tails at position 2 appears to be mandatory. This is further supported by the strong CD1b-binding of the otherwise inactive SGL16. In SGL16, the acyl chains at positions 2 and 3 are permuted as compared to SGL10. The presence of one C₁₆ chain is compatible with insertion into the C' pocket, and with the formation of stable complexes with shCD1b. However, the permuted C₁₆ chain might impose a change of the position of the trehalose-sulfate epitope which prevents TCR recognition (**Figure 36**). Overall, these data suggest that the C' pocket is in a closed state, and does not allow accommodation of fatty acid tails longer than C₁₈. This is in accordance with the recent crystal structure of natively folded CD1b [133], and contrasts with previous crystallographic structures obtained from *in vitro* refolded CD1b that point to the

existence of a C' portal [39]. Whether *in vitro*, but not *in vivo*, refolding causes opening of the C' portal remains to be investigated. The presence of an open C' pocket was also proposed by studies showing that GlcMM with a C₂₄ α -mycolic chain stimulates specific T cells without trimming of this acyl chain [436]. These results might be explained with the possibility that different lipid antigens differ in the capacity to induce opening of the C' pocket. Alternatively, the GlcMM-specific TCR might recognize the epitope generated by incomplete insertion into the C' pocket, whereas the Ac₂SGL-specific TCR might require a complete insertion.

In a recent publication [196], the importance of acyl chains with branched-methyl groups has been described for mannosyl β -1-phosphomyketides (MPMs), a group of CD1c-presented mycobacterial antigens. Like the response to Ac₂SGL, also the response to MPMs is strictly dependent on the chiral conformation of the branched-methyl groups. Our data are in line with this possibility and extend this type of recognition to CD1b-presented lipid antigens. In addition, our findings show that a wrong chiral conformation does not prevent binding to the CD1 presenting molecule, but directly affects TCR activation. It should be noticed that branched lipids are synthesized by bacterial cells and not by mammalian cells. The fact that the immune system also discriminates microbial from host glycolipids by recognizing the presence of acyl appendages unique to microbial cells remains an open possibility. The present study, combining antigen binding to CD1b and T cell activation assays, aims at clarifying the requirements for binding onto the antigen-presenting molecule and for productive TCR engagement. These informations are of primary importance for the design of strong agonist lipid molecules to be used as subunit vaccines in tuberculosis. Chemical synthesis of antigenic SGL analogs aims at facilitating large scale production of immunogenic compounds, and allows to get rid of tedious lipid extraction from cultured *M. tuberculosis* strains. Immunisation studies with synthetic SGL analogs involving CD1b-transgenic mice are ongoing, and preliminary data will be presented in the next chapter of this thesis.

CHAPTER 3

Design of lipid-based subunit vaccines

Approximately one third of the world's population is infected with the causative bacterial agent *Mycobacterium tuberculosis*, and roughly 10% of these individuals will develop active tuberculosis within their lifetime. Of these individuals, approximately 2 millions per year do not survive [443]. Antimicrobial drugs are available, but treatment is costly, lasts a minimum of 6 months, and results in substantial hepatotoxicity. The most frequently recommended and effective combination is isoniazid, rifampicin, pyrazinamide, and ethambutol for 2 months, followed by isoniazid and rifampicin for 4 months [444]. In addition, the number of cases of multidrug-resistant tuberculosis (MDR-TB), *i.e.* resistant to rifampicin and isoniazid, and extensively resistant tuberculosis (XDR-TB), *i.e.* resistant to at least rifampicin and isoniazid, increases, multiplying the cost of treatment by a factor of 100 or rendering it ineffective [445]. It is interesting to notice that isoniazid and pyrazinamide function by inhibiting mycolic acids biosynthesis. When the disease becomes active, 75% of the cases are pulmonary TB, with a large spectrum of symptoms including prolonged cough, bloody cough, fever and weight loss. In the other 25% of active cases, the infection moves from the lung to extrapulmonary infection sites including the central nervous system (CNS) and the lymphatic system, and may infect other organs in rare cases. Diagnosis rely on acid-fast staining of sputum samples and skin testing with tuberculin (PPD), but new blood tests relying on IFN γ production by T cells in response to the presence of protein antigens from *M. tuberculosis* are on the way [446, 447]. BCG, an attenuated *M. bovis* strain, is widely administered worldwide as a vaccine against tuberculosis, but its efficacy remains controversial. BCG effectively protects infants from tuberculosis, but immunity declines with age and fails to protect adults against pulmonary tuberculosis, that is the primary source of dissemination [448-450]. In addition, BCG vaccination is ineffective for people that have been pre-sensitized to some species of environmental mycobacteria [451]. Therefore, a more effective vaccine against tuberculosis would be highly desirable.

It is important to mention that all successful vaccines developed thus far against acute diseases like smallpox, anthrax and rabies, function largely through production of specific antibodies. Design of vaccines against intracellular bacterial pathogens like *M. tuberculosis* remains more challenging since the pathogen hides within cells and thus escapes immune attack of antibodies. The novel vaccines against tuberculosis can be broadly divided into subunit vaccines, on one hand, and live attenuated vaccines, on the other. Subunit vaccines are made of one or two antigens, delivered with powerful adjuvants or by novel systems such as modified vaccinia virus Ankara, so the immune response during infection is directed against these antigens. Such antigens are selected on the basis of criteria such as strong recognition by the immune system during tuberculosis and high abundance or active secretion by *M. tuberculosis* during infection. It is the case for secreted mycobacterial antigens from the Ag85 complex, that might induce protective memory T lymphocytes when given as fusion proteins [452-454] or if expressed in a modified vaccinia virus Ankara [455]. This is based on the assumption that a protective immune response can be constituted by potent reactivity against a limited number of antigens. Concerning live attenuated vaccines, attempts have been made to genetically modify BCG, by inserting Ag85B [456] or by inserting listeriolysin to facilitate the escape of the bacilli from the phagosome into the cytoplasm [457], to improve its immunogenicity and thus vaccine efficacy. These vaccines are aimed at replacing BCG and must therefore be either safer or more effective than BCG. During infection of the lung, *M. tuberculosis* most likely enters alveolar macrophages and traffics to draining lymph nodes. The entry of *M. tuberculosis* into macrophages and DCs can occur via different receptor molecules including complement receptors, mannose receptor, DC-SIGN and Fc receptors [458-460], but also via uptake of apoptotic bodies and exosomes [217]. Upon internalization, mycobacterial phagosomes undergo maturation and fuse with lysosomes where the bacteria are degraded [461-467]. Resulting peptidic and lipidic fragments are then generated, enter respective presentation pathways and are loaded onto antigen-presenting molecules. In draining lymph nodes, macrophages and DCs present mycobacterial antigens to T cells which become activated and traffic back to the lung, where waves of infiltrating cells wall off infected macrophages present in structures called granulomas, resulting from the dynamic interaction between *M. tuberculosis* and the macrophages and T cells trying to kill them. Within these structures, and as long as the host immunity is effective, there's usually no adverse effect of *M. tuberculosis* on the host's

health [468]. This means that priming of T cells and rapid migration into the infected lungs are of critical importance in protection. The priming of specific T cells requires efficient presentation of mycobacterial antigens, and both *M. tuberculosis* and BCG are able to interfere with these processes to persist in the host. As described above, on entering macrophages, *M. tuberculosis* and BCG reside within phagosomes, which, under normal circumstances, undergo maturation, become acidified and fuse with lysosomes which contain hydrolases, lipases and peptidases that kill the bacillus. *M. tuberculosis* and BCG are able to arrest acidification of phagosome, enabling them to grow and persist within these vacuoles [222]. *M. tuberculosis* interferes with phagosome-lysosome fusion by preventing phosphatidylinositol 3-phosphate (PI3P) accumulation on phagosomal membranes [469]; by secreting the soluble kinase PknG inside the macrophage phagosomes that is further translocated into the host's cytosol [470]; and by recruiting coronin 1 to phagosomes that leads to influx of calcium and activation of calcineurin [223]. Despite this, the host responds by cross-priming both CD8⁺ and CD4⁺ T cells via MHC class I and MHC class II presentation pathways, respectively [217, 471]. In addition, unconventional T cells, that are glycolipid-specific and CD1-restricted, are also stimulated during *M. tuberculosis* infection [152, 178, 217]. Immunity generated by BCG vaccination comprises a wide spectrum of T cell phenotypes stimulated by protein and lipid antigens. However, the capacity of *M. tuberculosis* to block their transfer to lysosomes is operational almost exclusively in nonactivated macrophages. Once macrophages have become activated, *M. tuberculosis* is rapidly transferred to lysosomes where they are destroyed by bactericidal activities such as the generation of reactive oxygen and nitrogen. Here should also be noticed that other mechanisms allowing *M. tuberculosis* survival include its ability to inhibit antigen processing and expression of MHC class II molecules on the surface of infected APCs via TLR2 [472, 473], to induce T cell apoptosis [474-476], to neutralize the effect of nitric oxide generated within activated macrophages [477-479], to modulate macrophage activation via LAM-related lipid species [480, 481], and to reduce cross-priming between infected and non-infected cells by inhibiting apoptosis of infected cells [482, 483]. Recently, an additional evasion strategy that has been proposed consists of uncoupling the sequential relationship between MHC class II antigen loading and maturation of DCs, leading to evasion of peptide, but not lipid antigen presentation [484]. Here must also be noticed that both *M. tuberculosis*

and BCG interfere with the generation and function of APCs by reducing group 1 CD1 expression and subsequent T cell responses [290, 291].

Studies in mice have demonstrated that a Th1 cytokine profile is required for control of infection, with Th2 cells having little or no protective capacity. Moreover, IFN γ and TNF α are key cytokines in that they activate macrophages to control bacterial proliferation by increasing phagosomal-lysosomal fusion [485, 486] and autophagy [487]. Macrophage activation can also occur via TLR signaling [488, 489], and regulation of phagosome maturation seems to occur through the TLR adaptor protein myeloid differentiation factor 88 (MyD88) and the mitogen-associated protein kinase (MAPK) p38 protein [490, 491].

One key in optimizing vaccination strategies against tuberculosis may lie in improving access of antigen to presentation pathways, thus enabling highly efficient T cell priming to mycobacterial antigens. The lipids that we identified and generated, namely GroMM and SGL12, might constitute minimal structures to be loaded onto CD1b molecules via internalization without processing, thus facilitating efficient and specific T cell priming. Here, we further evaluated the potential use of these lipidic antigens in subunit vaccines, and propose some clues to enhance their immunogenic properties.

Results

GroMM immunogenicity is increased by lipidic adjuvants and structural modifications of its hydrophobic tail

During GroMM characterization (see Chapter 1), we noticed that GroMM-reactive T cells (Z5B71) were also responding to polar lipidic fractions isolated from *M. bovis* BCG that should not contain GroMM. Indeed, MALDI-*Tof*-MS analysis of these fractions did not reveal the presence of GroMM (not shown). However, they were enriched in PIMs, that do not stimulate Z5B71 T cells. These findings led us to the hypothesis that these immunogenic polar fractions may contain traces of GroMM in non-detectable quantities, whose antigenic properties may be enhanced by the presence of PIMs. Therefore, we tested mixtures of GroMM/PIM₂ in T cell stimulation assays using DCs as APCs and the Z5B71 T cell clone (**Figure 38**). The presence of PIMs markedly increased GroMM stimulatory capacity, in a dose-dependent manner, whereas PIM₂ alone did not elicit any T cell response.

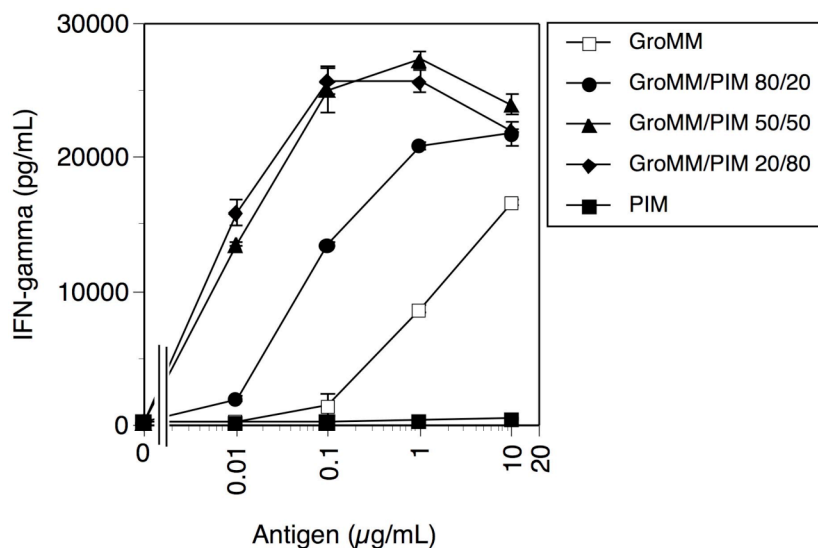


Figure 38: Effect of PIM₂ on GroMM stimulatory capacity. Human DCs were pre-incubated with different concentrations of GroMM/PIM₂ before addition of T cells. The antigen concentration on the x axis corresponds to GroMM concentration, except for the negative control. IFN γ release was used to quantify T cell activation and is expressed as the mean pg/mL (\pm SD; n=3). The data are representative of three independent experiments.

Maximal adjuvant effect was obtained with 50% PIM₂. Both efficacy and potency of GroMM were increased. Comparable results were obtained with PIM₆ (not shown). Other PI-related lipids, *i.e.* PI, LM and LAM, were also tested in mixture with GroMM and showed the same tendency whereas, alone, they did not elicit any response from GroMM-specific T cells (**Figure 39A, 39B and 39C**).

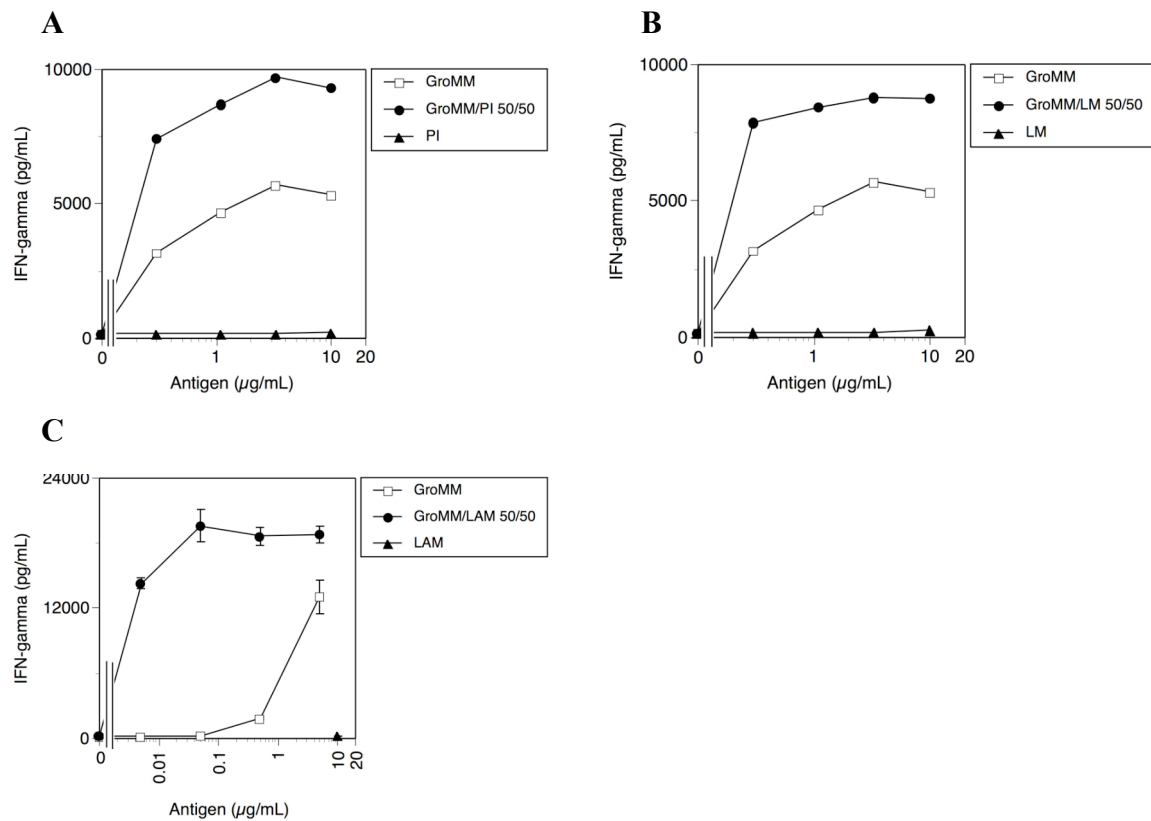


Figure 39: Effect of PI (A), LM (B) and LAM (C) on GroMM stimulatory capacity. Human DCs were pre-incubated with different concentrations of GroMM/adjuvant before addition of T cells. The antigen concentration on the x axis corresponds to GroMM concentration, except for the negative control. IFN γ release was used to quantify T cell activation and is expressed as the mean pg/mL. The data are representative of three independent experiments.

It is interesting to notice that also non PI-related lipids are capable of enhancing GroMM stimulatory capacity. It is the case for Ac₂SGL, that increases both efficacy and potency of GroMM, in a manner comparable to PI, PIMs, LM and LAM (Figure 40A).

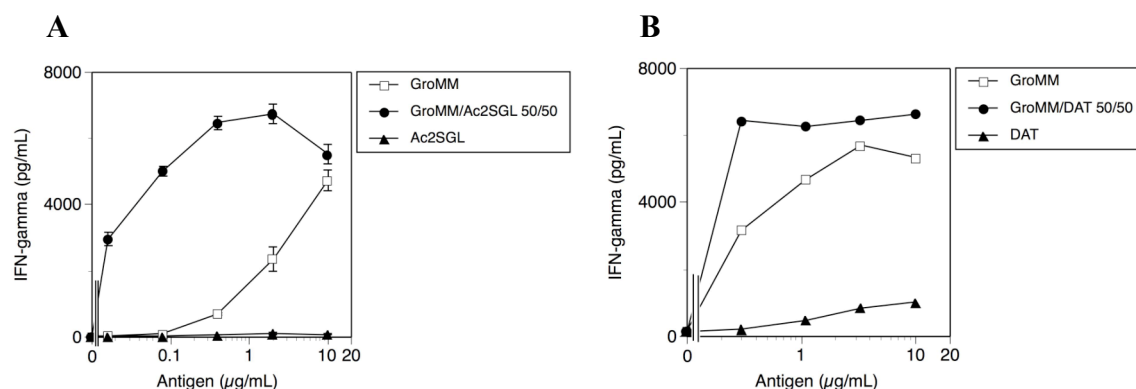


Figure 40: Effect of Ac₂SGL (A) and DAT (B) on GroMM stimulatory capacity. Human DCs were pre-incubated with different concentrations of GroMM/adjuvant before addition of T cells. The antigen concentration on the x axis corresponds to GroMM concentration, except for the negative control. IFN γ release was used to quantify T cell activation and is expressed as the mean pg/mL. The data are representative of three independent experiments.

Ac₂SGL, PI, PIMs, LM and LAM are all negatively charged. To evaluate the putative effect of the charge, activation experiments were carried out using DAT, that possess a structure similar to Ac₂SGL but are not sulfated, therefore bearing no negative charges. These compounds still have an enhancing effect when mixed with GroMM, but markedly reduced as compared to Ac₂SGL (**Figure 40B**).

It is interesting to notice that also chemical modifications of the structure of the hydrophobic tail of GroMM might influence GroMM immunogenicity, as reduction of a ketonic group to an alcohol at position 41 of the meromycolic chain strongly increases specific T cell pro-inflammatory response (**Figure 41**). One possible explanation is that this reduction may modify positioning of the glycerol head and subsequent recognition by the TCR by interfering with the way the end of the meromycolic chain protrudes out of the F' channel.

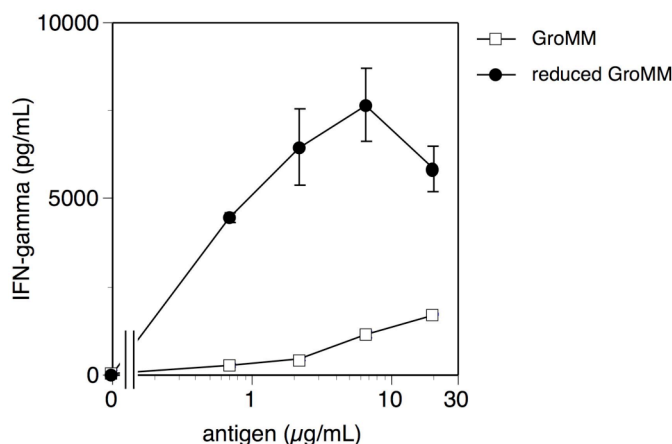


Figure 41: Effect of chemical structural modification of the lipid tail on GroMM stimulatory capacity. Human DCs were pre-incubated with different concentrations of GroMM or reduced GroMM before addition of T cells. IFN γ release was used to quantify T cell activation and is expressed as the mean pg/mL. The data are representative of three independent experiments.

These data show that other lipids may enhance GroMM immunogenicity, and that this effect might be related to their negative charges. In addition, structural modifications of the hydrophobic tail also seem to influence the immunogenic properties of GroMM.

PIMs and GroMM do not increase Ac₂SGL immunogenicity

In a second series of experiments, we tried to determine whether polar or apolar lipids could increase Ac₂SGL immunogenicity, as SGLs are promising compounds to be used in vaccines. Therefore, we tested mixtures of Ac₂SGL/PIM₂ and Ac₂SGL/GroMM in T cell stimulation assays using DCs as APCs and the Z4B27 Ac₂SGL-specific T cells as responder cells (**Figure 42**). In this case, the presence of PIMs did not influence Ac₂SGL antigenic properties. The decrease of activity of the mixtures was even proportional to the decrease of Ac₂SGL present in the sample (**Figure 42**).

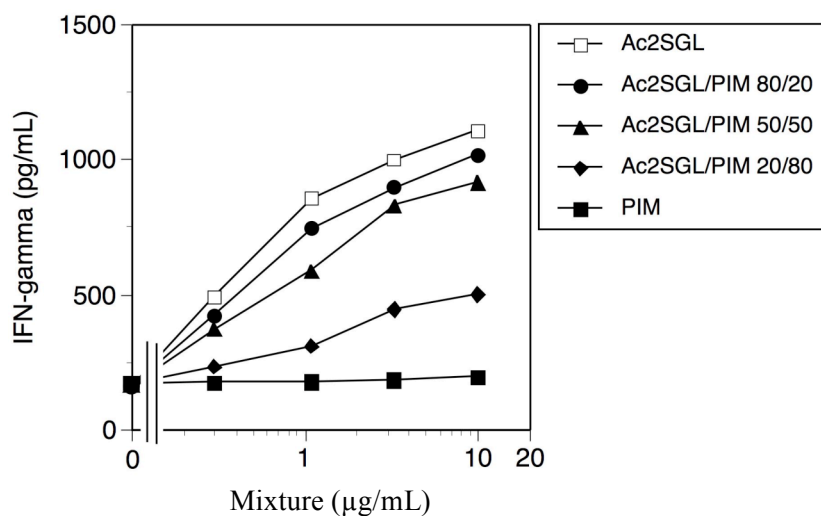


Figure 42: Effect of PIM₂ on Ac₂SGL stimulatory capacity. Human DCs were pre-incubated with different concentrations of Ac₂SGL/PIM₂ before addition of T cells. The concentration on the x axis corresponds to the complete mixture concentration. IFN γ release was used to quantify T cell activation and is expressed as the mean pg/mL. The data are representative of three independent experiments.

Use of GroMM to increase Ac₂SGL stimulatory capacity failed as well (**Figure 43**).

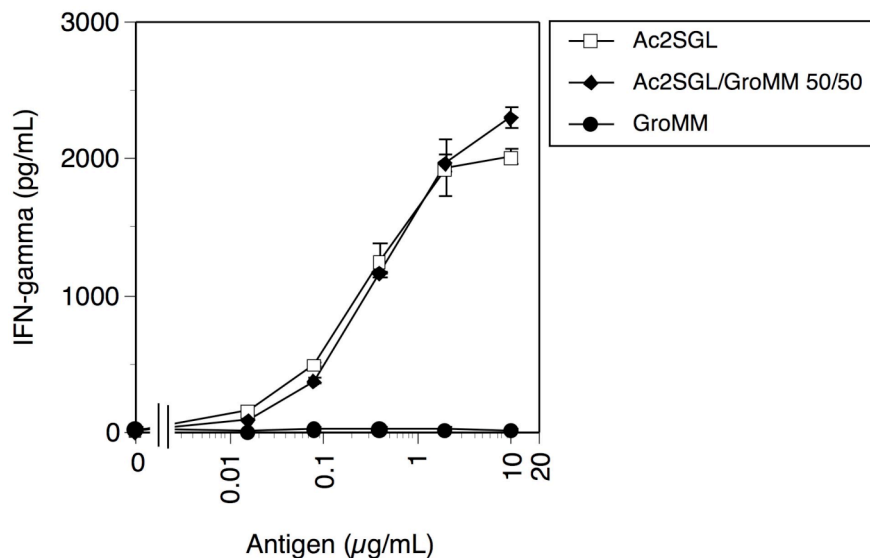


Figure 43: Effect of GroMM on Ac₂SGL stimulatory capacity. Human DCs were pre-incubated with different concentrations of Ac₂SGL/GroMM before addition of T cells. The antigen concentration on the x axis corresponds to Ac₂SGL concentration, except for the negative control. IFN γ release was used to quantify T cell activation and is expressed as the mean pg/mL. The data are representative of three independent experiments.

These data show that neither PIMs (polar) nor GroMM (apolar) lipids enhance Ac₂SGL antigenicity.

Lipid binding proteins can be used to increase Ac₂SGL immunogenicity

Lipid binding proteins (LBPs) are proteins ubiquitously distributed inside the cell, and also present in the extracellular milieu. Some have been shown to be involved in lipid loading/unloading onto CD1 molecules, pointing out crucial roles for LBPs in lipid immunogenicity. Precise function remains unclear for most of them, but several studies have shown their involvement in lipid solubilization and trafficking to acceptor membranes. Sterol carrier protein-2 (SCP-2) and human tocopherol associated protein (hTAP) have been shown to bind a wide variety of lipids [492-498], and shuttle them between membranes [492, 499-

506]. For these reasons, they were tested for their ability to increase stimulatory capacities of SGLs. When used in mixture with Ac₂SGL in activation assays, SCP-2 showed a striking ability to facilitate T cell response (**Figure 44A**), especially in the first hours of antigen uptake and presentation by DCs (**Figure 44B**).

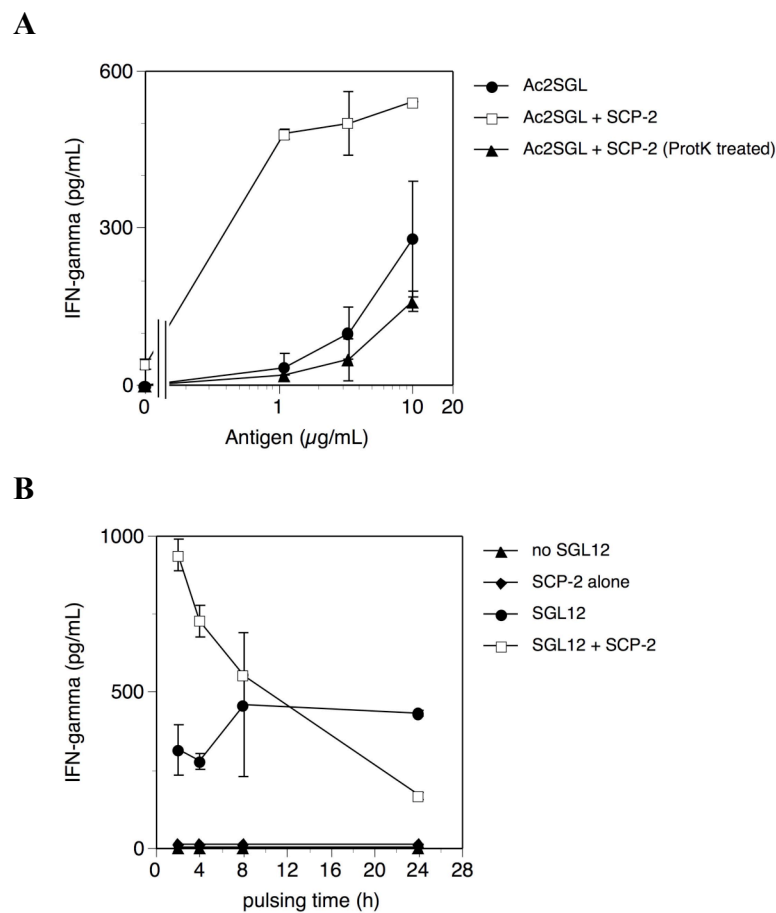


Figure 44: SCP-2 increases Ac₂SGL stimulatory capacity. **(A)** Human DCs were pre-incubated with different concentrations of Ac₂SGL in the presence or absence of SCP-2 before addition of T cells. **(B)** Human DCs were pulsed with SGL12 in the presence or absence of SCP-2 for different amounts of time, and washed before addition of T cells. IFN γ release was used to quantify T cell activation and is expressed as the mean pg/mL. The data are representative of three independent experiments.

Similar results were obtained with hTAP (**Figure 45**), clearly indicating that LBPs have the ability to increase the stimulatory capacity of polar lipid antigens, probably by allowing better solubilization, thus facilitating uptake by APCs and increasing availability for presentation to T cells.

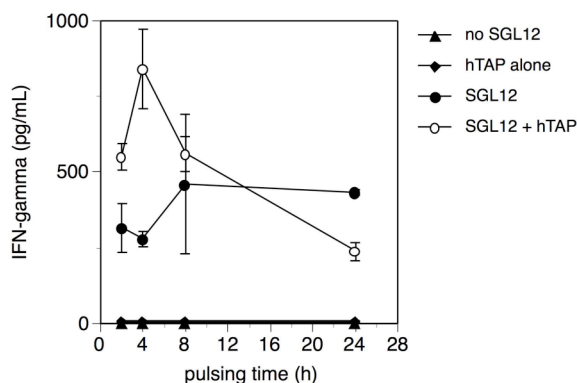


Figure 45: hTAP increases Ac₂SGL stimulatory capacity. Human DCs were pulsed with SGL12 in the presence or absence of hTAP for different amounts of time, then washed before addition of T cells. IFN γ release was used to quantify T cell activation and is expressed as the mean pg/mL. The data are representative of three independent experiments.

DCs from CD1b-transgenic mice present SGLs to Ac₂SGL-specific T cells in a CD1b-restricted manner

To further carry out preclinical studies involving SGLs, we generated transgenic mice expressing CD1b antigen-presenting molecule. CD1b functionality was assessed by activation assays using DCs from CD1b-transgenic mice as APCs to stimulate CD1b-restricted Ac₂SGL-specific human T cells (**Figure 46**). CD1b-transgenic DCs were able to elicit a strong T cell response by presenting synthetic SGL12 analog (**Table I**), whereas DCs from wild-type (WT) mice did not activate T cells (**Figure 46**). CD1b-restriction was further confirmed by inhibition with mAbs (**Figure 47**).

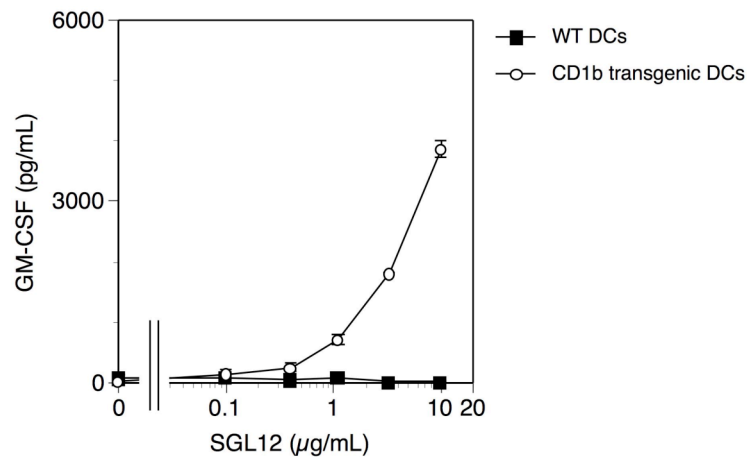


Figure 46: DCs from CD1b-transgenic mice successfully present SGLs to Ac₂SGL-specific human T cells. GM-CSF release was used to quantify T cell activation and is expressed as the mean pg/mL (\pm SD; n=3). The data are representative of three independent experiments.

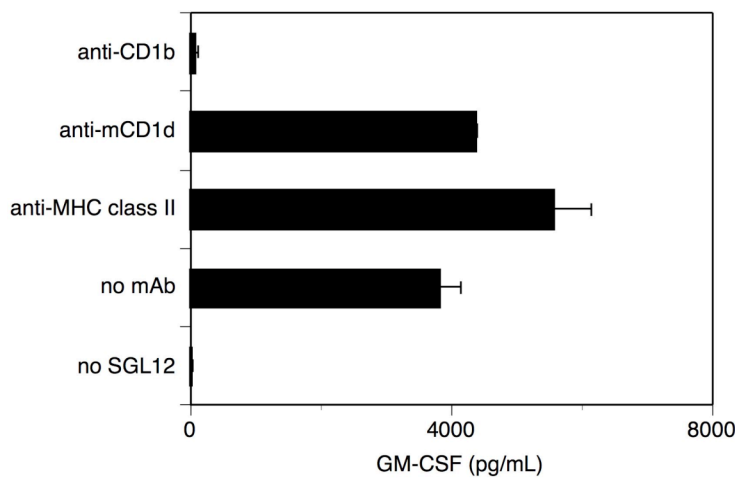


Figure 47: Presentation of SGLs using DCs from CD1b-transgenic mice to Ac₂SGL-specific T cells is CD1b-restricted. Mouse DCs were incubated with or without SGL12 and mAbs before addition of T cells. GM-CSF release was used to quantify T cell activation and is expressed as the mean pg/mL (\pm SD; n=3). The data are representative of three independent experiments.

We concluded that the CD1b molecule expressed by CD1b-transgenic mice is fully functional, and that these mice are suitable for pre-clinical purposes.

Generation of shCD1b:SGL12 dimers to stain CD1b-restricted Ac₂SGL-specific T cells

The current lack of molecular tools to stain CD1b-restricted T cells is a major limitation to the study of antigens presented by CD1b molecules. Therefore, we generated shCD1b:SGL12 complexes and used them to stain CD1b-restricted Ac₂SGL-specific T cells. First, we produced and purified recombinant shCD1b as described before [133]. Second, shCD1b molecules were mixed with a mAb directed against the BirA tag of shCD1b, and loaded with SGL12. Plate-bound activation assays using these complexes confirmed their ability to stimulate only CD1b-restricted Ac₂SGL-specific T cells (**Figure 48A**). Then, we used these dimers for flow cytometry analyses, and they successfully stained the TCR of Z4B27 cells (**Figure 48B**).

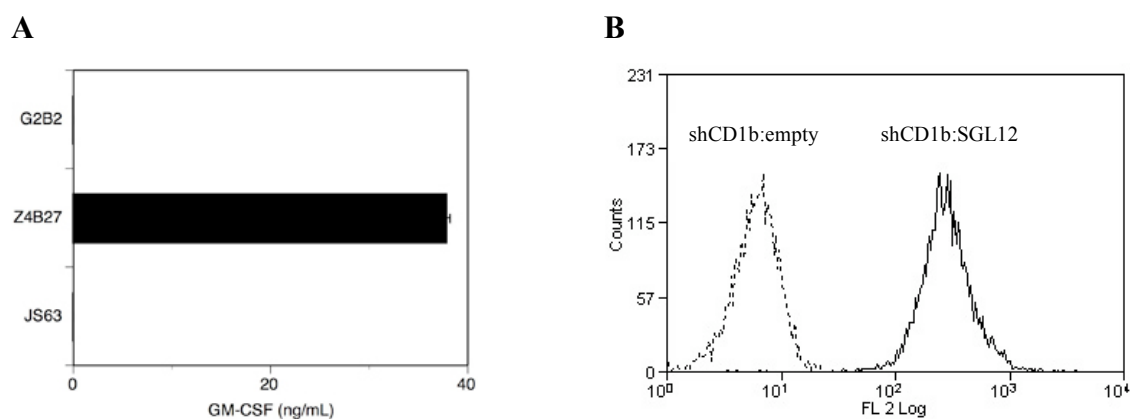


Figure 48: (A) shCD1b:SGL12 complexes exclusively stimulate CD1b-restricted Ac₂SGL-specific T cells (Z4B27), as $\gamma\delta$ T cells (G2B2) and CD1d-restricted cells (JS63) do not respond. Complexes were coated on 96 well plates before addition of T cells. GM-CSF release was used to quantify T cell activation and is expressed as the mean ng/mL (\pm SD; n=3). The data are representative of three independent experiments. (B) Human Ac₂SGL-specific T cell clone stained by shCD1b:SGL12 dimers. Numbers on the x axis correspond to the median fluorescence intensity. Numbers on the y axis corresponds to the number of events/cells acquired.

Immunization of CD1b-transgenic mice with synthetic SGLs leads to priming and expansion of SGL-specific T cells

Next, the potential of synthetic SGLs to prime T cells *in vivo* was tested. CD1b-transgenic mice were immunized with SGL12. To detect SGL-specific T cells by flow cytometry, we used shCD1b:SGL12 dimers. After immunization, phenotypic analysis of cells from lymph nodes confirmed the presence of shCD1b:SGL12-positive CD4⁺ and shCD1b:SGL12-positive CD8⁺ T cells in CD1b-transgenic mice (**Figure 49**).

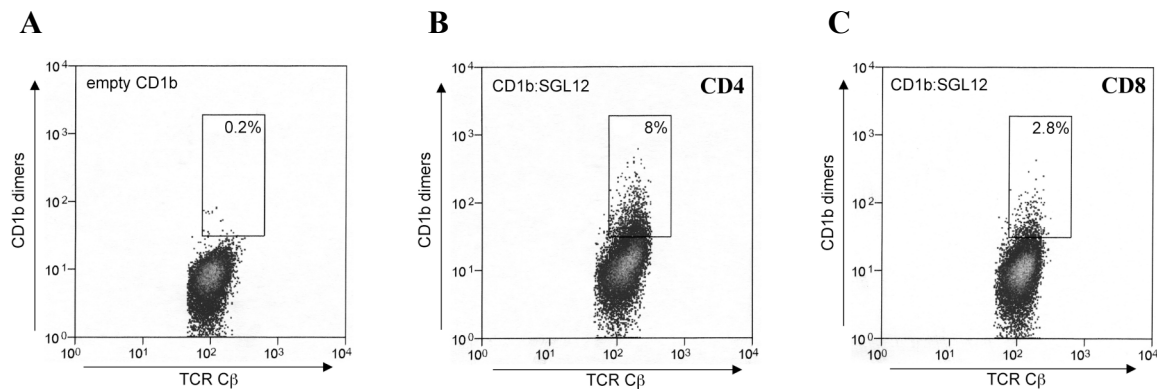


Figure 49: Immunization of CD1b-transgenic mice with SGL12 leads to priming and expansion of both CD4⁺ and CD8⁺ SGL12-specific T cells. **(A)** T cells were stained using unloaded CD1b dimers. **(B and C)** T cells were stained using CD1b dimers loaded with SGL12. Dead cells, B cells and macrophages were gated out. Numbers on the x and y axis correspond to the median fluorescence intensities.

These data suggest that immunization with SGL12 leads to consequent priming and expansion of SGL-specific T cells, thus confirming the potential of SGLs to be used in subunit vaccines.

Discussion

GroMM and diacylated sulfoglycolipids are CD1b-restricted antigens that have been identified as potential candidates for the design of lipid-based vaccines [178] [This thesis].

In order to increase their immunogenicity, we tried different approaches to facilitate their solubilization, thus enhancing their availability for APC uptake and presentation to T cells. In the case of GroMM, that is quite apolar, we found that mixtures with polar compounds like PI-related species remarkably increased both its potency and efficacy. One explanation to this phenomenon could be related to the charge of the polar lipids, as compounds like DAT, that bears no negative charges, showed only a minor effect on GroMM stimulatory capacity. This approach presents another considerable advantage due to the fact that antigenic bacterial lipids used to solubilize GroMM are also immunogenic, and might thus act in combination with GroMM to confer further protection in subunit vaccines. It is also interesting to notice that chemical modifications of GroMM structure enhances its stimulatory capacity as well, indicating that analogues with stronger antigenicity can be synthesized.

In the case of Ac₂SGLs, attempts to increase solubilization using both polar and apolar compounds failed. We speculated that lipid binding proteins capable of binding a large panel of lipid ligands might be able to behave as “solubilizers” too. Indeed, proteins like SCP-2 and hTAP have been shown to be able to transfer lipids to enzymes or between membranes [492, 499-506]. The results presented here confirm their capability to enhance the stimulatory capacity of polar lipid antigens, especially in the first hours of antigen uptake and presentation by professional APCs. These LBPs might allow better solubilization of lipid antigens, thus facilitating lipid uptake by APCs and increasing lipid availability for presentation to T cells. For both SCP-2 and hTAP, we also noticed a tendency to interfere with T cell activation after long incubation with APCs (24 hrs). This phenomenon might be toxicity due to high amounts of the LBPs in the culture medium, and should be avoided by tuning the concentration of the LBPs. Even if the safety and effectiveness of such approaches has still to be tested *in vivo*, they provide new hints to optimize the immunogenicity of lipid antigens.

One major limitation to the study of antigens presented by CD1b molecules is the current lack of molecular tools to stain CD1b-restricted T cells. Therefore, we generated shCD1b:SGL12 dimers, that specifically stimulated CD1b-restricted Ac₂SGL-specific T cells

in plate-bound activation assays. These dimers were also able to stain the TCR of Z4B27 cells, and can be used for flow cytometry analyses. The field of application of such dimers is wide, and they may allow study of CD1b-restricted SGL-specific T cell priming and expansion upon immunization, but also how these T cells behave in diseases. Successful loading of lipid ligands other than SGLs in these complexes may allow precise study of CD1b-restricted T cells.

Another limitation to the establishment of vaccines relying on lipids presented by CD1b molecules was the absence of a suitable animal model easy to handle. Mice do not express group 1 CD1 molecules, preventing any *in vivo* experimentation in these animals. Therefore, CD1b-transgenic mice were generated in our laboratory, and the functionality of the CD1b molecule expressed on the surface of APCs is shown here. We started to carry out immunization studies with our most stimulatory SGL analog, and our data using shCD1b:SGL12 dimers confirm priming and expansion of specific T cells *in vivo*. These findings are very encouraging, as we found that human Ac₂SGL-specific T cells kill intracellular *M. tuberculosis* [178]. It seems that also CD4⁺ T cells are expanded after immunization with SGL12. It is not known whether this type of cells directly contributes to cytotoxic and antimicrobial response in our case, but recent findings do not exclude such possibility [507]. Further characterization of these T cells is ongoing.

Overall, the data described in this last chapter confirm that lipid antigens presented by group 1 CD1 molecules can successfully prime and expand lipid-specific T cells *in vivo*. In addition, they prove that potent stimulatory analogs can be chemically produced and provide some clues about the way to optimize their properties using other antigenic or non antigenic compounds. The advantage of a vaccine that would kill bacteria instead of simply controlling their pathogenicity mostly relies on the cost of the treatment, as antibiotics are hardly affordable for low-income countries. In addition, it might prevent further development of resistant strains. Use of lipid antigens rather than peptides might also limit immune escape due to mutations, as lipids are products of multi-step synthesis. In the case of GroMM- and Ac₂SGL-based vaccination, another important point is their potential to be used as pre- and post-exposure vaccines. Indeed, because they are important constituents of the mycobacterial cell wall, they might be present in the structure of both active and dormant *M. tuberculosis*, that may not be the case for peptidic antigens.

Further studies, conducted *in vivo* in our CD1b-transgenic mice will evaluate safety and protective effect of lipid vaccination upon infection.

CONCLUSIONS

The work presented in this thesis aimed to identify and evaluate natural and synthetic lipid antigens as potential candidates to be included in subunit anti-mycobacterial vaccines. Indeed, lipid-based vaccines have already been shown to provide protection against *M. tuberculosis* [293].

Identification of GroMM as a lipid antigen widely distributed among bacteria belonging to the Corynebacteria-Mycobacteria-Nocardia group required use of a whole panel of techniques, from lipid extraction and fractionation, to *in vitro* assays using human cells and blood samples from patients. The fact that PPD⁺ patients, developing active tuberculosis, lack GroMM-reactive T cells is of primary interest. Whether their priming prevents re-activation of dormant *M. tuberculosis* needs to be carefully assessed.

Ac₂SGLs are immunogenic lipids found in the external part of the mycobacterial cell wall and are typical of virulent mycobacteria [178, 508, 509]. Combined analysis of binding and stimulatory capacity of synthetic SGL analogs allowed us to define structural features that permit fine tuning of their antigenicity. These features might help in the design of chemical compounds produced in large-scale for vaccinal purposes. Structural variations around the same antigenic moiety have the potential to precisely induce the required specific-T cell response, possibly avoiding side-effects, anergy, or auto-immune drifts.

Another interesting finding is the fact that different antigenic lipids have the ability to enhance their respective stimulatory capacity when mixed together. This means that a combination of lipids injected together during immunization may stimulate a whole panel of T cells differing in their specificity in a stronger manner compared to the same lipid species alone. In addition, the presence of recombinant LBPs seems to facilitate lipid uptake by professional APCs and subsequent presentation to T cells.

For the first time, CD1b dimers were generated and proven successful in the staining of CD1b-restricted T cells. Such molecular tool should greatly help to study these T cells, that are of primary importance in the immune response to mycobacteria.

Here are also shown for the first time data using a suitable mouse model to study lipid-based immunization. CD1b-transgenic mice immunized with synthetic SGL do show priming and expansion of SGL-specific T cells, confirming that pure lipids are immunogenic

in vivo. Analysis of these mice after *M. tuberculosis* infection will definitely shed light on the protective effect of SGL-related compounds.

Peptide-based subunit vaccines aim at improving protection by being administered after BCG vaccination, and already showed convincing effect in animal models [510-513]. However, without previous BCG vaccination, peptide-based mixtures might fail to stimulate lipid-reactive T cells required for protection. Thus, new vaccination strategies can easily be imagined, *e.g.* vaccination with BCG in combination with defined lipid/protein mixtures, or with defined lipid/protein mixtures without BCG, followed by a lipid/protein boost. In addition, lipid-based subunit vaccines might be used as pre- and post-exposure vaccines, allowing precise targeting of T cell populations that need to be re-stimulated after infection. Recently, the Global Advisory Committee on Vaccine Safety established by the World Health Organization recommended that BCG should not be administered to children known to be HIV infected for matter of safety [514]. This could present a major obstacle to novel vaccine approaches for vaccines relying on BCG prime. Prime vaccination relying on defined lipid species may represent an alternative.

MATERIALS AND METHODS

Synthesis of analogs, Mass Spectrometry and NMR were done by collaborators

Reagents. (R)-isopropylidene-glycerol and (S)-isopropylidene-glycerol, glyceryl tripalmitate (tripalmitin), 1,2 dipalmitoyl-sn-glycerol ((S)-glycerol 1,2-dipalmitate) and monopalmitoyl glycerol (1-O-palmityl-rac-glycerol) were purchased from Sigma (Saint Quentin Fallavier, France).

Bacterial Strain and Culture Conditions. *Nocardia asteroides* and *Corynebacterium glutamicum* were grown in suspension during 2 to 3 days at 32°C on Luria Broth and Brain Heart Infusion medium, respectively. Mycobacteria were grown during 4 to 8 weeks at 37°C on Sauton's medium as surface biofilm. Cells were harvested, separated from the culture media, and left in chloroform/methanol (2:1, v/v) at room temperature to kill bacteria.

Cell Culture. Human promyelocytic THP-1 cells were transfected with cDNA of human CD1A, or CD1B, or CD1C genes or double-transfected with CD1B and CD1E using the BCMGS-Neo and -Hygro vectors by electroporation. Cells were grown in RPMI-1640 supplemented with 10% fetal calf serum (FCS), 10 mM HEPES, 2 mM UltraGlutamine II, MEM nonessential amino acids, 1 mM Na-pyruvate and 100 µg/mL kanamycin (all from Invitrogen, Basel, Switzerland). DCs were isolated from peripheral blood mononuclear cells (PBMCs) of healthy donors by culturing in the presence of recombinant IL-4 and GM-CSF, as described previously [13]. T cell clones were generated as described [515], and grown in RPMI-1640 supplemented with 5% AB human serum (Swiss Red Cross), 10 mM HEPES, 2 mM UltraGlutamine II, MEM nonessential amino acids, 1 mM Na-pyruvate, 100 µg/mL kanamycin and 100 units/mL human recombinant IL-2. **In Chapter 3:** mouse DCs were derived from bone marrow after 8 days differentiation in RPMI-1640 supplemented with 10% fetal calf serum (FCS), 10 mM HEPES, 2 mM UltraGlutamine II, MEM nonessential amino acids, 1 mM Na-pyruvate, 100 µg/mL kanamycin (Invitrogen) and 10 µg/mL mouse GM-CSF.

T Cell Activation Assays. In Chapter 1 and Chapter 3: DCs (3×10^4 /well) or CD1-transfected THP-1 cells (3×10^4 /well) were incubated for 2 hr at 37°C with different concentrations of sonicated antigens before the addition of T cells (10^5 /well in triplicate). Supernatants were harvested after 36 hr of incubation, and cytokine release was measured by using enzyme-linked immunosorbent assay (ELISA) kits (IFN γ from Instrumentation Laboratory, Schlieren, Switzerland; TNF α from BD Pharmingen, Basel, Switzerland). Data are expressed as mean pg/mL or ng/mL \pm standard deviation (SD) of triplicates. **In Chapter 2 and Chapter 3:** The Ac $_2$ SGL-specific and CD1b-restricted Z4B27 T cell clone has been characterized previously [178]. T cell activation assays with human DCs as APCs were performed as previously described [178]. Briefly, DCs (3×10^4 /well) in RPMI-1640 medium containing 10% FCS (Invitrogen, Switzerland) were preincubated for 2 hr at 37°C with different concentrations of sonicated Ac $_2$ SGL or synthetic SGL analogs before the addition of T cells (10^5 /well in triplicate). Supernatants were harvested after 18 hr of incubation, and GM-CSF release was measured by using enzyme-linked immunosorbent assay (ELISA) (R&D, Europe). Data are expressed as mean ng/mL \pm SD of triplicates. For the plate-bound activation assays, 128 nM of each shCD1b:Ac $_2$ SGL or shCD1b:SGL complex were coated on Nunc MaxisorpTM flat-bottom 96 well plate (NUNC, Roskilde, Denmark) for 16 hr at 4°C . Plates were then washed before addition of T cells (10^5 /well in triplicate) in RPMI-1640 medium containing 10% FCS. Supernatants were collected after 18 hr of incubation, and GM-CSF release was measured by ELISA (R&D, Europe). Data are expressed as mean ng/mL \pm SD of triplicates. **In Chapter 3:** For classical T cell activation assays, SCP-2 was used at 25 $\mu\text{g/mL}$, after overnight incubation at 56°C with or without treatment with 50 $\mu\text{g/mL}$ proteinase K. For kinetic experiments using LBPs, human DCs were incubated for different amounts of time with 3 $\mu\text{g/mL}$ of SGL12, in presence or absence of 4 $\mu\text{g/mL}$ of LBP before washing and incubation with T cells.

Analysis of CD1 Restriction. CD1 restriction was investigated by evaluating the inhibition of the T cell response in the presence of the following mAb supplemented at 10 $\mu\text{g/mL}$ 30 min before the addition of T cells: **In Chapter 1:** OKT6 (anti-CD1a, American Type Culture Collection ATCC CRL-8019), WM-25 (anti-CD1b; Immunokontakt, Lugano, Switzerland), L161 (anti-CD1c; Instrumentation Laboratory), W6-32 (anti-MHC class I, ATCC) and L243 (anti-MHC class II, ATCC). Anti-TCRV γ 9 (B3) mAb was used as

irrelevant mAb. **In Chapter 3:** M5-114 (anti-mouse MHC class II), 15F7 (anti-mouse CD1d, ATCC HB322) and BCD1b3.1 (anti-CD1b).

Pulsing and infection of DCs with *M. tuberculosis*. *M. tuberculosis* was killed at 80°C for 20 min and incubated in RPMI-1640 medium containing 10% FCS for 2 hr at 37°C with DCs (3×10^4 /well) before addition of T cells (10^5 /well in triplicate). DCs were infected as previously described [175] and IFN γ release was monitored by ELISA.

Lipidic Fractions Used for Generation of T Cell Clone. The Z5B71 T cell clone was generated as described [178] by stimulating PBMCs of a PPD⁺ healthy donor with a *M. bovis* BCG PIM₂-enriched fraction [516]. Briefly, *M. bovis* BCG cells were suspended in chloroform/methanol (1:1, v/v) and filtered four times. The chloroform/methanol extract was concentrated and constituted the lipidic fraction, which was further partitioned between water and chloroform. The chloroform phase was evaporated and suspended in a minimum volume of chloroform. The addition of acetone overnight at 4°C led to formation of a precipitate, which was centrifuged (3,000 g at 4°C for 15 min) to generate an “acetone-soluble” phase and an “acetone-insoluble” phase. The “acetone-soluble” phase was applied to a QMA-Spherosil M (BioSeptra SA, Villeneuve-la-Garonne, France) column eluted successively with chloroform, chloroform/methanol (1:1, v/v), methanol to elute neutral compounds and then with chloroform/methanol (1:2, v/v) containing 0.1 M ammonium acetate to elute negatively charged compounds. This last fraction corresponds to the “PIM₂-enriched fraction”.

Lipidic fractions from several actinomycetes. Different lipidic fractions were prepared (as described above) from several actinomycetes species and tested against the Z5B71 T cell clone. The lipidic fractions from the following bacteria were tested: *M. smegmatis*, *M. tuberculosis* H37Ra, *M. fortuitum*, *M. xenopi*, *N. asteroides* and *C. glutamicum*, the “acetone-soluble” phase from *M. smegmatis*, *M. tuberculosis* H37Rv, *M. gastri*, *M. kansasii*, *M. marinum* and *M. bovis* BCG. The “acetone-insoluble” lipids from *M. tuberculosis* H37Rv, *M. gastri*, *M. kansasii*, *M. marinum* and *M. bovis* BCG were also tested.

Purification of the GroMM from *M. bovis* BCG. The “acetone-insoluble” fraction from *M. bovis* BCG, obtained as described above, was subjected to methanol precipitation

giving “methanol soluble” and “methanol insoluble” fractions. The “methanol-insoluble” fraction (150 mg) was fractionated on a silica acid column (1.3 x 23 cm) eluted with 7x175 mL of chloroform (fractions 1-7), 8x200 mL of chloroform/methanol (95:5, v/v) (fractions 8-15), 9x225 mL of chloroform/methanol (9:1, v/v) (fractions 16-24), 7x175 mL of chloroform/methanol (85:15, v/v) (fractions 25-31) and 7x175 mL of chloroform/methanol (7:3, v/v) (fractions 32-38). Fractions 5 to 8 were found to contain GroMM and were pooled. Purifications were checked by TLC on aluminium-backed silica gel plates (Alugram Sil G; Macherey-Nagel) using as migration solvent chloroform/methanol (95:5, v/v). Anthrone (9,10-dihydro-9-oxo-anthracene) (Sigma) at 0.2% dissolved in H₂SO₄ at 85% was used to detect glycolipids.

GroMM Acetylation. Peracetylation was performed on 200 µg of GroMM which were dissolved in acetic anhydride/anhydrous pyridine (1:1, v/v) and heated at 80°C for 30 min. The reaction mixture was dried under a stream of nitrogen and dissolved in chloroform for MALDI-*Tof*-MS analysis. For selective acetylation of GroMM hydroxyl functions, 16 µL of acetic acid were added to 10 mg of GroMM dissolved in 150 µL of pyridine and kept 3 hr at 0°C. Mono- and di-acetylated GroMM were extracted by CHCl₃ and purified on silica column eluted successively by CHCl₃ and CHCl₃/CH₃OH 95/5 (v/v). The number of acetyl substituents and their location on GroMM were determined by MALDI-*Tof*-MS and NMR analysis.

GroMM Saponification. 800 µL of methoxyethanol/KOH 20% (7:1, v/v) were added to 500 µg of GroMM. The mixture was then heated at 100°C for 3 h. After cooling and acidification by aqueous sulphuric acid at pH 3.0, mycolic acids were extracted three times by diethyl ether (v/v). Ether phases were pooled, washed five times with water and dried under a stream of nitrogen. Mycolic acids were redissolved in 100 µL chloroform for MALDI-*Tof*-MS analysis.

GroMM Synthesis. Reactions were performed under argon in anhydrous solvents. (*S*)-1-O-(4-Methylbenzene sulfonyl)-2,3-O-isopropylidene-glycerol [425]: p-toluene sulfonyl chloride (0.3 g, 1.57 mmol) was added at 0°C to (R)-isopropylidene-glycerol (230 mg, 1.74 mmol) dissolved in anhydrous pyridine (0.8 mL). After 24 hr at room temperature,

diethyl ether was added to the reaction mixture and the organic phase was washed sequentially with cold, 1 M hydrochloric acid, water, saturated sodium bicarbonate solution and water. The ether extract was dried on magnesium sulphate and concentrated. Chromatography on silica gel (elution with petroleum ether / ethyl acetate 4/1, v/v) gave the product (around 100 mg, 0.35 mmol). In the same manner, (R)-1-O-(4-methylbenzenesulfonyl)-2,3-O,O-isopropylidene-glycerol was obtained from (S)-isopropylidene-glycerol.

Potassium mycolates: Mycolic acids (gift of Dr. M.A. Lanéeelle, IPBS, Toulouse) were released from *M. tuberculosis* H37Rv cells as described [420]. Potassium mycolates were obtained by two successive washings of mycolic acids dissolved in chloroform with 10 mM hydrochloric acid and 5 M potassium hydroxide. After extraction with chloroform, potassium mycolates were dried on magnesium sulphate and concentrated.

(S)-1-O-Mycoloyl-2,3-O,O-isopropylidene-glycerol [426]: Potassium mycolates (8 mg, ~6 μmol) were added to (S)-1-O-(4-methylbenzenesulfonyl)-2,3-O,O-isopropylidene-glycerol (2 mg, 7 μmol) in anhydrous dimethylformamide (0.150 mL) and stirred for 3 days at 135 °C. The reaction mixture was acidified by 1 M hydrochloric acid and extracted by diethyl ether. Ether extract was then washed with water, dried on magnesium sulphate and concentrated. Chromatography on silica gel (elution with petroleum ether / diethyl ether 5/1, v/v) gave the product (around 4 mg, 2.9 μmol). In the same way, (R)-1-O-mycoloyl-2,3-O,O-isopropylidene-glycerol was obtained from (R)-1-O-(4-methylbenzenesulfonyl)-2,3-O,O-isopropylidene-glycerol.

(S)-1-O-Mycoloyl-glycerol (GroMM) [425]: 100 μL of concentrated hydrochloric acid ($d=1.017$) were added to (S)-1-O-Mycoloyl-2,3-O,O-isopropylidene-glycerol (4 mg, 2.9 μmol) dissolved in diethyl ether (0.1 mL). After 10 min of stirring at room temperature, water was added to the reaction mixture and the product (3 mg, 2.3 μmol) was extracted with diethyl ether. The ether extract was dried on magnesium sulphate and concentrated. Supplemental purification was not necessary. (R)-1-O-mycoloyl-glycerol was also obtained using (R)-1-O-mycoloyl-2,3-O,O-isopropylidene-glycerol.

MALDI-Tof-MS. In Chapter 1: MALDI-Tof-MS analysis were performed on a 4700 Proteomics Analyser (with Tof-Tof Optics, Applied Biosystems) using the reflectron mode. Ionization was effected by irradiation with pulsed UV light (355 nm) from an Nd:YAG laser. GroMM samples were analyzed by the instrument operating at 20 kV in the positive ion

mode using an extraction delay time set at 20 ns. Typically, spectra from 100 to 250 laser shots were summed to obtain the final spectrum. The HABA (2-[4-hydroxy-phenylazo]-benzoic acid) matrix (Sigma-Aldrich) was used at a concentration of ~10 mg/mL in ethanol/water (1:1, v/v). Then, 0.5 μ L sample solution and 0.5 μ L of the matrix solution were deposited on the target, mixed with a micropipette and dried under a gentle stream of warm air. The measurements were externally calibrated at two points with mycobacterial PIM. ***In Chapter 2:*** Analysis by MALDI-Tof-MS was performed on a Voyager DE-STR (PerSeptive Biosystems) using the reflectron mode. Ionization was effected by irradiation with pulsed UV light (337 nm) from an N₂ laser. SGL samples were analyzed by the instrument operating at 20 kV in the negative ion mode using an extraction delay time set at 200 ns. Typically, spectra from 2500 laser shots were summed to obtain the final spectrum. All of the samples were prepared for MALDI analysis using the on-probe sample cleanup procedure with cation exchange resin. The HABA matrix (2-[4-hydroxyphenylazo]-benzoic acid; Sigma-Aldrich) was used at a concentration of ~10 mg/mL in ethanol/water (1/1, vol/vol). Typically, 0.5 μ L of SGL sample (10 μ g) in a CHCl₃/CH₃OH (4/1) solution and 0.5 μ L of the matrix solution, containing ~5-10 cation exchange beads, were deposited on the target, mixed with a micropipette, and dried under a gentle stream of warm air. The measurements were externally calibrated at two points with mycobacterial PIM.

NMR Analysis. *In Chapter 1:* NMR spectra were recorded with an Avance DMX500 spectrometer (Bruker) equipped with an Origin 200 SGI using Xwinnmx 2.6. GroMM was dissolved in CDCl₃-CD₃OD, (9:1, v/v) and analyzed in 200 x 5 mm 535-PP NMR tubes at 298 K. Proton chemical shifts are expressed in parts per million downfield from the signal of the chloroform ($\delta_{\text{H/TMS}}$ 7.27). All the details concerning correlation spectroscopy and homonuclear Hartmann-Hahn spectroscopy sequences used and experimental procedures were as previously described [517]. ***In Chapter 2:*** ¹H and ¹³C NMR spectra were recorded on Bruker ARX250, AV300 and DMX500 spectrometers, working at 250, 300 and 500 MHz respectively for the ¹H and at 63, 75 and 126 MHz for the ¹³C.

Recognition of GroMM by Lymphocytes from Tuberculosis Patients and Healthy Donors. PBMCs were purified from blood of healthy donors and tuberculosis patients after informed consent was given. All patients included in this study suffered from

culture proven pulmonary tuberculosis and were undergoing treatment with anti-tuberculosis drugs for 2 to 8 weeks at the time of blood donation. PBMCs (10^5 /well) were cultured with autologous DCs (2×10^4 /well) in the presence or absence of 10 $\mu\text{g}/\text{mL}$ natural GroMM, PIM₂ or DAT. After 6 days supernatants were collected and tested for the presence of IFN γ by sandwich ELISA. PBMCs were kept at 37°C in supplemented RPMI 1640 medium (see above) during the 2 days of autologous monocytes differentiation to DCs. In parallel PBMCs were stimulated with 10 $\mu\text{g}/\text{mL}$ PPD (Chiron) and recombinant ESAT6 (Lionex). Healthy donors that responded by releasing at least 250 pg/mL IFN γ in response to PPD were scored as BCG immunized. Donors that responded to both antigens were considered as latently *M. tuberculosis* infected. Those that did not respond to PPD were scored as PPD-negative. For individual experiments, a cocktail of CD1b- and CD1c-blocking antibodies (BCD1b3.1 and F10 at 10 $\mu\text{g}/\text{mL}$ each) was added 30 min prior to GroMM to block CD1 presentation.

Molecular Modeling. CD1b in complex with GroMM was obtained from GlcMM by replacing the glucose moiety in the glycolipid head of the molecule by glycerol. The starting point for this work was the crystal structure of the CD1b-GlcMM complex [432]. We have used the Builder and Biopolymer modules of InsightII (BIOSYM/MSI, San Diego) to replace the glucose moiety by glycerol. The bonds and partial charges have been corrected and adjusted to the CVFF force field. In order to position the new fragment optimally with respect to the neighboring residues, we minimized the energy of the molecule with the Discover module, following the standard simulated annealing (SA) protocol. During the procedure, only the glycerol atoms were allowed to move, along with the side chains of Phe75 and Arg79, the closest spatial neighbors. Molecular dynamics was simulated during 20 ps with the time step of 1 fs, with temperature initially raised to 1000K and gradually lowered to 300K. The minimization was performed with the Conjugate Gradient algorithm, and was terminated upon reaching the threshold value for the root mean square gradients of 0.001 kcal/mol. In order to be able to compare the results directly with the original complex, we have subjected the CD1b-GlcMM complex to the identical procedure.

Synthesis of sulfoglycolipids. Details of the preparation of all synthetic sulfoglycolipids and their physicochemical data will be described in a separate manuscript. Briefly, the synthesis of SGL analogs is based on a 7-reaction sequence with an overall

product yield of about 5%. Preparation of SGL analogs started from known 4,6,4',6'-benzylidene protected trehalose derivative **1** [518] which was selectively acylated on the 2 position using palmitoyl chloride (or any other acid chloride) in pyridine. Use of a bidentate reagent (1,3-dichloro-1,1,3,3-tetraisopropylidisiloxane TCI_2) allowed the selective protection of the 2' and 3' positions of **2** in one step [519] and gave alcohol **3**. This reagent was selected owing to its easy deprotection in the presence of the benzylidene groups. This approach leaves the hydroxyl on position 3 as the only potential acylation site for esterification of compound **3** by the second fatty acid. Unmasking of the 2' and 3' positions of **4** afforded diol **5** which was selectively sulfated on the 2' position [520]. The synthesis of SGLs was completed after removal of the benzylidene protecting groups under carefully controlled acidic conditions. Compound structures were analysed by ^1H and ^{13}C NMR at each step of the synthesis and final SGLs structures were confirmed by MALDI-*Tof*-MS analysis.

Preparation of *M. tuberculosis* multimethyl fatty acids for hemisynthesis. *M. tuberculosis* DAT and TAT were purified following the method described in [178] for the purification of Ac_2SGL . DAT and TAT were eluted with Ac_3SGL and Ac_4SGL . The mix of lipidic compounds (127.4 mg) obtained were ethanolysed in a solution of sodium ethanolate (0.2 M) in ethanol/petroleum ether (1:2, vol) at room temperature for 20 hr. The reaction mixture was acidified with HCl solution (1 M) until pH 1.0, and the fatty esters were extracted with ethyl acetate/petroleum ether (1:4, vol) four times. The combined organic extracts were washed with water and dried over anhydrous magnesium sulfate. The solvent was removed and 107.3 mg of esters were obtained. All these compounds were separated by “flash” column chromatography eluted with petroleum ether/ether/acetic acid (9:1:0.1, 200 mL; 8.5:1.5:0.1, 100 mL; 8:2:0.2, 100 mL). The first fractions contained multimethylated non hydroxylated fatty esters (6 mg), then a mix with linear ones is eluted (69 mg) and after there were the multimethylated hydroxylated ones (3 mg). The first were pooled and saponified with 10 eq. of KOH in ethanol/water (3:2, vol) at 80°C overnight. The reaction was acidified with an HCl solution (1 M), acids were extracted with ether and the solvent was evaporated (5 mg). Then the corresponding SGL4 was synthesized following the general strategy depicted in the (**Figure 29**).

Synthesis of multimethylated fatty acids. Saturated and α,β -unsaturated dextrogyre mono-, di-, tri-, and tetramethyl-branched fatty acids and the unsaturated pentamethyl-branched fatty acid were synthesized following two different methods. The first one involves an iterative six-step sequence for the introduction of each branched-methyl group [521]. Although resulting in products of very high optical purity, the overall efficiency of this procedure is poor, and could not be used for the synthesis of acids with more than 3 asymmetric carbon atoms. A more efficient method, based on the asymmetric alkylation of SAMP-derived hydrazone enolates with alkyl-iodides [522], was used for the synthesis of the different multimethyl-branched saturated and α,β -unsaturated fatty acids (data not shown).

Analysis of shCD1b protein:SGL complexes by IEF. Lipid loading onto shCD1b was measured as described in [133]. Briefly, 10-20 μM of LysC-treated shCD1b and 100 μM of the sulfoglycolipid were shaken at 600 rpm for 1 hr at 37°C in a solution containing 50 mM Na acetate / 50 mM NaCl / 1 mM DTT / 1 mM EDTA at pH 4.0. After 6 hr the solution was cooled on ice, 2 μL were loaded onto the IEF 4-6.5 gel (Amersham Biosciences). A second aliquot of 1-2 μL was withdrawn for cIEF analysis (see below). Incubation in the presence of taurocholate (10 mM final conc.) was carried out similarly, with the exception that the pH of the solution was adjusted to 5.0 and the incubation time was reduced to 1 hr. Isoelectric-focusing electrophoresis (IEF) was performed in a PhastGel system (Amersham Biosciences) for 600 accumulated Volt hours (AVh). Protein bands were detected by staining with Coomassie R 350.

Generation of shCD1b and *in vitro* SGL binding assays. The extracellular soluble domain of human CD1b expressed in mouse cells, was purified by anti-CD1b affinity chromatography as described in [133]. To reduce the extent of uncontrolled proteolysis of the C-terminal extension BirA tag, the last 18 residues of shCD1b were removed by treatment with the endoprotease LysC. This preparation was then incubated with natural Ac₂SGL or synthetic SGL analogs at 37°C and pH 4.0 for 6 hr. In parallel experiments, Ac₂SGL or SGL were mixed with the mild taurocholate detergent at above CMC concentrations, and then incubated with shCD1b for 1 hr at 37°C and pH 5.0. The binding of Ac₂SGL or synthetic SGL to sCD1b proteins was monitored by isoelectric-focusing electrophoresis (IEF) in gel or by capillary electrophoresis (cIEF).

Capillary isoelectrofocusing (cIEF). The ProteomLab™ Capillary Isoelectric Focusing Kit (Beckman Coulter, Inc., Fullerton, CA) was used. It contains a neutral coated capillary, cIEF gel, ampholytes and protein standard markers. CE separations were performed on a ProteomeLab PA 800 System (Beckman Coulter, Inc., Fullerton, CA) with UV detection and neutral coated capillary, 50 µm ID x 30.2 cm (20 cm effective length to detector), was used for separations. Anolyte was 100 mM H₃PO₄ in cIEF gel (polymeric solution) and catholyte was 20 mM NaOH in water. An aliquot of 1-2 µL sample (prepared for IEF/gel) was mixed with 0.9 µL ampholyte 3-10 and 0.5 µL carbonic anhydrase 0.4 mg/mL (pI 5.9) in 50 µL cIEF gel. After filling the capillary with a sample/ampholyte mixture at 30 psi for 1.5 min, focusing was performed by applying a constant voltage of 15 kV for 6 min with normal polarity and 0.7 psi pressure both at the anode and cathode side. The mobilisation step was completed after 30 min at 21 kV by applying 0.7 psi pressure at the anode side. During separation, the capillary temperature was maintained at 20°C, CD1b and CD1b:lipid complexes were detected at 280 nm [523, 524].

Cloning, expression and purification of SCP-2 and hTAP. Oligonucleotide primers were synthesized based on the genomic SCP-2 sequence with a sense oligonucleotide primer (5'-CCCATGGGAAGCTCTGCAAGTGATGGA-3') and an antisense oligonucleotide primer (5'-AGGATCCGAGCTTAGCGTTGCCTGGC-3') (Operon Biotechnologies, Cologne, Germany). PCR was carried out by using the Advantage HF 2 PCR Kit (Clontech, Mountain View, CA) in a GeneAmp PCR System 9600 (Perkin-Elmer, Waltham, MA), with human spleen cDNA as a template. PCR conditions were: denaturation for 60 s at 94°C, and then 30 cycles under the following conditions: 20 s at 94°C, 30 s at 56°C, 90 s at 68°C. The resulting PCR product was purified with the QIAquick Gel Extraction Kit (Qiagen, Basel, Switzerland), subcloned into the pCR 2.1-TOPO vector (Invitrogen, Basel, Switzerland) and transformed in TOP 10 competent *E. coli* (Invitrogen). Clones were sequenced using M13 forward and reverse oligonucleotide primers (Microsynth, Balgach, Switzerland), and sequence analysis was done using MacVector. Purification of the plasmid was done using the NucleoSpin Plasmid Kit (Macherey-Nagel, Düren, Germany). SCP-2 coding sequence was removed from pCR 2.1-TOPO using *Nco* I and *Bam*H I, and subcloned into the pQE-60 vector (Qiagen), which contains the 6xHis-tag coding sequence. The pQE-60 vector

containing SCP-2 fused in-frame with the C-terminal 6xHis tag sequence was then transformed in BL21(DE3)pLysS *E. coli* bacterial strain (Promega, Madison, WI) for production. BL21(DE3)pLysS containing the construct were expanded at 37°C in LB broth (Difco Laboratories, Detroit, MI) + 100 µg/mL ampicillin (Sigma-Aldrich, Buchs, Switzerland) until OD₆₀₀ reaches 0.4-0.6. Transcription was then induced using 1 mM IPTG (Applichem GmbH, Darmstadt, Germany) and the bacterial pellet was collected 5 hr after induction. The pellet was resuspended in PBS 10 mM pH 7.5 and cells were lysed by sonication. Supernatant was collected after centrifugation and SCP-2 was purified using HIS-Select™ Spin Columns (Sigma-Aldrich).

The N-terminal 6xHis hTAP is a gift from JM Zingg (Tufts University, Boston, MA) and was cloned, produced and purified as previously described [525].

Generation of shCD1b:SGL12 dimers. 5 µM of shCD1b and 1 µM of mouse anti-BirA monoclonal antibody were incubated for 15 min at room temperature, then with 100 µM of SGL12, all in a solution containing 50 mM Na acetate / 50 mM NaCl / 1 mM DTT / 1 mM EDTA at pH 5.0. The mixture was shaken at 400 rpm for 1 hr at 37°C, then kept at 37°C for additional 3 hrs without shaking. Dimers are stable at +4°C for at least one week.

Flow Cytometry. shCD1b:SGL12 dimers were detected using goat anti-mouse IgG2b-RPE mAb (SBA, Birmingham, AL). Cells were stained with combinations of the following mAb conjugates, B220/Mac-PB (BioLegend, San Diego, CA), anti-TCRβ-AlexaFluor (H57-597), CD4/CD8-biotin (BioLegend), SAV-APC (Invitrogen). Samples were passed on a CyAn ADP flow cytometer (DakoCytomation, Baar, Switzerland), gated to exclude nonviable cells on the basis of light scatter and incorporation of propidium iodide. Data were analysed using Summit 4.3 software (DakoCytomation).

APPENDIX

Work discussed in the present thesis

Mycolic acids constitute a scaffold for mycobacterial lipidic antigens stimulating CD1b-restricted T cells

Collmann A, Layre E, Bastian M, Mariotti S, Czaplicki J, Prandi J, Mori L, Stenger S, De Libero G, Puzo G, Gilleron M.

These results have been accepted for publication in *Chemistry & Biology*.

Fatty acyl structures of *Mycobacterium tuberculosis* sulfoglycolipid govern T cell immunogenicity

Collmann A, Guiard J, Garcia-Alles LF, Mourey L, Brando T, Mori L, Gilleron M, Prandi J, De Libero G, Puzo G.

These results have been submitted to the *Journal of Immunology*.

Other participations

Synthesis of Diacylated Trehalose Sulfates: Candidates for a Tuberculosis Vaccine**

Julie Guiard, Anthony Collmann, Martine Gilleron, Lucia Mori, Gennaro De Libero, Jacques Prandi,* and Germain Puzo

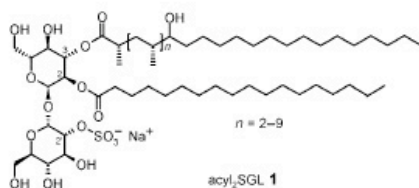
Tuberculosis remains a major world-wide health problem and results in the loss of almost 2 million lives annually, with the majority of deaths occurring in the developing world.^[1] Despite the discovery of active antibiotics in the 1960s and the production of the Bacillus Calmette–Guérin (BCG) vaccine in the early 20th century, tuberculosis is still not under control. The increasing incidence of human immunodeficiency virus (HIV) epidemics and the emergence of multidrug-resistant strains of *Mycobacterium tuberculosis*, the causative agent of tuberculosis, impair the eradication of the disease. New therapeutic approaches and the development of new vaccines to fight tuberculosis are thus urgently needed.

Recently, a diacylated sulfolglycolipid, acyl₂SGL (**1**),^[2] was characterized and identified as a new mycobacterial antigen able to stimulate populations of CD1b-restricted human T lymphocytes during infection with *M. tuberculosis*. Furthermore, these acyl₂SGL-specific activated T cells were shown to: 1) release interferon- γ (IFN- γ), 2) recognize *M. tuberculosis* infected antigen-presenting cells, and 3) kill intracellular mycobacteria in vitro.^[2] In light of these properties, sulfolglycolipid **1** seemed to be a promising candidate for the

development of a new tuberculosis vaccine. Compound **1** is specific to the *M. tuberculosis* species and is not present in *M. bovis* BCG, the species used in the current vaccine. The structure of acyl₂SGL encompasses an α,α -D-trehalose core, which is esterified at the 2-position with a palmitic (or stearic) acid, esterified at the 3-position with a hydroxyphthioceranoic acid, and O-sulfated at the 2'-position. Hydroxyphthioceranoic acids are a family of complex dextrorotatory fatty acids specific to the *Mycobacterium* genus, which contain a hydroxy group and methyl groups arranged in a 2,4,6 pattern.^[3] All methyl-substituted stereocenters are of the L series,^[3] whereas the configuration of the hydroxy-substituted carbon atom has not been assigned.

Compound **1** was isolated in tiny amounts (about 1 mgL⁻¹) from cultures of *M. tuberculosis*. Its low availability limits its further development as a potential tuberculosis vaccine. We therefore devised a synthetic route to this class of diacylated sulfated trehalose compounds and hypothesized that the hydroxyphthioceranoic acid, which is not readily available from natural sources, might be replaced by simpler fatty acids. Herein we report the preparation of various sulfolglycolipid (SGL) analogues of the natural compound acyl₂SGL (**1**) in which the hydroxyphthioceranoic acid has been replaced by less complex acids. Some of these analogues were able, like the natural product, to activate the acyl₂SGL-specific T-cell clone with the production of (IFN- γ). Of the utmost importance, it was found that small modifications to the structure of the hydroxyphthioceranoic acid substituent can modulate the immunogenicity of the analogues. Recent interest in the synthesis of mycobacterial sulfolglycolipids has led to the preparation of a tetraacylated trehalose sulfate.^[4,5]

The elaboration of the trisubstituted α,α -D-trehalose core of the sulfolglycolipids on the basis of the pioneering synthetic studies of Goren and co-workers, and Baer and Wu was straightforward.^[3,6,7] The known compound 4,6,4',6'-dibenzylidene α,α -D-trehalose (**2**)^[8] was acylated selectively at the 2-position (or 2'-position) by using palmitoyl chloride (or another acyl chloride) in pyridine to give a trehalose derivative **3** in 45% yield (Scheme 1). This direct acylation reaction avoided the dibutylstannylene procedure,^[6] which involves toxic tin derivatives and which was found to be difficult to carry out on a larger scale. The use of the bifunctional reagent 1,3-dichloro-1,1,3,3-tetraisopropylidioxane (TIPSCl₂) enabled the selective protection of the 2'- and 3'-positions of **3** in one step and gave alcohol **4** in good yield (60%). Owing to the steric crowding around the alcohol functionality of **4**, the nucleophilicity of the oxygen atom was low, and the esterification of compound **4** with fatty-acid derivatives proved to be difficult. The best yields of **5** (up to

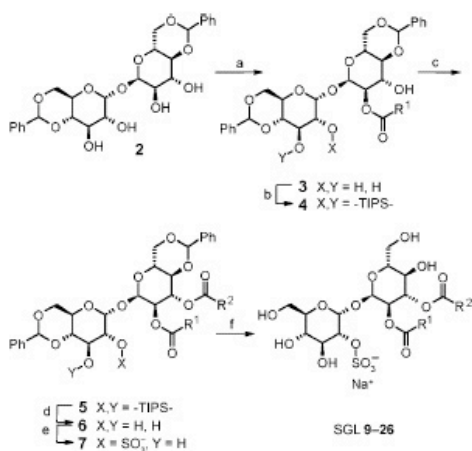


[*] J. Guiard, Dr. M. Gilleron, Dr. J. Prandi, Dr. G. Puzo
Département des Mécanismes Moléculaires des Infections
Mycobactériennes, Institut de Pharmacologie et de Biologie
Structurale du CNRS, UMR 5089, Université de Toulouse III
205 route de Narbonne, 31077 Toulouse Cedex (France)
Fax: (+33)5-61-17-59-94
E-mail: Jacques.Prandi@ipbs.fr

A. Collmann, Dr. L. Mori, Prof. Dr. G. De Libero
Experimental Immunology, Department of Biomedicine
University Hospital Basel
Hebelstrasse 20, 4031 Basel (Switzerland)

[**] Participating laboratories were funded by the 6th European Union
Framework Program (TB-VAC program, LSHP-CT-2003-503367).
M.G., J.P., and G.P. received funding from the Centre National de la
Recherche Scientifique (CNRS).

Supporting information for this article is available on the WWW
under <http://dx.doi.org/10.1002/anie.200803835>.

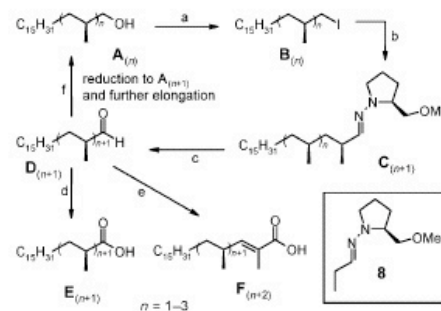


Scheme 1. General synthesis of sulfoglycolipids 9–26: a) R¹COCl, pyridine, DMAP, room temperature; b) TIPSCl₂ (1.2 equiv), pyridine, room temperature, 48 h; c) R²COCl (2.0 equiv), pyridine, DMAP, or R²COOH (2.0 equiv), DCC (2.0 equiv), toluene, microwave irradiation; d) 1 M *n*Bu₄NF in THF, room temperature, 24 h; e) SO₃·pyridine (1.5 equiv), DMF, room temperature, 24 h; f) 1.7% aqueous H₂SO₄/CHCl₃/MeOH, room temperature, 24 h. R¹ and R² groups are shown in Table 1. DCC = dicyclohexylcarbodiimide, DMAP = 4-dimethylaminopyridine, TIPS = tetraisopropylsilyloxane.

68%) were observed when the free fatty acid was activated with dicyclohexylcarbodiimide in toluene under microwave irradiation, but this method precluded the recycling of the fatty acid. When precious chiral polymethyl fatty acids were used, despite the lower acylation yields (26–54%), the reaction was carried out more classically in pyridine after activation of the acid by conversion into the acid chloride through treatment with oxalyl chloride. The 2'- and 3'-positions of diester 5 were unmasked with 1 M tetrabutylammonium fluoride in THF to afford diol 6 in high yield (>90%), provided that the slightly basic commercial solution had been neutralized to pH 6.5 (pH paper) with trifluoroacetic acid before use. Without this precaution, some scrambling of the acyl groups on the two glucose units of the trehalose was observed. Selective 2'-O-sulfation of diol 6 with the SO₃·pyridine complex in anhydrous *N,N*-dimethylformamide (DMF) at room temperature gave a mixture of 2'-O- and 3'-O-monosulfated trehalose derivatives. The observed regioselectivity was 5:1 in favor of the desired 2'-O-sulfate, and the regioisomers were separated readily by chromatography on silica gel. Compound 7 was isolated in 40–50% yield. The synthesis of the SGLs was completed by removal of the benzylidene protecting groups under carefully controlled acidic conditions (chloroform/methanol/1.7% aqueous H₂SO₄ 60:40:8 (v/v/v), room temperature), and the final products were isolated in almost quantitative yield. All compounds in Table 1 were prepared by this route.

Preliminary testing of the antigenic properties of sulfoglycolipids 9–11, which contain linear fatty acids with chain

lengths from C₁₆ to C₃₀, showed that they were unable to activate T cells specific for the acyl₂SGL complexes (data not shown). As the only difference between these compounds and the natural antigen is the nature of the 3-O-acyl group, these data emphasized the crucial role of the hydroxyphthiocerano-acyl group for CD1b presentation, T-cell-receptor (TCR) engagement, and T-lymphocyte activation. We therefore prepared polymethyl chiral fatty acids and incorporated them into the synthesis of the sulfoglycolipids. Hydroxyphthioceranoic and phthioceranoic acids belong to the deoxypolypropionate family of natural products. Numerous approaches to the stereoselective construction of the 1,3,5... polymethyl pattern on the basis of enolate alkylation,^[9–11] conjugate addition,^[12–14] or other methods^[15–17] have been reported. Recently, the first synthesis of phthioceranoic acid was completed by using an iterative catalytic asymmetric 1,4-conjugate addition of a Grignard reagent to an unsaturated thioester.^[18] As the synthesis of these polymethyl fatty acids is linear and use of a cycle of reactions, the number of steps involved, the reaction times, and the number of chromatographic purification steps are important parameters for the efficiency of the synthetic route. For these reasons, we chose the asymmetric alkylation of hydrazone enolates derived from (*S*)-1-amino-2-methoxymethylpyrrolidine (SAMP) with iodides, a method developed by Enders and co-workers,^[19,20] as the whole cycle of four reactions can be carried out in less than three days with only two chromatographic steps (Scheme 2).

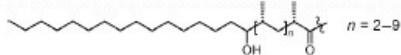
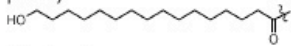
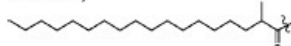
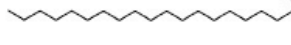



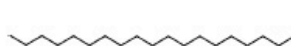
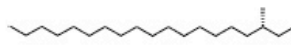
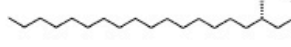
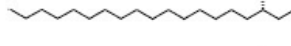


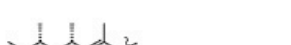
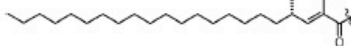



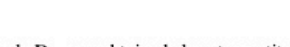


Scheme 2. General synthesis of polymethylated fatty acids: a) A_(n) (1.0 equiv), PPh₃ (1.2 equiv), I₂ (1.3 equiv), imidazole (3.1 equiv), toluene, reflux, 1 h; b) 8 (2.0 equiv), LDA (2.0 equiv), THF, 0°C, 1 h, then B_(n) (1.0 equiv), -50 → -25°C, overnight; c) 4 M HCl, petroleum ether, room temperature, 3 h; d) Jones reagent, acetone, 0°C, 30 min; e) (carboxyethylidene)triphenylphosphorane (1.2 equiv), CH₂Cl₂, room temperature, overnight, then 3 M KOH, H₂O/EtOH, reflux; f) BH₃·THF complex (1.7 equiv), THF, 0°C → RT, overnight. LDA = lithium diisopropylamide.

The starting material used was the long-chain alcohol A₍₁₎, which was obtained in 98% yield after the reduction with BH₃·THF of (2*S*)-2-methyloctadecanoic acid E₍₁₎^[21] in THF. The treatment of alcohol A₍₁₎ under conditions developed by Garegg and Samuelsson (PPh₃, imidazole, I₂ in toluene)^[22] gave iodide B₍₁₎ in 93% yield. This iodide was treated with the

Communications

Table 1: Synthetic analogues of 1.

Product	R ¹ CO	R ² CO
1	palmitoyl/stearoyl	
9	palmitoyl	palmitoyl 
10	palmitoyl	triacontanoyl 
12	palmitoyl	
13	palmitoyl	
14	palmitoyl	
15	palmitoyl	
16	palmitoyl	
17	palmitoyl	
18	palmitoyl	
19	palmitoyl	
20	palmitoyl	
21	octanoyl	
22	tetracosanoyl	
23		palmitoyl 
24	palmitoyl	
25	palmitoyl	
26	palmitoyl	

lithium enolate of SAMP propanal hydrazone (**8**)^[23] in THF to give the 2*S* alkylated product **C**₍₂₎ in good yield (72%). Owing to the very low solubility of the long-chain iodides **B**_(n) at -78°C in THF, alkylation reactions had to be performed at -50°C with warming to -25°C , and erosion of the optical purity of the products occurred to a small extent. The diastereomeric ratio for each alkylation was 94:6. The key

aldehyde **D**₍₂₎ was obtained almost quantitatively after acidic hydrolysis of hydrazone **C**₍₂₎ in a petroleum ether/aqueous HCl biphasic mixture at room temperature. This aldehyde could then be oxidized quantitatively with the Jones reagent^[24] to the saturated acid **E**₍₂₎ or submitted to a Wittig reaction with (carboxyethylidene)triphenylphosphorane followed by saponification to give the unsaturated acid **F**₍₃₎

in 80–85% yield. Aldehyde **D**₍₂₎ could also be reduced with the BH₃·THF complex in THF to alcohol **A**₍₂₎ in quantitative yield and the whole cycle repeated with comparable overall yield for the introduction of additional methyl groups.

This procedure is short and efficient (only four steps and 60% overall yield for each cycle) and can be scaled up easily. All polymethyl fatty acids prepared by this route are presented in Table 1 (third column). They were used for the synthesis of the corresponding sulfolipids **13–26** according to the general procedure described herein.

Sulfolipids **9–26** were tested for their ability to activate the acyl-SGL-specific T cells by following the reported procedure.^[2] Human dendritic cells that express the CD1b protein were incubated with varying amounts of the antigen, and the T-lymphocyte clone was added. The amount of IFN- γ released by the T cells was quantified, and dose-dependent curves were obtained (Figure 1a). As also

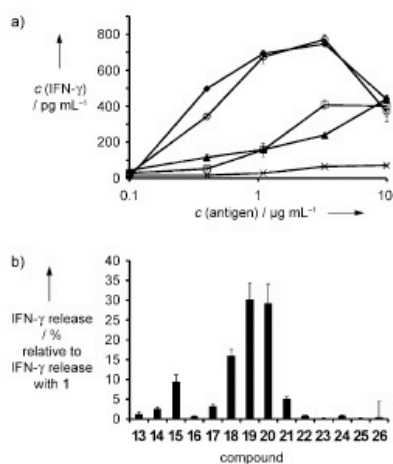


Figure 1. IFN- γ release by the T-cell clone. a) Response curves for compounds **14**, **15**, and **18–20**: \times **14**, \blacktriangle **15**, \square **18**, \circ **19**, \blacklozenge **20**. b) Relative intensity of IFN- γ release for analogues **13–26** compared to that for **1**, for a fixed antigen concentration of 3.3 $\mu\text{g mL}^{-1}$.

observed with the natural product, the maximum activity was usually observed for an antigen concentration of around 3 $\mu\text{g mL}^{-1}$. More importantly, it was found that the level of T-lymphocyte activation was highly dependent on the length, the position, and the structure of the fatty-acid residues connected to the trehalose core. When the hydroxyphthioceranoic acid moiety was replaced by linear fatty acids (products **9–11**, data not shown) or with saturated fatty acids containing one or two methyl groups (compounds **12** and **13**), no T-cell activation was observed (Figure 1b). When this fatty-acid chain was substituted with additional methyl groups (compounds **14** and **15**), a steady increase in the immunogenicity of the sulfolipids was observed. A similar relationship between the immunogenicity and the number of methyl

groups was observed when a chiral polymethylated α,β -unsaturated fatty acid was used in place of the hydroxyphthioceranoic acid moiety (see compounds **16–20**). However, with these unsaturated acids, there was no further improvement of the antigenic activity upon the introduction of a further methyl group once four methyl groups had been incorporated in the fatty-acid chain (compounds **19** and **20**).

Other structural variations on the SGLs gave more insight into the parameters which are crucial for the antigenic activity of these analogues. The length and the respective positions of the fatty acyl chains at the 2- and 3-positions of the trehalose unit were found to be very important. Shortening of the 2-*O*-acyl chain of the SGL from a palmitoyl (in **19**) to an octanoyl group gave compound **21**, the potency of which was greatly diminished with respect to that of **19**. An even more pronounced effect on the activity was observed when the 3-*O*-acyl group was shortened from a trimethyltracosanoyl chain to a trimethyloctanoyl chain (compare the results for **18** and **25**). Lengthening of the 2-*O*-acyl chain from a palmitoyl (in **19**) to a tetracosanoyl group (in **22**) was also deleterious to the T-cell-stimulatory activity. The immunogenicity was also lost when the two acyl groups in **17** were permuted, as in **23**. Finally, the introduction of further unsaturation at the γ,δ -position of the 3-*O*-fatty acid (in **26**) and the use of a methylated fatty acid with an *R* stereocenter (in **24**) gave inactive products.

A general and convenient synthesis of 2,3-di-*O*-acyl-2'-*O*-sulfate trehalose derivatives has been developed. This route enables the preparation of numerous analogues of the natural *M. tuberculosis* antigen sulfolipid **1**, with the incorporation of polymethylated chiral fatty acids in place of the complex hydroxyphthioceranoic acid moiety. Although none of the synthetic compounds were as potent as the natural sulfolipid **1**, some of these sulfolipids showed promising T-lymphocyte-activation properties. All active analogues have a saturated or monounsaturated polymethylated fatty acid with stereocenters of the *S* configuration at the 3-position of the trehalose core. These synthetic sulfolipids are available in large amounts, and their protective effects against tuberculosis infection might be investigated further. The synthesis of analogues with other variations of the fatty-acid structure is underway in an attempt to gain a better understanding of the factors that influence their interaction with CD1 proteins^[25,26] and their recognition by the TCR.

Received: August 4, 2008

Published online: November 3, 2008

Keywords: antigens · fatty acids · glycolipids · tuberculosis · vaccines

[1] <http://www.who.int/tb/en/>.

[2] M. Gilleron, S. Stenger, Z. Mazorra, F. Wittke, S. Mariotti, G. Böhrer, J. Prandi, L. Mori, G. Puzo, G. De Libero, *J. Exp. Med.* **2004**, *199*, 649–659.

[3] M. B. Goren, O. Brokl, B. C. Das, E. Lederer, *Biochemistry* **1971**, *10*, 72–81.

- [4] F. Lin, L. H. van Halbeek, C. R. Bertozzi, *Carbohydr. Res.* **2007**, *342*, 2014–2030.
- [5] C. D. Leigh, C. R. Bertozzi, *J. Org. Chem.* **2008**, *73*, 1008–1017.
- [6] H. H. Baer, X. Wu, *Carbohydr. Res.* **1993**, *238*, 215–230.
- [7] A. Liav, M. B. Goren, *Carbohydr. Res.* **1984**, *127*, 211–216.
- [8] H. H. Baer, B. Radatus, *Carbohydr. Res.* **1984**, *128*, 165–174.
- [9] A. Abiko, S. Masamune, *Tetrahedron Lett.* **1996**, *37*, 1081–1084.
- [10] A. G. Myers, B. H. Yang, H. Chen, L. McKinstry, D. J. Kopecky, J. L. Gleason, *J. Am. Chem. Soc.* **1997**, *119*, 6496–6511.
- [11] M. O. Duffey, A. LeTiran, J. P. Morken, *J. Am. Chem. Soc.* **2003**, *125*, 1458–1459.
- [12] D. R. Williams, A. L. Nold, R. J. Mullins, *J. Org. Chem.* **2004**, *69*, 5374–5382.
- [13] R. Des Mazery, M. Pullez, F. Lopez, S. R. Hanutyunyan, A. J. Minnaard, B. L. Feringa, *J. Am. Chem. Soc.* **2005**, *127*, 9966–9967.
- [14] B. ter Horst, B. L. Feringa, A. J. Minnaard, *Chem. Commun.* **2007**, 489–491.
- [15] T. Novak, Z. Tan, B. Liang, E.-i. Negishi, *J. Am. Chem. Soc.* **2005**, *127*, 2838–2839.
- [16] E.-i. Negishi, Z. Tan, B. Liang, T. Novak, *Proc. Natl. Acad. Sci. USA* **2004**, *101*, 5782–5787.
- [17] S. Hanessian, S. Giroux, V. Mascitti, *Synthesis* **2006**, 1057–1076.
- [18] B. ter Horst, B. L. Feringa, A. J. Minnaard, *Org. Lett.* **2007**, *9*, 3013–3015.
- [19] A. A. Birkbeck, D. Enders, *Tetrahedron Lett.* **1998**, *39*, 7823–7826.
- [20] D. Enders, J. Tiebes, N. De Kimpe, M. Keppens, C. Stevens, G. Smaghe, O. Betz, *J. Org. Chem.* **1993**, *58*, 4881–4884.
- [21] G. S. Besra, D. E. Minnikin, P. R. Wheeler, C. Ratledge, *Chem. Phys. Lipids* **1993**, *66*, 23–34.
- [22] P. J. Garegg, B. Samuelsson, *J. Chem. Soc. Chem. Commun.* **1979**, 978–980.
- [23] D. Enders, H. Eichenauer, *Tetrahedron Lett.* **1977**, *18*, 191–194.
- [24] K. Bowden, I. M. Heilbron, E. R. H. Jones, B. C. L. Weedon, *J. Chem. Soc.* **1946**, 39–45.
- [25] G. De Libero, L. Moti, *Trends Immunol.* **2006**, *27*, 485–492.
- [26] A. de Jong, E. Casas Arce, T.-Y. Cheng, R. P. van Summeren, B. L. Feringa, V. Dudkin, D. Crich, I. Matsunaga, A. J. Minnaard, D. B. Moody, *Chem. Biol.* **2007**, *14*, 1232–1242.

CUTTING EDGE

Cutting Edge: A Naturally Occurring Mutation in CD1e Impairs Lipid Antigen Presentation¹

Sylvie Tourne,^{2*§} Blandine Maitre,^{*†‡§} Anthony Collmann,[¶] Emilie Layre,^{||} Sabrina Mariotti,[¶] François Signorino-Gelo,^{*‡§} Caroline Loch,[#] Jean Salamero,^{**††} Martine Gilleron,^{||} Catherine Angénieux,^{*‡§} Jean-Pierre Cazenave,^{†‡§} Lucia Mori,[¶] Daniel Hanau,^{*‡§} Germain Puzo,^{||} Gennaro De Libero,[¶] and Henri de la Salle^{2*‡§}

The human CD1a–d proteins are plasma membrane molecules involved in the presentation of lipid Ags to T cells. In contrast, CD1e is an intracellular protein present in a soluble form in late endosomes or lysosomes and is essential for the processing of complex glycolipid Ags such as hexamannosylated phosphatidyl-myo-inositol, PIM₆. CD1e is formed by the association of β_2 -microglobulin with an α -chain encoded by a polymorphic gene. We report here that one variant of CD1e with a proline at position 194, encoded by allele 4, does not assist PIM₆ presentation to CD1b-restricted specific T cells. The immunological incompetence of this CD1e variant is mainly due to inefficient assembly and poor transport of this molecule to late endosomal compartments. Although the allele 4 of CD1E is not frequent in the population, our findings suggest that homozygous individuals might display an altered immune response to complex glycolipid Ags. *The Journal of Immunology*, 2008, 180: 3642–3646.

In humans, CD1a–d present lipids to T cells (1). They acquire self-lipid ligands in the endoplasmic reticulum (ER),³ where they are assembled, and lipid Ags in the endosomal compartments, where they cycle through after a transit from the cell surface (2). CD1e also participates in the presentation of lipids to T cells, but not as an Ag-presenting molecule. CD1e never transits through the plasma membrane but is directly targeted from Golgi compartments to early endosomes before reaching late endosomes and lysosomes (3). In these lat-

ter compartments CD1e facilitates the processing of complex glycolipids, which is required for their presentation by CD1b molecules. In particular, CD1e is essential in the processing of hexamannosylated phosphatidyl-myo-inositol (PIM₆) by the lysosomal α -mannosidase (4).

CD1, like MHC class I molecules, is composed of a transmembrane α -chain that noncovalently associates with the β_2 -microglobulin (β_2m). The α -chain folds in three structural α domains ($\alpha 1$ – 3), with the $\alpha 1$ and $\alpha 2$ domains delimiting a hydrophobic pocket-containing groove in which lipid ligands bind. For CD1e, the α -chain is cleaved between the $\alpha 3$ and the transmembrane domains in late endosomal compartments, generating by this way soluble CD1e, which represents the CD1e active form (4, 5). The human CD1 genes are poorly polymorphic. Only two alleles have been described for CD1A, B, C, and D (6, 7), the polymorphism of CD1B and C being silent (6, 7). CD1E is the most polymorphic CD1 gene, six alleles having been reported (6, 8, 9). Among individuals from diverse ethnic backgrounds, alleles 1 and 2 display a frequency of 49 and 51%, respectively (6), whereas the four other alleles have been described once (8, 9). The polymorphic nucleotides are located in exons 2 or 3 of the CD1E gene, encoding the $\alpha 1$ and $\alpha 2$ domains, respectively (see Fig. 1) (6, 8, 9).

The impact of the polymorphism of the CD1 gene on the structure and function of the encoded protein has been poorly addressed. The products of CD1A alleles are similarly expressed on the cell surface and display similar structural characteristics (10), whereas no significant correlation between the CD1 genotype and susceptibility to *Mycobacterium mageritense* pulmonary disease (11) or chronic dysimmune neuropathies (12) could be inferred.

*Unité 725 "Biology of Human Dendritic Cells" and †Unité 311, Institut National de la Santé et de la Recherche Médicale (INSERM), Strasbourg, France; ‡Etablissement Français du Sang-Alsace, Strasbourg, France; §Université Louis-Pasteur, Strasbourg, France; ¶Experimental Immunology, Department of Research, Basel University Hospital, Basel, Switzerland; #Institut de Pharmacologie et de Biologie Structurale, Centre National de la Recherche Scientifique (CNRS) Unité Mixte de Recherche (UMR) 5089, Department of Molecular Mechanisms of Mycobacterial Infections, Toulouse, France; ||Institut de Génétique et de Biologie Moléculaire et Cellulaire, CNRS/INSERM, Université Louis-Pasteur, Illkirch-Graffenstaden, France; and **Imaging Center and ††Molecular Mechanisms of Intracellular Transport, UMR144 CNRS, Institut Curie, Paris, France

Received for publication November 5, 2007. Accepted for publication January 25, 2008. The costs of publication of this article were defrayed in part by the payment of page charges. This article must therefore be hereby marked *advertisement* in accordance with 18 U.S.C. Section 1734 solely to indicate this fact.

¹ This work was supported by Institut National de la Santé et de la Recherche Médicale, Etablissement Français du Sang-Alsace and Agence Nationale de Recherche Microbiolo-

gie-Maladie Emergentes (ANR-05-MIME-006), the European Union funded TB-VAC tuberculosis vaccine project (LSHP-CT-2003-503367), Swiss National Fund Grant 3100A0-109918, and the Basel Cancer League (Krebsliga Beider Basel). B.M. was the recipient of a grant from Association de Recherche et de Développement en Médecine et en Santé Publique (ARMESA).

² Address correspondence and reprint requests to Dr. Sylvie Tourne or Dr. Henri de la Salle, Institut National de la Santé et de la Recherche Médicale, Unité 725, Etablissement Français du Sang-Alsace, 10 Rue Spielmann, 67065 Strasbourg Cedex, France. E-mail addresses: sylvie.tourne@efs-alsace.fr and henri.delasalle@efs-alsace.fr

³ Abbreviations used in this paper: ER, endoplasmic reticulum; β_2m , β_2 -microglobulin; Endo-H, endoglycosidase H; GM1, monosialoganglioside GM1; MFI, median fluorescence intensity; PIM, phosphatidyl-myo-inositol-mannoside; PIM₆, hexamannosylated phosphatidyl-myo-inositol; PNGase F, peptide N-glycosidase F; rs, recombinant soluble (prefix); WB, Western blotting.

Copyright © 2008 by The American Association of Immunologists, Inc. 0022-1767/08/\$2.00

In this study, we examine the impact of the polymorphism of *CD1E* gene on the function of the encoded proteins.

Materials and Methods

DNA constructs and cell transfection

The cDNAs encoding the CD1e variants were derived from CD1e-2 cDNA by PCR-based mutagenesis methods. These cDNA were cloned in the pEGFP-N3 expression vector (Clontech) and transfected, as previously described (5), into the melanoma M10 cells already transfected, or not, with CD1b cDNA. The cDNA encoding recombinant soluble (rs) CD1e-4, from residue Asp²¹ to residue Ser³⁰⁵, was cloned in a pMTV5His plasmid (Invitrogen Life Technologies) and coexpressed with human β_2m in *Drosophila* S2 cells as described (4).

Antibodies

The anti-CD1e mAb VIIC7, 1.22 and 20.6, have been described (5). Polyclonal IgGs specific for the denatured CD1e H chain were obtained by immunizing a rabbit with a recombinant protein consisting of the CD1e $\alpha 1$, $\alpha 2$, and $\alpha 3$ domains fused to GST. An anti-CD1b mAb (clone 4A7.6) was purchased from Beckman Coulter and an anti-CD63 mAb (clone H5C6) was conjugated to Alexa Fluor 488 (5). Cyanine 3- or PE-conjugated F(ab')₂ specific for mouse IgG was obtained from respectively Jackson ImmunoResearch or DakoCytomation. HRP-conjugated polyclonal Abs specific for rabbit and mouse Ig were purchased from Jackson ImmunoResearch and DakoCytomation, respectively. IgG1 (clone 679.1 Mc7) and IgG2a (clone U7.27) mAbs from Beckman Coulter were used as isotypic controls and normal mouse serum was obtained from Rockland.

Immunostaining and analyses

Cells, fixed and permeabilized for intracellular labeling, were stained as described (5) and analyzed on a FACSCalibur flow cytometer (BD Biosciences) or under a Leica SP5 AOBs confocal microscope (Leica Microsystems). The specific median fluorescence intensities (MFIs) were obtained by subtracting the MFI of cells stained with an IgG isotype-matched control from the MFI of cells stained with the Ab of interest. Colocalization was quantified as described (3).

Cell extracts

Cells, labeled or not with [³⁵S]methionine and cysteine as previously described (5), were resuspended in lysis buffer containing 1% Triton X-100, Nonidet P-40, digitonin or CHAPS, 150 mM NaCl, 20 mM Tris (pH 8), and a mixture of protease inhibitors (Complete Mini; Roche Applied Science) for 30 min on ice and then cleared by a 10-min centrifugation at 13,000 × g.

Immunoprecipitations and Western blotting (WB)

Immunoprecipitations and treatment with glycosidases were performed as described (5) before separation on SDS-PAGE. When necessary, gels were fixed, dried, and exposed to autoradiography or to PhosphorImager screens. The radioactive signals were quantified by Quantity One software after scanning on a Typhoon Trio PhosphorImager (GE-Healthcare). For WB, proteins were transferred to nitrocellulose membranes (Bio-Rad) and CD1e molecules were detected according to the usual protocols using West Pico chemiluminescent substrate (Perbio Science).

Ag presentation assays

APCs (3×10^4 cells) were preincubated for 2 h at 37°C with monosialoganglioside (GM1; Matreya) or *Mycobacterium tuberculosis* PIM₆ extracted, and purified according to the procedure described in Ref. 13. T cell clones (10^5 cells in triplicate) GG33A recognizing the CD1e-independent Ag GM1 (14) and DL15A30 recognizing PIMs in a CD1b-restricted manner, obtained as described in Ref. 4, were then added and, after 36 h, GM-CSF release was measured by ELISA (R&D Systems), as well as IFN- γ release (data not shown).

In vitro mannosidase digestion assays

In vitro digestion assays of PIM₆ by mannosidase and mass spectrum analyses were performed as previously described (4).

Results and Discussion

CD1e with P194 is not able to assist CD1b presentation of PIM₆Ag

Human CD1e is essential for the lysosomal processing of PIM₆ into antigenic molecule(s) presented by CD1b (4). This function was initially described for the product of *CD1E-2* gene, the most common allele (6). In this study we investigated whether

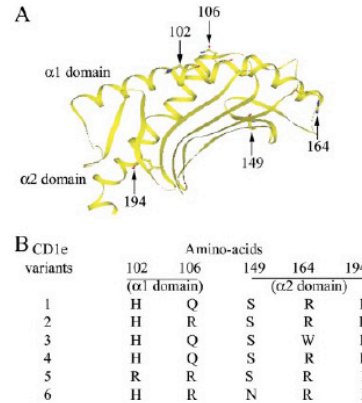


FIGURE 1. CD1e residues affected by the polymorphism of the *CD1E* gene. *A*, Model of the three-dimensional structure of the $\alpha 1$ and $\alpha 2$ domains of CD1e-2 and the locations of the residues affected by the polymorphism of *CD1E*. *B*, Nature of the amino acids located at positions 102, 106, 149, 164, and 194 in the sequences of the different CD1e variants.

the products of the five other alleles of *CD1E* gene display similar properties.

We constructed cDNAs encoding CD1e molecules with residues specifically found in the proteins encoded by the alleles 1, 2, 3, 4, 5, and 6 of *CD1E*, referred to in this paper as CD1e-1, CD1e-2, CD1e-3, CD1e-4, CD1e-5, and CD1e-6, respectively (Fig. 1*B*). M10 cells expressing CD1b (M10-CD1b), which have already been used as APCs to study CD1e function (4), were stably transfected with each of these cDNAs. Clones expressing the CD1e variants were selected by immunofluorescence staining of fixed, permeabilized cells with the conformation-dependent mAbs 1.22 and 20.6, previously raised and selected using CD1e-2 molecules (5). FACS analyses showed that all of the variants were recognized by 1.22 and all but CD1e-3 were recognized by 20.6 (data not shown), which means that arginine 164, substituted by a tryptophan in CD1e-3, contributes to the epitope recognized by the mAb 20.6. These analyses also showed that all of the clones displayed a similar MFI of staining with the mAb 1.22, indicating that they expressed similar amounts of CD1e (data not shown).

These doubly transfected cells were used as APCs for the CD1b-restricted presentation of PIM₆ to the specific T cell clone DL15A30. The GM-CSF release of T cells in response to different concentrations of Ag revealed that cells coexpressing CD1b and CD1e-1, CD1e-2, CD1e-3, CD1e-5, or CD1e-6 were able to present PIM₆ to T cells in a dose-dependent manner (Fig. 2*A*). In contrast, PIM₆ presentation by M10-CD1b-CD1e-4 cells was significantly reduced and comparable to that obtained with single CD1b-transfected APCs (Fig. 2*A*). Similar data were obtained by measuring IFN- γ release and by using another CD1b-restricted and PIM₆-specific T cell clone (data not shown).

The poor capacity of CD1e-4-expressing cells to assist PIM₆ presentation was not due to a lower expression of CD1b, because FACS analyses showed that the specific MFIs of M10-CD1b-CD1e-4 and -CD1e-2 cells stained with an anti-CD1b mAb were comparable (346 and 225, respectively, with M10

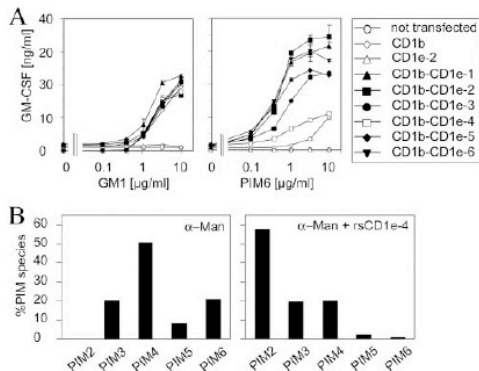


FIGURE 2. *A*, Assistance of CD1e-4 in PIM₆ presentation to T cells. M10 (not transfected), M10-CD1b, M10-CD1e-2, M10-CD1b-CD1e-1, -CD1e-2, -CD1e-3, -CD1e-4, -CD1e-5, or -CD1e-6 cells were preincubated with different doses of PIM₆ or GM1 before addition of DL15A30 or GG33A T cells, respectively. GM-CSF release was used to quantify the T cells. The experiments illustrated have been performed twice with the same results. *B*, Assistance of rsCD1e-4 in the *in vitro* digestion of PIM₆ by α -mannosidase (α -Man). PIM₆ was incubated for 1 h at 37°C with jack bean α -mannosidase in the presence or absence of rsCD1e-4, after which PIMs were extracted and analyzed by MALDI-TOF mass spectrometry. Relative abundance of the different PIM glycoforms is presented.

cells having a specific MFI of 0.4) (data not shown). This reduced T cell response was also not caused by a general defect in Ag presentation of CD1e-4 expressing cells, as these cells very efficiently presented the CD1e-independent Ag GM1 to the specific CD1b-restricted T cell clone GG33A (Fig. 2*A*).

To determine whether the inability of CD1e-4 to assist PIM₆ presentation was due to incapacity of the protein to participate in the processing of PIM₆ into PIM₂ by α -mannosidase, we produced rsCD1e-4 molecules in insect cells. The activity of rsCD1e-4 in the *in vitro* enzymatic digestion of PIM₆ by α -mannosidase is reported in Fig. 2*B*. MALDI-TOF analyses showed that in the presence of rsCD1e-4, as previously reported for rsCD1e-2 (4), α -mannosidase was able to generate PIM₂ molecules. Thus, the rsCD1e-4 produced in insect cells was biochemically functional *in vitro*.

CD1e-4 exhibits a singular intracellular fate

Because CD1e-4 appeared to be active in biochemical but not in Ag presentation assays, we examined whether CD1e-4 underwent a different intracellular fate as compared with the other CD1e variants. We first established that the other CD1e variants displayed subcellular localization (in late endosomal compartments) and maturation processes (cleavage and resistance to Endo-H) similar to those of CD1e-2 (data not shown), and we then chose to compare CD1e-1 and CD1e-4, which only differ at residue 194 (Fig. 1*B*).

We first showed that CD1e-4 remained strictly intracellular, as does CD1e-1 (data not shown). To examine the intracellular localization of the protein, fixed and permeabilized transfected cells were costained with anti-CD1e and anti-CD63 mAbs and analyzed by confocal microscopy. CD1e-4 colocalized with CD63 molecules and hence was present in late endosomal compartments, like CD1e-1 (Fig. 3*A*). However, quantitative mea-

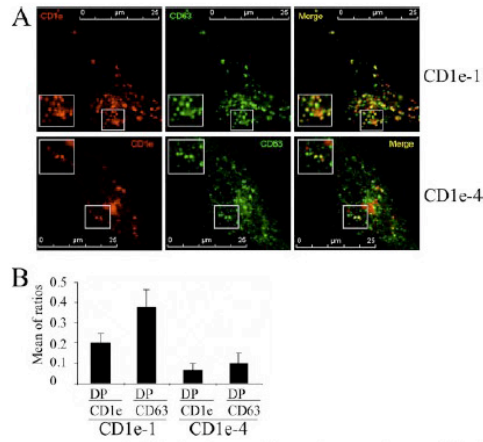


FIGURE 3. Subcellular distribution of CD1e-4. *A*, Fixed, permeabilized M10-CD1b-CD1e-1 or -CD1e-4 cells were stained with the mAb 20.6 and revealed with cyanine 3-conjugated polyclonal Abs and an Alexa Fluor 488-conjugated anti-CD63 mAb before analysis by confocal microscopy. *Insets* are a focal view of a part of the cell. *B*, The colocalization of CD1e and CD63 was quantified by counting CD63 and CD1e single and double positive structures in seven M10-CD1b-CD1e-1 or -CD1e-4 cells as previously described (3). The total numbers of double positive organelles in CD1e-1- or CD1e-4-expressing cells were 900 and 160, respectively. The histograms represent the means of the ratios of the numbers of double positive (DP) to single positive vesicles (DP⁺CD1e⁺ and DP⁺CD63⁺, respectively). The SD for each condition is indicated.

surements revealed that CD1e-4 colocalized with CD63 about four times less than CD1e-1 did (Fig. 3*B*).

During its intracellular transport, CD1e becomes Endo-H resistant in the Golgi apparatus and soluble in the late endosomal compartments. To investigate the biochemical maturation of CD1e-4, transfected cells were metabolically labeled for 45 min, chased for 0, 4, or 8 h, and lysed in buffer containing Triton X-100, after which CD1e molecules were immunoprecipitated with the mAb 20.6, treated or not with PNGase F or Endo-H, and separated by SDS-PAGE. In contrast to CD1e-1, which was progressively converted into a cleaved form during chase, cleaved CD1e-4 remained undetectable after 4 h (Fig. 4*A*) and up to 8 h of chase (data not shown). Moreover, when CD1e-4 was immunoprecipitated with the mAb 20.6 from detergent-solubilized extracts of transfected cells, no cleaved proteins were detected by WB using polyclonal rabbit IgGs specific for the denatured luminal part of CD1e. These Abs nevertheless revealed the uncleaved form, as did the mAb VIIC7 (Fig. 4*B*). In contrast, cleaved CD1e molecules were detected in control experiments using extracts from cells expressing CD1e-2 or CD1e-1 (Fig. 4*B*). Pulse-chase experiments also revealed that unlike CD1e-1, which became Endo-H resistant during chase, CD1e-4 remained Endo-H sensitive (Fig. 4*A*). Nonetheless, WB analyses of CD1e, immunoprecipitated from detergent-solubilized extracts of transfected cells, demonstrated that at least a small fraction of CD1e-4 molecules became Endo-H resistant (Fig. 4*C*), consistent with its detection in CD63⁺ compartments (Fig. 3*A*). Similar results were obtained when pulse-chase experiments were performed using the mAb 1.22 instead of 20.6 or CHAPS instead of Triton X-100 (data not shown).

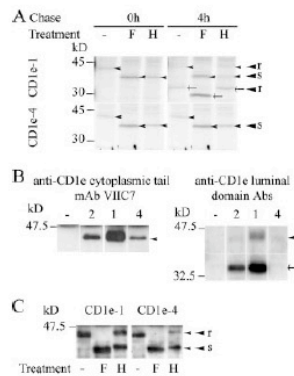


FIGURE 4. Maturation of CD1e-4. *A*, M10-CD1b-CD1e-1 or -CD1e-4 cells were metabolically labeled for 45 min and chased for 0 or 4 h. CD1e molecules were immunoadsorbed on the mAb 20.6, digested with PNGase F (F) or Endo-H (H) or not (-) and separated by SDS-PAGE. The positions of the uncleaved and cleaved CD1e forms are indicated by an arrowhead and an arrow, respectively. The positions of Endo-H-sensitive and Endo-H-resistant species are indicated by a larger arrowhead followed by s (sensitive) and r (resistant), respectively (at 4-h chase time point). *B*, Cell extracts were prepared from M10-CD1b (-) or M10-CD1b-CD1e-1 (1), CD1e-2 (2), or CD1e-4 (4), and CD1e molecules were immunoadsorbed using the mAb 20.6. Uncleaved forms were revealed by WB with the mAb VIIIC7, while uncleaved and cleaved forms were detected with polyclonal rabbit IgGs specific for the denatured luminal part of CD1e. Symbols are defined in *A*. *C*, Cell extracts were prepared from M10-CD1b-CD1e-1 or -CD1e-4 cells and uncleaved CD1e molecules were immunoadsorbed with the mAb VIIIC7, digested with PNGase F (F) or Endo-H (H) or not (-) and analyzed by WB using the mAb VIIIC7. Symbols are defined in *A*.

Altogether, these observations suggested that either only small amounts of CD1e-4 reach late endosomal compartments or that CD1e-4 is degraded in these compartments.

CD1e assembly and traffic are affected by the L194P substitution

To study the stability of CD1e-4 in late endosomal compartments, M10-CD1b-CD1e-1 or -CD1e-4 cells were metabolically labeled during 5 h in the absence or presence of bafilomycin, which blocks acidification of the late endosomal compartments. Immunoprecipitation of CD1e with the mAb 20.6 followed or not by a treatment with glycosidases showed that uncleaved Endo-H resistant forms of both CD1e-1 and CD1e-4 accumulated in cells treated with bafilomycin (Fig. 5*A*). Nevertheless, the Endo-H resistant CD1e-4 forms were far less abundant than the CD1e-1 ones, suggesting that only small amounts of CD1e-4 reach endosomes (Fig. 5*A*).

This defect might result from an altered association of the CD1e α -chain with β_2 m in the ER. Indeed, the exit of CD1a, CD1b, and CD1c from the ER has been reported to be strictly dependent on the association of CD1 α -chains with β_2 m (15), while only a fraction of newly synthesized CD1d H chains reach the plasma membrane not associated with β_2 m (16). In agreement with this hypothesis, fewer β_2 m molecules were coimmunoprecipitated with the CD1e-4 α -chain as compared with the CD1e-1 α -chain using the mAb VIIIC7 (Fig. 5*B*) or 20.6 (data not shown). This difference was also apparent when Nonidet P-40, digitonin, or CHAPS was used as the detergent (Fig. 5*B*).

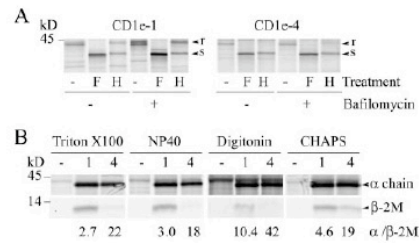


FIGURE 5. Assembly and export of CD1e-4 to late endosomal compartments. *A*, M10-CD1b-CD1e-1 or -CD1e-4 cells were metabolically labeled in the presence or absence of bafilomycin (0.1 μ M). After 5 h, CD1e molecules were immunoadsorbed with the mAb 20.6, digested with PNGase F (F) or Endo-H (H) or not (-) and separated by SDS-PAGE. Symbols are defined in Fig. 4*A*. *B*, M10-CD1b (-) cells or M10-CD1b-CD1e-1 (4) or M10-CD1b-CD1e-4 (4) cells were metabolically labeled for 1 h and cell extracts were prepared in Triton X-100, Nonidet P-40, digitonin, or CHAPS. CD1e molecules were immunoadsorbed with the mAb VIIIC7, separated by SDS-PAGE, and exposed for autoradiography. To determine the α -chain/ β_2 m ratios, gels were exposed to PhosphorImager screens.

The crystallographic resolution of other CD1 molecules provides no argument in favor of a direct participation of leucine 194 in the binding of CD1e to β_2 m (17). Nevertheless, proline is a residue known to potentially affect the conformation of proteins by introducing an elbow into the structure. Owing to the proximity of residue 194 to the $\alpha 3$ domain, which interacts with β_2 m, the association of β_2 m with the CD1e-4 α -chain might be affected. Next to residue 194, at position 193, is a conserved aromatic amino acid, a phenylalanine that contributes to the A' pocket of the CD1 binding groove. As CD1e binds lipids (4), the L194P substitution could affect the stereo arrangement of this aromatic residue and, consequently, the capture of an endogenous lipid required for the appropriate assembly and stability of CD1e molecules in the ER.

Conclusion

In summary, the polymorphism of the *CD1E* allele 4 represents the first example of a functional defect in the family of CD1 molecules. It alters the assembly and, consequently, the intracellular transport and function of the encoded molecule. Because the functional impairment resulting from this polymorphism relates to the capacity of the CD1e molecule to participate in the immune response to complex glycolipids, it is tempting to speculate that individuals homozygous for the allele 4 of *CD1E* might display an altered immune response to *M. tuberculosis* lipid Ags requiring endosomal processing. It will be important to determine whether the polymorphism of the *CD1E* gene represents a factor of susceptibility to human diseases involving the immune response to complex glycolipid Ags.

Acknowledgments

We are especially grateful to J. Mulvihill for excellent editorial assistance. We also thank the members of the RIO-Cell and Tissue Imaging Facility of UMR 144, CNRS-Institut Curie for their help with imaging approaches.

Disclosures

The authors have no financial conflict of interest.

References

- De Libero, G., and L. Mori. 2005. Recognition of lipid antigens by T cells. *Nat. Rev. Immunol.* 5: 485–496.
- Sugita, M., D. C. Barral, and M. B. Brenner. 2007. Pathways of CD1 and lipid antigen delivery, trafficking, processing, loading, and presentation. *Curr. Top. Microbiol. Immunol.* 314: 143–164.
- Angenieux, C., V. Fraissier, B. Maitre, V. Racine, N. van der Wel, D. Fricker, F. Proamer, M. Sachse, J. P. Cazenave, P. Peters, et al. 2005. The cellular pathway of CD1e in immature and maturing dendritic cells. *Traffic* 6: 286–302.
- de la Salle, H., S. Mariotti, C. Angenieux, M. Gilleron, L. F. Garcia-Alles, D. Malm, T. Berg, S. Paoletti, B. Maitre, L. Mourey, et al. 2005. Assistance of microbial glycolipid antigen processing by CD1e. *Science* 310: 1321–1324.
- Angenieux, C., J. Salameo, D. Fricker, J. P. Cazenave, B. Goud, D. Hanau, and H. de La Salle. 2000. Characterization of CD1e, a third type of CD1 molecule expressed in dendritic cells. *J. Biol. Chem.* 275: 37757–37764.
- Han, M., L. I. Hannick, M. DiBrino, and M. A. Robinson. 1999. Polymorphism of human CD1 genes. *Tissue Antigens* 54: 122–127.
- Oteo, M., J. F. Parra, I. Mirones, L. I. Gimenez, F. Setien, and E. Martinez-Naves. 1999. Single strand conformational polymorphism analysis of human CD1 genes in different ethnic groups. *Tissue Antigens* 53: 545–550.
- Mirones, I., M. Oteo, J. F. Parra-Cuadrado, and E. Martinez-Naves. 2000. Identification of two novel human CD1E alleles. *Tissue Antigens* 56: 159–161.
- Tamouza, R., R. Sghiri, R. Ramasawmy, M. G. Neonato, L. E. Mombo, J. C. Poirier, V. Schaeffer, C. Fortier, D. Labie, R. Giro, et al. 2002. Two novel CD1 E alleles identified in black African individuals. *Tissue Antigens* 59: 417–420.
- Oteo, M., P. Arribas, F. Setien, J. F. Parra, I. Mirones, M. Gomez del Moral, and E. Martinez-Naves. 2001. Structural characterization of two CD1A allelic variants. *Hum. Immunol.* 62: 1137–1141.
- Jones, D. C., C. M. Gelder, T. Ahmad, I. A. Campbell, M. C. Barnardo, K. I. Welsh, S. E. Marshall, and M. Bunce. 2001. CD1 genotyping of patients with *Mycobacterium tuberculosis* pulmonary disease. *Tissue Antigens* 58: 19–23.
- De Angelis, M. V., F. Notturno, C. M. Caporale, M. Pace, and A. Uncini. 2007. Polymorphisms of CD1 genes in chronic dysimmune neuropathies. *J. Neuroimmunol.* 186: 161–163.
- Gilleron, M., C. Ronet, M. Mempel, B. Monsarrat, G. Gachelin, and G. Puzo. 2001. Acylation state of the phosphatidylinositol mannosides from *Mycobacterium bovis* bacillus Calmette Guerin and ability to induce granuloma and recruit natural killer T cells. *J. Biol. Chem.* 276: 34896–34904.
- Shamshiev, A., A. Donda, I. Carena, I. Mori, L. Kappos, and G. De Libero. 1999. Self glycolipids as T-cell autoantigens. *Eur. J. Immunol.* 29: 1667–1675.
- Bauer, A., R. Huttinger, G. Staffler, C. Hansmann, W. Schmidt, O. Majdic, W. Knapp, and H. Stockinger. 1997. Analysis of the requirement for β_2 -microglobulin for expression and formation of human CD1 antigens. *Eur. J. Immunol.* 27: 1366–1373.
- Balk, S. P., S. Burke, J. E. Polischuk, M. E. Frantz, L. Yang, S. Porcelli, S. P. Colgan, and R. S. Blumberg. 1994. β_2 -Microglobulin-independent MHC class Ib molecule expressed by human intestinal epithelium. *Science* 265: 259–262.
- Moody, D. B., D. M. Zajonc, and I. A. Wilson. 2005. Anatomy of CD1-lipid antigen complexes. *Nat. Rev. Immunol.* 5: 387–399.

European Journal of
Immunology
Highlights

FRONTLINE:

Differential alteration of lipid antigen presentation to NKT cells due to imbalances in lipid metabolism

Jens Schümann^{*1}, Federica Facciotti^{*1}, Luigi Panza², Mario Michieletti², Federica Compostella³, Anthony Collmann¹, Lucia Mori¹ and Gennaro De Libero¹

¹ Experimental Immunology, Department of Research, University Hospital Basel, Basel, Switzerland

² Department of Chemical, Nutritional, Pharmaceutical, and Pharmacological Sciences, University of Piemonte Orientale, Novara, Italy

³ Department of Medical Chemistry, Biochemistry, and Biotechnology, University of Milano, Milano, Italy

Deficiencies in enzymes of the lysosomal glycosphingolipid degradation pathway or in lysosomal lipid transfer proteins cause an imbalance in lipid metabolism and induce accumulation of certain lipids. A possible impact of such an imbalance on the presentation of lipid antigens to lipid-reactive T cells has only been hypothesized but not extensively studied so far. Here we demonstrate that presentation of lipid antigens to, and development of, lipid-reactive CD1d-restricted NKT cells, are impaired in mice deficient in the lysosomal enzyme β -galactosidase (β Gal) or the lysosomal lipid transfer protein Niemann-Pick C (NPC) 2. Importantly, the residual populations of NKT cells selected in β Gal^{-/-} and NPC2^{-/-} mice showed differential TCR and CD4 repertoire characteristics, suggesting that differential selecting CD1d:lipid antigen complexes are formed. Furthermore, we provide direct evidence that accumulation of lipids impairs lipid antigen presentation in both cases. However, the mechanisms by which imbalanced lipid metabolism affected lipid antigen presentation were different. Based on these results, the impact of lipid accumulation should be generally considered in the interpretation of immunological deficiencies found in mice suffering from lipid metabolic disorders.

Received 8/2/07

Accepted 10/4/07

[DOI 10.1002/eji.200737160]

■ **Key words:**

β -Galactosidase · CD1
 · NKT cells
 · Niemann-Pick C2



Supporting information for this article is available at
http://www.wiley-vch.de/contents/jc_2040/2007/37160_s.pdf

* These authors contributed equally to this work.

Correspondence: Gennaro De Libero, Experimental Immunology, Department of Research, University Hospital Basel, Hebelstr. 20, 4031 Basel, Switzerland
 Fax: +41-61-2652350
 e-mail: gennaro.delibero@unibas.ch

Abbreviations: α -GalCer: α -galactosylceramide (KRN7000) · α/β Gal: α/β -galactosidase · DN: CD4⁺ CD8⁻ double negative · DP: CD4⁺ CD8⁺ double positive · Hex: hexosaminidase · HSA: heat-stable Ag · i: invariant · iGb3: isoglobotrihexosylceramide · NB-DNJ: N-butyldeoxynojirimycin · NPC: Niemann-Pick C

Introduction

Defects in lysosomal lipid trafficking or degradation result in a severe imbalance of lipid metabolism. Little is known about the consequences of such an imbalance on the presentation of lipid antigens to lipid-reactive T cells, e.g., the important immunoregulatory invariant (i) NKT cell subset (Va14i and Va24i NKT cells in mice and humans, respectively), which recognizes glycolipid antigens presented by the MHC class I-like molecule

CD1d. In mice, the TCR of $V\alpha 14i$ NKT cells is composed of an invariant $V\alpha 14-J\alpha 18$ chain, paired preferentially with a restricted β chain, mostly containing $V\beta 8.2$ or $V\beta 7$ (the human equivalents are $V\alpha 24-J\alpha 18$ and $V\beta 11$) [1–4]. $V\alpha 14i$ NKT cells are implicated in the regulation of antitumor immunity, antimicrobial responses, and the balance between tolerance and autoimmunity [5, 6].

$V\alpha 14i$ NKT cells, which can be either $CD4^+$ or $CD4^-CD8^-$ double negative (DN), are a thymus-dependent population derived from $CD4^+CD8^+$ double-positive (DP) thymocytes [7–11]. Different maturation stages of developing thymic $V\alpha 14i$ NKT cells have been described, characterized by the sequential acquisition of CD44 and NK1.1 in C57BL/6 mice [12–14]. Unlike conventional MHC-dependent T cells, $V\alpha 14i$ NKT cells are not positively selected by thymic epithelial cells but rather by hematopoietic cells [2, 15–18], in particular by CD1d-expressing DP cortical thymocytes [19, 20], which alone are sufficient for positive selection of $V\alpha 14i$ NKT cells [21, 22]. Furthermore, $V\alpha 14i$ NKT cells can be negatively selected by very strong activation signals provided by thymic DC [22, 23] or DP cortical thymocytes [22].

The key event deciding for selection of $V\alpha 14i$ NKT cells is the appropriate presentation of endogenous thymic lipid antigen(s) by CD1d. Many steps are involved in this process, including proper conformation of the CD1d molecule, correct intracellular trafficking of lipids and CD1d, generation of lipid antigen(s), and loading of the lipid antigen(s) onto CD1d in late endosomes/lysosomes [24–27].

Recent work suggested that isoglobotrihexosylceramide (iGb3), a lysosomal glycosphingolipid that is absent in mice deficient in β -hexosaminidases A and B ($Hexb^{-/-}$), is involved in thymic selection of $V\alpha 14i$ NKT cells [28]. Furthermore, different lysosomal lipid transfer proteins, *i.e.*, saposins and GM2 activator protein, have been implicated in loading of endogenous and exogenous lipid antigens onto CD1d and thus in CD1d-restricted presentation of selection-relevant lipid antigens to $V\alpha 14i$ NKT cells [29, 30]. Indeed, development of $V\alpha 14i$ NKT cells is completely abolished in mice deficient in saposins [29]. However, deficiency in $Hexb$ or saposins causes severe imbalances in lipid metabolism, and in more recent studies it has been discussed that lipids accumulating in lysosomes might impair presentation of lipid antigens by CD1d, and thus thymic selection of $V\alpha 14i$ NKT cells. Presentation of lipid antigens to, and thymic development of, $V\alpha 14i$ NKT cells are also deficient in mouse models of different other types of lysosomal lipid storage diseases, *i.e.*, in mice deficient in β -hexosaminidases A and S ($Hexa^{-/-}$), α -galactosidase ($\alpha Gal^{-/-}$), β -galactosidase ($\beta Gal^{-/-}$), or the lysosomal Niemann-Pick C (NPC) 1 protein [31, 32]. Nevertheless, the impact of accumulating lipids in lysosomes to the impairment of lipid antigen presenta-

tion has not been directly investigated, and the mechanism by which lipid antigen presentation is disturbed in this context remains enigmatic.

To gain a better understanding of the influence of disturbed lipid metabolism and lysosomal lipid storage on the presentation of lipid antigens and the development of $V\alpha 14i$ NKT cells, we investigated these aspects using two mouse models of imbalanced lipid metabolism, *i.e.*, mice deficient in the lysosomal enzyme βGal (EC 3.2.1.23), which is involved in the glycosphingolipid degradation pathway, and mice deficient in the lysosomal lipid transfer protein NPC2, whose precise functions are still largely unknown. We found that presentation of lipid antigens and development of $V\alpha 14i$ NKT cells are differentially impaired in the absence of βGal or NPC2. In both cases the accumulation of lipids is involved in this impairment. Nevertheless, differential mechanisms account for the defects in lipid antigen presentation to, and selection of, $V\alpha 14i$ NKT cells.

Results

Thymic selection of $V\alpha 14i$ NKT cells is impaired in $\beta Gal^{-/-}$ mice

The absence of βGal impaired thymic development of $V\alpha 14i$ NKT cells by ~70–80%. This was determined by flow-cytometric analysis of thymocytes from $\beta Gal^{-/-}$ and WT mice (Fig. 1A). Thymocyte numbers and frequencies of conventional TCR- $\alpha\beta$ and TCR- $\gamma\delta$ T cells, as well as DN, DP, $CD4^+$, and $CD8^+$ cells were normal (Fig. 1A). CD1d expression levels on DP thymocytes (*i.e.*, the cell type driving positive selection of $V\alpha 14i$ NKT cells) also remained unchanged (Fig. 1A). The residual population of $V\alpha 14i$ NKT cells that was selected in the absence of βGal bound CD1d: α -galactosylceramide (CD1d: α -GalCer) dimers with remarkably high avidity (Fig. 1A).

Liver and spleen are the major organs to which thymus-derived $V\alpha 14i$ NKT cells home. Interestingly, the frequencies of $V\alpha 14i$ NKT cells were reduced in livers and spleens of $\beta Gal^{-/-}$ mice to a similar extent as in the thymus (Fig. 1B; *cf* Fig. 1A). The numbers of mononuclear cells and the frequencies of conventional TCR- $\alpha\beta$ T cells were normal in livers and spleens of $\beta Gal^{-/-}$ mice. As in the thymus, the small residual population of $V\alpha 14i$ NKT cells bound CD1d: α -GalCer dimers with high avidity. Since the $V\beta$ domain is known to influence the avidity of CD1d:glycolipid binding by $V\alpha 14i$ NKT cells [33–36], the residual $V\alpha 14i$ NKT cell populations were further analyzed for expression of the two major $V\beta$ chains, which mostly pair with the invariant TCR- α chain of $V\alpha 14i$ NKT cells, *i.e.*, $V\beta 8.2$ and $V\beta 7$. Interestingly, the $V\alpha 14i$ NKT cell population that was selected in

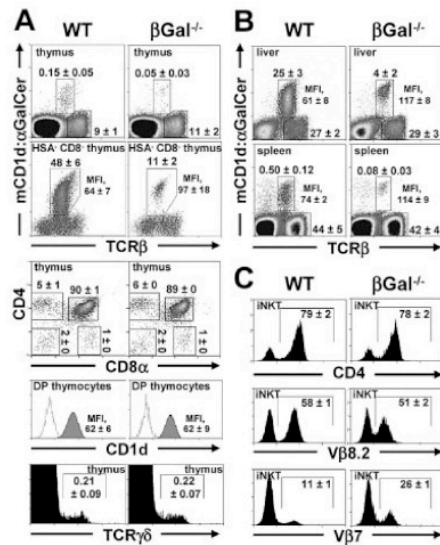


Figure 1. Thymic selection of *Vα14i* NKT cells is impaired in β Gal^{-/-} mice. (A) Complete or HSA/CD8-depleted thymocytes from β Gal^{-/-} or WT mice were stained with mouse CD1d: α -GalCer dimers and mAb against TCR β and analyzed by flow cytometry. The first set of cytograms depicts the gates defining *Vα14i* NKT (TCR β ⁺ mouse CD1d: α -GalCer dimer⁺) and conventional TCR $\alpha\beta$ T cells (TCR β ⁺ mouse CD1d: α -GalCer dimer⁻). Furthermore, thymocytes were analyzed for expression of CD4, CD8 α , and CD1d, or TCR $\gamma\delta$. CD1d expression is shown for DP thymocytes. (B, C) Liver mononuclear cells or splenocytes from β Gal^{-/-} or WT mice were stained with mouse CD1d: α -GalCer dimers and mAb against TCR β and CD4 or V β 8.2 or V β 7, and analyzed by flow cytometry. The cytograms in (B) depict the gates defining *Vα14i* NKT and conventional TCR $\alpha\beta$ T cells, as described for (A). The histograms in (C) show the expression of CD4, V β 8.2, or V β 7 among hepatic *Vα14i* NKT cells. Numbers represent the mean percentage of positive cells (\pm SD) in the indicated gates ($n=3$).

the absence of β Gal showed a remarkable shift in the V β 8.2/V β 7 ratio towards V β 7 expression, whereas CD4 was expressed at normal frequency and intensity (Fig. 1C). Frequencies of V β 8.2⁺, V β 7⁺, and CD4⁺ cells were not changed among conventional TCR- $\alpha\beta$ T cells in β Gal-deficient mice (unpublished data).

Presentation of lipid antigens is impaired in β Gal^{-/-} thymocytes

Since thymic development of *Vα14i* NKT cells was impaired in β Gal^{-/-} mice, we wondered whether presentation of lipid antigens is impaired if β Gal is missing. We utilized an *in vitro* system in which a human *Vα24i* NKT clone is stimulated by mouse thymocytes in

the absence of additional lipid antigens. Under these conditions, thymocytes from WT mice caused the release of human IL-4 by the *Vα24i* NKT clone (Fig. 2A). This stimulation was completely abolished when β Gal^{-/-} thymocytes were used as APC (Fig. 2A). DC were also able to induce the secretion of human IL-4 by the *Vα24i* NKT clone (Fig. 2A), but deficiency of β Gal in DC did not impair this cytokine release (Fig. 2A). This points to a certain degree of cell type-specific differences and indicates that β Gal *per se* is not involved in the stimulation of the *Vα24i* NKT clone in the described *in vitro* system.

To check whether presentation of exogenously given lipid antigens is also disturbed in the absence of β Gal, a mouse *Vα14i* NKT hybridoma was stimulated with β Gal^{-/-} or WT thymocytes in the presence of the pan-iNKT cell activating glycolipid agonist α -GalCer or of iGb3. Both α -GalCer and iGb3 were less efficiently presented by β Gal^{-/-} as compared to WT thymocytes (Fig. 2B). In contrast, DC from β Gal^{-/-} mice were not impaired in presenting α -GalCer or iGb3 (unpublished data).

Presentation of peptides *via* MHC class II was not affected by the lack of β Gal, since β Gal^{-/-} splenocytes perfectly presented purified protein derivative to a specific T cell line (Supporting Information Fig. S1A).

These results show that presentation of lipid antigens is disturbed in β Gal^{-/-} thymocytes, and this might explain the impairment of thymic selection of *Vα14i* NKT cells in β Gal^{-/-} mice.

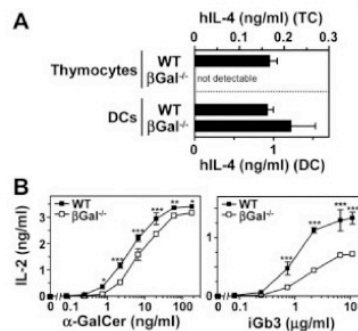


Figure 2. Presentation of lipid antigens is impaired in β Gal^{-/-} thymocytes. (A) Thymocytes (TC) or DC from β Gal^{-/-} or WT mice were incubated with a human *Vα24i* NKT clone, and human (h) IL-4 release to cell culture supernatant was determined. (B) Thymocytes from β Gal^{-/-} or WT mice were incubated with different concentrations of α -GalCer or iGb3 before the addition of *Vα14i* NKT hybridoma cells. IL-2 release to cell culture supernatant was determined. Diagrams show the mean release of cytokine (\pm SD; $n=3$). * $p<0.05$, ** $p<0.01$, *** $p<0.001$ comparing WT and β Gal^{-/-}.

Pharmacological reduction of lipid accumulation in β Gal^{-/-} thymocytes improves lipid antigen presentation

β Gal hydrolyses the terminal β -galactosidic residues of different glycoconjugates, including the gangliosides GM1 and GA1, and lactosylceramide [37]. A deficiency of β Gal could therefore cause the lack of a lipid antigen involved in thymic selection of V α 14i NKT cells. However, our findings that β Gal^{-/-} DC were able to stimulate V α 24i NKT cells in the absence of additional lipid antigen and that presentation of exogenously given lipid antigens was impaired in β Gal^{-/-} thymocytes suggest that an indirect rather than a direct mechanism is responsible for impaired selection of V α 14i NKT cells in β Gal^{-/-} mice. To test for the hypothesis that the accumulation of lipids negatively influences lipid antigen presentation in β Gal^{-/-} mice, we took advantage of an inhibitor of glycosphingolipid biosynthesis, N-butyldeoxynojirimycin (NB-DNJ), which reduces pathological lipid storage *in vitro* and *in vivo* [38]. Incubation of β Gal^{-/-} thymocytes with NB-DNJ significantly improved their capacity to present α -GalCer to V α 14i NKT hybridoma cells (Fig. 3A), indicating that accumulating lipids disturb lipid antigen presentation in β Gal^{-/-} thymocytes. This mechanism might also explain why thymic selection of V α 14i NKT cells is impaired in β Gal^{-/-} mice.

Intracellular defects account for impairment of lipid antigen presentation in β Gal^{-/-} cells

Accumulating lipids might disturb lipid antigen presentation by directly blocking or modifying CD1d, by changing membrane structures, and/or by disturbing proteins involved in the transport of lipid antigens, in the unloading of non-antigenic lipids from CD1d, and/or in the loading of lipid antigens onto CD1d. To investigate whether the formation of functional CD1d:lipid antigen complexes on the cell surface is impaired in β Gal^{-/-} thymocytes, these cells were fixed with glutaraldehyde and tested for their capacity to present α -GalCer to V α 14i NKT hybridoma cells [39]. Interestingly, upon fixation β Gal^{-/-} and WT thymocytes presented α -GalCer equally to V α 14i NKT hybridoma cells (Fig. 3B), showing that the formation of functional CD1d: α -GalCer complexes directly on the cell surface is not disturbed in β Gal-deficient thymocytes.

Thymic selection of V α 14i NKT cells is impaired in NPC2^{-/-} mice

The absence of NPC2 inhibited thymic development of V α 14i NKT cells by ~60–70%. This was determined by flow-cytometric analysis of thymocytes from NPC2^{-/-}

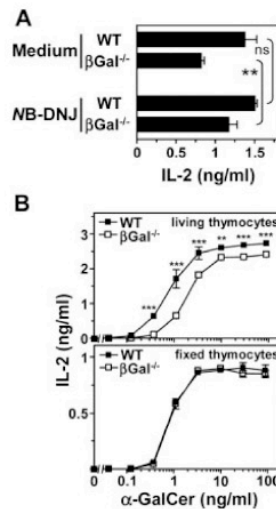


Figure 3. Accumulation of lysosomal storage lipids and intracellular defects with no disturbance of the CD1d molecule account for the impairment of lipid antigen presentation in β Gal^{-/-} cells. (A) Thymocytes from β Gal^{-/-} or WT mice were incubated with NB-DNJ or medium before α -GalCer (1 ng/mL) and V α 14i NKT hybridoma cells were added. IL-2 release to cell culture supernatant was determined. The bar chart shows the mean release of IL-2 (\pm SD; n=3). ** $p < 0.01$; ns, not significant. (B) Living or fixed thymocytes from β Gal^{-/-} or WT mice were incubated with various concentrations of α -GalCer before the addition of V α 14i NKT hybridoma cells. IL-2 release to cell culture supernatant was determined. Diagrams show the mean release of IL-2 (\pm SD; n=3). ** $p < 0.01$, *** $p < 0.001$ comparing WT and β Gal^{-/-}.

and WT mice (Fig. 4A). Thymocyte numbers and frequencies of conventional TCR- $\alpha\beta$ and TCR- $\gamma\delta$ T cells, as well as DN, DP, CD4⁺, and CD8⁺ cells were normal (Fig. 4A). CD1d surface expression was somewhat lower on DP thymocytes in the absence of NPC2 (Fig. 4A). However, this decreased surface expression is not sufficient to explain the low numbers of V α 14i NKT cells selected in NPC2^{-/-} mice since CD1d^{+/-} mice, expressing half the amount of CD1d as compared to CD1d^{+/+} mice, have normal numbers of V α 14i NKT cells [17, 35]. Also, in the periphery, *i.e.*, in liver and spleen, frequencies and numbers of V α 14i NKT cells were greatly reduced in NPC2^{-/-} mice (Fig. 4B), although total mononuclear cell numbers were significantly increased, especially in the liver. Further analysis revealed that this increase is mainly due to elevated numbers of B cells (unpublished data), whereas conventional TCR- $\alpha\beta$ T cell numbers remained normal. Despite the fact that both β Gal^{-/-} and NPC2^{-/-} mice were deficient in V α 14i NKT

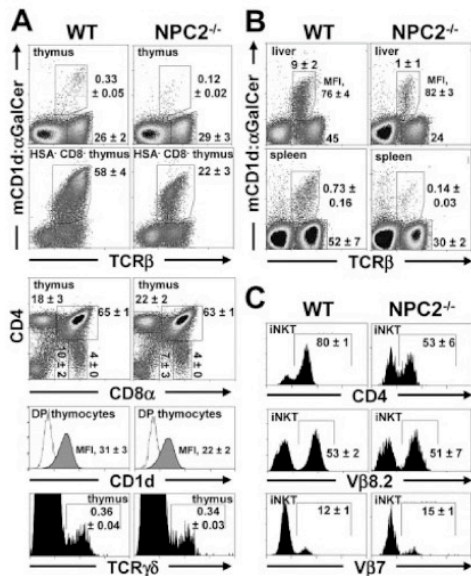


Figure 4. Thymic selection of Va14i NKT cells is impaired in NPC2^{-/-} mice. (A) Complete or HSA/CD8-depleted thymocytes from NPC2^{-/-} or WT mice were stained with mouse CD1d:αGalCer dimers and mAb against TCRβ and analyzed by flow cytometry. The first set of cytograms depicts the gates defining Va14i NKT and conventional TCRαβ T cells. Furthermore, thymocytes were analyzed for expression of CD4, CD8α, and CD1d, or TCRγδ. CD1d expression is shown for DP thymocytes. (B, C) Liver mononuclear cells or splenocytes from NPC2^{-/-} or WT mice were stained with mouse CD1d:αGalCer dimers and mAb against TCRβ and CD4 or Vβ8.2 or Vβ7, and analyzed by flow cytometry. The cytograms in (B) depict the gates defining Va14i NKT and conventional TCRαβ T cells, as described for (A). The histograms in (C) show the expression of CD4, Vβ8.2, or Vβ7 among hepatic Va14i NKT cells. Numbers represent the mean percentage of positive cells (± SD) in the indicated gates (n=3).

cells, there are some interesting differences regarding the residual populations of Va14i NKT cells: (i) The small population of Va14i NKT cells, selected in the absence of NPC2, bound CD1d:αGalCer dimers with similar avidity as Va14i NKT cells from WT mice, whereas in βGal^{-/-} mice only Va14i NKT cells binding these dimers with high avidity could be detected (Figs. 1 and 4). (ii) The ratio of CD4⁺/CD4⁻ cells among Va14i NKT (but not among conventional TCR-αβ T) cells in NPC2^{-/-} mice was significantly increased by a factor of ~ 3.5, whereas CD4 expression was normal among Va14i NKT cells in βGal^{-/-} mice (Figs. 1C and 4C). (iii) The ratio of Vβ8.2/Vβ7 among Va14i NKT cells in NPC2^{-/-} mice was only slightly decreased, whereas in βGal^{-/-} mice these cells clearly expressed Vβ7 at higher frequency. These

repertoire differences point to differential mechanisms causing impaired selection of Va14i NKT cells in βGal^{-/-} and NPC2^{-/-} mice.

Presentation of lipid antigens is impaired in NPC2^{-/-} APC

To investigate whether presentation of lipid antigens is impaired in NPC2^{-/-} APC, we first checked for the capability of NPC2^{-/-} thymocytes or DC to stimulate a human Va24i NKT clone in the absence of additional lipid antigens, as described above. Thymocytes or DC from WT mice stimulated the human Va24i NKT clone to release human IL-4, whereas this stimulation was strongly impaired if cells were deficient in NPC2 (Fig. 5A). It should be noted that, in contrast to thymocytes (Fig. 4A), NPC2^{-/-} DC had normal expres-

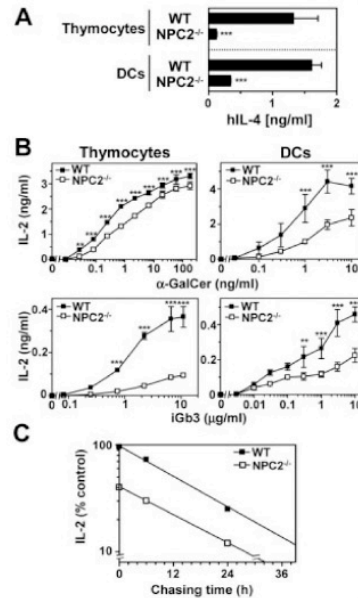


Figure 5. Presentation of lipid antigens is impaired in NPC2^{-/-} APC. (A) Thymocytes or DC from NPC2^{-/-} or WT mice were incubated with a human Va24i NKT clone, and human (h) IL-4 release to cell culture supernatant was determined. (B) Thymocytes or DC from NPC2^{-/-} or WT mice were incubated with different concentrations of αGalCer or iGb3 before the addition of Va14i NKT hybridoma cells. IL-2 release to cell culture supernatant was determined. (C) DC from NPC2^{-/-} or WT mice were pulsed with αGalCer (100 ng/mL) for 2 h and chased for different periods of time before addition of Va14i NKT hybridoma cells. Diagrams show the mean release of cytokine (± SD in A and B; n=3). ** p<0.01, *** p<0.001 comparing WT and NPC2^{-/-} (in A and B).

sion levels of CD1d on the surface (unpublished data) and nevertheless were weak APC.

The stimulation of mouse $V\alpha 14i$ NKT hybridoma cells in the presence of α -GalCer or iGb3 was also impaired if thymocytes or DC were deficient in NPC2 (Fig. 5B). Presentation of peptides via MHC class II was not influenced by the lack of NPC2, since NPC2^{-/-} DC perfectly presented ovalbumin to specific T cells derived from OT-II transgenic mice (Supporting Information Fig. S1B).

Since NPC2 is thought to be involved in lipid transport [40–42], we wondered whether the lower efficacy of lipid antigens in NPC2^{-/-} cells is due to a changed half-life of functional CD1d:lipid antigen complexes. To this end, NPC2^{-/-} or WT DC were pulsed with α -GalCer for 2 h and chased for different periods of time before addition of $V\alpha 14i$ NKT hybridoma cells. The kinetics by which the stimulatory capacity of DC decreased, and thus the half-life of functional CD1d: α -GalCer complexes, were identical between NPC2^{-/-} and WT cells ($t_{1/2} \sim 14$ h) (Fig. 5C). Therefore, it is the formation of such complexes, rather than their maintenance, which is affected in NPC2^{-/-} cells.

The deficiency in lipid antigen presentation might explain the low numbers of $V\alpha 14i$ NKT cells selected in NPC2^{-/-} mice.

Pharmacological reduction of lipid accumulation in NPC2^{-/-} thymocytes improves lipid antigen presentation

To better understand the mechanism of impaired lipid antigen presentation in NPC2^{-/-} APC, we tested whether accumulation of lipids might play a role. Glycosphingolipid biosynthesis was pharmacologically inhibited in thymocytes with NB-DNJ, as described above. Analogous experiments with DC could not be performed because of toxicity of NB-DNJ at pharmacological concentrations (unpublished data), similar to observations described for the analogous drug *N*-butyldeoxygalactonojirimycin [31]. Incubation of NPC2^{-/-} thymocytes with NB-DNJ significantly improved their capacity to present α -GalCer to the $V\alpha 14i$ NKT hybridoma (Fig. 6A), indicating that accumulating lipids contribute to the impairment of lipid antigen presentation in NPC2^{-/-} thymocytes. This mechanism might also explain why thymic selection of $V\alpha 14i$ NKT cells is impaired in NPC2^{-/-} mice.

The formation of stimulatory CD1d:lipid antigen complexes is impaired in NPC2^{-/-} APC

To investigate whether the formation of functional CD1d:lipid antigen complexes on the cell surface is impaired in NPC2^{-/-} APC, DC from NPC2^{-/-} and WT

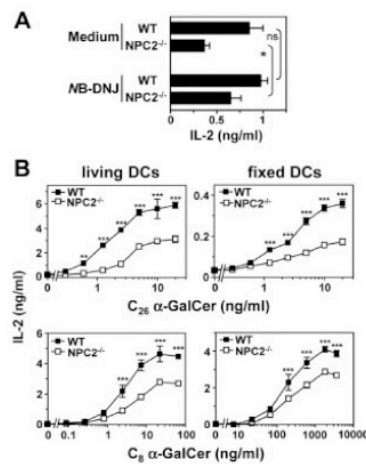


Figure 6. Accumulation of lysosomal storage lipids accounts for the impairment of lipid antigen presentation in NPC2^{-/-} cells, characterized by a disturbance of CD1d in forming functional complexes with lipid antigen. (A) Thymocytes from NPC2^{-/-} or WT mice were incubated with NB-DNJ or medium before α -GalCer (1 ng/mL) and $V\alpha 14i$ NKT hybridoma cells were added. IL-2 release to cell culture supernatant was determined. The bar chart shows the mean release of IL-2 (\pm SD; $n=3$). * $p < 0.05$; ns, not significant. (B) Living or fixed DC from NPC2^{-/-} or WT mice were incubated with various concentrations of "classical" C₂₆ α -GalCer or a C₈ α -GalCer analogue before the addition of $V\alpha 14i$ NKT hybridoma cells. IL-2 release to cell culture supernatant was determined. Diagrams show the mean release of IL-2 (\pm SD; $n=3$). ** $p < 0.01$, *** $p < 0.001$ comparing WT and NPC2^{-/-}.

mice were fixed with glutaraldehyde and then incubated with α -GalCer to test their presentation capacity to $V\alpha 14i$ NKT hybridoma cells. For this experiment we chose DC rather than thymocytes because surface CD1d levels were not reduced in the case of NPC2^{-/-} DC, as mentioned above. Fixation did not improve the efficacy of α -GalCer stimulation by NPC2-deficient APC (Fig. 6B). Increasing concentrations of α -GalCer could not overcome this defect, suggesting that the CD1d: α -GalCer complexes formed on NPC2^{-/-} DC might have intrinsic differences limiting the stimulation of $V\alpha 14i$ NKT cells. These differences could depend on the presence of spacer molecules disturbing proper binding of stimulatory lipid antigens or, alternatively, could be ascribed to a reduced number of CD1d molecules freely available for binding α -GalCer. To test for the first possibility, lipid antigens with short alkyl chains were used together with NPC2^{-/-} DC. Indeed, α -GalCer containing a C₈ alkyl chain binds to CD1d also in the presence of spacer molecules inserted in the A' pocket [43]. We compared the $V\alpha 14i$ NKT cell stimulatory

capacity of two α -GalCer molecules containing a C₈ and a C₂₆ alkyl chain, respectively. As shown in Fig. 6B, these experiments revealed three main findings: (i) The reduction of the alkyl chain length from C₂₆ to C₈ did not improve the efficacy of α -GalCer stimulation by living or fixed NPC2^{-/-} DC. This suggests that a smaller number of stimulatory CD1d: α -GalCer complexes is formed on NPC2^{-/-} cells regardless of the alkyl chain length. (ii) When fixed DC were used, about 100 times more C₈ α -GalCer was required for maximal T cell stimulation as compared to living DC. Instead, C₂₆ α -GalCer was equally potent with both fixed and living DC. This indicates that the presence of short alkyl chains affects the formation of stable complexes with CD1d molecules modified by fixation. (iii) The maximal cytokine release induced by C₈ α -GalCer was similar when living or fixed DC were used, thus indicating that the CD1d: α -GalCer complexes formed with this analogue stimulate V α 14i NKT cells very efficiently.

Discussion

Deficiencies in enzymes of the lysosomal glycosphingolipid degradation pathway or in lysosomal lipid transfer proteins cause imbalances in lipid metabolism. Recently, mouse models of lipid storage diseases have been studied with respect to the relevance of lysosomal enzymes and lipid transfer proteins for stimulation and selection of a specialized population of T cells, *i.e.*, V α 14i NKT cells, recognizing glycolipid antigens in the context of CD1d antigen-presenting molecules. These studies revealed that Hexb^{-/-} [28, 32], Hexa^{-/-} [32], α Gal^{-/-} [32], β Gal^{-/-} [32], saposin^{-/-} [29], or NPC1^{-/-} [31, 32] deficient mice have reduced numbers of V α 14i NKT cells and, in the cases of Hexb^{-/-}, β Gal^{-/-}, saposin^{-/-}, and NPC1^{-/-} mice, defects in lipid antigen presentation. V α 14i NKT cell deficiency has originally been explained as a result of lacking iGb3 in the case of Hexb^{-/-}, and of impaired saposin-mediated lipid transfer onto CD1d molecules in the case of saposin^{-/-} mice. More recently, Sagiv *et al.* [31] and Gadola *et al.* [32] hypothesized that lysosomal lipid storage might have an independent, nonspecific negative effect on lipid antigen presentation to, and thymic selection of, V α 14i NKT cells. However, the contribution of lysosomal storage lipids to an impairment of lipid antigen presentation has not been investigated, so far.

Here we investigated two mouse models of imbalanced lipid metabolism, *i.e.*, β Gal^{-/-} mice (a model for GM1 gangliosidosis) and NPC2^{-/-} mice (a model for Niemann Pick C2 disease). In both models, development of V α 14i NKT but not of other T cells was impaired by ~70%. The simplest explanation for V α 14i NKT cell deficiency in these mice would be a specific involvement

of β Gal in the generation of iNKT cell-selecting lipid antigen(s) in the thymus and a specific role of NPC2 as a lipid transfer protein for iNKT cell-selecting lipid antigen(s) or their precursors. However, our data suggest that it is rather indirect mechanisms, *i.e.*, particularly the accumulation of different types of lipids, which are responsible for impaired selection of V α 14i NKT cells in the two mouse models.

The enzyme β Gal is involved in the hydrolyzation of terminal β -galactosidic residues of glycoconjugates, including the gangliosides GM1 and GA1, and lactosylceramide [37]. GM1/GA1 can no longer be degraded to GM2/GA2 and GM3/GA3 and represent the most prominent glycolipids accumulating in patients and mice deficient in β Gal [44–46]. However, the lack of gangliosides such as GM2/GA2 or GM3/GA3 probably does not explain deficient development of V α 14i NKT cells in β Gal^{-/-} mice since mice lacking ganglio-series glycolipids as a result of genetic deficiency of GM2 or GM3 synthase, *i.e.*, the key enzymes for their synthesis, displayed no apparent defect in development of V α 14i NKT cells [28]. Lactosylceramide does not accumulate in β Gal^{-/-} mice because its degradation, involving the removal of terminal β -galactose residues, can be exerted by an alternative enzyme, galactosylceramidase (EC 3.2.1.46) [47, 48]. Hence, assuming that accumulating lipids in lysosomes would not interfere with the glycosphingolipid degradation pathways, the degradation products of lactosylceramide would be generated normally in these mice. iGb3 would also be generated normally because β Gal is not involved in the globoside degradation pathway. Overall, we therefore considered the possibility that deficiency of β Gal indirectly, rather than directly, causes the impairment of V α 14i NKT cell development. This consideration was supported by our observations that β Gal^{-/-} DC, in contrast to β Gal^{-/-} thymocytes, were able to stimulate V α 24i NKT cells in the absence of additional lipid antigens and that presentation of exogenous lipid antigens (α -GalCer or iGb3) by β Gal^{-/-} thymocytes was impaired. Similarly, Gadola *et al.* [32] recently showed impaired presentation of α -GalCer by β Gal^{-/-} splenocytes. Furthermore, we found that presentation of exogenous lipid antigen is improved by pre-treatment of β Gal^{-/-} thymocytes with NB-DNJ, an inhibitor of glycosphingolipid biosynthesis known to reduce pathological lipid storage *in vitro* and *in vivo* [38]. This indicates that accumulating lipids disturb lipid antigen presentation in β Gal^{-/-} thymocytes. GM1, the major glycolipid accumulating in β Gal-deficient patients and mice, competes with other glycolipids for binding to CD1d [49]. This mechanism would affect the formation of stimulatory CD1d:lipid antigen complexes on the cell surface. However, since upon fixation β Gal^{-/-} and WT thymocytes presented lipid antigen equally, it is intracellular defects that

account for the impairment of lipid antigen presentation in $\beta\text{Gal}^{-/-}$ cells. Disturbance of proteins involved in the transport of lipid antigens, in the unloading of non-antigenic lipids from CD1d, in the loading of lipid antigens onto CD1d, and/or in the maintenance of functional CD1d:lipid antigen complexes might occur. The effect of βGal deficiency on lipid antigen presentation could be observed with thymocytes and splenocytes, but not with DC (cf Figure 2 and [32]). Different quantities or types of accumulating lipids might explain why lipid antigen presentation is impaired in $\beta\text{Gal}^{-/-}$ thymocytes but not DC. Therefore, this demands caution with the cell type used for lipid antigen-presentation experiments to avoid misinterpretations, e.g., regarding thymic selection.

The proteins NPC1 and NPC2 are thought to be involved in the transport of different lipids [40, 41]. Deficiency of either NPC1 or NPC2 results in lysosomal storage of cholesterol, phospholipids, GM2 and GM3, glucosylceramide, lactosylceramide, sphingomyelin, and other lipids [40]. The precise mechanisms of action or the substrates of these putative transporters have not been fully defined, yet. However, it is inferred that NPC1 and NPC2 have nonredundant functions in a common pathway of lipid transport [40] with a particular role for NPC2 as a lysosomal cholesterol transfer protein [42]. Recently, impaired glycosphingolipid trafficking, lipid antigen presentation, and development of V α 14i NKT cells in NPC1 $^{-/-}$ mice have been described [31, 32]. Glycosphingolipid trafficking was partly restored by pre-treatment of NPC1-deficient cells with *N*-butyldeoxygalactonojirimycin *in vitro* [31]. The impact of this partial restoration on lipid antigen presentation to V α 14i NKT cells has not been studied. However, since accumulating lipids disturb glycosphingolipid trafficking in NPC1 $^{-/-}$ cells [31, 41], they might also contribute to impaired lipid antigen presentation if NPC1 is absent. In the present study, we demonstrated that lipid antigen presentation is impaired in NPC2 $^{-/-}$ APC, including thymocytes, and that thymic selection of V α 14i NKT cells is disturbed in NPC2 $^{-/-}$ mice. Impaired presentation of lipid antigens was not due to a change in the half-life of CD1d:lipid antigen complexes thus excluding faster degradation of CDd:lipid antigen complexes. Importantly, lipid antigen presentation could be improved by pre-treatment of NPC2 $^{-/-}$ APC with NB-DNJ, directly demonstrating that accumulating glycosphingolipids disturb lipid presentation in NPC2 $^{-/-}$ APC. Two mechanisms describing how the accumulating lipids might inhibit CD1d antigen presentation can be envisaged. First, they could hinder unloading of the spacer molecules that are associated with CD1d [43]. However, this possibility is not supported by the results obtained with the C $_3$ α -GalCer analogue. This lipid antigen can effectively bind to CD1d in the presence of

spacers [43]. Nevertheless, it does not restore the presentation capacity of NPC2 $^{-/-}$ APC. A second mechanism is that accumulating glycosphingolipids could form very stable complexes with CD1d and prevent the formation of complexes containing the stimulatory lipid antigens. Indeed, a number of lipids are able to bind to CD1d without being antigenic for V α 14i NKT cells, including phospholipids [49, 50] and glucosylceramide [50], which accumulate in NPC2 $^{-/-}$ cells. Although this mechanism is difficult to prove experimentally, it is in agreement with our findings showing that pre-treatment of NPC2 $^{-/-}$ DC with NB-DNJ partially restores lipid antigen presentation and that even high concentrations of α -GalCer could not overcome the presentation defect.

Although the accumulation of lipids impairs lipid antigen presentation in both $\beta\text{Gal}^{-/-}$ and NPC2 $^{-/-}$ cells, the underlying mechanisms are different. We can not exclude that also the mouse strain background (C57BL/6 in the case of $\beta\text{Gal}^{-/-}$ and BALB/c in the case of NPC2 $^{-/-}$ mice) may influence the effect of accumulating lipids on the phenotype of V α 14i NKT cells. However, because of the characteristic types of lipids accumulating in $\beta\text{Gal}^{-/-}$ vs. NPC2 $^{-/-}$ mice, we favor the hypothesis that it is mainly a change in the quantity and type(s) of presented lipid antigens that influences the phenotype and TCR repertoire among the residual V α 14i NKT cell populations in $\beta\text{Gal}^{-/-}$ vs. NPC2 $^{-/-}$ mice. This includes a remarkable decrease of the V β 8.2/V β 7 ratio in $\beta\text{Gal}^{-/-}$, but not NPC2 $^{-/-}$, and an increase of the CD4 $^{-}$ /CD4 $^{+}$ ratio in NPC2 $^{-/-}$, but not $\beta\text{Gal}^{-/-}$, mice. In $\beta\text{Gal}^{-/-}$ mice, limiting quantities of available lipids responsible for positive selection might favor development of V α 14i NKT cells expressing V β 7, which confers high avidity binding to CD1d in the context of endogenous selecting lipid antigen(s) [35, 36]. In NPC2 $^{-/-}$ mice, changes in the types of selecting lipid antigens might affect the strength of TCR signaling and cause more frequent down-regulation of CD4, resembling down-regulation of CD4 and CD8 on DP thymocytes caused by stimulation of the TCR [51].

In summary, dysregulation of lipid metabolism and accumulation of lipids cause defective presentation of lipid antigens to, and impaired thymic selection of, V α 14i NKT cells. The exact underlying mechanisms are diverse, depending on the cause of imbalance, and, as a consequence, different subsets of V α 14i NKT cells are selected in thymi of mice suffering from different lipid storage diseases. It will be interesting to investigate to what extent alterations in lipid metabolism in other diseases, e.g., atherosclerosis, tumors, and infections, change the capacity of APC to present lipid antigens via CD1 molecules and thus affect the immune response.

Materials and methods

Mice

C57BL/6 and BALB/c mice were bred at our institute. β Gal^{-/-} [44, 45] and NPC2^{-/-} [40] mice were backcrossed to C57BL/6 and BALB/c mice, respectively. This study was reviewed and approved by the “Kantonales Veterinäramt Basel-Stadt” in Basel, Switzerland.

Cell preparations

Thymocytes were prepared by grinding thymi through tea strainers. For further analysis of Va14i NKT cells, thymocytes were depleted of heat-stable Ag (HSA)⁺ and CD8⁺ cells by treatment with rat IgM mAb B2A2 and rat IgM mAb 3.168.8.1 plus rabbit complement. Viable recovered cells were purified on a lympholyte M gradient (Cedarlane Laboratories, Hornby, Ontario, Canada). Liver mononuclear cells were prepared as described previously [2]. Splenocytes and bone marrow cells were obtained using standard methods. DC were prepared by culturing bone marrow progenitors with mouse GM-CSF for 8 days.

Flow cytometry

Va14i NKT cells were specifically identified by mouse CD1d: α -GalCer dimers as described previously [33]. Cells were further stained with combinations of the following mAb conjugates, anti-TCR β -FITC (H57–597), anti-CD8 α -FITC (53–6.7), anti-CD4-PE (RM4–5), anti-CD1d-biotin (1B1), anti-TCR γ δ -biotin (GL3), anti-CD4-biotin (RM4–5), anti-V β 8.2-biotin (F23–2), and anti-V β 7-biotin (TR310). The biotinylated mAb were revealed with streptavidin-allophycocyanin. Samples were passed on a CyAn ADP flow cytometer (DakoCytomation, Baar, Switzerland), gated to exclude nonviable cells on the basis of light scatter and incorporation of propidium iodide. Data were analyzed using Summit 4.2 software (DakoCytomation).

Fixation of APC

Thymocytes or bone marrow-derived DC were washed and suspended in PBS (3×10^6 /mL) containing 0.05% glutaraldehyde for 20 s. Additional fixation was blocked with 0.2 M lysine/PBS.

Generation of human Va24i NKT clones and mouse Va14i NKT hybridomas

CD1d-restricted human Va24i NKT cells were expanded *in vitro* by stimulation of human PBMC with 100 ng/mL α -GalCer. After 14 days, Va24i NKT clones were derived and maintained according to standard procedures. To generate mouse Va14i NKT hybridomas, Va14i NKT cells sorted from α -GalCer-treated C57BL/6 mice on the basis of human CD1d: α -GalCer dimer binding were fused with mouse BW5147 thymic lymphoma cells using standard procedures.

In vitro stimulation of iNKT cells

Thymocytes (500 000/well) or bone marrow-derived DC (50 000/well) were either incubated with the human Va24i NKT clone JS63 (100 000/well) or with the mouse Va14i NKT hybridoma FF13 (50 000/well) for 40 h. In some experiments, living or fixed thymocytes or bone marrow-derived DC were incubated for 2 h with different concentrations of sonicated α -GalCer or iGb3 (Alexis Corporation, Lausen, Switzerland) before addition of iNKT cells. In some experiments, thymocytes were pre-incubated for 24 h with 50 μ M NB-DNJ (Calbiochem, Merck Biosciences, Nottingham, UK) before the stimulation experiment started. NB-DNJ was also present during the stimulation experiments at 50 μ M. Human IL-4 or mouse IL-2 released to cell culture supernatants were measured by ELISA using antibody pairs from BD Biosciences PharMingen (San Diego, CA).

Synthesis of C₈ α -GalCer

α -GalCer containing a C₈ acyl chain was prepared following, in part, literature procedures. Briefly, glycosylation of properly protected azidophytosphingosine, obtained according to Schmidt and Maier [52], with tetra-O-benzyl- α -D-galactopyranosyl bromide [53] using the “*in situ* anomerization” [54] protocol gave the corresponding α -glycoside. Reduction of the azide by hydrogenation with Lindlar catalyst [54] and conventional acylation with octanoyl chloride gave the protected C₈ α -GalCer. Removal of the isopropylidene group by acidic hydrolysis and of the benzyl groups from galactosyl moiety by hydrogenolysis catalyzed by Pd(OH)₂/C gave the desired C₈ α -GalCer.

Statistical analysis

The results were analyzed using ANOVA with the Bonferroni multiple comparison post test. All data in this study are expressed as the mean \pm SD. $p < 0.05$ was considered significant.

Acknowledgements: We thank J. Matsuda (Laboratory of Experimental Animal Models, National Institute of Biomedical Innovation, Osaka, Japan) for providing β Gal^{-/-}, P. Lobel (Center of Advanced Biotechnology and Medicine, University of Medicine & Dentistry of New Jersey, Piscataway, NJ, USA) for providing NPC2^{-/-}, and U. Günthert (Institute for Medical Microbiology, University of Basel, Basel, Switzerland) for providing OT-II transgenic (DO11.10) mice. We are indebted to Y. Kozuka (Kirin Brewery, Gunma, Japan) for providing α -GalCer (KRN7000). This work was supported by the Swiss National Foundation grant 3100A0-109918 (to G.D.L.), the MOLSTROKE project, contract no. LSH-CT-2004-005206, funded under the EU FP6-2003 LIFESCI-HEALTH program (to G.D.L.), the University of Piemonte Orientale (to L.P.) and IRCAD-Novara (to L.P.). The authors have no conflicting financial interests.

References

- Arase, H., Arase, N., Ogasawara, K., Good, R. A. and Onoe, K., An NK1.1⁺CD4⁺8⁻ single-positive thymocyte population that expresses a highly skewed T-cell antigen V β family. *Proc. Natl. Acad. Sci. USA* 1992. **89**: 6506–6510.
- Ohteki, T. and MacDonald, H. R., Major histocompatibility complex class I related molecules control the development of CD4⁺8⁻ and CD4⁺8⁺ subsets of natural killer 1.1⁺ T cell receptor- α/β ⁺ cells in the liver of mice. *J. Exp. Med.* 1994. **180**: 699–704.
- Lantz, O. and Bendelac, A., An invariant T cell receptor α chain is used by a unique subset of major histocompatibility complex I-specific CD4⁺ and CD4⁺8⁻ T cells in mice and humans. *J. Exp. Med.* 1994. **180**: 1097–1106.
- Ohteki, T. and MacDonald, H. R., Stringent V β requirement for the development of NK1.1⁺ T cell receptor- α/β ⁺ cells in mouse liver. *J. Exp. Med.* 1996. **183**: 1277–1282.
- Godfrey, D. I. and Kronenberg, M., Going both ways: immune regulation via CD1d-dependent NKT cells. *J. Clin. Invest.* 2004. **114**: 1379–1388.
- Yu, K. O. A. and Porcelli, S. A., The diverse functions of CD1d-restricted NKT cells and their potential for immunotherapy. *Immunol. Lett.* 2005. **100**: 42–55.
- Gapin, L., Matsuda, J. L., Surh, C. D. and Kronenberg, M., NKT cells derive from double-positive thymocytes that are positively selected by CD1d. *Nat. Immunol.* 2001. **2**: 971–978.
- Dao, T., Guo, D., Ploss, A., Stolzer, A., Saylor, C., Boursalian, T. E., Im, J. S. and Sant'Angelo, D. B., Development of CD1d-restricted NKT cells in the mouse thymus. *Eur. J. Immunol.* 2004. **34**: 3542–3552.
- Bezradica, J. S., Hill, T., Stanic, A. K., Van Kaer, L. and Joyce, S., Commitment toward the natural T (iNKT) cell lineage occurs at the CD4⁺8⁺ stage of thymic ontogeny. *Proc. Natl. Acad. Sci. USA* 2005. **102**: 5114–5119.
- Egawa, T., Eberl, G., Taniuchi, I., Benlagha, K., Geissmann, F., Hennighausen, L., Bendelac, A. and Littman, D. R., Genetic evidence supporting selection of the V α 14i NKT cell lineage from double-positive thymocyte precursors. *Immunity* 2005. **22**: 705–716.
- Benlagha, K., Wei, D. G., Veiga, J., Teyton, L. and Bendelac, A., Characterization of the early stages of thymic NKT cell development. *J. Exp. Med.* 2005. **202**: 485–492.
- Fellicci, D. G., Hammond, K. J. L., Uldrich, A. P., Baxter, A. G., Smyth, M. J. and Godfrey, D. I., A natural killer T (NKT) cell developmental pathway involving a thymus-dependent NK1.1⁺ CD4⁺ CD1d-dependent precursor stage. *J. Exp. Med.* 2002. **195**: 835–844.
- Benlagha, K., Kyin, T., Beavis, A., Teyton, L. and Bendelac, A., A thymic precursor to the NK T cell lineage. *Science* 2002. **296**: 553–555.
- Gadue, P. and Stein, P. L., NK T cell precursors exhibit differential cytokine regulation and require Itk for efficient maturation. *J. Immunol.* 2002. **169**: 2397–2406.
- Bix, M., Coles, M. and Raulet, D., Positive selection of V β 8⁺ CD4⁺8⁻ thymocytes by class I molecules expressed by hematopoietic cells. *J. Exp. Med.* 1993. **178**: 901–908.
- Bendelac, A., Killeen, N., Littman, D. and Schwartz, R. H., A subset of CD4⁺ thymocytes selected by MHC class I molecules. *Science* 1994. **263**: 1774–1778.
- Forestier, C., Park, S. H., Wei, D., Benlagha, K., Teyton, L. and Bendelac, A., T cell development in mice expressing CD1d directed by a classical MHC class II promoter. *J. Immunol.* 2003. **171**: 4096–4104.
- Xu, H., Chun, T., Colmone, A., Nguyen, H. and Wang, C. R., Expression of CD1d under the control of a MHC class Ia promoter skews the development of NKT cells, but not CD8⁺ T cells. *J. Immunol.* 2003. **171**: 4105–4112.
- Coles, M. C. and Raulet, D. H., NK1.1⁺ T cells in the liver arise in the thymus and are selected by interactions with class I molecules on CD4⁺ CD8⁺ cells. *J. Immunol.* 2000. **164**: 2412–2418.
- Bendelac, A., Positive selection of mouse NK1⁺ T cells by CD1-expressing cortical thymocytes. *J. Exp. Med.* 1995. **182**: 2091–2096.
- Wei, D. G., Lee, H., Park, S. H., Beaudoin, L., Teyton, L., Lehuen, A. and Bendelac, A., Expansion and long-range differentiation of the NKT cell lineage in mice expressing CD1d exclusively on cortical thymocytes. *J. Exp. Med.* 2005. **202**: 239–248.
- Schümann, J., Pittoni, P., Tonti, E., MacDonald, H. R., Dellabona, P. and Casorati, G., Targeted expression of human CD1d in transgenic mice reveals independent roles for thymocytes and thymic antigen-presenting cells in positive and negative selection of V α 14i NKT cells. *J. Immunol.* 2005. **175**: 7303–7310.
- Chun, T., Page, M. J., Gapin, L., Matsuda, J. L., Xu, H., Nguyen, H., Kang, H. S. et al., CD1d-expressing dendritic cells but not thymic epithelial cells can mediate negative selection of NKT cells. *J. Exp. Med.* 2003. **197**: 907–918.
- De Libero, G. and Mori, L., Mechanisms of lipid-antigen generation and presentation to T cells. *Trends Immunol.* 2006. **27**: 485–492.
- Savage, P. B., Teyton, L. and Bendelac, A., Glycolipids for natural killer T cells. *Chem. Soc. Rev.* 2006. **35**: 771–779.
- Sullivan, B. A., Nagarajan, N. A. and Kronenberg, M., CD1 and MHC II find different means to the same end. *Trends Immunol.* 2005. **26**: 282–288.
- Hava, D. L., Brigl, M., Van den Elzen, P., Zajonc, D. M., Wilson, I. A. and Brenner, M. B., CD1 assembly and the formation of CD1-antigen complexes. *Curr. Opin. Immunol.* 2005. **17**: 88–94.
- Zhou, D., Mattner, J., Cantu, C. III, Schrantz, N., Yin, N., Gao, Y., Sagiv, Y. et al., Lysosomal glycosphingolipid recognition by NKT cells. *Science* 2004. **306**: 1786–1789.
- Zhou, D., Cantu, C. III, Sagiv, Y., Schrantz, N., Kulkarni, A. B., Qi, X., Mahuran, D. J. et al., Editing of CD1d-bound lipid antigens by endosomal lipid transfer proteins. *Science* 2004. **303**: 523–527.
- Kang, S. J. and Cresswell, P., Saposins facilitate CD1d-restricted presentation of an exogenous lipid antigen to T cells. *Nat. Immunol.* 2004. **5**: 175–181.
- Sagiv, Y., Hudspeth, K., Mattner, J., Schrantz, N., Stern, R. K., Zhou, D., Savage, P. B. et al., Cutting edge: Impaired glycosphingolipid trafficking and NKT cell development in mice lacking Niemann-Pick type C1 protein. *J. Immunol.* 2006. **177**: 26–30.
- Gadola, S. D., Silk, J. D., Jeans, A., Illarionov, P. A., Salio, M., Besra, G. S., Dwek, R. et al., Impaired selection of invariant natural killer T cells in diverse mouse models of glycosphingolipid lysosomal storage diseases. *J. Exp. Med.* 2006. **203**: 2293–2303.
- Schümann, J., Voyle, R. B., Wei, B. Y. and MacDonald, H. R., Cutting edge: Influence of the TCR V β domain on the avidity of CD1d: α -galactosylceramide binding by invariant V α 14 NKT cells. *J. Immunol.* 2003. **170**: 5815–5819.
- Stanic, A. K., Shashidharamurthy, R., Bezradica, J. S., Matsuki, N., Yoshimura, Y., Miyake, S., Choi, E. Y. et al., Another view of T cell antigen recognition: cooperative engagement of glycolipid antigens by V α 14i natural T (iNKT) cell receptor. *J. Immunol.* 2003. **171**: 4539–4551.
- Schümann, J., Mycko, M. P., Dellabona, P., Casorati, G. and MacDonald, H. R., Cutting edge: Influence of the TCR V β domain on the selection of semi-invariant NKT cells by endogenous ligands. *J. Immunol.* 2006. **176**: 2064–2068.
- Wei, D. G., Curran, S. A., Savage, P. B., Teyton, L. and Bendelac, A., Mechanisms imposing the V β bias of V α 14 natural killer T cells and consequences for microbial glycolipid recognition. *J. Exp. Med.* 2006. **203**: 1197–1207.
- Kolter, T. and Sandhoff, K., Principles of lysosomal membrane digestion: Stimulation of sphingolipid degradation by sphingolipid activator proteins and anionic lysosomal lipids. *Annu. Rev. Cell. Dev. Biol.* 2005. **21**: 81–103.
- Platt, F. M. and Butters, T. D., New therapeutic prospects for the glycosphingolipid lysosomal storage diseases. *Biochem. Pharmacol.* 1998. **56**: 421–430.
- Yu, K. O. A., Im, J. S., Molano, A., Dutronc, Y., Illarionov, P. A., Forestier, C., Fujiwara, N. et al., Modulation of CD1d-restricted NKT cell responses by using N-acetyl variants of α -galactosylceramides. *Proc. Natl. Acad. Sci. USA* 2005. **102**: 3383–3388.
- Sleat, D. E., Wiseman, J. A., El-Banna, M., Price, S. M., Verot, L., Shen, M. M., Tint, G. S. et al., Genetic evidence for nonredundant functional cooperativity between NPC1 and NPC2 in lipid transport. *Proc. Natl. Acad. Sci. USA* 2004. **101**: 5886–5891.
- Mukherjee, S. and Maxfield, F. R., Lipid and cholesterol trafficking in NPC. *Biochim. Biophys. Acta* 2004. **1685**: 28–37.

- 42 Cheruku, S. R., Xu, Z., Dutia, R., Lobel, P. and Storch, J., Mechanism of cholesterol transfer from the Niemann-Pick type C2 protein to model membranes supports a role in lysosomal cholesterol transport. *J. Biol. Chem.* 2006. **281**: 31594–31604.
- 43 Zajonc, D. M., Cantu, C. III, Mattner, J., Zhou, D., Savage, P. B., Bendelac, A., Wilson, I. A. and Teyton, L., Structure and function of a potent agonist for the semi-invariant natural killer T cell receptor. *Nat. Immunol.* 2005. **6**: 810–818.
- 44 Matsuda, J., Suzuki, O., Oshima, A., Ogura, A., Naiki, M. and Suzuki, Y., Neurological manifestations of knockout mice with β -galactosidase deficiency. *Brain Dev.* 1997. **19**: 19–20.
- 45 Matsuda, J., Suzuki, O., Oshima, A., Ogura, A., Noguchi, Y., Yamamoto, Y., Asano, T. et al., β -Galactosidase-deficient mouse as an animal model for GM₁-gangliosidosis. *Glycoconj. J.* 1997. **14**: 729–736.
- 46 Hahn, C. N., Del Pilar Martin, M., Schröder, M., Vanier, M. T., Hara, Y., Suzuki, K., Suzuki, K. and d'Azzo, A., Generalized CNS disease and massive GM₁-ganglioside accumulation in mice defective in lysosomal acid β -galactosidase. *Hum. Mol. Genet.* 1997. **6**: 205–211.
- 47 Zschoche, A., Fürst, W., Schwarzmann, G. and Sandhoff, K., Hydrolysis of lactosylceramide by human galactosylceramidase and GM1- β -galactosidase in a detergent-free system and its stimulation by sphingolipid activator proteins, sap-B and sap-C. *Eur. J. Biochem.* 1994. **222**: 83–90.
- 48 Tohyama, J., Vanier, M. T., Suzuki, K., Ezoe, T., Matsuda, J. and Suzuki, K., Paradoxical influence of acid β -galactosidase gene dosage on phenotype of the twitcher mouse (genetic galactosylceramidase deficiency). *Hum. Mol. Genet.* 2000. **9**: 1699–1707.
- 49 Naidenko, O. V., Maher, J. K., Ernst, W. A., Sakai, T., Modlin, R. L. and Kronenberg, M., Binding and antigen presentation of ceramide-containing glycolipids by soluble mouse and human CD1d molecules. *J. Exp. Med.* 1999. **190**: 1069–1079.
- 50 Stanic, A. K., De Silva, A. D., Park, J. J., Sriram, V., Ichikawa, S., Hirabayashi, Y., Hayakawa, K. et al., Defective presentation of the CD1d1-restricted Va14Ja18 NKT lymphocyte antigen caused by β -d-glucosylceramide synthase deficiency. *Proc. Natl. Acad. Sci. USA* 2003. **100**: 1849–1854.
- 51 Page, D. M., Kane, L. P., Allison, J. P. and Hedrick, S. M., Two signals are required for negative selection of CD4⁺ CD8⁺ thymocytes. *J. Immunol.* 1993. **151**: 1868–1880.
- 52 Schmidt, R. R. and Maier, T., Synthesis of d-ribo- and l-lyxo-phyto-sphingosine: transformation into the corresponding lactosyl-ceramides. *Carbohydr. Res.* 1988. **174**: 169–179.
- 53 Wessel, H.-P. and Bundle, D. R., Strategies for the synthesis of branched oligosaccharides of the *Shigella flexneri* 5a, 5b, and variant X serogroups employing a multifunctional rhamnose precursor. *J. Chem. Soc. Perkin Trans.* 1985I, 2251–2260.
- 54 Murata, K., Toba, T., Nakanishi, K., Takahashi, B., Yamamura, T., Miyake, S. and Annoura, H., Total Synthesis of an Immunosuppressive Glycolipid, (2S,3S,4R)-1-O-(α -d-Galactosyl)-2-tetracosanoylamino-1,3,4-nonanetriol. *J. Org. Chem.* 2005. **70**: 2398–2401.

CURRICULUM VITAE

EDUCATION

2003 - MASTER'S DEGREE in MOLECULAR AND CELL BIOLOGY

Academic Honors: CUM LAUDE

Awards: Fellowship Award from VML (a French Society promoting research against rare diseases - <http://www.vml-asso.org>)

Louis Pasteur University, Strasbourg, FRANCE

2002 - MAITRISE in BIOCHEMISTRY

Academic Honors: CUM LAUDE

Awards: Merit Scholarship Award (top 5% in the discipline nationwide)

Henri Poincare University, Nancy, FRANCE

2001 - BACHELOR'S DEGREE in BIOCHEMISTRY

Academic Honors: CUM LAUDE

Henri Poincare University, Nancy, FRANCE

RESEARCH AND PROFESSIONAL EXPERIENCE

December 2003 - present: Ph.D. student

Experimental Immunology, Department of Biomedicine, University Hospital Basel, Basel, SWITZERLAND

Identified glycerol monomycolate as a bacterial lipid antigen capable of T cell stimulation and potential candidate for use in subunit vaccines. Defined structural requirements for design of immunogenic synthetic sulfoglycolipid analogs to be used in subunit vaccines against tuberculosis. Established molecular tools to characterize and evaluate expansion of specific T cells upon immunization with synthetic sulfoglycolipids. Participated in diverse studies assessing involvement of CD1e, lipid binding proteins and lipid metabolism alterations in lipid immunogenicity.

September 2002 - December 2003: Graduate Student

Cancer Biology, Institute of Genetics and Molecular and Cellular Biology (IGBMC), Illkirch, FRANCE

Participated in defining the function of MLN64, a protein involved in breast cancer progression.

July 2002 - September 2002: Quality Control Analyst

Total Petrochemicals, Carling, FRANCE

Responsible for computer analysis of chemical compounds verified by High Performance Liquid Chromatography (HPLC).

June 2001 - August 2001: Microbiologist

Alsa Bestfoods, Ludres, FRANCE

Responsible for Quality Control analysis and Microbiological testing, databases updating and suppliers relationships.

**SKILLS AND
TECHNIQUES**

Common use:

Molecular/Cellular Biology: Cell Culture in a Biosafety Level 2 (BSL2) environment, including handling of blood samples, isolation of Peripheral Blood Mononuclear Cells (PBMC), generation of monocytes-derived Dendritic Cells (DC), restimulation and handling of T cells, surface and intracellular staining of adherent and non-adherent cells, antibody and protein production, generation of transient- and stable transfectants. DNA cloning, design of oligonucleotides for polymerase chain reaction (PCR), PCR, DNA isolation from blood and tissues, genotyping of mice by PCR. Bacterial cell culture, transformation, and purification of plasmid DNA from bacterial cells.

Biochemistry: Western blot, Immunoprecipitation, Enzyme-linked immunosorbent assay (ELISA)

Spectroscopy: Fluorescence Activated Cell Sorting (FACS) analysis, Confocal Microscopy.

Occasional use:

Molecular/Cellular Biology: Cloning of cells. DNA purification, point mutagenesis and work with radioactivity (generation of DNA probes and genotyping). Preparation of competent bacterial cells. Reverse transcriptase-polymerase chain reaction (RT-PCR).

Biochemistry: Protein purification by chromatography and HPLC, biotinylation, dialysis and concentration.

Others: Handling of mice (once dead) under supervision, isolation of organs, generation of Bone-Marrow derived Dendritic Cells and splenocytes.

PUBLICATIONS

Collmann A, Guiard J, Garcia-Alles LF, Mourey L, Brando T, Mori L, Gilleron M, Prandi J, De Libero G, Puzo G. Fatty acyl structures of *Mycobacterium tuberculosis* sulfolipid govern T cell immunogenicity. (Submitted to the Journal of Immunology)

Maître B, Angénieux C, Wurtz V, Layre E, Gilleron M, Collmann A, Mariotti S, Mori L, Fricker D, Cazenave JP, Van Dorsselaer A, Gachet C, De Libero G, Puzo G, Hanau D, De La Salle H. The assembly of CD1e is controlled by an N-terminal propeptide which is processed in endosomal compartments. (Submitted to The Biochemical Journal)

Collmann A, Layre E, Bastian M, Mariotti S, Czaplicki J, Prandi J, Mori L, Stenger S, De Libero G, Puzo G, Gilleron M. Mycolic acids constitute a scaffold for mycobacterial lipidic antigens stimulating CD1b-restricted T cells. *Chem Biol.* (*in Press*)

Guiard J, Collmann A, Gilleron M, Mori L, De Libero G, Prandi J, Puzo G. Synthesis of diacylated trehalose sulfates: candidates for a tuberculosis vaccine. *Angew Chem Int Ed Engl.* 2008;47(50):9734-8.

Tourne S, Maitre B, Collmann A, Layre E, Mariotti S, Signorino-Gelo F, Loch C, Salamero J, Gilleron M, Angénieux C, Cazenave JP, Mori L, Hanau D, Puzo G, De Libero G, de la Salle H. Cutting Edge: A Naturally Occurring Mutation in CD1e Impairs Lipid Antigen Presentation. *J Immunol.* 2008 Mar 15;180(6):3642-6.

Schümann J, Facciotti F, Panza L, Michieletti M, Compostella F, Collmann A, Mori L, De Libero G. Differential alteration of lipid antigen presentation to NKT cells due to imbalances in lipid metabolism. *Eur J Immunol.* 2007 Jun;37(6):1431-41

Collmann A, Paoletti S, Sansano S, Angman L, Zingg JM, Mori L, De Libero G. Human tocopherol-associated protein 1 (hTAP1) reduces lipid antigen presentation to T cells. *Swiss Med Wkly.* 2007 Mar;137:5S

COMMUNICATIONS

May 19th, 2008

Immunology meeting of the Department of Biomedicine (DBM),
Basel, SWITZERLAND

Oral communication: Microbial antigens: variations on a scaffold
lipid

October 23rd, 2007

Biovalley Science day, Basel, SWITZERLAND

Poster title: Human Tocopherol-Associated Protein 1 (hTAP1)
reduces lipid antigen presentation to T cells

April 19-20th, 2007

Annual Congress SGAI-SSAI, Basel, SWITZERLAND

Poster title: Human Tocopherol-Associated Protein 1 (hTAP1)
reduces lipid antigen presentation to T cells

November 20th, 2006

Immunology meeting of the Department of Biomedicine (DBM),
Basel, SWITZERLAND

Oral communication: Are cytoplasmic Lipid Binding Proteins
relevant for lipid immunogenicity?

October 4-8th, 2006

4th Annual NKT Cell & CD1 Workshop, Tuscany, ITALY

Poster title: The role of human Tocopherol-Associated Protein 1
(hTAP1) in lipid antigen presentation

March 30-April 1st, 2005

XVII. Meeting of the Swiss Immunology Ph.D. students,
Wolfsberg, SWITZERLAND

Oral communication: The role of saposin lipid transfer proteins
in lipid antigen presentation

LANGUAGES

English Fluent

French Native speaker

German Basic

REFERENCES

1. Complete sequence and gene map of a human major histocompatibility complex. *The MHC sequencing consortium*. *Nature*, 1999. **401**(6756): p. 921-3.
2. Beck, S. and J. Trowsdale, *The human major histocompatibility complex: lessons from the DNA sequence*. *Annu Rev Genomics Hum Genet*, 2000. **1**: p. 117-37.
3. Kumanovics, A., T. Takada, and K.F. Lindahl, *Genomic organization of the mammalian MHC*. *Annu Rev Immunol*, 2003. **21**: p. 629-57.
4. Abi-Rached, L., et al., *Evidence of en bloc duplication in vertebrate genomes*. *Nat Genet*, 2002. **31**(1): p. 100-5.
5. Danchin, E.G. and P. Pontarotti, *Towards the reconstruction of the bilaterian ancestral pre-MHC region*. *Trends Genet*, 2004. **20**(12): p. 587-91.
6. Holland, L.Z., V. Laudet, and M. Schubert, *The chordate amphioxus: an emerging model organism for developmental biology*. *Cell Mol Life Sci*, 2004. **61**(18): p. 2290-308.
7. Blomme, T., et al., *The gain and loss of genes during 600 million years of vertebrate evolution*. *Genome Biol*, 2006. **7**(5): p. R43.
8. Wang, Y. and X. Gu, *Evolutionary patterns of gene families generated in the early stage of vertebrates*. *J Mol Evol*, 2000. **51**(1): p. 88-96.
9. Dehal, P. and J.L. Boore, *Two rounds of whole genome duplication in the ancestral vertebrate*. *PLoS Biol*, 2005. **3**(10): p. e314.
10. Force, A., A. Amores, and J.H. Postlethwait, *Hox cluster organization in the jawless vertebrate *Petromyzon marinus**. *J Exp Zool*, 2002. **294**(1): p. 30-46.
11. Flajnik, M.F. and M. Kasahara, *Comparative genomics of the MHC: glimpses into the evolution of the adaptive immune system*. *Immunity*, 2001. **15**(3): p. 351-62.
12. McMichael, A.J., et al., *A human thymocyte antigen defined by a hybrid myeloma monoclonal antibody*. *Eur J Immunol*, 1979. **9**(3): p. 205-10.
13. Porcelli, S., C.T. Morita, and M.B. Brenner, *CD1b restricts the response of human CD4-8- T lymphocytes to a microbial antigen*. *Nature*, 1992. **360**(6404): p. 593-7.
14. Kumar, S. and S.B. Hedges, *A molecular timescale for vertebrate evolution*. *Nature*, 1998. **392**(6679): p. 917-20.
15. Lee, M.S., *Molecular clock calibrations and metazoan divergence dates*. *J Mol Evol*, 1999. **49**(3): p. 385-91.
16. Moody, D.B., *T Cell Activation by CD1 and Lipid Antigens*. CTMI 314. 2007.
17. Ahlberg, P.E. and J.A. Clack, *Palaeontology: a firm step from water to land*. *Nature*, 2006. **440**(7085): p. 747-9.
18. Albertson, D.G., et al., *Sensitive and high resolution in situ hybridization to human chromosomes using biotin labelled probes: assignment of the human thymocyte CD1 antigen genes to chromosome 1*. *Embo J*, 1988. **7**(9): p. 2801-5.
19. Kasahara, M., et al., *Origin and evolution of the class I gene family: why are some of the mammalian class I genes encoded outside the major histocompatibility complex?* *Res Immunol*, 1996. **147**(5): p. 278-84; discussion 284-5.
20. Calabi, F., et al., *Two classes of CD1 genes*. *Eur J Immunol*, 1989. **19**(2): p. 285-92.
21. Ji, Q., et al., *The earliest known eutherian mammal*. *Nature*, 2002. **416**(6883): p. 816-22.

22. Novacek, M.J., *Mammalian evolution: an early record bristling with evidence*. *Curr Biol*, 1997. **7**(8): p. R489-91.
23. Danchin, E., et al., *The major histocompatibility complex origin*. *Immunol Rev*, 2004. **198**: p. 216-32.
24. Manolova, V., et al., *Functional CD1a is stabilized by exogenous lipids*. *Eur J Immunol*, 2006. **36**(5): p. 1083-92.
25. Moody, D.B., et al., *Lipid length controls antigen entry into endosomal and nonendosomal pathways for CD1b presentation*. *Nat Immunol*, 2002. **3**(5): p. 435-42.
26. Moody, D.B. and S.A. Porcelli, *Intracellular pathways of CD1 antigen presentation*. *Nat Rev Immunol*, 2003. **3**(1): p. 11-22.
27. Sugita, M., et al., *Separate pathways for antigen presentation by CD1 molecules*. *Immunity*, 1999. **11**(6): p. 743-52.
28. Shamshiev, A., et al., *The alphabeta T cell response to self-glycolipids shows a novel mechanism of CD1b loading and a requirement for complex oligosaccharides*. *Immunity*, 2000. **13**(2): p. 255-64.
29. van den Elzen, P., et al., *Apolipoprotein-mediated pathways of lipid antigen presentation*. *Nature*, 2005. **437**(7060): p. 906-10.
30. Zhou, D., et al., *Editing of CD1d-bound lipid antigens by endosomal lipid transfer proteins*. *Science*, 2004. **303**(5657): p. 523-7.
31. Dascher, C.C. and M.B. Brenner, *Evolutionary constraints on CD1 structure: insights from comparative genomic analysis*. *Trends Immunol*, 2003. **24**(8): p. 412-8.
32. Sugita, M., P.J. Peters, and M.B. Brenner, *Pathways for lipid antigen presentation by CD1 molecules: nowhere for intracellular pathogens to hide*. *Traffic*, 2000. **1**(4): p. 295-300.
33. Angenieux, C., et al., *Characterization of CD1e, a third type of CD1 molecule expressed in dendritic cells*. *J Biol Chem*, 2000. **275**(48): p. 37757-64.
34. de la Salle, H., et al., *Assistance of microbial glycolipid antigen processing by CD1e*. *Science*, 2005. **310**(5752): p. 1321-4.
35. Sugita, M., M. Cernadas, and M.B. Brenner, *New insights into pathways for CD1-mediated antigen presentation*. *Curr Opin Immunol*, 2004. **16**(1): p. 90-5.
36. Jackman, R.M., et al., *The tyrosine-containing cytoplasmic tail of CD1b is essential for its efficient presentation of bacterial lipid antigens*. *Immunity*, 1998. **8**(3): p. 341-51.
37. Salamero, J., et al., *CD1a molecules traffic through the early recycling endosomal pathway in human Langerhans cells*. *J Invest Dermatol*, 2001. **116**(3): p. 401-8.
38. Zeng, Z., et al., *Crystal structure of mouse CD1: An MHC-like fold with a large hydrophobic binding groove*. *Science*, 1997. **277**(5324): p. 339-45.
39. Gadola, S.D., et al., *Structure of human CD1b with bound ligands at 2.3 Å, a maze for alkyl chains*. *Nat Immunol*, 2002. **3**(8): p. 721-6.
40. Moody, D.B., D.M. Zajonc, and I.A. Wilson, *Anatomy of CD1-lipid antigen complexes*. *Nat Rev Immunol*, 2005. **5**(5): p. 387-99.
41. Zajonc, D.M., et al., *Crystal structure of CD1a in complex with a sulfatide self antigen at a resolution of 2.15 Å*. *Nat Immunol*, 2003. **4**(8): p. 808-15.
42. Koch, M., et al., *The crystal structure of human CD1d with and without alpha-galactosylceramide*. *Nat Immunol*, 2005. **6**(8): p. 819-26.
43. Zajonc, D.M., et al., *Structure and function of a potent agonist for the semi-invariant natural killer T cell receptor*. *Nat Immunol*, 2005. **6**(8): p. 810-8.

44. Wu, D., et al., *Design of natural killer T cell activators: structure and function of a microbial glycosphingolipid bound to mouse CD1d*. Proc Natl Acad Sci U S A, 2006. **103**(11): p. 3972-7.
45. Giabbai, B., et al., *Crystal structure of mouse CD1d bound to the self ligand phosphatidylcholine: a molecular basis for NKT cell activation*. J Immunol, 2005. **175**(2): p. 977-84.
46. Zajonc, D.M., et al., *Structural basis for CD1d presentation of a sulfatide derived from myelin and its implications for autoimmunity*. J Exp Med, 2005. **202**(11): p. 1517-26.
47. Zajonc, D.M., et al., *Crystal structures of mouse CD1d-iGb3 complex and its cognate Valpha14 T cell receptor suggest a model for dual recognition of foreign and self glycolipids*. J Mol Biol, 2008. **377**(4): p. 1104-16.
48. Zajonc, D.M., et al., *Molecular mechanism of lipopeptide presentation by CD1a*. Immunity, 2005. **22**(2): p. 209-19.
49. Grant, E.P., et al., *Fine specificity of TCR complementarity-determining region residues and lipid antigen hydrophilic moieties in the recognition of a CD1-lipid complex*. J Immunol, 2002. **168**(8): p. 3933-40.
50. Borg, N.A., et al., *CD1d-lipid-antigen recognition by the semi-invariant NKT T-cell receptor*. Nature, 2007. **448**(7149): p. 44-9.
51. Rudolph, M.G., R.L. Stanfield, and I.A. Wilson, *How TCRs bind MHCs, peptides, and coreceptors*. Annu Rev Immunol, 2006. **24**: p. 419-66.
52. Fainboim, L. and C. Salamone Mdel, *CD1: a family of glycolipid-presenting molecules or also immunoregulatory proteins?* J Biol Regul Homeost Agents, 2002. **16**(2): p. 125-35.
53. Pena-Cruz, V., et al., *Epidermal Langerhans cells efficiently mediate CD1a-dependent presentation of microbial lipid antigens to T cells*. J Invest Dermatol, 2003. **121**(3): p. 517-21.
54. Small, T.N., et al., *M241 (CD1) expression on B lymphocytes*. J Immunol, 1987. **138**(9): p. 2864-8.
55. Duperrier, K., et al., *Distinct subsets of dendritic cells resembling dermal DCs can be generated in vitro from monocytes, in the presence of different serum supplements*. J Immunol Methods, 2000. **238**(1-2): p. 119-31.
56. Pietschmann, P., et al., *Functional and phenotypic characteristics of dendritic cells generated in human plasma supplemented medium*. Scand J Immunol, 2000. **51**(4): p. 377-83.
57. Xia, C.Q. and K.J. Kao, *Heparin induces differentiation of CD1a+ dendritic cells from monocytes: phenotypic and functional characterization*. J Immunol, 2002. **168**(3): p. 1131-8.
58. Martino, A., et al., *Influence of pertussis toxin on CD1a isoform expression in human dendritic cells*. J Clin Immunol, 2006. **26**(2): p. 153-9.
59. Caux, C., et al., *GM-CSF and TNF-alpha cooperate in the generation of dendritic Langerhans cells*. Nature, 1992. **360**(6401): p. 258-61.
60. Caux, C., et al., *CD34+ hematopoietic progenitors from human cord blood differentiate along two independent dendritic cell pathways in response to GM-CSF+TNF alpha*. J Exp Med, 1996. **184**(2): p. 695-706.
61. Banchereau, J., et al., *Immunobiology of dendritic cells*. Annu Rev Immunol, 2000. **18**: p. 767-811.

62. Cao, X., et al., *CD1 molecules efficiently present antigen in immature dendritic cells and traffic independently of MHC class II during dendritic cell maturation.* J Immunol, 2002. **169**(9): p. 4770-7.
63. van der Wel, N.N., et al., *CD1 and major histocompatibility complex II molecules follow a different course during dendritic cell maturation.* Mol Biol Cell, 2003. **14**(8): p. 3378-88.
64. McMichael, A., *Leucocyte typing III: white cell differentiation antigens.* 1987.
65. Battistini, L., et al., *CD1b is expressed in multiple sclerosis lesions.* J Neuroimmunol, 1996. **67**(2): p. 145-51.
66. Plebani, A., et al., *B and T lymphocyte subsets in fetal and cord blood: age-related modulation of CD1c expression.* Biol Neonate, 1993. **63**(1): p. 1-7.
67. Smith, M.E., J.A. Thomas, and W.F. Bodmer, *CD1c antigens are present in normal and neoplastic B-cells.* J Pathol, 1988. **156**(2): p. 169-77.
68. Roura-Mir, C., et al., *CD1a and CD1c activate intrathyroidal T cells during Graves' disease and Hashimoto's thyroiditis.* J Immunol, 2005. **174**(6): p. 3773-80.
69. Delia, D., et al., *CD1c but neither CD1a nor CD1b molecules are expressed on normal, activated, and malignant human B cells: identification of a new B-cell subset.* Blood, 1988. **72**(1): p. 241-7.
70. Roura-Mir, C., et al., *Mycobacterium tuberculosis regulates CD1 antigen presentation pathways through TLR-2.* J Immunol, 2005. **175**(3): p. 1758-66.
71. Sieling, P.A., et al., *CD1 expression by dendritic cells in human leprosy lesions: correlation with effective host immunity.* J Immunol, 1999. **162**(3): p. 1851-8.
72. Page, G., S. Lebecque, and P. Miossec, *Anatomic localization of immature and mature dendritic cells in an ectopic lymphoid organ: correlation with selective chemokine expression in rheumatoid synovium.* J Immunol, 2002. **168**(10): p. 5333-41.
73. Bell, D., et al., *In breast carcinoma tissue, immature dendritic cells reside within the tumor, whereas mature dendritic cells are located in peritumoral areas.* J Exp Med, 1999. **190**(10): p. 1417-26.
74. Iwamoto, M., et al., *Prognostic value of tumor-infiltrating dendritic cells expressing CD83 in human breast carcinomas.* Int J Cancer, 2003. **104**(1): p. 92-7.
75. Fivenson, D.P. and B.J. Nickoloff, *Distinctive dendritic cell subsets expressing factor XIIIa, CD1a, CD1b and CD1c in mycosis fungoides and psoriasis.* J Cutan Pathol, 1995. **22**(3): p. 223-8.
76. Zheng, Z., et al., *Expression profiling of B cell chronic lymphocytic leukemia suggests deficient CD1-mediated immunity, polarized cytokine response, altered adhesion and increased intracellular protein transport and processing of leukemic cells.* Leukemia, 2002. **16**(12): p. 2429-37.
77. Raftery, M.J., et al., *Inhibition of CD1 antigen presentation by human cytomegalovirus.* J Virol, 2008. **82**(9): p. 4308-19.
78. Exley, M., et al., *CD1d structure and regulation on human thymocytes, peripheral blood T cells, B cells and monocytes.* Immunology, 2000. **100**(1): p. 37-47.
79. Ulanova, M., et al., *Antigen-specific regulation of CD1 expression in humans.* J Clin Immunol, 2000. **20**(3): p. 203-11.
80. Salamone, M.C., et al., *Activation-induced expression of CD1d antigen on mature T cells.* J Leukoc Biol, 2001. **69**(2): p. 207-14.

81. Spada, F.M., et al., *Low expression level but potent antigen presenting function of CD1d on monocyte lineage cells.* Eur J Immunol, 2000. **30**(12): p. 3468-77.
82. Gerlini, G., et al., *Cd1d is expressed on dermal dendritic cells and monocyte-derived dendritic cells.* J Invest Dermatol, 2001. **117**(3): p. 576-82.
83. Yang, O.O., et al., *CD1d on myeloid dendritic cells stimulates cytokine secretion from and cytolytic activity of V alpha 24J alpha Q T cells: a feedback mechanism for immune regulation.* J Immunol, 2000. **165**(7): p. 3756-62.
84. Blumberg, R.S., et al., *Expression of a nonpolymorphic MHC class I-like molecule, CD1D, by human intestinal epithelial cells.* J Immunol, 1991. **147**(8): p. 2518-24.
85. Canchis, P.W., et al., *Tissue distribution of the non-polymorphic major histocompatibility complex class I-like molecule, CD1d.* Immunology, 1993. **80**(4): p. 561-5.
86. Bonish, B., et al., *Overexpression of CD1d by keratinocytes in psoriasis and CD1d-dependent IFN-gamma production by NK-T cells.* J Immunol, 2000. **165**(7): p. 4076-85.
87. Adly, M.A., H.A. Assaf, and M. Hussein, *Expression of CD1d in human scalp skin and hair follicles: hair cycle related alterations.* J Clin Pathol, 2005. **58**(12): p. 1278-82.
88. Yamazaki, K., Y. Ohsawa, and H. Yoshie, *Elevated proportion of natural killer T cells in periodontitis lesions: a common feature of chronic inflammatory diseases.* Am J Pathol, 2001. **158**(4): p. 1391-8.
89. Jenkinson, H.J., et al., *Expression of CD1D mRNA transcripts in human choriocarcinoma cell lines and placentally derived trophoblast cells.* Immunology, 1999. **96**(4): p. 649-55.
90. Kojo, S., et al., *Alternative splicing forms of the human CD1D gene in mononuclear cells.* Biochem Biophys Res Commun, 2000. **276**(1): p. 107-11.
91. Balk, S.P., et al., *Beta 2-microglobulin-independent MHC class Ib molecule expressed by human intestinal epithelium.* Science, 1994. **265**(5169): p. 259-62.
92. Somnay-Wadgaonkar, K., *Immunolocalization of CD1d in human intestinal epithelial cells and identification of a beta2-microglobulin-associated form.* Int Immunol, 1999. **11**: p. 383-392.
93. Kim, H.S., et al., *Human CD1d associates with prolyl-4-hydroxylase during its biosynthesis.* Mol Immunol, 2000. **37**(14): p. 861-8.
94. Chen, Q.Y. and N. Jackson, *Human CD1D gene has TATA boxless dual promoters: an SPI-binding element determines the function of the proximal promoter.* J Immunol, 2004. **172**(9): p. 5512-21.
95. Page, M.J., et al., *Cd1d-restricted cellular lysis by peripheral blood lymphocytes: relevance to the inflammatory bowel diseases.* J Surg Res, 2000. **92**(2): p. 214-21.
96. Bleicher, P.A., et al., *Expression of murine CD1 on gastrointestinal epithelium.* Science, 1990. **250**(4981): p. 679-82.
97. Burke, S., et al., *Rat cluster of differentiation 1 molecule: expression on the surface of intestinal epithelial cells and hepatocytes.* Gastroenterology, 1994. **106**(5): p. 1143-9.
98. Tsuneyama, K., et al., *Increased CD1d expression on small bile duct epithelium and epithelioid granuloma in livers in primary biliary cirrhosis.* Hepatology, 1998. **28**(3): p. 620-3.

99. Durante-Mangoni, E., et al., *Hepatic CD1d expression in hepatitis C virus infection and recognition by resident proinflammatory CD1d-reactive T cells*. J Immunol, 2004. **173**(3): p. 2159-66.
100. Busshoff, U., et al., *CD1 expression is differentially regulated by microglia, macrophages and T cells in the central nervous system upon inflammation and demyelination*. J Neuroimmunol, 2001. **113**(2): p. 220-30.
101. Metelitsa, L.S., et al., *Expression of CD1d by myelomonocytic leukemias provides a target for cytotoxic NKT cells*. Leukemia, 2003. **17**(6): p. 1068-77.
102. Takahashi, T., et al., *Valpha24+ natural killer T-cell responses against T-acute lymphoblastic leukaemia cells: implications for immunotherapy*. Br J Haematol, 2003. **122**(2): p. 231-9.
103. Dhodapkar, K.M., et al., *Invariant natural killer T cells are preserved in patients with glioma and exhibit antitumor lytic activity following dendritic cell-mediated expansion*. Int J Cancer, 2004. **109**(6): p. 893-9.
104. Fais, F., et al., *CD1d is expressed on B-chronic lymphocytic leukemia cells and mediates alpha-galactosylceramide presentation to natural killer T lymphocytes*. Int J Cancer, 2004. **109**(3): p. 402-11.
105. Nebozhyn, M., et al., *Quantitative PCR on 5 genes reliably identifies CTCL patients with 5% to 99% circulating tumor cells with 90% accuracy*. Blood, 2006. **107**(8): p. 3189-96.
106. Mosser, D.D., J. Duchaine, and L.H. Martin, *Biochemical and developmental characterization of the murine cluster of differentiation 1 antigen*. Immunology, 1991. **73**(3): p. 298-303.
107. Brossay, L., et al., *Mouse CD1 is mainly expressed on hemopoietic-derived cells*. J Immunol, 1997. **159**(3): p. 1216-24.
108. Mandal, M., et al., *Tissue distribution, regulation and intracellular localization of murine CD1 molecules*. Mol Immunol, 1998. **35**(9): p. 525-36.
109. Roark, J.H., et al., *CD1.1 expression by mouse antigen-presenting cells and marginal zone B cells*. J Immunol, 1998. **160**(7): p. 3121-7.
110. Chun, T., et al., *CD1d-expressing dendritic cells but not thymic epithelial cells can mediate negative selection of NKT cells*. J Exp Med, 2003. **197**(7): p. 907-18.
111. Amano, M., et al., *CD1 expression defines subsets of follicular and marginal zone B cells in the spleen: beta 2-microglobulin-dependent and independent forms*. J Immunol, 1998. **161**(4): p. 1710-7.
112. Makowska, A., et al., *CD1high B cells: a population of mixed origin*. Eur J Immunol, 1999. **29**(10): p. 3285-94.
113. Sallinen, K., E. Verajankorva, and P. Pollanen, *Expression of antigens involved in the presentation of lipid antigens and induction of clonal anergy in the female reproductive tract*. J Reprod Immunol, 2000. **46**(2): p. 91-101.
114. Ylinen, L., et al., *The role of lipid antigen presentation, cytokine balance, and major histocompatibility complex in a novel murine model of adoptive transfer of insulinitis*. Pancreas, 2000. **20**(2): p. 197-205.
115. Bradbury, A., et al., *Mouse CD1 is distinct from and co-exists with TL in the same thymus*. Embo J, 1988. **7**(10): p. 3081-6.
116. Geng, Y., et al., *Transcriptional regulation of CD1D1 by Ets family transcription factors*. J Immunol, 2005. **175**(2): p. 1022-9.

117. Chen, Y.H., et al., *Expression of CD1d2 on thymocytes is not sufficient for the development of NK T cells in CD1d1-deficient mice.* J Immunol, 1999. **162**(8): p. 4560-6.
118. Campos-Martin, Y., et al., *Immature human dendritic cells infected with Leishmania infantum are resistant to NK-mediated cytotoxicity but are efficiently recognized by NKT cells.* J Immunol, 2006. **176**(10): p. 6172-9.
119. Skold, M., et al., *Interplay of cytokines and microbial signals in regulation of CD1d expression and NKT cell activation.* J Immunol, 2005. **175**(6): p. 3584-93.
120. Chen, N., et al., *HIV-1 down-regulates the expression of CD1d via Nef.* Eur J Immunol, 2006. **36**(2): p. 278-86.
121. Sanchez, D.J., J.E. Gumperz, and D. Ganem, *Regulation of CD1d expression and function by a herpesvirus infection.* J Clin Invest, 2005. **115**(5): p. 1369-78.
122. Renukaradhya, G.J., et al., *Virus-induced inhibition of CD1d1-mediated antigen presentation: reciprocal regulation by p38 and ERK.* J Immunol, 2005. **175**(7): p. 4301-8.
123. Ichimiya, S., K. Kikuchi, and A. Matsuura, *Structural analysis of the rat homologue of CD1. Evidence for evolutionary conservation of the CD1D class and widespread transcription by rat cells.* J Immunol, 1994. **153**(3): p. 1112-23.
124. Kasai, K., et al., *Localization of rat CD1 transcripts and protein in rat tissues--an analysis of rat CD1 expression by in situ hybridization and immunohistochemistry.* Clin Exp Immunol, 1997. **109**(2): p. 317-22.
125. Melian, A., et al., *CD1 expression in human atherosclerosis. A potential mechanism for T cell activation by foam cells.* Am J Pathol, 1999. **155**(3): p. 775-86.
126. Angenieux, C., et al., *The cellular pathway of CD1e in immature and maturing dendritic cells.* Traffic, 2005. **6**(4): p. 286-302.
127. Tourne, S., et al., *Cutting edge: a naturally occurring mutation in CD1e impairs lipid antigen presentation.* J Immunol, 2008. **180**(6): p. 3642-6.
128. Woolfson, A. and C. Milstein, *Alternative splicing generates secretory isoforms of human CD1.* Proc Natl Acad Sci U S A, 1994. **91**(14): p. 6683-7.
129. Kang, S.J. and P. Cresswell, *Regulation of intracellular trafficking of human CD1d by association with MHC class II molecules.* Embo J, 2002. **21**(7): p. 1650-60.
130. Kim, H.S., et al., *Biochemical characterization of CD1d expression in the absence of beta2-microglobulin.* J Biol Chem, 1999. **274**(14): p. 9289-95.
131. Trombetta, E.S. and I. Mellman, *Cell biology of antigen processing in vitro and in vivo.* Annu Rev Immunol, 2005. **23**: p. 975-1028.
132. Pamer, E. and P. Cresswell, *Mechanisms of MHC class I--restricted antigen processing.* Annu Rev Immunol, 1998. **16**: p. 323-58.
133. Garcia-Alles, L.F., et al., *Endogenous phosphatidylcholine and a long spacer ligand stabilize the lipid-binding groove of CD1b.* Embo J, 2006. **25**(15): p. 3684-92.
134. Joyce, S., et al., *Natural ligand of mouse CD1d1: cellular glycosylphosphatidylinositol.* Science, 1998. **279**(5356): p. 1541-4.
135. De Silva, A.D., et al., *Lipid protein interactions: the assembly of CD1d1 with cellular phospholipids occurs in the endoplasmic reticulum.* J Immunol, 2002. **168**(2): p. 723-33.
136. Park, J.J., et al., *Lipid-protein interactions: biosynthetic assembly of CD1 with lipids in the endoplasmic reticulum is evolutionarily conserved.* Proc Natl Acad Sci U S A, 2004. **101**(4): p. 1022-6.

137. Jamil, H., et al., *Microsomal triglyceride transfer protein. Specificity of lipid binding and transport.* J Biol Chem, 1995. **270**(12): p. 6549-54.
138. Brozovic, S., et al., *CD1d function is regulated by microsomal triglyceride transfer protein.* Nat Med, 2004. **10**(5): p. 535-9.
139. Dougan, S.K., et al., *Microsomal triglyceride transfer protein lipidation and control of CD1d on antigen-presenting cells.* J Exp Med, 2005. **202**(4): p. 529-39.
140. Kaser, A., et al., *Microsomal triglyceride transfer protein regulates endogenous and exogenous antigen presentation by group 1 CD1 molecules.* Eur J Immunol, 2008. **38**(8): p. 2351-9.
141. Briken, V., et al., *Intracellular trafficking pathway of newly synthesized CD1b molecules.* Embo J, 2002. **21**(4): p. 825-34.
142. Sugita, M., et al., *Cytoplasmic tail-dependent localization of CD1b antigen-presenting molecules to MIICs.* Science, 1996. **273**(5273): p. 349-52.
143. Chiu, Y.H., et al., *Multiple defects in antigen presentation and T cell development by mice expressing cytoplasmic tail-truncated CD1d.* Nat Immunol, 2002. **3**(1): p. 55-60.
144. Sugita, M., et al., *CD1c molecules broadly survey the endocytic system.* Proc Natl Acad Sci U S A, 2000. **97**(15): p. 8445-50.
145. Barral, D.C., et al., *CD1a and MHC Class I Follow a Similar Endocytic Recycling Pathway.* Traffic, 2008.
146. Sloma, I., et al., *Regulation of CD1a surface expression and antigen presentation by invariant chain and lipid rafts.* J Immunol, 2008. **180**(2): p. 980-7.
147. Sugita, M., et al., *Failure of trafficking and antigen presentation by CD1 in AP-3-deficient cells.* Immunity, 2002. **16**(5): p. 697-706.
148. Cernadas, M., et al., *Lysosomal localization of murine CD1d mediated by AP-3 is necessary for NK T cell development.* J Immunol, 2003. **171**(8): p. 4149-55.
149. Elewaut, D., et al., *The adaptor protein AP-3 is required for CD1d-mediated antigen presentation of glycosphingolipids and development of Valpha14i NKT cells.* J Exp Med, 2003. **198**(8): p. 1133-46.
150. Maitre, B., et al., *Control of the intracellular pathway of CD1e.* Traffic, 2008. **9**(4): p. 431-45.
151. Kawashima, T., et al., *Cutting edge: major CD8 T cell response to live bacillus Calmette-Guerin is mediated by CD1 molecules.* J Immunol, 2003. **170**(11): p. 5345-8.
152. Ulrichs, T., et al., *T-cell responses to CD1-presented lipid antigens in humans with Mycobacterium tuberculosis infection.* Infect Immun, 2003. **71**(6): p. 3076-87.
153. Shamshiev, A., et al., *Self glycolipids as T-cell autoantigens.* Eur J Immunol, 1999. **29**(5): p. 1667-75.
154. Rauch, J., et al., *Structural features of the acyl chain determine self-phospholipid antigen recognition by a CD1d-restricted invariant NKT (iNKT) cell.* J Biol Chem, 2003. **278**(48): p. 47508-15.
155. Agea, E., et al., *Human CD1-restricted T cell recognition of lipids from pollens.* J Exp Med, 2005. **202**(2): p. 295-308.
156. Miyamoto, K., S. Miyake, and T. Yamamura, *A synthetic glycolipid prevents autoimmune encephalomyelitis by inducing TH2 bias of natural killer T cells.* Nature, 2001. **413**(6855): p. 531-4.

157. Oki, S., et al., *The clinical implication and molecular mechanism of preferential IL-4 production by modified glycolipid-stimulated NKT cells*. J Clin Invest, 2004. **113**(11): p. 1631-40.
158. Mandon, E.C., et al., *Subcellular localization and membrane topology of serine palmitoyltransferase, 3-dehydrosphinganine reductase, and sphinganine N-acyltransferase in mouse liver*. J Biol Chem, 1992. **267**(16): p. 11144-8.
159. Hanada, K., et al., *Molecular machinery for non-vesicular trafficking of ceramide*. Nature, 2003. **426**(6968): p. 803-9.
160. van Meer, G. and J.C. Holthuis, *Sphingolipid transport in eukaryotic cells*. Biochim Biophys Acta, 2000. **1486**(1): p. 145-70.
161. Futerman, A.H., et al., *Sphingomyelin synthesis in rat liver occurs predominantly at the cis and medial cisternae of the Golgi apparatus*. J Biol Chem, 1990. **265**(15): p. 8650-7.
162. Jeckel, D., et al., *Glucosylceramide is synthesized at the cytosolic surface of various Golgi subfractions*. J Cell Biol, 1992. **117**(2): p. 259-67.
163. Warnock, D.E., et al., *Transport of newly synthesized glucosylceramide to the plasma membrane by a non-Golgi pathway*. Proc Natl Acad Sci U S A, 1994. **91**(7): p. 2708-12.
164. Allende, M.L., et al., *Evidence supporting a late Golgi location for lactosylceramide to ganglioside GM3 conversion*. Glycobiology, 2000. **10**(10): p. 1025-32.
165. Giraudo, C.G., V.M. Rosales Fritz, and H.J. Maccioni, *GA2/GM2/GD2 synthase localizes to the trans-golgi network of CHO-K1 cells*. Biochem J, 1999. **342 Pt 3**: p. 633-40.
166. Ruan, S. and K.O. Lloyd, *Glycosylation pathways in the biosynthesis of gangliosides in melanoma and neuroblastoma cells: relative glycosyltransferase levels determine ganglioside patterns*. Cancer Res, 1992. **52**(20): p. 5725-31.
167. Yamashiro, S., et al., *Genetic and enzymatic basis for the differential expression of GM2 and GD2 gangliosides in human cancer cell lines*. Cancer Res, 1993. **53**(22): p. 5395-400.
168. Holthuis, J.C. and T.P. Levine, *Lipid traffic: floppy drives and a superhighway*. Nat Rev Mol Cell Biol, 2005. **6**(3): p. 209-20.
169. Relloso, M., et al., *pH-dependent interdomain tethers of CD1b regulate its antigen capture*. Immunity, 2008. **28**(6): p. 774-86.
170. Jayawardena-Wolf, J., et al., *CD1d endosomal trafficking is independently regulated by an intrinsic CD1d-encoded tyrosine motif and by the invariant chain*. Immunity, 2001. **15**(6): p. 897-908.
171. Shamshiev, A., et al., *Presentation of the same glycolipid by different CD1 molecules*. J Exp Med, 2002. **195**(8): p. 1013-21.
172. Pender, M.P., et al., *Increased circulating T cell reactivity to GM3 and GQ1b gangliosides in primary progressive multiple sclerosis*. J Clin Neurosci, 2003. **10**(1): p. 63-6.
173. Acarin, N., et al., *Different antiganglioside antibody pattern between relapsing-remitting and progressive multiple sclerosis*. Acta Neurol Scand, 1996. **93**(2-3): p. 99-103.
174. Sadatipour, B.T., J.M. Greer, and M.P. Pender, *Increased circulating antiganglioside antibodies in primary and secondary progressive multiple sclerosis*. Ann Neurol, 1998. **44**(6): p. 980-3.

175. De Libero, G., et al., *Bacterial infections promote T cell recognition of self-glycolipids*. *Immunity*, 2005. **22**(6): p. 763-72.
176. Beckman, E.M., et al., *Recognition of a lipid antigen by CD1-restricted alpha beta+ T cells*. *Nature*, 1994. **372**(6507): p. 691-4.
177. Moody, D.B., et al., *T cell activation by lipopeptide antigens*. *Science*, 2004. **303**(5657): p. 527-31.
178. Gilleron, M., et al., *Diacylated sulfoglycolipids are novel mycobacterial antigens stimulating CD1-restricted T cells during infection with Mycobacterium tuberculosis*. *J Exp Med*, 2004. **199**(5): p. 649-59.
179. Moody, D.B., et al., *Structural requirements for glycolipid antigen recognition by CD1b-restricted T cells*. *Science*, 1997. **278**(5336): p. 283-6.
180. Sieling, P.A., et al., *CD1-restricted T cell recognition of microbial lipoglycan antigens*. *Science*, 1995. **269**(5221): p. 227-30.
181. Moody, D.B., et al., *CD1c-mediated T-cell recognition of isoprenoid glycolipids in Mycobacterium tuberculosis infection*. *Nature*, 2000. **404**(6780): p. 884-8.
182. Amprey, J.L., et al., *A subset of liver NK T cells is activated during Leishmania donovani infection by CD1d-bound lipophosphoglycan*. *J Exp Med*, 2004. **200**(7): p. 895-904.
183. Fischer, K., et al., *Mycobacterial phosphatidylinositol mannoside is a natural antigen for CD1d-restricted T cells*. *Proc Natl Acad Sci U S A*, 2004. **101**(29): p. 10685-90.
184. Kinjo, Y., et al., *Recognition of bacterial glycosphingolipids by natural killer T cells*. *Nature*, 2005. **434**(7032): p. 520-5.
185. Mattner, J., et al., *Exogenous and endogenous glycolipid antigens activate NKT cells during microbial infections*. *Nature*, 2005. **434**(7032): p. 525-9.
186. Sriram, V., et al., *Cell wall glycosphingolipids of Sphingomonas paucimobilis are CD1d-specific ligands for NKT cells*. *Eur J Immunol*, 2005. **35**(6): p. 1692-701.
187. Wu, D., et al., *Bacterial glycolipids and analogs as antigens for CD1d-restricted NKT cells*. *Proc Natl Acad Sci U S A*, 2005. **102**(5): p. 1351-6.
188. Ernst, W.A., et al., *Molecular interaction of CD1b with lipoglycan antigens*. *Immunity*, 1998. **8**(3): p. 331-40.
189. Brennan, P.J. and H. Nikaido, *The envelope of mycobacteria*. *Annu Rev Biochem*, 1995. **64**: p. 29-63.
190. Moody, D.B., et al., *CD1b-mediated T cell recognition of a glycolipid antigen generated from mycobacterial lipid and host carbohydrate during infection*. *J Exp Med*, 2000. **192**(7): p. 965-76.
191. Karakousis, P.C., W.R. Bishai, and S.E. Dorman, *Mycobacterium tuberculosis cell envelope lipids and the host immune response*. *Cell Microbiol*, 2004. **6**(2): p. 105-16.
192. Padovan, E., R.M. Landmann, and G. De Libero, *How pattern recognition receptor triggering influences T cell responses: a new look into the system*. *Trends Immunol*, 2007. **28**(7): p. 308-14.
193. Yarkoni, E., M.B. Goren, and H.J. Rapp, *Regression of a transplanted guinea pig hepatoma after intralesional injection of an emulsified mixture of endotoxin and mycobacterial sulfolipid*. *Infect Immun*, 1979. **24**(2): p. 357-62.
194. Goren, M.B., *Immunoreactive substances of mycobacteria*. *Am Rev Respir Dis*, 1982. **125**(3 Pt 2): p. 50-69.
195. Matsunaga, I., et al., *Mycobacterium tuberculosis pks12 produces a novel polyketide presented by CD1c to T cells*. *J Exp Med*, 2004. **200**(12): p. 1559-69.

196. de Jong, A., et al., *CD1c presentation of synthetic glycolipid antigens with foreign alkyl branching motifs*. Chem Biol, 2007. **14**(11): p. 1232-42.
197. Narayanan, R.B., A. Girdhar, and B.K. Girdhar, *CD1-positive epidermal Langerhans cells in regressed tuberculoid and lepromatous leprosy lesions*. Int Arch Allergy Appl Immunol, 1990. **92**(1): p. 94-6.
198. Uehira, K., et al., *Dendritic cells are decreased in blood and accumulated in granuloma in tuberculosis*. Clin Immunol, 2002. **105**(3): p. 296-303.
199. Rosat, J.P., et al., *CD1-restricted microbial lipid antigen-specific recognition found in the CD8+ alpha beta T cell pool*. J Immunol, 1999. **162**(1): p. 366-71.
200. Sieling, P.A., et al., *Evidence for human CD4+ T cells in the CD1-restricted repertoire: derivation of mycobacteria-reactive T cells from leprosy lesions*. J Immunol, 2000. **164**(9): p. 4790-6.
201. Natori, T., Morita, M., Akimoto, K., Koezuka, Y., *Agelasphins novel antitumor and immunostimulatory cerebroside from the marine sponge Agelas-Mauritanus*. Tetrahedron, 1994. **50**: p. 2711-2784.
202. Schofield, L., et al., *CD1d-restricted immunoglobulin G formation to GPI-anchored antigens mediated by NKT cells*. Science, 1999. **283**(5399): p. 225-9.
203. Silk, J.D., et al., *Cutting edge: nonglycosidic CD1d lipid ligands activate human and murine invariant NKT cells*. J Immunol, 2008. **180**(10): p. 6452-6.
204. Brigl, M. and M.B. Brenner, *CD1: antigen presentation and T cell function*. Annu Rev Immunol, 2004. **22**: p. 817-90.
205. Willnow, T.E., A. Nykjaer, and J. Herz, *Lipoprotein receptors: new roles for ancient proteins*. Nat Cell Biol, 1999. **1**(6): p. E157-62.
206. Herz, J. and D.K. Strickland, *LRP: a multifunctional scavenger and signaling receptor*. J Clin Invest, 2001. **108**(6): p. 779-84.
207. Greaves, D.R. and S. Gordon, *Thematic review series: the immune system and atherogenesis. Recent insights into the biology of macrophage scavenger receptors*. J Lipid Res, 2005. **46**(1): p. 11-20.
208. Hoebe, K., et al., *CD36 is a sensor of diacylglycerides*. Nature, 2005. **433**(7025): p. 523-7.
209. Prigozy, T.I., et al., *The mannose receptor delivers lipoglycan antigens to endosomes for presentation to T cells by CD1b molecules*. Immunity, 1997. **6**(2): p. 187-97.
210. Hunger, R.E., et al., *Langerhans cells utilize CD1a and langerin to efficiently present nonpeptide antigens to T cells*. J Clin Invest, 2004. **113**(5): p. 701-8.
211. Conner, S.D. and S.L. Schmid, *Regulated portals of entry into the cell*. Nature, 2003. **422**(6927): p. 37-44.
212. Ikonen, E., *Roles of lipid rafts in membrane transport*. Curr Opin Cell Biol, 2001. **13**(4): p. 470-7.
213. Nabi, I.R. and P.U. Le, *Caveolae/raft-dependent endocytosis*. J Cell Biol, 2003. **161**(4): p. 673-7.
214. Ruggers, R.J., et al., *Lipid traffic: the ABC of transbilayer movement*. Traffic, 2000. **1**(3): p. 226-34.
215. Eehalt, R., et al., *Translocation of long chain fatty acids across the plasma membrane--lipid rafts and fatty acid transport proteins*. Mol Cell Biochem, 2006. **284**(1-2): p. 135-40.
216. Schaffer, J.E. and H.F. Lodish, *Expression cloning and characterization of a novel adipocyte long chain fatty acid transport protein*. Cell, 1994. **79**(3): p. 427-36.

217. Schaible, U.E., et al., *Apoptosis facilitates antigen presentation to T lymphocytes through MHC-I and CD1 in tuberculosis*. Nat Med, 2003. **9**(8): p. 1039-46.
218. Kobayashi, T., F. Gu, and J. Gruenberg, *Lipids, lipid domains and lipid-protein interactions in endocytic membrane traffic*. Semin Cell Dev Biol, 1998. **9**(5): p. 517-26.
219. Mukherjee, S. and F.R. Maxfield, *Role of membrane organization and membrane domains in endocytic lipid trafficking*. Traffic, 2000. **1**(3): p. 203-11.
220. Mukherjee, S., T.T. Soe, and F.R. Maxfield, *Endocytic sorting of lipid analogues differing solely in the chemistry of their hydrophobic tails*. J Cell Biol, 1999. **144**(6): p. 1271-84.
221. Armstrong, J.A. and P.D. Hart, *Response of cultured macrophages to Mycobacterium tuberculosis, with observations on fusion of lysosomes with phagosomes*. J Exp Med, 1971. **134**(3 Pt 1): p. 713-40.
222. Russell, D.G., *Mycobacterium tuberculosis: here today, and here tomorrow*. Nat Rev Mol Cell Biol, 2001. **2**(8): p. 569-77.
223. Jayachandran, R., et al., *Survival of mycobacteria in macrophages is mediated by coronin 1-dependent activation of calcineurin*. Cell, 2007. **130**(1): p. 37-50.
224. Prigozy, T.I., et al., *Glycolipid antigen processing for presentation by CD1d molecules*. Science, 2001. **291**(5504): p. 664-7.
225. Kang, S.J. and P. Cresswell, *Saposins facilitate CD1d-restricted presentation of an exogenous lipid antigen to T cells*. Nat Immunol, 2004. **5**(2): p. 175-81.
226. Winau, F., et al., *Saposin C is required for lipid presentation by human CD1b*. Nat Immunol, 2004. **5**(2): p. 169-74.
227. Kolter, T. and K. Sandhoff, *Principles of lysosomal membrane digestion: stimulation of sphingolipid degradation by sphingolipid activator proteins and anionic lysosomal lipids*. Annu Rev Cell Dev Biol, 2005. **21**: p. 81-103.
228. Morimoto, S., et al., *Interaction of saposins, acidic lipids, and glucosylceramidase*. J Biol Chem, 1990. **265**(4): p. 1933-7.
229. Schuette, C.G., et al., *Sphingolipid activator proteins: proteins with complex functions in lipid degradation and skin biogenesis*. Glycobiology, 2001. **11**(6): p. 81R-90R.
230. Qi, X. and G.A. Grabowski, *Acid beta-glucosidase: intrinsic fluorescence and conformational changes induced by phospholipids and saposin C*. Biochemistry, 1998. **37**(33): p. 11544-54.
231. Ciaffoni, F., et al., *Saposin B binds and transfers phospholipids*. J Lipid Res, 2006. **47**(5): p. 1045-53.
232. Vogel, A., G. Schwarzmann, and K. Sandhoff, *Glycosphingolipid specificity of the human sulfatide activator protein*. Eur J Biochem, 1991. **200**(2): p. 591-7.
233. Li, S.C., et al., *Activator protein required for the enzymatic hydrolysis of cerebroside sulfate. Deficiency in urine of patients affected with cerebroside sulfatase activator deficiency and identity with activators for the enzymatic hydrolysis of GM1 ganglioside and globotriaosylceramide*. J Biol Chem, 1985. **260**(3): p. 1867-71.
234. Li, S.C., et al., *Characterization of a nonspecific activator protein for the enzymatic hydrolysis of glycolipids*. J Biol Chem, 1988. **263**(14): p. 6588-91.
235. Fluharty, C.B., et al., *Comparative lipid binding study on the cerebroside sulfate activator (saposin B)*. J Neurosci Res, 2001. **63**(1): p. 82-9.

236. Fischer, G. and H. Jatzkewitz, *The activator of cerebroside-sulphatase. A model of the activation.* Biochim Biophys Acta, 1978. **528**(1): p. 69-76.
237. Schumann, J., et al., *Differential alteration of lipid antigen presentation to NKT cells due to imbalances in lipid metabolism.* Eur J Immunol, 2007. **37**(6): p. 1431-41.
238. Cantu, C., 3rd, et al., *The paradox of immune molecular recognition of alpha-galactosylceramide: low affinity, low specificity for CD1d, high affinity for alpha beta TCRs.* J Immunol, 2003. **170**(9): p. 4673-82.
239. Stanic, A.K., et al., *Another view of T cell antigen recognition: cooperative engagement of glycolipid antigens by Va14Ja18 natural T(iNKT) cell receptor [corrected].* J Immunol, 2003. **171**(9): p. 4539-51.
240. Bendelac, A., et al., *Mouse CD1-specific NK1 T cells: development, specificity, and function.* Annu Rev Immunol, 1997. **15**: p. 535-62.
241. Gui, M., et al., *TCR beta chain influences but does not solely control autoreactivity of V alpha 14J281T cells.* J Immunol, 2001. **167**(11): p. 6239-46.
242. Matsuda, J.L., et al., *Natural killer T cells reactive to a single glycolipid exhibit a highly diverse T cell receptor beta repertoire and small clone size.* Proc Natl Acad Sci U S A, 2001. **98**(22): p. 12636-41.
243. Ronet, C., et al., *Role of the complementarity-determining region 3 (CDR3) of the TCR-beta chains associated with the V alpha 14 semi-invariant TCR alpha-chain in the selection of CD4+ NK T Cells.* J Immunol, 2001. **166**(3): p. 1755-62.
244. Cardell, S., et al., *CD1-restricted CD4+ T cells in major histocompatibility complex class II-deficient mice.* J Exp Med, 1995. **182**(4): p. 993-1004.
245. Jahng, A., et al., *Prevention of autoimmunity by targeting a distinct, noninvariant CD1d-reactive T cell population reactive to sulfatide.* J Exp Med, 2004. **199**(7): p. 947-57.
246. Grant, E.P., et al., *Molecular recognition of lipid antigens by T cell receptors.* J Exp Med, 1999. **189**(1): p. 195-205.
247. Porcelli, S.A. and R.L. Modlin, *The CD1 system: antigen-presenting molecules for T cell recognition of lipids and glycolipids.* Annu Rev Immunol, 1999. **17**: p. 297-329.
248. Garcia, K.C., et al., *CD8 enhances formation of stable T-cell receptor/MHC class I molecule complexes.* Nature, 1996. **384**(6609): p. 577-81.
249. Zamoyska, R., *CD4 and CD8: modulators of T-cell receptor recognition of antigen and of immune responses?* Curr Opin Immunol, 1998. **10**(1): p. 82-7.
250. Wei, D.G., et al., *Expansion and long-range differentiation of the NKT cell lineage in mice expressing CD1d exclusively on cortical thymocytes.* J Exp Med, 2005. **202**(2): p. 239-48.
251. Schumann, J., et al., *Targeted expression of human CD1d in transgenic mice reveals independent roles for thymocytes and thymic APCs in positive and negative selection of Valpha14i NKT cells.* J Immunol, 2005. **175**(11): p. 7303-10.
252. Zhou, D., et al., *Lysosomal glycosphingolipid recognition by NKT cells.* Science, 2004. **306**(5702): p. 1786-9.
253. Benlagha, K., et al., *A thymic precursor to the NK T cell lineage.* Science, 2002. **296**(5567): p. 553-5.
254. Benlagha, K., et al., *Characterization of the early stages of thymic NKT cell development.* J Exp Med, 2005. **202**(4): p. 485-92.
255. Gadue, P. and P.L. Stein, *NK T cell precursors exhibit differential cytokine regulation and require Itk for efficient maturation.* J Immunol, 2002. **169**(5): p. 2397-406.

256. Pellicci, D.G., et al., *A natural killer T (NKT) cell developmental pathway involving a thymus-dependent NK1.1(-)CD4(+) CD1d-dependent precursor stage*. J Exp Med, 2002. **195**(7): p. 835-44.
257. Kronenberg, M. and L. Gapin, *The unconventional lifestyle of NKT cells*. Nat Rev Immunol, 2002. **2**(8): p. 557-68.
258. Matsuda, J.L. and L. Gapin, *Developmental program of mouse Valpha14i NKT cells*. Curr Opin Immunol, 2005. **17**(2): p. 122-30.
259. Kunisaki, Y., et al., *DOCK2 is required in T cell precursors for development of Valpha14 NK T cells*. J Immunol, 2006. **176**(8): p. 4640-5.
260. Kennedy, M.K., et al., *Reversible defects in natural killer and memory CD8 T cell lineages in interleukin 15-deficient mice*. J Exp Med, 2000. **191**(5): p. 771-80.
261. Wu, L.C., et al., *Two-step binding mechanism for T-cell receptor recognition of peptide MHC*. Nature, 2002. **418**(6897): p. 552-6.
262. Sidobre, S., et al., *The T cell antigen receptor expressed by Valpha14i NKT cells has a unique mode of glycosphingolipid antigen recognition*. Proc Natl Acad Sci U S A, 2004. **101**(33): p. 12254-9.
263. Sidobre, S., et al., *The V alpha 14 NKT cell TCR exhibits high-affinity binding to a glycolipid/CD1d complex*. J Immunol, 2002. **169**(3): p. 1340-8.
264. Sim, B.C., et al., *Surprisingly minor influence of TRAV11 (Valpha14) polymorphism on NK T-receptor mCD1/alpha-galactosylceramide binding kinetics*. Immunogenetics, 2003. **54**(12): p. 874-83.
265. Gadola, S.D., et al., *Structure and binding kinetics of three different human CD1d-alpha-galactosylceramide-specific T cell receptors*. J Exp Med, 2006. **203**(3): p. 699-710.
266. Kjer-Nielsen, L., et al., *A structural basis for selection and cross-species reactivity of the semi-invariant NKT cell receptor in CD1d/glycolipid recognition*. J Exp Med, 2006. **203**(3): p. 661-73.
267. Wu, D.Y., et al., *Cross-presentation of disialoganglioside GD3 to natural killer T cells*. J Exp Med, 2003. **198**(1): p. 173-81.
268. Brigl, M., et al., *Conserved and heterogeneous lipid antigen specificities of CD1d-restricted NKT cell receptors*. J Immunol, 2006. **176**(6): p. 3625-34.
269. Gumperz, J.E., et al., *Murine CD1d-restricted T cell recognition of cellular lipids*. Immunity, 2000. **12**(2): p. 211-21.
270. Park, S.H., et al., *The mouse CD1d-restricted repertoire is dominated by a few autoreactive T cell receptor families*. J Exp Med, 2001. **193**(8): p. 893-904.
271. Behar, S.M., et al., *Diverse TCRs recognize murine CD1*. J Immunol, 1999. **162**(1): p. 161-7.
272. Godfrey, D.I., et al., *NKT cells: what's in a name?* Nat Rev Immunol, 2004. **4**(3): p. 231-7.
273. Chiu, Y.H., et al., *Distinct subsets of CD1d-restricted T cells recognize self-antigens loaded in different cellular compartments*. J Exp Med, 1999. **189**(1): p. 103-10.
274. Baron, J.L., et al., *Activation of a nonclassical NKT cell subset in a transgenic mouse model of hepatitis B virus infection*. Immunity, 2002. **16**(4): p. 583-94.
275. Terabe, M., et al., *CD1d-restricted natural killer T cells can down-regulate tumor immunosurveillance independent of interleukin-4 receptor-signal transducer and activator of transcription 6 or transforming growth factor-beta*. Cancer Res, 2006. **66**(7): p. 3869-75.

276. Exley, M.A., et al., *A major fraction of human bone marrow lymphocytes are Th2-like CD1d-reactive T cells that can suppress mixed lymphocyte responses.* J Immunol, 2001. **167**(10): p. 5531-4.
277. Van Rhijn, I., et al., *CD1d-restricted T cell activation by nonlipidic small molecules.* Proc Natl Acad Sci U S A, 2004. **101**(37): p. 13578-83.
278. Shiina, T., et al., *Genomic anatomy of a premier major histocompatibility complex paralogous region on chromosome 1q21-q22.* Genome Res, 2001. **11**(5): p. 789-802.
279. Kawachi, I., et al., *MRI-restricted V alpha 19i mucosal-associated invariant T cells are innate T cells in the gut lamina propria that provide a rapid and diverse cytokine response.* J Immunol, 2006. **176**(3): p. 1618-27.
280. Treiner, E., et al., *Mucosal-associated invariant T (MAIT) cells: an evolutionarily conserved T cell subset.* Microbes Infect, 2005. **7**(3): p. 552-9.
281. Okamoto, N., et al., *Synthetic alpha-mannosyl ceramide as a potent stimulant for an NKT cell repertoire bearing the invariant Valpha19-Jalpha26 TCR alpha chain.* Chem Biol, 2005. **12**(6): p. 677-83.
282. Shimamura, M., et al., *Induction of promotive rather than suppressive immune responses from a novel NKT cell repertoire Valpha19 NKT cell with alpha-mannosyl ceramide analogues consisting of the immunosuppressant ISP-I as the sphingosine unit.* Eur J Med Chem, 2006. **41**(5): p. 569-76.
283. Vincent, M.S., et al., *CD1a-, b-, and c-restricted TCRs recognize both self and foreign antigens.* J Immunol, 2005. **175**(10): p. 6344-51.
284. Spada, F.M., et al., *Self-recognition of CD1 by gamma/delta T cells: implications for innate immunity.* J Exp Med, 2000. **191**(6): p. 937-48.
285. Stenger, S., K.R. Niazi, and R.L. Modlin, *Down-regulation of CD1 on antigen-presenting cells by infection with Mycobacterium tuberculosis.* J Immunol, 1998. **161**(7): p. 3582-8.
286. Giuliani, A., et al., *Influence of Mycobacterium bovis bacillus Calmette Guerin on in vitro induction of CD1 molecules in human adherent mononuclear cells.* Infect Immun, 2001. **69**(12): p. 7461-70.
287. Prete, S.P., et al., *Bacillus Calmette-Guerin down-regulates CD1b induction by granulocyte-macrophage colony stimulating factor in human peripheral blood monocytes.* J Chemother, 2001. **13**(1): p. 52-8.
288. Amprey, J.L., G.F. Spath, and S.A. Porcelli, *Inhibition of CD1 expression in human dendritic cells during intracellular infection with Leishmania donovani.* Infect Immun, 2004. **72**(1): p. 589-92.
289. Gagliardi, M.C., et al., *Cell wall-associated alpha-glucan is instrumental for Mycobacterium tuberculosis to block CD1 molecule expression and disable the function of dendritic cell derived from infected monocyte.* Cell Microbiol, 2007. **9**(8): p. 2081-92.
290. Gagliardi, M.C., et al., *Bacillus Calmette-Guerin shares with virulent Mycobacterium tuberculosis the capacity to subvert monocyte differentiation into dendritic cell: implication for its efficacy as a vaccine preventing tuberculosis.* Vaccine, 2004. **22**(29-30): p. 3848-57.
291. Mariotti, S., et al., *Mycobacterium tuberculosis diverts alpha interferon-induced monocyte differentiation from dendritic cells into immunoprivileged macrophage-like host cells.* Infect Immun, 2004. **72**(8): p. 4385-92.

292. Hiromatsu, K., et al., *Induction of CD1-restricted immune responses in guinea pigs by immunization with mycobacterial lipid antigens*. J Immunol, 2002. **169**(1): p. 330-9.
293. Dascher, C.C., et al., *Immunization with a mycobacterial lipid vaccine improves pulmonary pathology in the guinea pig model of tuberculosis*. Int Immunol, 2003. **15**(8): p. 915-25.
294. Gonzalez-Aseguinolaza, G., et al., *alpha -galactosylceramide-activated Valpha 14 natural killer T cells mediate protection against murine malaria*. Proc Natl Acad Sci U S A, 2000. **97**(15): p. 8461-6.
295. Kakimi, K., et al., *Natural killer T cell activation inhibits hepatitis B virus replication in vivo*. J Exp Med, 2000. **192**(7): p. 921-30.
296. Kawakami, K., et al., *Activation of Valpha14(+) natural killer T cells by alpha-galactosylceramide results in development of Th1 response and local host resistance in mice infected with Cryptococcus neoformans*. Infect Immun, 2001. **69**(1): p. 213-20.
297. Benlagha, K., et al., *In vivo identification of glycolipid antigen-specific T cells using fluorescent CD1d tetramers*. J Exp Med, 2000. **191**(11): p. 1895-903.
298. Procopio, D.O., et al., *Glycosylphosphatidylinositol-anchored mucin-like glycoproteins from Trypanosoma cruzi bind to CD1d but do not elicit dominant innate or adaptive immune responses via the CD1d/NKT cell pathway*. J Immunol, 2002. **169**(7): p. 3926-33.
299. Berntman, E., et al., *The role of CD1d-restricted NK T lymphocytes in the immune response to oral infection with Salmonella typhimurium*. Eur J Immunol, 2005. **35**(7): p. 2100-9.
300. Brigl, M., et al., *Mechanism of CD1d-restricted natural killer T cell activation during microbial infection*. Nat Immunol, 2003. **4**(12): p. 1230-7.
301. Gansert, J.L., et al., *Human NKT cells express granulysin and exhibit antimycobacterial activity*. J Immunol, 2003. **170**(6): p. 3154-61.
302. Carnaud, C., et al., *Cutting edge: Cross-talk between cells of the innate immune system: NKT cells rapidly activate NK cells*. J Immunol, 1999. **163**(9): p. 4647-50.
303. Kamath, A.B., et al., *Cytolytic CD8+ T cells recognizing CFP10 are recruited to the lung after Mycobacterium tuberculosis infection*. J Exp Med, 2004. **200**(11): p. 1479-89.
304. Godfrey, D.I. and M. Kronenberg, *Going both ways: immune regulation via CD1d-dependent NKT cells*. J Clin Invest, 2004. **114**(10): p. 1379-88.
305. Yu, K.O. and S.A. Porcelli, *The diverse functions of CD1d-restricted NKT cells and their potential for immunotherapy*. Immunol Lett, 2005. **100**(1): p. 42-55.
306. Schmiege, J., et al., *Superior protection against malaria and melanoma metastases by a C-glycoside analogue of the natural killer T cell ligand alpha-Galactosylceramide*. J Exp Med, 2003. **198**(11): p. 1631-41.
307. McCarthy, C., et al., *The length of lipids bound to human CD1d molecules modulates the affinity of NKT cell TCR and the threshold of NKT cell activation*. J Exp Med, 2007. **204**(5): p. 1131-44.
308. Kawakami, K., et al., *Critical role of Valpha14+ natural killer T cells in the innate phase of host protection against Streptococcus pneumoniae infection*. Eur J Immunol, 2003. **33**(12): p. 3322-30.
309. Nieuwenhuis, E.E., et al., *CD1d-dependent macrophage-mediated clearance of Pseudomonas aeruginosa from lung*. Nat Med, 2002. **8**(6): p. 588-93.

310. Kumar, H., et al., *Cutting edge: CD1d deficiency impairs murine host defense against the spirochete, Borrelia burgdorferi*. J Immunol, 2000. **165**(9): p. 4797-801.
311. Duthie, M.S., et al., *During Trypanosoma cruzi infection CD1d-restricted NK T cells limit parasitemia and augment the antibody response to a glycosphosphoinositol-modified surface protein*. Infect Immun, 2002. **70**(1): p. 36-48.
312. Duthie, M.S., et al., *Critical proinflammatory and anti-inflammatory functions of different subsets of CD1d-restricted natural killer T cells during Trypanosoma cruzi infection*. Infect Immun, 2005. **73**(1): p. 181-92.
313. Faveeuw, C., et al., *Antigen presentation by CD1d contributes to the amplification of Th2 responses to Schistosoma mansoni glycoconjugates in mice*. J Immunol, 2002. **169**(2): p. 906-12.
314. Ishikawa, H., et al., *CD4(+) v(alpha)14 NKT cells play a crucial role in an early stage of protective immunity against infection with Leishmania major*. Int Immunol, 2000. **12**(9): p. 1267-74.
315. Mattner, J., et al., *NKT cells mediate organ-specific resistance against Leishmania major infection*. Microbes Infect, 2006. **8**(2): p. 354-62.
316. Svensson, M., et al., *Invariant NKT cells are essential for the regulation of hepatic CXCL10 gene expression during Leishmania donovani infection*. Infect Immun, 2005. **73**(11): p. 7541-7.
317. Ronet, C., et al., *NKT cells are critical for the initiation of an inflammatory bowel response against Toxoplasma gondii*. J Immunol, 2005. **175**(2): p. 899-908.
318. Lin, Y., et al., *Long-term loss of canonical NKT cells following an acute virus infection*. Eur J Immunol, 2005. **35**(3): p. 879-89.
319. de Lalla, C., et al., *Production of profibrotic cytokines by invariant NKT cells characterizes cirrhosis progression in chronic viral hepatitis*. J Immunol, 2004. **173**(2): p. 1417-25.
320. Singh, A.K., et al., *Natural killer T cell activation protects mice against experimental autoimmune encephalomyelitis*. J Exp Med, 2001. **194**(12): p. 1801-11.
321. Jahng, A.W., et al., *Activation of natural killer T cells potentiates or prevents experimental autoimmune encephalomyelitis*. J Exp Med, 2001. **194**(12): p. 1789-99.
322. Pal, E., et al., *Costimulation-dependent modulation of experimental autoimmune encephalomyelitis by ligand stimulation of V alpha 14 NK T cells*. J Immunol, 2001. **166**(1): p. 662-8.
323. Goff, R.D., et al., *Effects of lipid chain lengths in alpha-galactosylceramides on cytokine release by natural killer T cells*. J Am Chem Soc, 2004. **126**(42): p. 13602-3.
324. Oki, S., et al., *Preferential T(h)2 polarization by OCH is supported by incompetent NKT cell induction of CD40L and following production of inflammatory cytokines by bystander cells in vivo*. Int Immunol, 2005. **17**(12): p. 1619-29.
325. Naumov, Y.N., et al., *Activation of CD1d-restricted T cells protects NOD mice from developing diabetes by regulating dendritic cell subsets*. Proc Natl Acad Sci U S A, 2001. **98**(24): p. 13838-43.
326. Wang, B., Y.B. Geng, and C.R. Wang, *CD1-restricted NK T cells protect nonobese diabetic mice from developing diabetes*. J Exp Med, 2001. **194**(3): p. 313-20.
327. Hammond, K.J., et al., *alpha/beta-T cell receptor (TCR)+CD4-CD8- (NKT) thymocytes prevent insulin-dependent diabetes mellitus in nonobese diabetic (NOD)/Lt mice by the influence of interleukin (IL)-4 and/or IL-10*. J Exp Med, 1998. **187**(7): p. 1047-56.

328. Hong, S., et al., *The natural killer T-cell ligand alpha-galactosylceramide prevents autoimmune diabetes in non-obese diabetic mice*. Nat Med, 2001. **7**(9): p. 1052-6.
329. Sharif, S., et al., *Activation of natural killer T cells by alpha-galactosylceramide treatment prevents the onset and recurrence of autoimmune Type 1 diabetes*. Nat Med, 2001. **7**(9): p. 1057-62.
330. Mizuno, M., et al., *Synthetic glycolipid OCH prevents insulinitis and diabetes in NOD mice*. J Autoimmun, 2004. **23**(4): p. 293-300.
331. Laloux, V., et al., *NK T cell-induced protection against diabetes in V alpha 14-J alpha 281 transgenic nonobese diabetic mice is associated with a Th2 shift circumscribed regionally to the islets and functionally to islet autoantigen*. J Immunol, 2001. **166**(6): p. 3749-56.
332. Chiba, A., et al., *The involvement of V(alpha)14 natural killer T cells in the pathogenesis of arthritis in murine models*. Arthritis Rheum, 2005. **52**(6): p. 1941-8.
333. Yang, J.Q., et al., *Repeated alpha-galactosylceramide administration results in expansion of NK T cells and alleviates inflammatory dermatitis in MRL-lpr/lpr mice*. J Immunol, 2003. **171**(8): p. 4439-46.
334. Singh, A.K., et al., *The natural killer T cell ligand alpha-galactosylceramide prevents or promotes pristane-induced lupus in mice*. Eur J Immunol, 2005. **35**(4): p. 1143-54.
335. Zeng, D., et al., *Activation of natural killer T cells in NZB/W mice induces Th1-type immune responses exacerbating lupus*. J Clin Invest, 2003. **112**(8): p. 1211-22.
336. Ueno, Y., et al., *Single dose of OCH improves mucosal T helper type 1/T helper type 2 cytokine balance and prevents experimental colitis in the presence of valpha14 natural killer T cells in mice*. Inflamm Bowel Dis, 2005. **11**(1): p. 35-41.
337. Sumida, T., et al., *Selective reduction of T cells bearing invariant V alpha 24J alpha Q antigen receptor in patients with systemic sclerosis*. J Exp Med, 1995. **182**(4): p. 1163-8.
338. Illes, Z., et al., *Differential expression of NK T cell V alpha 24J alpha Q invariant TCR chain in the lesions of multiple sclerosis and chronic inflammatory demyelinating polyneuropathy*. J Immunol, 2000. **164**(8): p. 4375-81.
339. Araki, M., et al., *Th2 bias of CD4+ NKT cells derived from multiple sclerosis in remission*. Int Immunol, 2003. **15**(2): p. 279-88.
340. Demoulin, T., et al., *A biased Valpha24+ T-cell repertoire leads to circulating NKT-cell defects in a multiple sclerosis patient at the onset of his disease*. Immunol Lett, 2003. **90**(2-3): p. 223-8.
341. Oishi, Y., et al., *Selective reduction and recovery of invariant Valpha24JalphaQ T cell receptor T cells in correlation with disease activity in patients with systemic lupus erythematosus*. J Rheumatol, 2001. **28**(2): p. 275-83.
342. Kojo, S., et al., *Dysfunction of T cell receptor AV24AJ18+, BV11+ double-negative regulatory natural killer T cells in autoimmune diseases*. Arthritis Rheum, 2001. **44**(5): p. 1127-38.
343. van der Vliet, H.J., et al., *Circulating V(alpha24+) Vbeta11+ NKT cell numbers are decreased in a wide variety of diseases that are characterized by autoreactive tissue damage*. Clin Immunol, 2001. **100**(2): p. 144-8.
344. Wilson, S.B., et al., *Extreme Th1 bias of invariant Valpha24JalphaQ T cells in type 1 diabetes*. Nature, 1998. **391**(6663): p. 177-81.
345. Kukreja, A., et al., *Multiple immuno-regulatory defects in type-1 diabetes*. J Clin Invest, 2002. **109**(1): p. 131-40.

346. Lee, P.T., et al., *Testing the NKT cell hypothesis of human IDDM pathogenesis*. J Clin Invest, 2002. **110**(6): p. 793-800.
347. Oikawa, Y., et al., *High frequency of valpha24(+) vbeta11(+) T-cells observed in type 1 diabetes*. Diabetes Care, 2002. **25**(10): p. 1818-23.
348. Akbari, O., et al., *CD4+ invariant T-cell-receptor+ natural killer T cells in bronchial asthma*. N Engl J Med, 2006. **354**(11): p. 1117-29.
349. Akbari, O., et al., *Essential role of NKT cells producing IL-4 and IL-13 in the development of allergen-induced airway hyperreactivity*. Nat Med, 2003. **9**(5): p. 582-8.
350. Lisbonne, M., et al., *Cutting edge: invariant V alpha 14 NKT cells are required for allergen-induced airway inflammation and hyperreactivity in an experimental asthma model*. J Immunol, 2003. **171**(4): p. 1637-41.
351. Meyer, E.H., et al., *Glycolipid activation of invariant T cell receptor+ NK T cells is sufficient to induce airway hyperreactivity independent of conventional CD4+ T cells*. Proc Natl Acad Sci U S A, 2006. **103**(8): p. 2782-7.
352. Milner, J.D., et al., *Differential responses of invariant V alpha 24J alpha Q T cells and MHC class II-restricted CD4+ T cells to dexamethasone*. J Immunol, 1999. **163**(5): p. 2522-9.
353. Tamada, K., et al., *IL-4-producing NK1.1+ T cells are resistant to glucocorticoid-induced apoptosis: implications for the Th1/Th2 balance*. J Immunol, 1998. **161**(3): p. 1239-47.
354. Adcock, I.M. and K. Ito, *Steroid resistance in asthma: a major problem requiring novel solutions or a non-issue?* Curr Opin Pharmacol, 2004. **4**(3): p. 257-62.
355. Ito, K., K.F. Chung, and I.M. Adcock, *Update on glucocorticoid action and resistance*. J Allergy Clin Immunol, 2006. **117**(3): p. 522-43.
356. Kim, C.H., B. Johnston, and E.C. Butcher, *Trafficking machinery of NKT cells: shared and differential chemokine receptor expression among V alpha 24(+)V beta 11(+) NKT cell subsets with distinct cytokine-producing capacity*. Blood, 2002. **100**(1): p. 11-6.
357. Gumperz, J.E., et al., *Functionally distinct subsets of CD1d-restricted natural killer T cells revealed by CD1d tetramer staining*. J Exp Med, 2002. **195**(5): p. 625-36.
358. Campos, R.A., et al., *Cutaneous immunization rapidly activates liver invariant Valpha14 NKT cells stimulating B-1 B cells to initiate T cell recruitment for elicitation of contact sensitivity*. J Exp Med, 2003. **198**(12): p. 1785-96.
359. Nieuwenhuis, E.E., et al., *CD1d and CD1d-restricted iNKT-cells play a pivotal role in contact hypersensitivity*. Exp Dermatol, 2005. **14**(4): p. 250-8.
360. Oishi, Y., et al., *CD4-CD8- T cells bearing invariant Valpha24JalphaQ TCR alpha-chain are decreased in patients with atopic diseases*. Clin Exp Immunol, 2000. **119**(3): p. 404-11.
361. Takahashi, T., et al., *V alpha 24+ natural killer T cells are markedly decreased in atopic dermatitis patients*. Hum Immunol, 2003. **64**(6): p. 586-92.
362. Magnan, A., et al., *Relationships between natural T cells, atopy, IgE levels, and IL-4 production*. Allergy, 2000. **55**(3): p. 286-90.
363. Smyth, M.J., et al., *Differential tumor surveillance by natural killer (NK) and NKT cells*. J Exp Med, 2000. **191**(4): p. 661-8.
364. Kobayashi, E., et al., *KRN7000, a novel immunomodulator, and its antitumor activities*. Oncol Res, 1995. **7**(10-11): p. 529-34.

365. Yamaguchi, Y., et al., *Enhancing effects of (2S,3S,4R)-1-O-(alpha-D-galactopyranosyl)-2-(N-hexacosanoylamino) -1,3,4-octadecanetriol (KRN7000) on antigen-presenting function of antigen-presenting cells and antimetastatic activity of KRN7000-pretreated antigen-presenting cells.* Oncol Res, 1996. **8**(10-11): p. 399-407.
366. Nakagawa, R., et al., *Treatment of hepatic metastasis of the colon26 adenocarcinoma with an alpha-galactosylceramide, KRN7000.* Cancer Res, 1998. **58**(6): p. 1202-7.
367. Nakagawa, R., et al., *Antitumor activity of alpha-galactosylceramide, KRN7000, in mice with EL-4 hepatic metastasis and its cytokine production.* Oncol Res, 1998. **10**(11-12): p. 561-8.
368. Smyth, M.J., et al., *Sequential production of interferon-gamma by NK1.1(+) T cells and natural killer cells is essential for the antimetastatic effect of alpha-galactosylceramide.* Blood, 2002. **99**(4): p. 1259-66.
369. Hayakawa, Y., et al., *Alpha-galactosylceramide (KRN7000) suppression of chemical- and oncogene-dependent carcinogenesis.* Proc Natl Acad Sci U S A, 2003. **100**(16): p. 9464-9.
370. Hayakawa, Y., et al., *Critical contribution of IFN-gamma and NK cells, but not perforin-mediated cytotoxicity, to anti-metastatic effect of alpha-galactosylceramide.* Eur J Immunol, 2001. **31**(6): p. 1720-7.
371. Kawano, T., et al., *Antitumor cytotoxicity mediated by ligand-activated human V alpha24 NKT cells.* Cancer Res, 1999. **59**(20): p. 5102-5.
372. Tahir, S.M., et al., *Loss of IFN-gamma production by invariant NK T cells in advanced cancer.* J Immunol, 2001. **167**(7): p. 4046-50.
373. Dhodapkar, M.V., et al., *A reversible defect in natural killer T cell function characterizes the progression of premalignant to malignant multiple myeloma.* J Exp Med, 2003. **197**(12): p. 1667-76.
374. Tachibana, T., et al., *Increased intratumor V alpha24-positive natural killer T cells: a prognostic factor for primary colorectal carcinomas.* Clin Cancer Res, 2005. **11**(20): p. 7322-7.
375. Kenna, T., et al., *NKT cells from normal and tumor-bearing human livers are phenotypically and functionally distinct from murine NKT cells.* J Immunol, 2003. **171**(4): p. 1775-9.
376. Park, J.M., et al., *Unmasking immunosurveillance against a syngeneic colon cancer by elimination of CD4+ NKT regulatory cells and IL-13.* Int J Cancer, 2005. **114**(1): p. 80-7.
377. Ostrand-Rosenberg, S., M.J. Grusby, and V.K. Clements, *Cutting edge: STAT6-deficient mice have enhanced tumor immunity to primary and metastatic mammary carcinoma.* J Immunol, 2000. **165**(11): p. 6015-9.
378. Terabe, M., et al., *A nonclassical non-Valpha14Jalpha18 CD1d-restricted (type II) NKT cell is sufficient for down-regulation of tumor immunosurveillance.* J Exp Med, 2005. **202**(12): p. 1627-33.
379. Sfondrini, L., et al., *Absence of the CD1 molecule up-regulates antitumor activity induced by CpG oligodeoxynucleotides in mice.* J Immunol, 2002. **169**(1): p. 151-8.
380. Duarte, N., et al., *Prevention of diabetes in nonobese diabetic mice mediated by CD1d-restricted nonclassical NKT cells.* J Immunol, 2004. **173**(5): p. 3112-8.

381. Exley, M.A., et al., *Cutting edge: Compartmentalization of Th1-like noninvariant CD1d-reactive T cells in hepatitis C virus-infected liver*. J Immunol, 2002. **168**(4): p. 1519-23.
382. Smith, C.L., et al., *Recombinant modified vaccinia Ankara primes functionally activated CTL specific for a melanoma tumor antigen epitope in melanoma patients with a high risk of disease recurrence*. Int J Cancer, 2005. **113**(2): p. 259-66.
383. Smith, C.L., et al., *Immunodominance of poxviral-specific CTL in a human trial of recombinant-modified vaccinia Ankara*. J Immunol, 2005. **175**(12): p. 8431-7.
384. Lee, P.T., et al., *Distinct functional lineages of human V(alpha)24 natural killer T cells*. J Exp Med, 2002. **195**(5): p. 637-41.
385. Seino, K. and M. Taniguchi, *Functionally distinct NKT cell subsets and subtypes*. J Exp Med, 2005. **202**(12): p. 1623-6.
386. Giaccone, G., et al., *A phase I study of the natural killer T-cell ligand alpha-galactosylceramide (KRN7000) in patients with solid tumors*. Clin Cancer Res, 2002. **8**(12): p. 3702-9.
387. Nieda, M., et al., *Therapeutic activation of Valpha24+Vbeta11+ NKT cells in human subjects results in highly coordinated secondary activation of acquired and innate immunity*. Blood, 2004. **103**(2): p. 383-9.
388. Ishikawa, A., et al., *A phase I study of alpha-galactosylceramide (KRN7000)-pulsed dendritic cells in patients with advanced and recurrent non-small cell lung cancer*. Clin Cancer Res, 2005. **11**(5): p. 1910-7.
389. Chang, D.H., et al., *Sustained expansion of NKT cells and antigen-specific T cells after injection of alpha-galactosyl-ceramide loaded mature dendritic cells in cancer patients*. J Exp Med, 2005. **201**(9): p. 1503-17.
390. van der Vliet, H.J., et al., *Potent expansion of human natural killer T cells using alpha-galactosylceramide (KRN7000)-loaded monocyte-derived dendritic cells, cultured in the presence of IL-7 and IL-15*. J Immunol Methods, 2001. **247**(1-2): p. 61-72.
391. Nakui, M., et al., *Potential of antitumor effect of NKT cell ligand, alpha-galactosylceramide by combination with IL-12 on lung metastasis of malignant melanoma cells*. Clin Exp Metastasis, 2000. **18**(2): p. 147-53.
392. Smyth, M.J., et al., *Sequential activation of NKT cells and NK cells provides effective innate immunotherapy of cancer*. J Exp Med, 2005. **201**(12): p. 1973-85.
393. Fujii, S., et al., *Activation of natural killer T cells by alpha-galactosylceramide rapidly induces the full maturation of dendritic cells in vivo and thereby acts as an adjuvant for combined CD4 and CD8 T cell immunity to a coadministered protein*. J Exp Med, 2003. **198**(2): p. 267-79.
394. Liu, K., et al., *Innate NKT lymphocytes confer superior adaptive immunity via tumor-capturing dendritic cells*. J Exp Med, 2005. **202**(11): p. 1507-16.
395. Hermans, I.F., et al., *NKT cells enhance CD4+ and CD8+ T cell responses to soluble antigen in vivo through direct interaction with dendritic cells*. J Immunol, 2003. **171**(10): p. 5140-7.
396. Cardell, S.L., *The natural killer T lymphocyte: a player in the complex regulation of autoimmune diabetes in non-obese diabetic mice*. Clin Exp Immunol, 2006. **143**(2): p. 194-202.

397. Miyake, S. and T. Yamamura, *Therapeutic potential of glycolipid ligands for natural killer (NK) T cells in the suppression of autoimmune diseases*. *Curr Drug Targets Immune Endocr Metabol Disord*, 2005. **5**(3): p. 315-22.
398. Fujii, S., et al., *Prolonged IFN-gamma-producing NKT response induced with alpha-galactosylceramide-loaded DCs*. *Nat Immunol*, 2002. **3**(9): p. 867-74.
399. Uldrich, A.P., et al., *NKT cell stimulation with glycolipid antigen in vivo: costimulation-dependent expansion, Bim-dependent contraction, and hyporesponsiveness to further antigenic challenge*. *J Immunol*, 2005. **175**(5): p. 3092-101.
400. Parekh, V.V., et al., *Glycolipid antigen induces long-term natural killer T cell anergy in mice*. *J Clin Invest*, 2005. **115**(9): p. 2572-83.
401. Cui, J., et al., *Requirement for Valpha14 NKT cells in IL-12-mediated rejection of tumors*. *Science*, 1997. **278**(5343): p. 1623-6.
402. Takeda, K., et al., *Liver NK1.1+ CD4+ alpha beta T cells activated by IL-12 as a major effector in inhibition of experimental tumor metastasis*. *J Immunol*, 1996. **156**(9): p. 3366-73.
403. Kobayashi, T., et al., *Interleukin-12 administration is more effective for preventing metastasis than for inhibiting primary established tumors in a murine model of spontaneous hepatic metastasis*. *Surg Today*, 2002. **32**(3): p. 236-42.
404. Shin, T., et al., *Inhibition of tumor metastasis by adoptive transfer of IL-12-activated Valpha14 NKT cells*. *Int J Cancer*, 2001. **91**(4): p. 523-8.
405. Smyth, M.J., M. Taniguchi, and S.E. Street, *The anti-tumor activity of IL-12: mechanisms of innate immunity that are model and dose dependent*. *J Immunol*, 2000. **165**(5): p. 2665-70.
406. Takeda, K., et al., *Relative contribution of NK and NKT cells to the anti-metastatic activities of IL-12*. *Int Immunol*, 2000. **12**(6): p. 909-14.
407. Baxevanis, C.N., A.D. Gritzapis, and M. Papamichail, *In vivo antitumor activity of NKT cells activated by the combination of IL-12 and IL-18*. *J Immunol*, 2003. **171**(6): p. 2953-9.
408. Jaffee, E.M., *Immunotherapy of cancer*. *Ann N Y Acad Sci*, 1999. **886**: p. 67-72.
409. Gillessen, S., et al., *CD1d-restricted T cells regulate dendritic cell function and antitumor immunity in a granulocyte-macrophage colony-stimulating factor-dependent fashion*. *Proc Natl Acad Sci U S A*, 2003. **100**(15): p. 8874-9.
410. Eager, R. and J. Nemunaitis, *GM-CSF gene-transduced tumor vaccines*. *Mol Ther*, 2005. **12**(1): p. 18-27.
411. Morris, E.S., et al., *NKT cell-dependent leukemia eradication following stem cell mobilization with potent G-CSF analogs*. *J Clin Invest*, 2005. **115**(11): p. 3093-103.
412. Ko, S.Y., et al., *alpha-Galactosylceramide can act as a nasal vaccine adjuvant inducing protective immune responses against viral infection and tumor*. *J Immunol*, 2005. **175**(5): p. 3309-17.
413. Chung, Y., et al., *NKT cell ligand alpha-galactosylceramide blocks the induction of oral tolerance by triggering dendritic cell maturation*. *Eur J Immunol*, 2004. **34**(9): p. 2471-9.
414. Silk, J.D., et al., *Utilizing the adjuvant properties of CD1d-dependent NK T cells in T cell-mediated immunotherapy*. *J Clin Invest*, 2004. **114**(12): p. 1800-11.
415. Matsuyoshi, H., et al., *Therapeutic effect of alpha-galactosylceramide-loaded dendritic cells genetically engineered to express SLC/CCL21 along with tumor*

- antigen against peritoneally disseminated tumor cells*. *Cancer Sci*, 2005. **96**(12): p. 889-96.
416. Skold, M. and S.M. Behar, *The role of group 1 and group 2 CD1-restricted T cells in microbial immunity*. *Microbes Infect*, 2005. **7**(3): p. 544-51.
 417. De Libero, G. and L. Mori, *Recognition of lipid antigens by T cells*. *Nat Rev Immunol*, 2005. **5**(6): p. 485-96.
 418. Martin, C., *The dream of a vaccine against tuberculosis; new vaccines improving or replacing BCG?* *Eur Respir J*, 2005. **26**(1): p. 162-7.
 419. Skeiky, Y.A. and J.C. Sadoff, *Advances in tuberculosis vaccine strategies*. *Nat Rev Microbiol*, 2006. **4**(6): p. 469-76.
 420. Laval, F., et al., *Accurate molecular mass determination of mycolic acids by MALDI-TOF mass spectrometry*. *Anal Chem*, 2001. **73**(18): p. 4537-44.
 421. Daffe, M. and P. Draper, *The envelope layers of mycobacteria with reference to their pathogenicity*. *Adv Microb Physiol*, 1998. **39**: p. 131-203.
 422. Watanabe, M., et al., *Separation and characterization of individual mycolic acids in representative mycobacteria*. *Microbiology*, 2001. **147**(Pt 7): p. 1825-37.
 423. Schroeder, B.G. and C.E. Barry, 3rd, *The specificity of methyl transferases involved in trans mycolic acid biosynthesis in Mycobacterium tuberculosis and Mycobacterium smegmatis*. *Bioorg Chem*, 2001. **29**(3): p. 164-77.
 424. Quemard, A., et al., *Structure of a hydroxymycolic acid potentially involved in the synthesis of oxygenated mycolic acids of the Mycobacterium tuberculosis complex*. *Eur J Biochem*, 1997. **250**(3): p. 758-63.
 425. Sowden, J.C. and H.O.L. Fischer, *l-Glycidol*. *J Am Chem Soc*, 1942. **42**: p. 1291-1293.
 426. Defaye, J. and E. Lederer, *Synthesis of a glycerin-alpha-monomycolate*. *J Bull Soc Chim Biol (Paris)*, 1956. **38**: p. 1301-1304.
 427. Tsumita, T., *Studies on the lipid of BCG. I. Glyceryl mono-mycolate in wax C fraction of the lipid of BCG*. *Jpn J Med Sci Biol*, 1956. **9**: p. 205-216.
 428. Noll, H., *The chemistry of some native constituents of the purified wax of Mycobacterium tuberculosis*. *J Biol Chem*, 1957. **224**(1): p. 149-64.
 429. Bloch, H., et al., *Constituents of a toxic-lipid obtained from Mycobacterium tuberculosis*. *Biochim Biophys Acta*, 1957. **23**(2): p. 312-21.
 430. Noll, H. and E. Jackim, *The chemistry of the native constituents of the acetone-soluble fat of Mycobacterium tuberculosis (Brevannes). I. Glycerides and phosphoglycolipides*. *J Biol Chem*, 1958. **232**(2): p. 903-17.
 431. Batrakov, S.G., *Specific lipids of mycobacteria and related organisms*. *Chem of Nat Compounds*, 1985. **21**: p. 137-159.
 432. Batuwangala, T., et al., *The crystal structure of human CD1b with a bound bacterial glycolipid*. *J Immunol*, 2004. **172**(4): p. 2382-8.
 433. Tsuji, M., *Glycolipids and phospholipids as natural CD1d-binding NKT cell ligands*. *Cell Mol Life Sci*, 2006. **63**(16): p. 1889-98.
 434. Kinjo, Y., et al., *Natural killer T cells recognize diacylglycerol antigens from pathogenic bacteria*. *Nat Immunol*, 2006. **7**(9): p. 978-86.
 435. Schaible, U.E., et al., *Intersection of group I CD1 molecules and mycobacteria in different intracellular compartments of dendritic cells*. *J Immunol*, 2000. **164**(9): p. 4843-52.

436. Cheng, T.Y., et al., *Role of lipid trimming and CDI groove size in cellular antigen presentation*. *Embo J*, 2006. **25**(13): p. 2989-99.
437. Hirsch, C.S., et al., *Cross-modulation by transforming growth factor beta in human tuberculosis: suppression of antigen-driven blastogenesis and interferon gamma production*. *Proc Natl Acad Sci U S A*, 1996. **93**(8): p. 3193-8.
438. Caccamo, N., et al., *Phenotypical and functional analysis of memory and effector human CD8 T cells specific for mycobacterial antigens*. *J Immunol*, 2006. **177**(3): p. 1780-5.
439. Moody, D.B., et al., *The molecular basis of CDI-mediated presentation of lipid antigens*. *Immunol Rev*, 1999. **172**: p. 285-96.
440. Goren, M.B., et al., *Sulfolipid I of Mycobacterium tuberculosis, strain H37RV. Nature of the acyl substituents*. *Biochemistry*, 1971. **10**(1): p. 72-81.
441. Minnikin, D.E., et al., *The methyl-branched fortifications of Mycobacterium tuberculosis*. *Chem Biol*, 2002. **9**(5): p. 545-53.
442. Goren, M.B., *The Mycobacteria: A sourcebook, Part A*. eds Kubica GP, Wayne LG (Dekker, New York), 1984: p. 379-415.
443. Kaufmann, S.H. and A.J. McMichael, *Annulling a dangerous liaison: vaccination strategies against AIDS and tuberculosis*. *Nat Med*, 2005. **11**(4 Suppl): p. S33-44.
444. Jindani, A., A.J. Nunn, and D.A. Enarson, *Two 8-month regimens of chemotherapy for treatment of newly diagnosed pulmonary tuberculosis: international multicentre randomised trial*. *Lancet*, 2004. **364**(9441): p. 1244-51.
445. Glynn, J.R., et al., *Worldwide occurrence of Beijing/W strains of Mycobacterium tuberculosis: a systematic review*. *Emerg Infect Dis*, 2002. **8**(8): p. 843-9.
446. Diel, R., et al., *Avoiding the effect of BCG vaccination in detecting Mycobacterium tuberculosis infection with a blood test*. *Eur Respir J*, 2006. **28**(1): p. 16-23.
447. Dheda, K., et al., *Utility of the antigen-specific interferon-gamma assay for the management of tuberculosis*. *Curr Opin Pulm Med*, 2005. **11**(3): p. 195-202.
448. Fine, P.E., *The BCG story: lessons from the past and implications for the future*. *Rev Infect Dis*, 1989. **11 Suppl 2**: p. S353-9.
449. Rodrigues, L.C., V.K. Diwan, and J.G. Wheeler, *Protective effect of BCG against tuberculous meningitis and miliary tuberculosis: a meta-analysis*. *Int J Epidemiol*, 1993. **22**(6): p. 1154-8.
450. Colditz, G.A., et al., *Efficacy of BCG vaccine in the prevention of tuberculosis. Meta-analysis of the published literature*. *JAMA*, 1994. **271**: p. 698-702.
451. Brandt, L., et al., *Failure of the Mycobacterium bovis BCG vaccine: some species of environmental mycobacteria block multiplication of BCG and induction of protective immunity to tuberculosis*. *Infect Immun*, 2002. **70**(2): p. 672-8.
452. Olsen, A.W., et al., *Protective effect of a tuberculosis subunit vaccine based on a fusion of antigen 85B and ESAT-6 in the aerosol guinea pig model*. *Infect Immun*, 2004. **72**(10): p. 6148-50.
453. Langermans, J.A., et al., *Protection of macaques against Mycobacterium tuberculosis infection by a subunit vaccine based on a fusion protein of antigen 85B and ESAT-6*. *Vaccine*, 2005. **23**(21): p. 2740-50.
454. Brandt, L., et al., *The protective effect of the Mycobacterium bovis BCG vaccine is increased by coadministration with the Mycobacterium tuberculosis 72-kilodalton fusion polyprotein Mtb72F in M. tuberculosis-infected guinea pigs*. *Infect Immun*, 2004. **72**(11): p. 6622-32.

455. McShane, H., et al., *Recombinant modified vaccinia virus Ankara expressing antigen 85A boosts BCG-primed and naturally acquired antimycobacterial immunity in humans*. *Nat Med*, 2004. **10**(11): p. 1240-4.
456. Horwitz, M.A. and G. Harth, *A new vaccine against tuberculosis affords greater survival after challenge than the current vaccine in the guinea pig model of pulmonary tuberculosis*. *Infect Immun*, 2003. **71**(4): p. 1672-9.
457. Grode, L., et al., *Increased vaccine efficacy against tuberculosis of recombinant Mycobacterium bovis bacille Calmette-Guerin mutants that secrete listeriolysin*. *J Clin Invest*, 2005. **115**(9): p. 2472-9.
458. Ernst, J.D., *Macrophage receptors for Mycobacterium tuberculosis*. *Infect Immun*, 1998. **66**(4): p. 1277-81.
459. Cambi, A., M. Koopman, and C.G. Figdor, *How C-type lectins detect pathogens*. *Cell Microbiol*, 2005. **7**(4): p. 481-8.
460. Tailleux, L., et al., *DC-SIGN is the major Mycobacterium tuberculosis receptor on human dendritic cells*. *J Exp Med*, 2003. **197**(1): p. 121-7.
461. Duclos, S., et al., *Rab5 regulates the kiss and run fusion between phagosomes and endosomes and the acquisition of phagosome leishmanicidal properties in RAW 264.7 macrophages*. *J Cell Sci*, 2000. **113 Pt 19**: p. 3531-41.
462. Claus, V., et al., *Lysosomal enzyme trafficking between phagosomes, endosomes, and lysosomes in J774 macrophages. Enrichment of cathepsin H in early endosomes*. *J Biol Chem*, 1998. **273**(16): p. 9842-51.
463. Vieira, O.V., R.J. Botelho, and S. Grinstein, *Phagosome maturation: aging gracefully*. *Biochem J*, 2002. **366**(Pt 3): p. 689-704.
464. Koul, A., et al., *Interplay between mycobacteria and host signalling pathways*. *Nat Rev Microbiol*, 2004. **2**(3): p. 189-202.
465. Schuller, S., et al., *Coronin is involved in uptake of Mycobacterium bovis BCG in human macrophages but not in phagosome maintenance*. *Cell Microbiol*, 2001. **3**(12): p. 785-93.
466. Via, L.E., et al., *Arrest of mycobacterial phagosome maturation is caused by a block in vesicle fusion between stages controlled by rab5 and rab7*. *J Biol Chem*, 1997. **272**(20): p. 13326-31.
467. Fratti, R.A., et al., *Role of phosphatidylinositol 3-kinase and Rab5 effectors in phagosomal biogenesis and mycobacterial phagosome maturation arrest*. *J Cell Biol*, 2001. **154**(3): p. 631-44.
468. Saunders, B.M. and W.J. Britton, *Life and death in the granuloma: immunopathology of tuberculosis*. *Immunol Cell Biol*, 2007. **85**(2): p. 103-11.
469. Fratti, R.A., et al., *Mycobacterium tuberculosis glycosylated phosphatidylinositol causes phagosome maturation arrest*. *Proc Natl Acad Sci U S A*, 2003. **100**(9): p. 5437-42.
470. Walburger, A., et al., *Protein kinase G from pathogenic mycobacteria promotes survival within macrophages*. *Science*, 2004. **304**(5678): p. 1800-4.
471. Blachere, N.E., R.B. Darnell, and M.L. Albert, *Apoptotic cells deliver processed antigen to dendritic cells for cross-presentation*. *PLoS Biol*, 2005. **3**(6): p. e185.
472. Noss, E.H., C.V. Harding, and W.H. Boom, *Mycobacterium tuberculosis inhibits MHC class II antigen processing in murine bone marrow macrophages*. *Cell Immunol*, 2000. **201**(1): p. 63-74.

473. Noss, E.H., et al., *Toll-like receptor 2-dependent inhibition of macrophage class II MHC expression and antigen processing by 19-kDa lipoprotein of Mycobacterium tuberculosis*. J Immunol, 2001. **167**(2): p. 910-8.
474. Hirsch, C.S., et al., *Augmentation of apoptosis and interferon-gamma production at sites of active Mycobacterium tuberculosis infection in human tuberculosis*. J Infect Dis, 2001. **183**(5): p. 779-88.
475. Hirsch, C.S., et al., *Apoptosis and T cell hyporesponsiveness in pulmonary tuberculosis*. J Infect Dis, 1999. **179**(4): p. 945-53.
476. Kremer, L., et al., *Ineffective cellular immune response associated with T-cell apoptosis in susceptible Mycobacterium bovis BCG-infected mice*. Infect Immun, 2000. **68**(7): p. 4264-73.
477. Li, Z., et al., *Expression of katG in Mycobacterium tuberculosis is associated with its growth and persistence in mice and guinea pigs*. J Infect Dis, 1998. **177**(4): p. 1030-5.
478. Darwin, K.H., et al., *The proteasome of Mycobacterium tuberculosis is required for resistance to nitric oxide*. Science, 2003. **302**(5652): p. 1963-6.
479. Pieters, J. and H. Ploegh, *Microbiology. Chemical warfare and mycobacterial defense*. Science, 2003. **302**(5652): p. 1900-2.
480. Chan, J., et al., *Lipoarabinomannan, a possible virulence factor involved in persistence of Mycobacterium tuberculosis within macrophages*. Infect Immun, 1991. **59**(5): p. 1755-61.
481. Knutson, K.L., et al., *Lipoarabinomannan of Mycobacterium tuberculosis promotes protein tyrosine dephosphorylation and inhibition of mitogen-activated protein kinase in human mononuclear phagocytes. Role of the Src homology 2 containing tyrosine phosphatase 1*. J Biol Chem, 1998. **273**(1): p. 645-52.
482. Nigou, J., et al., *Mycobacterial lipoarabinomannans: modulators of dendritic cell function and the apoptotic response*. Microbes Infect, 2002. **4**(9): p. 945-53.
483. Rojas, M., et al., *Mannosylated lipoarabinomannan antagonizes Mycobacterium tuberculosis-induced macrophage apoptosis by altering Ca²⁺-dependent cell signaling*. J Infect Dis, 2000. **182**(1): p. 240-51.
484. Hava, D.L., et al., *Evasion of peptide, but not lipid antigen presentation, through pathogen-induced dendritic cell maturation*. Proc Natl Acad Sci U S A, 2008. **105**(32): p. 11281-6.
485. Schaible, U.E., et al., *Cytokine activation leads to acidification and increases maturation of Mycobacterium avium-containing phagosomes in murine macrophages*. J Immunol, 1998. **160**(3): p. 1290-6.
486. MacMicking, J.D., G.A. Taylor, and J.D. McKinney, *Immune control of tuberculosis by IFN-gamma-inducible LRG-47*. Science, 2003. **302**(5645): p. 654-9.
487. Gutierrez, M.G., et al., *Autophagy is a defense mechanism inhibiting BCG and Mycobacterium tuberculosis survival in infected macrophages*. Cell, 2004. **119**(6): p. 753-66.
488. Medzhitov, R. and C.A. Janeway, Jr., *An ancient system of host defense*. Curr Opin Immunol, 1998. **10**(1): p. 12-5.
489. Takeda, K., T. Kaisho, and S. Akira, *Toll-like receptors*. Annu Rev Immunol, 2003. **21**: p. 335-76.
490. Blander, J.M. and R. Medzhitov, *On regulation of phagosome maturation and antigen presentation*. Nat Immunol, 2006. **7**(10): p. 1029-35.

491. Fremond, C.M., et al., *Fatal Mycobacterium tuberculosis infection despite adaptive immune response in the absence of MyD88*. J Clin Invest, 2004. **114**(12): p. 1790-9.
492. Kempna, P., et al., *Cloning of novel human SEC14p-like proteins: ligand binding and functional properties*. Free Radic Biol Med, 2003. **34**(11): p. 1458-72.
493. Zimmer, S., et al., *A novel human tocopherol-associated protein: cloning, in vitro expression, and characterization*. J Biol Chem, 2000. **275**(33): p. 25672-80.
494. Dansen, T.B., et al., *High-affinity binding of very-long-chain fatty acyl-CoA esters to the peroxisomal non-specific lipid-transfer protein (sterol carrier protein-2)*. Biochem J, 1999. **339** (Pt 1): p. 193-9.
495. Frolov, A., et al., *Sterol carrier protein-2, a new fatty acyl coenzyme A-binding protein*. J Biol Chem, 1996. **271**(50): p. 31878-84.
496. Gallegos, A.M., et al., *Gene structure, intracellular localization, and functional roles of sterol carrier protein-2*. Prog Lipid Res, 2001. **40**(6): p. 498-563.
497. Nichols, J.W., *Binding of fluorescent-labeled phosphatidylcholine to rat liver nonspecific lipid transfer protein*. J Biol Chem, 1987. **262**(29): p. 14172-7.
498. Avdulov, N.A., et al., *Lipid binding to sterol carrier protein-2 is inhibited by ethanol*. Biochim Biophys Acta, 1999. **1437**(1): p. 37-45.
499. Zingg, J.M., et al., *Characterization of three human sec14p-like proteins: alpha-Tocopherol transport activity and expression pattern in tissues*. Biochimie, 2008.
500. Wanders, R.J., et al., *Peroxisomal fatty acid alpha- and beta-oxidation in humans: enzymology, peroxisomal metabolite transporters and peroxisomal diseases*. Biochem Soc Trans, 2001. **29**(Pt 2): p. 250-67.
501. Billheimer, J.T. and J.L. Gaylor, *Effect of lipid composition on the transfer of sterols mediated by non-specific lipid transfer protein (sterol carrier protein2)*. Biochim Biophys Acta, 1990. **1046**(2): p. 136-43.
502. Gadella, T.W., Jr. and K.W. Wirtz, *Phospholipid binding and transfer by the nonspecific lipid-transfer protein (sterol carrier protein 2). A kinetic model*. Eur J Biochem, 1994. **220**(3): p. 1019-28.
503. Frolov, A., et al., *Fibroblast membrane sterol kinetic domains: modulation by sterol carrier protein-2 and liver fatty acid binding protein*. J Lipid Res, 1996. **37**(9): p. 1862-74.
504. Vila, A., et al., *Sterol carrier protein-2-facilitated intermembrane transfer of cholesterol- and phospholipid-derived hydroperoxides*. Biochemistry, 2004. **43**(39): p. 12592-605.
505. Kriska, T., et al., *Intracellular dissemination of peroxidative stress. Internalization, transport, and lethal targeting of a cholesterol hydroperoxide species by sterol carrier protein-2-overexpressing hepatoma cells*. J Biol Chem, 2006. **281**(33): p. 23643-51.
506. Kernstock, R.M. and A.W. Girotti, *Lipid transfer protein binding of unmodified natural lipids as assessed by surface plasmon resonance methodology*. Anal Biochem, 2007. **365**(1): p. 111-21.
507. Bastian, M., et al., *Mycobacterial lipopeptides elicit CD4+ CTLs in Mycobacterium tuberculosis-infected humans*. J Immunol, 2008. **180**(5): p. 3436-46.
508. Middlebrook, G., C.M. Coleman, and W.B. Schaefer, *Sulfolipid from Virulent Tubercle Bacilli*. Proc Natl Acad Sci U S A, 1959. **45**(12): p. 1801-4.

509. Goren, M.B., O. Brokl, and W.B. Schaefer, *Lipids of putative relevance to virulence in Mycobacterium tuberculosis: correlation of virulence with elaboration of sulfatides and strongly acidic lipids*. Infect Immun, 1974. **9**(1): p. 142-9.
510. Weinrich Olsen, A., et al., *Protection of mice with a tuberculosis subunit vaccine based on a fusion protein of antigen 85b and esat-6*. Infect Immun, 2001. **69**(5): p. 2773-8.
511. Skeiky, Y.A., et al., *Differential immune responses and protective efficacy induced by components of a tuberculosis polyprotein vaccine, Mtb72F, delivered as naked DNA or recombinant protein*. J Immunol, 2004. **172**(12): p. 7618-28.
512. Williams, A., et al., *Evaluation of vaccines in the EU TB Vaccine Cluster using a guinea pig aerosol infection model of tuberculosis*. Tuberculosis (Edinb), 2005. **85**(1-2): p. 29-38.
513. Dietrich, J., et al., *Synergistic effect of bacillus calmette guerin and a tuberculosis subunit vaccine in cationic liposomes: increased immunogenicity and protection*. J Immunol, 2007. **178**(6): p. 3721-30.
514. WHO, *Global Advisory Committee on Vaccine Safety, 29-30 November 2006*. Wkly Epidemiol Rec, 2007. **82**(3): p. 18-24.
515. De Libero, G., *Methods for the generation of T cell clones and epithelial cell lines from excised human biopsies or needle aspirates*. N.F.a.G. Butcher, ed. (Oxford:IRL), 1997: p. 123-140.
516. Gilleron, M., et al., *Acylation state of the phosphatidylinositol mannosides from Mycobacterium bovis bacillus Calmette Guerin and ability to induce granuloma and recruit natural killer T cells*. J Biol Chem, 2001. **276**(37): p. 34896-904.
517. Gilleron, M., V.F. Quesniaux, and G. Puzo, *Acylation state of the phosphatidylinositol hexamannosides from Mycobacterium bovis bacillus Calmette Guerin and mycobacterium tuberculosis H37Rv and its implication in Toll-like receptor response*. J Biol Chem, 2003. **278**(32): p. 29880-9.
518. Baer, H. and B. Radatus, *Preparation of some partially protected, α,α -trehalose-type disaccharides having the D-altro configuration*. Carbohydr Res, 1984. **128**: p. 165-174.
519. Baer, H.H. and X. Wu, *Synthesis of alpha, alpha-trehalose 2,3- and 2,3'-diesters with palmitic and stearic acid: potential immunoreactants for the serodiagnosis of tuberculosis*. Carbohydr Res, 1993. **238**: p. 215-30.
520. Liav, A. and M.B. Goren, *Sulfatides of Mycobacterium tuberculosis. Synthesis of the core alpha, alpha-trehalose 2-sulfate*. Carbohydr Res, 1984. **127**(2): p. 211-6.
521. Besra, G.S., et al., *Synthesis of methyl (Z)-tetracos-5-enoate and both enantiomers of ethyl (E)-6-methyltetracos-4-enoate: possible intermediates in the biosynthesis of mycolic acids in mycobacteria*. Chem Phys Lipids, 1993. **66**(1-2): p. 23-34.
522. Birkbeck, A. and D. Enders, *The total synthesis of (+)-pectinatone: An iterative alkylation approach based on the SAMP-hydrazone method*. Tet Lett, 1998. **39**: p. 7823-7826.
523. Righetti, P.G., C. Gelfi, and M. Conti, *Current trends in capillary isoelectric focusing of proteins*. J Chromatogr B Biomed Sci Appl, 1997. **699**(1-2): p. 91-104.
524. Rodriguez-Diaz, R., T. Wehr, and M. Zhu, *Capillary isoelectric focusing*. Electrophoresis, 1997. **18**(12-13): p. 2134-44.
525. Habermehl, D., et al., *Recombinant SEC14-like proteins (TAP) possess GTPase activity*. Biochem Biophys Res Commun, 2005. **326**(1): p. 254-9.

